Physical properties of natural rubber

Payne, A. R.

PHYSICAL PROPERTIES OF NATURAL RUBBER.

PHYSICAL PROPERTIES OF NATURAL RUBBER.

THESIS

Presented for the degree of

MASTER OF SCIENCE

in the

UNIVERSITY OF DURHAM.

by

ARTHUR ROBERT PAYNE.

B.Sc. (Hons) DUNELM. Fellow of The Institute of Physics. Fellow of The Institution of The Rubber Industry.

Natural Rubber Producers' Research Association,

Welwyn Garden City,

Herts.

January 1966.

ABTRACT.

This Thesis is a review of the effect of temperature and frequency of oscillation on the viscoelastic properties of natural rubber when a sinusoidal oscillation, either electrical or mechanical, is used to stress the rubber.

The Thesis is divided into two sections. The first part discusses the dynamic mechanical properties of various types of natural rubber vulcanizate, with particular emphasis on the interdependence of temperature and frequency of oscillation. The second part discusses the dielectric properties of natural rubber and again treats the interdependence of temperature and frequency on the physical properties in detail. Molecular theories regarding the mechanical and dielectric properties are reviewed and applied to experimental data.

SUPPLEMENTARY CONTRIBUTIONS.

1. "Temperature-frequency relationships of dielectric and mechanical properties of polymers," by A.R. Payne.

   "Rheology of Elastomers", London (1958a) p 86-112. Edited by P. Mason and N. Wookey. Pergamon Press, for The British Society of Rheology meeting at Welwyn Garden City at which this paper was read by the author.

2. "The mechanical and dielectric temperature-frequency equivalence of polymers-GR-S", by A.R. Payne.

   Society of Chemical Industry Publication. Silver Jubilee Symposium of The Plastics and Polymer Group". Paper read at The symposium. (1958b), p 154-165, 186-191. Also appeared as Rubber and Plastics Research Association Report No 93.

3. "Dielectric properties of purified natural rubber" ~~by natural rubber~~" by R.H. Norman and A.R. Payne.

   Transactions of The Institution of The Rubber Industry. 41, No 5 (1965), p T 191-211. Awaiting reprinting in The American Chemical Society Publication, Rubber Chemistry and Technology.

ACKNOWLEDGEMENTS.

The author is indebted to the Board of The Natural Rubber Producers' Research Association for providing facilities for the compilation of this Thesis.

As the Thesis is essentially a review Thesis. reference has been made to some of the author's published work. This work has appeared in "Rheology of Elastomers' edited by P. Mason and N. Wookey, Pergamon Press, on behalf of The British Society of Rheology (1958) p 86-112. In Society of Chemical Industry Publication:- Silver Jubilee Symposium. (Plastics and Polymer Group.)(1958), p 154-165, 186-191. In the Transactions of The Institution of The Rubber Industry. (1965), 41, No 5, T.131. The paper appearing in The Transactions of The Institution of The Rubber Industry was published jointly with Mr. R.H. Norman of The Rubber and Plastics Research Association on work carried out several years ago with the author at the Research Association of British Rubber Manufacturers.

The author is also indebted to Dr. W.A. Prowse

Master of Van Mildert College for his very helpful advice during the preparation of this Thesis, and to Dr. L. Mullins, Director of The Natural Rubber Producers' Research Association for his comments and advice on the subject of this Thesis.

PHYSICAL PROPERTIES OF NATURAL RUBBER.

TABLE OF CONTENTS

PHYSICAL PROPERTIES OF NATURAL RUBBER

CHAPTER 1

1. INTRODUCTION

In describing the mechanical properties of materials, there are two basic theories which can be used :-

a) The classical theory of elasticity: for a material whose mechanical response is proportional to strain but independent of the rate of strain, or

b) The classical theory of hydrodynamics : for perfectly viscous liquids in which the material property is proportional to the rate of strain but independent of the strain itself.

The deviations from these two basic conditions which can occur in real materials can be summarised as :-

a) The strain (in a solid) or rate of strain (in a liquid) may <u>not</u> be directly proportional to stress but may depend upon stress in a more complicated manner - the material possesses stress anomalies

b) The stress may depend on both strain and rate of strain together, as well as on higher time derivatives of strain; - the material possesses time anomalies.

c) Both stress and time anomalies may occur together.

In viscoelastic materials such as rubber or plastics time anomalies reflect a behaviour which combines both liquid-like and solid-like characteristics. If time anomalies only are present, a material is said to possess linear viscoelasticity, and its behaviour can be simulated by a model consisting of suitable combinations of springs and dashpots with the springs obeying Hookes' law and the viscous dashpots obeying Newton's law. Such models are of limited applicability in describing the viscoelastic behaviour of real materials, such as natural rubber, and it appears both stress and time anomalies are present in a rubber.

Deformation of hard solids, such as diamond, sodium chloride and crystalline zinc involve displacement of atoms from equilibrium positions in localized fields

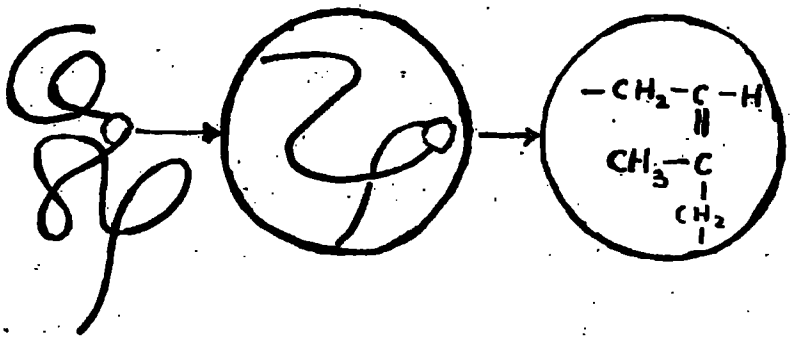

Fig 2·1 Symbolic representation of long range and short-range contour relationships in a flexible polymer molecule (natural rubber).

of force. From a knowledge of the interatomic potentials, the elastic constants of such materials can be calculated. Kittel (1956). In an ordinary liquid under stress, viscous flow reflects the change with time of the distribution of molecules surrounding a given molecule, and here, too, the relevant forces and processes of readjustment are quite local in character, and from a knowledge of them, the viscosity can, in principle, be calculated. Kirkwood, (1946).

In a polymer, on the other hand, each flexible threadlike molecule pervades an average volume much greater than atomic dimensions and is continuously changing its shape as it waggles and wreathes with its thermal energy. To characterise the various configurations or contour shapes the polymer molecules assume, it is necessary to consider ~~gross~~ not only long-range configurational relationships, but also more local relationships, over the whole range down to the orientation of bonds in the chain backbone with respect to each other on a scale of atomic dimensions. See Fig. 2.1.

Alfrey (1948) has referred to these spatial relationships, viewed over progressively longer ranges, as kinks, curls and convolutions. Rearrangements on a local scale (kinks) are relatively rapid, on a long range (convolutions) very slow, so there is a wide range of time scales covering the response of such a system under stress. Even at temperatures well below a glass-transition temperature, where the long range convolutional readjustments are severely restricted, polymers still show a wide range of response rates to external stress. Energy can be dispersed in a polymer by interaction of electrical as well as mechanical waves with the segmental modes of motion of the polymer chain. This is realised, if we note that the dipoles in a liquid follow an alternating field of suitable frequency by aligning themselves. For instance, in a polymer such as polyvinyl chloride, the strong C-Cℓ dipole can only become aligned by the motion of the chain segment to which it is attached. Similarly, with vulcanised natural rubber, the sulphur dipole introduced into a crosslink or into a cyclic chain by vulcanisation can only respond by

involving a segment of the polymer chain to which it is attached. As in the case of the mechanical excitation of segmental motions, heat can be generated by internal friction, and a resonant frequency obtained at the match point of segmental and applied frequencies. Therefore, a study of dielectric properties should aid a study of mechanical properties.

Technologically, dissipation of energy either mechanically or dielectrically in polymers is of importance. The mechanical dissipation of energy causes the 'power loss' in rubber tyres when they heat up under the cyclic deformation imposed by the tyre rolling on the road surface. This heating also causes oxidation, degradation and premature ageing of the rubber. Dielectric power loss is a serious drawback in insulators for cables carrying alternating currents.

Antivibration and shock mountings of rubber have critical requirements with regard to elasticity, damping and vibration transmissibility. It is apparent therefore that a study of mechanical and electrical response of polymers has a direct bearing on the practical

applications of elastomeric materials.

A convenient way of studying these time dependent properties is to impose both electrical and mechanical sinusoidal oscillations on the materials, and then to measure and characterise the subsequent response. This thesis confines itself to a review of the present state of knowledge of the effect of temperature and frequency when a sinusoidal oscillation, either electrical or mechanical, is used to stress or strain a polymer. Most of the data discussed refer to natural rubber, although some data referring to other rubbers is mentioned in the text, either for purposes of comparison, or when relevant information on natural rubber is too sparse to illustrate the point being discussed.

The thesis is also restricted to areas in which the author has himself contributed, either in published studies or in recent unpublished work.

CHAPTER 2.

DYNAMIC MECHANICAL PROPERTIES (Temperature and frequency dependence)

2.1 INTRODUCTION

This chapter reviews the effect of temperature and frequency on dynamic mechanical properties, stressing in particular the interrelationship between these two variables. The influence of compounding in modifying the dynamic properties will be summarised, and the experimentally derived data will be compared with current molecular theories.

LIST OF SYMBOLS USED

LIST OF SYMBOLS USED IN CHAPTER 2

SYMBOL	DEFINITION
E	Young's (tensile) modulus, dyne cm^{-2}
E^*	complex dynamic tensile modulus, dyne cm^{-2}
E'	tensile storage modulus, dyne cm^{-2}
E''	tensile loss modulus, dyne cm^{-2}
G	shear modulus, dyne cm^{-2}
G^*	complex dynamic shear modulus, dyne cm^{-2}
G'	shear storage modulus, dyne cm^{-2}
G''	shear loss modulus, dyne cm^{-2}
G''/G'	dissipation factor or loss tangent $\equiv \tan\delta$ or J''/J'
G_e	equilibrium or pseudo-equilibrium shear modulus dyne cm^{-2}
G_i	modulus contribution of model element
$G_{(t)}$	time dependent shear modulus, dyne cm^{-2}
H	relaxation spectrum (shear)
J	shear compliance , cm^2/dyne
J^*	complex dynamic shear compliance, cm^2/dyne
J'	shear storage compliance, cm^2/dyne
J''	shear loss compliance, cm^2/dyne
$J_{(t)}$	time dependent shear compliance, cm^2/dyne
J_e	equilibrium pseudo-equilibrium, or steady-state shear compliance, cm^2/dyne
J_i	compliance contribution of model element
L	retardation spectrum (shear)
M_o	molecular weight per monomer unit
M_e	average molecular weight between entanglement coupling points
M_c	average molecular weight of a network strand

SYMBOL	DEFINITION
N_o	Avogadro's number
T	absolute temperature
T_o	reference temperature for reduced variables
T_s	standard reference temperature for WLF equation in form of equation 2.19, chapter 2
T_g	glass transition temperature
Z_e	average degree of polymerisation between entanglement coupling points
a	root-mean-square end-to-end distance per square root of number of monomer units
a_T	ratio of relaxation times at two different temperatures
e	shear strain
f	force, or fractional free volume
f_g	fractional free volume at the glass transition temperature
f_o	translational friction coefficient of a sub-molecule
k	Boltzmann's constant
m	slope of logarithmic plot
n	number of molecules per cc
p	summation index
q	number of monomer units in a sub-molecule
t	time (seconds)
Γ	Gamma function
δ	phase cycle between stress and strain, or Dirac delta
ϵ	dielectric constant
ϵ'	real component of complex dielectric constant
ϵ''	imaginary component of complex dielectric constant
ζ_o	translational friction coefficient per monomer unit
ζ_1	translational friction coefficient for small foreign molecule
η	shear viscosity
η^*	complex dynamic shear viscosity
η'	real part of complex viscosity
η''	imaginary part of complex viscosity
η_i	viscosity contribution of model element

SYMBOL	DEFINITION
ρ	density
σ	root-mean-square end-to-end distance of a sub molecule
σ	shear stress
τ	relaxation or retardation time; argument of H or L
τ_i	relaxation or retardation time of element of mechanical model
τ'	reciprocal of the value of $\log H - \log \tau$ plot has a slope of $\frac{1}{2}$
ϕ	volume fraction (of filler)
ω	frequency in rad/sec.

PLEASE UNFOLD THIS PAGE TO SUPPLY AN EASY
REFERENCE TO A LIST OF SYMBOLS
USED IN THIS CHAPTER 2.

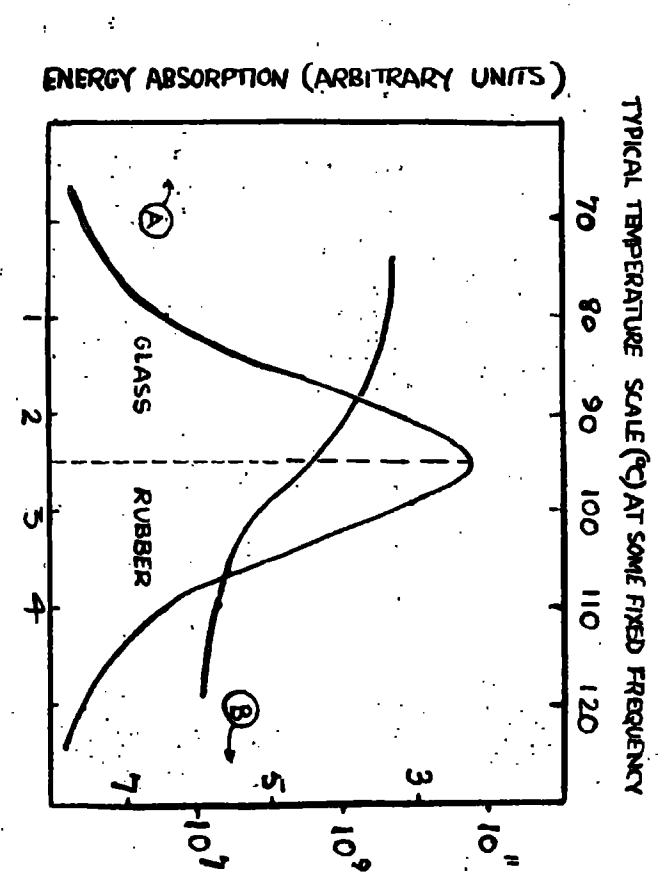

Fig 2.5. Relaxation behaviour of a polymer (schematic). Curve A: energy loss (left-hand scale). Curve B: dielectric constant (upper right-hand scale) or Young's modulus (middle right-hand scale). Both curves are functions of temperature (upper scale) or frequency (lower scale). The vertical broken line shows the glass-to-rubber transition.

where J' is the real component and J'' the imaginary component of the complex compliance, and can be represented vectorially as in Fig. 2.2b

The behaviour of polymers is best summarised by reference to Fig. 2.5, in which it can be seen that:-

a) the <u>energy absorption</u> rises to a peak as the applied frequency matches the average segmental relaxation rate of the polymer chains. Such a peak is obtainable, either as the temperature is varied at fixed frequency (segmental frequency variable, applied frequency fixed), or as the frequency is varied at constant temperature (applied frequency variable, segmental frequency fixed).

b) the <u>dynamic elastic modulus</u> rises from a low value in the soft or rubbery state to a high value in the hard or glassy state along a characteristic S shaped curve either as the frequency is raised or as the temperature is lowered. The modulus reaches its maximum rate of change with temperature or with frequency at the match-point of segmental and applied

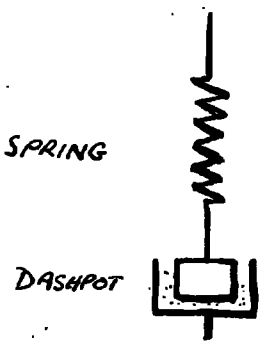

THE MAXWELL ELEMENT.

(a)

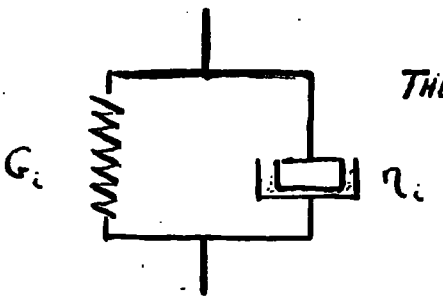

THE VOIGT ELEMENT.

(b)

FIG 2·6

frequencies, i.e. the point of inflexion of the S-shape coincides with the position of the energy absorption peak.

The following sections of this chapter discuss these phenomena in greater detail.

2.3 ELEMENTARY MODELS USED TO DESCRIBE MECHANICAL BEHAVIOUR OF VISCOELASTIC MATERIALS.

2.3.1 Maxwell Unit

The simplest model used to describe the time or frequency dependence of viscoelastic materials is a Maxwell unit - consisting of a spring and dashpot in series, and can be used to illustrate some aspects of the dynamic behaviour of rubber. Fig. 2.6a.

The equation of motion of a Maxwell unit is:-

$$\frac{de}{dt} = \frac{1}{G_i} \frac{d\sigma}{dt} + \frac{\sigma}{\tau_i G_i} \qquad (2.4)$$

where the relaxation time of the element is defined as

$$\tau_i = \eta_i / G_i$$

and e is shear strain, σ shear stress, η_i shear viscosity, G_i shear modulus of the element. This

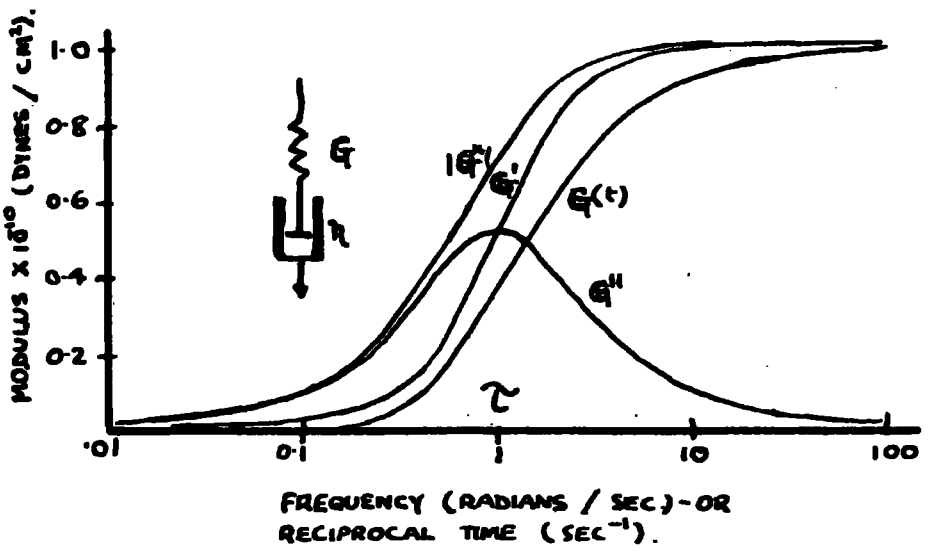

FIG 2·7. *Dynamic behaviour of a Maxwell unit as a function of frequency. The relaxation time is one second. The stress-relaxation modulus G(t) of the same model is given for comparison.* $|G^*| = \sqrt{(G'^2 + G''^2)}$.

equation can be solved to give :-

$$G' = \frac{\omega^2 \tau_i^2 G_i}{1 + \omega_i^2 \tau_i^2} \qquad (2.5)$$

$$G'' = \frac{\omega \tau_i G_i}{1 + \omega^2 \tau_i^2} \qquad (2.6a)$$

$$\tan = 1/\omega\tau_i \qquad (2.6b)$$

where ω is the frequency in radians per sec.

The dynamic modulus G' and damping G'' of a Maxwell unit as a function of frequency are shown in Fig. 2.7. In this example, the modulus G of the spring and the viscosity η of the dashpot are both 10^{10} units, so the relaxation τ is one second. At low frequencies, where most of the deformation comes from the dashpot, the dynamic modulus G' is very low. At very high frequencies there is not enough time for any appreciable flow to occur in the dashpot during the time of a cycle of oscillation, and therefore the motion at high

frequencies is due to the stretching of the spring, so that the dynamic modulus is equal to the modulus of the spring. At intermediate frequencies where the time for an oscillation is roughly equal to the relaxation time, motion of both the spring and the dashpot take place under the action of an applied force. In this frequency range, the dynamic modulus increases rapidly with frequency.

The loss modulus G'' approaches zero at both high and low frequencies. Energy dissipation comes from motion of the dashpot. At high frequencies a cycle of oscillation takes so little time that no motion can occur in the dashpot. At low frequencies, there is a lot of motion of the dashpot, but the motion is so slow that the rate of shear in the dashpot is small. Viscous damping leads to the dissipation of large amounts of energy only when the amounts of motion (total shear) and the rate of shear (frequency) are both large. At intermediate frequencies both the rate of shear and the motion of the dashpot are large, so the dissipation of energy is large. The loss

modulus goes through a maximum when $\omega = {}^{1}/_{\tau}$

The absolute value of the modulus $/G^{*}/$ is defined as

$$/G^{*}/ = \sqrt{(G')^2 + (G'')^2} \qquad 2.7$$

and is also plotted in Fig. 2.7. At low frequencies the absolute value of the modulus is equal to G'' while at high frequencies it equals G'. The dissipation G''/G' of a Maxwell element is equal to $1/\omega\tau$, so that G''/G' increases continuously as the frequency decreases. Natural and other rubbers show Maxwell-type behaviour only near their glass or high frequency transition, and it is necessary to use more complex models and to postulate a broad distribution of relaxation and retardation times in order to describe the mechanical response of rubber.

2.3.2 Voight (or Kelvin) Element

A single spring-dashpot point in parallel is called a Voight element, Fig 2.6b and it can be shown that

$$G' = G_i$$
$$G'' = G_i\omega\tau_i = \omega\eta_i \qquad 2.8$$
$$\tan\delta = \omega\tau_i$$
$$\text{etc.}$$

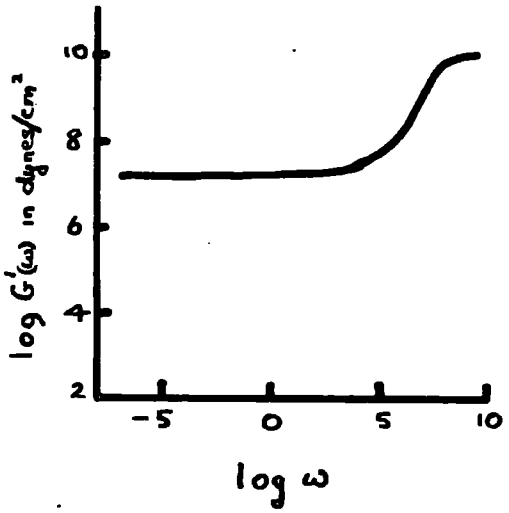

Fig 2·8 a

Storage modulus plotted against frequency with logarithmic scales.
Lightly vulcanised NR. 25°C.

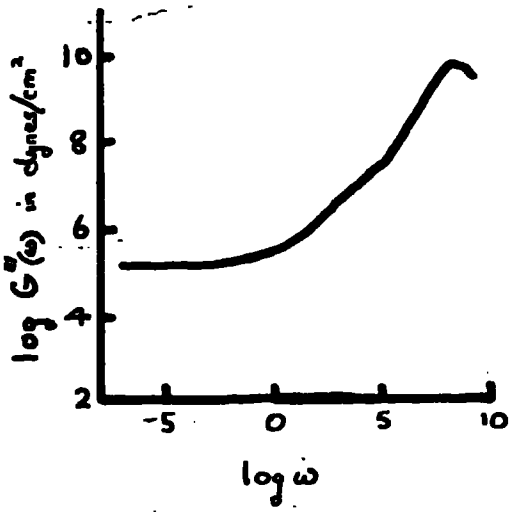

Fig 2·8 b

Loss modulus plotted against frequency with logarithmic scales
Lightly vulcanised NR at 25°C.

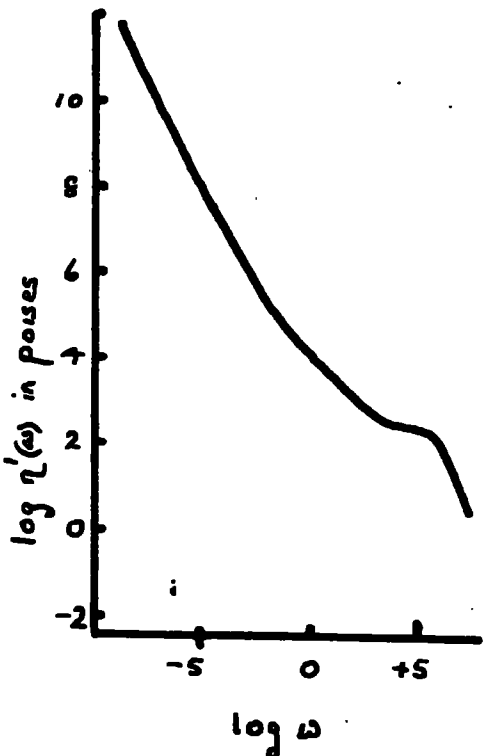

Fig 2·8 c

Real part of the complex dynamic viscosity with logarithmic scales.
Lightly vulcanised NR at 25°C.

For a spring corresponding to a shear modulus $G_i = {}^1/J_i$, and the dashpot to a viscosity η_i, τ_i is the retardation time = η_i/G_i.

Graphs of these functions have been given in many places, Alfrey (1941), Ferry (1961), Leaderman (1944), and will not be given here, because, as with a Maxwell element, they are too simple to correspond to the real viscoelastic behaviour in rubber.

2.4 A GENERAL DESCRIPTION OF THE DYNAMIC RESPONSE OF NATURAL RUBBER.

It is useful at this stage to consider in detail some results obtained by the author on a lightly vulcanised natural rubber and at the same time to define more precisely some of the terms used to describe its behaviour.

2.4.1 Storage modulus

The shear storage modulus G' is defined as the stress in phase with the strain in a sinusoidal deformation divided by the strain. log G' is plotted against log ω in Fig. 2.8a for a lightly vulcanised natural rubber.

2.4.2 The Loss Modulus

The loss modulus G'' is defined as the stress 90^o

out of phase with the strain divided by the strain. It is plotted as a function of frequency in Fig 2.8b. In frequency regions where G′ changed slowly (see Fig 2.8a), the behaviour is more nearly perfectly elastic, hence comparatively little energy is dissipated in periodic deformations.

At high frequencies, a generalised Maxwell model for instance would be expected to approach perfect elastic behaviour as the motion of the dashpot became negligible compared with that of the springs, and G″ should also approach zero. For lightly vulcanised natural rubber this is not the case as a slight maximum in G″ appears but does not drop down to zero at higher frequencies. There must therefore be some molecular or atomic adjustments capable of dissipating energy even at the highest frequencies.

At very low frequencies, a system corresponding to a finite mechanical model should exhibit direct proportionality of G″ to ω (a slope of 1), for lightly vulcanised NR this is certainly not the case.

2.4.3 The Dynamic Viscosity

The dissipative effect of an alternating stress can be

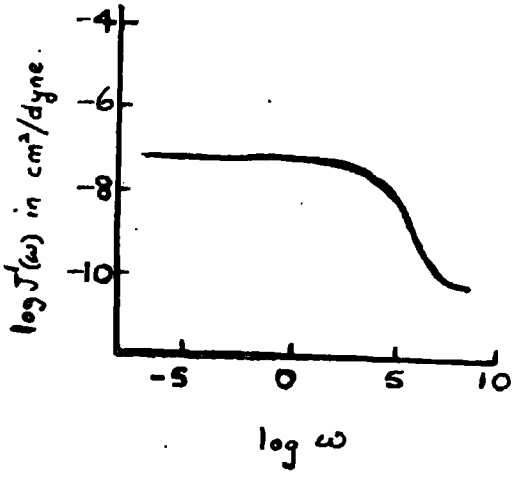

Fig 2·8 d:

Storage compliance plotted logarithmically.

Lightly vulcanised NR at 25°C

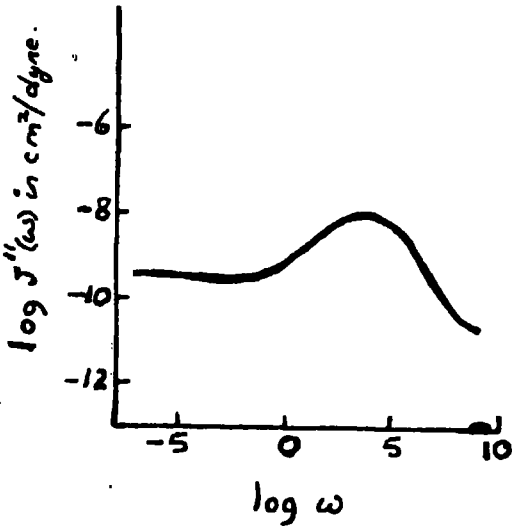

Fig 2·8 e

Loss compliance plotted logarithmically.

Lightly vulcanised NR at 25°C.

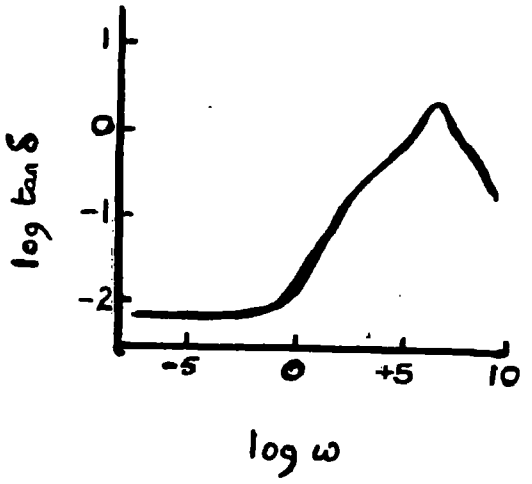

Fig 2·8 f

Loss tangent plotted logarithmically.

Lightly vulcanised NR at 25°C.

described by the stress in-phase with rate of strain divided by the strain. This has the dimensions of a viscosity, and is the real part η' of complex viscosity η^* where

$$\eta^* = \eta' - i\eta''$$
$$\eta' = G''/\omega \qquad 2.9$$
$$\eta = G'/\omega$$

With increasing frequency, η', falls monotonically for a lightly vulcanised natural rubber as shown in Fig 2.8c, reaching values many orders of magnitude smaller than η, the ordinary steady flow viscosity of the polymer.

2.4.4 The Storage Compliance

The storage compliance J' is defined as the strain in a sinusoidal deformation in-phase with the stress divided by the stress. It is plotted on logarithmic scales in Fig. 2.8d for a lightly vulcanised natural rubber. It can be seen that at low frequencies J' reaches a steady value and approaches J_e, the equilibrium compliance at low frequencies.

2.4.5 The Loss Compliance

The loss compliance J'' is defined as the strain 90^o

out of phase with the stress divided by the stress. It is plotted on logarithmic scales in Fig. 2.8e. This function is characterised by a broad maximum, for both vulcanised and unvulcanised polymers of high molecular weight, at a point corresponding to the low-frequency end of the transition zone. It is presumably characteristic of a network structure, whether the network is formed of permanently bonded molecular chains or chains coupled by entanglements. Simple finite mechanical models predict that J' becomes inversely proportional to ω (in fact $1/\omega\eta$), and, of course, this is not so for the lightly crosslinked natural rubber.

2.4.6 The Loss Tangent

A useful parameter which is a measure of the ratio of energy lost to energy stored in cyclic deformation is :-

$$\tan\delta = G''/G' = J''/J' \quad (=\text{dissipation factor}) \qquad 2.10$$

The logarithmic plot in Fig. 2.8f for lightly vulcanised rubber reveals that in the transition zone between glasslike and rubberlike states, the loss tangent goes through a pronounced maxima.

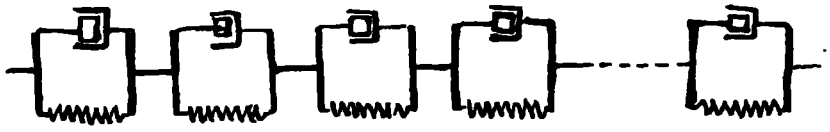

Fig 2·9 Generalised Voigt model of springs and dashpots representing the mechanical behaviour of a viscoelastic material.

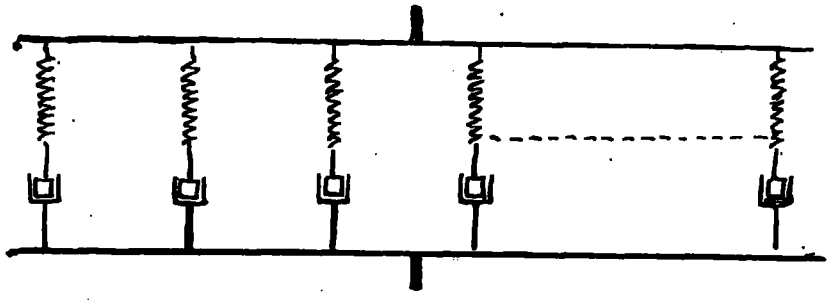

Fig. 2·10 Generalised Maxwell model of springs and dashpots representing the mechanical behaviour of a viscoelastic material.

It is of interest to note that the maxima in J'' occurs to the left of that in $\tan\delta$, and the maxima in G'' occur to the right of that in $\tan\delta$ on the frequency scale; the differences amount to several decades. As each of these three functions is a measure of elastic losses or heat dissipation, it is clear that the frequency region in which the "loss" occurs depends upon the choice of function by which the loss is specified.

2.4.7 Discrete Viscoelastic Spectra

Any number of Maxwell elements in series have the properties of a single Maxwell element with $J = \sum J_i$ and $1/\eta = \sum 1/\eta_i$. Any number of Voigt elements in parallel have the properties of a single Voigt element with $G = \sum G_i$ and $\eta = \sum \eta_i$.

Maxwell elements in parallel or Voigt elements in series as in Figs 2.9 and 2.10 obviously have much more complicated properties, and are more useful representations of viscoelastic behaviour than a single Maxwell or Voigt element. For instance, if the number of elements in the Maxwell model of Fig 2.10 is increased without limit, the

result is a <u>continuous spectrum</u> of relaxation times in which each infinitesimal contribution to the shear modulus is associated with relaxation times lying in the range between τ and $\tau + d\tau$. As is evident from the dynamic data plots, it is more useful to consider a <u>continuous relaxation spectrum</u> as defined by $Hd(\ln\tau)$, the contribution to rigidity associated with relaxation times whose logarithms lie in the range between $\ln\tau$ and $\ln\tau + d\ln\tau$, and it can be shown that :-

$$G(t) = G_e + \int_{-\infty}^{\infty} He^{-t/\tau}\, d(\ln\tau) \qquad 2.11$$

This equation may be taken to be a mathematical description of H without recourse to use of any models. Here G_e is added to allow for a finite value when the relaxation time is very long ($\tau \rightarrow \infty$). (G_e is usually assumed to be zero for uncrosslinked polymers, but this ignores the effects of entanglements which act as crosslinks, so G_e always has a finite value).

Fig. 2.11 is a plot of log H, the relaxation spectrum for lightly crosslinked natural rubber. The

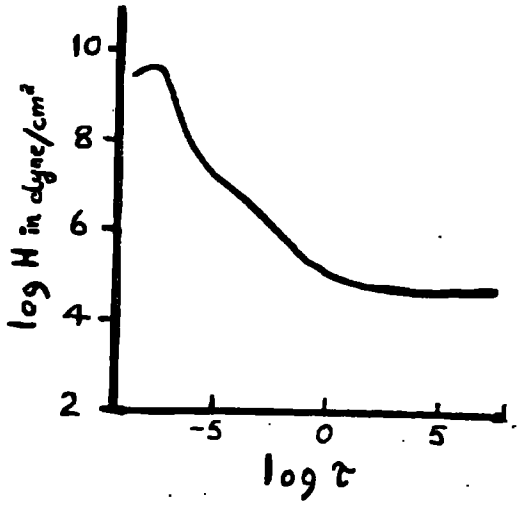

FIG 2·11

Relaxation Spectrum plotted logarithmically.

Lightly vulcanised NR at 25°C

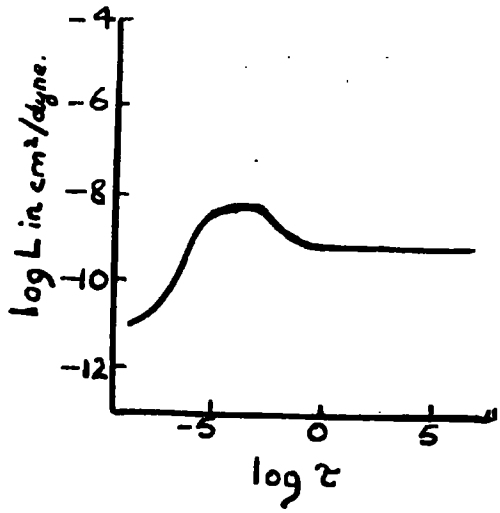

FIG 2·12

Retardation Spectrum plotted logarithmically

Lightly vulcanised NR at 25°C

maximum in log H represents a concentration of relaxation processes in a certain region of the logarithmic time scale. H attains quite a low value at long times but gives no indication of approaching any zero, showing that some degree of relaxation continues apparently indefinitely. Also H is finite at very short times indicating that some relaxation process occurs even at the shortest times.

2.4.8. The Retardation Spectrum.

In an entirely analogous manner, if the Voigt model in Fig 2.6b is made infinite in extent as in Fig 2.9, there results a continuous spectrum of retardation times, L, so :-

$$J(t) = J_\infty + \int_{-\infty}^{\infty} L(1-e^{-t/\tau}) \, d\ln\tau + t/\eta \qquad 2.12$$

J_∞ is instantaneous or glasslike shear compliance (shear compliance measured at very low temperatures or very high frequencies) Fig 2.12 plots the retardation spectrum of lightly vulcanised natural rubber and it is apparent that

some elastic compliance mechanisms persist beyond the longest times for which data is available. In this long time zone L is also relatively flat. The plateau zone in the spectrum H corresponds roughly to the maximum in the spectrum L.

2.5 EFFECTS OF TEMPERATURE AND FREQUENCY AND THEIR INTERRELATION.

The fundamental nature of rubber causes its deformation to be dependent on temperature as well as on the rate at which strain or stress is applied. When the temperature is reduced, the thermal motions of the molecules become slower, and since rubber-like deformation depends on these motions, the response to stress changes become more sluggish and the rubber appears stiffer, and the effective modulus increases. At a sufficiently low temperature, substantially no molecular motions can occur, behaviour then resembles that of a glass in which deformation is due to the straining of inter-atomic bonds; the deformation of inter-atomic bonds involves high forces and hence is associated with a very high modulus. If we analyse the

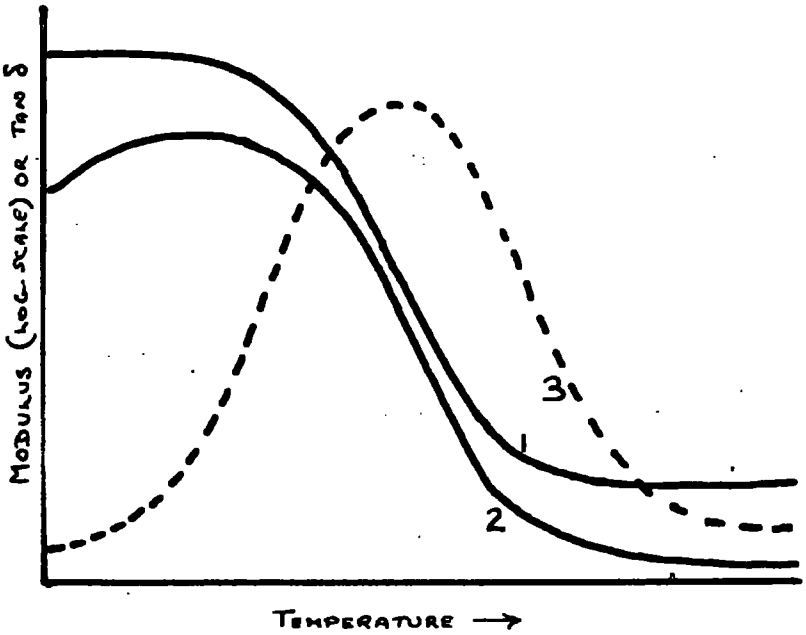

FIG 2·13. Temperature dependence of in-phase modulus component G' (cu
out-of-phase modulus component G'' (curve 2), and G''/G' or tan δ fu
(Not to scale).

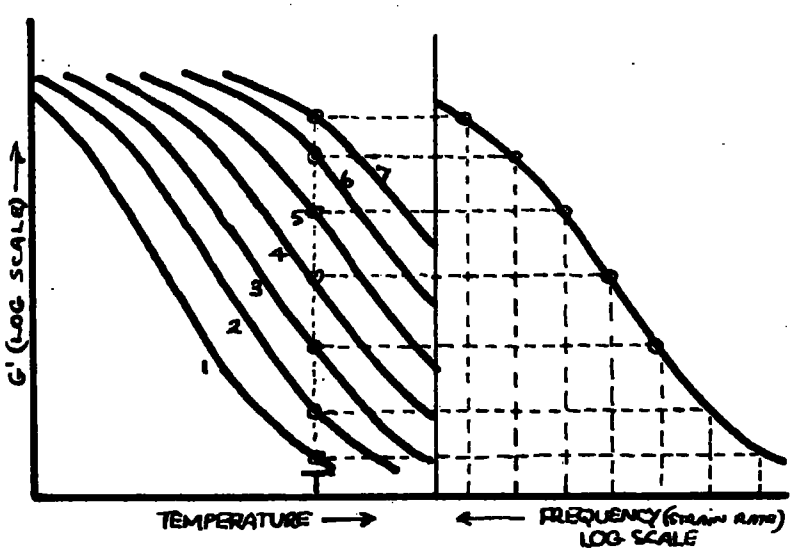

FIG 2·14. Construction of frequency/modulus (G') curve from a serie
temperature/modulus curves at different frequencies, curves 1 to 7 relate to
increasing frequencies (or strain rates).

effective or complex modulus G^* into its in-phase and out-of-phase components, we find the former (G') behaves much like G^*, giving the characteristic temperature variation shown diagrammatically by curve 1 in Fig. 2.13. The out-of-phase modulus G'' rises sooner (with lowered temperature) but falls again at very low temperatures (curve 2). The ratio G''/G' (or $\tan\delta$), therefore, passes through a maximum corresponding roughly to the middle of the rising part of the G' curve (see curve 3). Since G' and G'' vary over a range of 4 to 5 decades, they are generally plotted on logarithmic scales.

Figure 2.13 refers to tests at one fixed frequency. If this frequency is increased the curves move to the right (higher temperature), and if it is decreased, they move to the left. Thus for a series of frequencies we have for the in-phase modulus, G', a family of curves similar to curve 1 but spaced out along the temperature axis as in the left-hand half of Fig. 2.14. If now we select one temperature, T, the corresponding values of modulus plotted against frequency (or more

conveniently its logarithm) will form a curve broadly similar in shape to the temperature-modulus curve provided increase in frequency is plotted from right to left (right-hand half of Fig. 2.14).

A precisely analogous result follows, if we use the curve for the out-of-phase component G'' (curve 2 of Fig. 2.13.); and if we take G''/G' a peaked curve for G''/G' against log frequency will be obtained, similar to curve 3 in Fig. 2.13.

2.5.1 Method of Reduced Variables.

Ferry and Fitzgerald (1953) have developed a method of transforming the temperature and frequency scales, so that the observed values of a given property such as elastic modulus or dielectric constant can be brought on to a single curve covering a very wide range of temperature and frequency. This transformation of the data involves two stages.

Stage 1: Density and Kinetic Theory Changes

This stage arises because (i) rubber alters in density with change of temperature, (ii) the true elastic modulus is proportional to the absolute

temperature, as required by the kinetic theory of rubber elasticity. It is therefore necessary, from the observed modulus values at temperature T, to calculate 'reduced' values corresponding to a reference temperature T_o as follows:

In-Phase Component. From the mathematical point of view it is convenient to consider the compliance (inverse of modulus), since this is the sum of the true rubber-like ('storage') compliance and a very small compliance J_∞ corresponding to the limiting deformation in the glassy state; then the reduced compliance J'_r is given by:-

$$J'_r = (J'-J_\infty)\ (T\rho/T_o\rho_o) + J_\infty \qquad 2.13$$

where ρ and ρ_o, density at T and T_o respectively (note that these temperatures are all expressed on the absolute scale).

Since at the usual operating temperatures the J_∞ term is very small compared with the value of J', it can for practical purposes be ignored, thus enabling the relationship to be expressed directly in terms of

modulus:

$$G_r' = G' T_0 \rho_0 / T \rho \qquad 2.14$$

Out-of-Phase Component:—

$$G_r'' = G'' T_0 \rho_0 / T \rho \qquad 2.15$$

Complex modulus:—

Since $|G^*| = \sqrt{(G_r'^2 + G_r''^2)}$, we can (again neglecting J_∞) express the reduced complex modulus as

$$G_r^* = G^* T_0 \rho_0 / T \rho \qquad 2.16$$

Stage 2: Transformation Along Frequency Scale.

If now the values of the reduced in-phase modulus G_r' (from equation 2.3.20) are plotted against frequency for a series of temperatures, a family of curves similar to that in the right-hand half of Fig. 2.14 is obtained. If these curves are moved parallel to the frequency axis, it is found that they will all coincide and form a single curve of modulus against frequency.

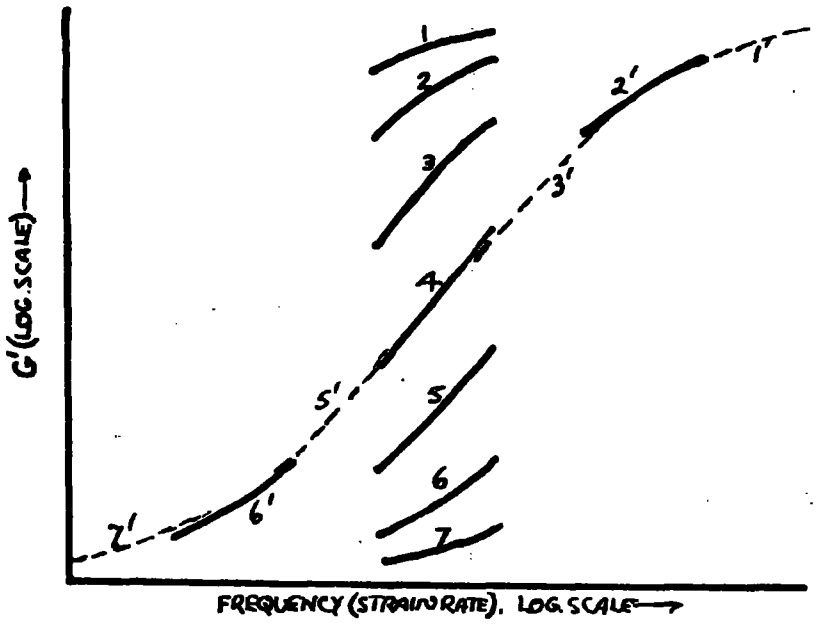

FIG 2·15. Construction of composite frequency/modulus (G') curve 1'–7' from short portions of curves obtained at different temperatures; Curves 1–7 relate to increasing temperatures, that for curve 4 being the 'reference temperature' T_0

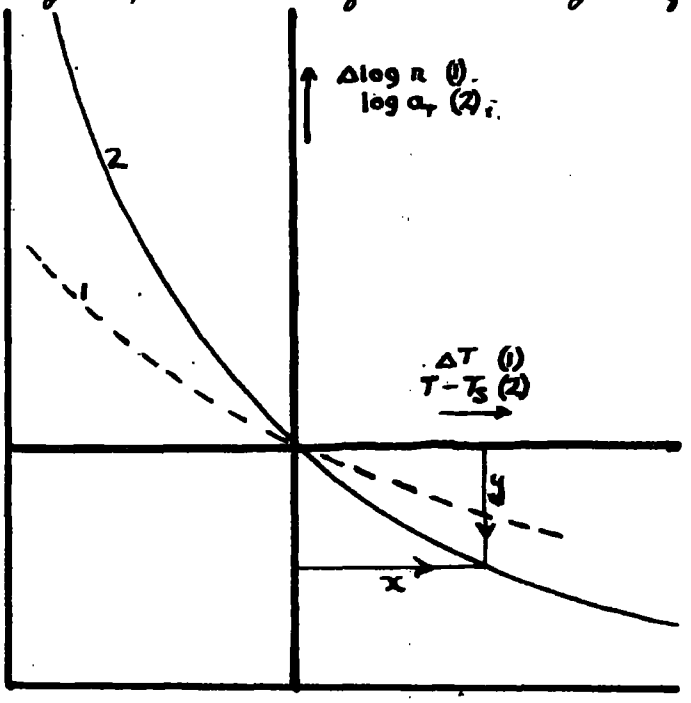

FIG 2·16. Relation between temperature difference, ΔT or $(T-T_S)$, and the corresponding log frequency difference, $\Delta \log R$ or $\log a_T$; 1 = experimental curve; 2 = master curve, equation 2·19.

In practice, of course, it may well happen that only short portions of each curve are available, because there may be only a limited range of test frequencies, but these short portions will be found to merge together into a smooth curve as shown in Fig. 2.15.

The practical importance of this result lies in the fact that, if the available frequency range is limited, as is often the case with the simpler types of test equipment used for technological purposes provided tests can be made at various temperatures, it is possible to predict the effect of a much wider range of frequencies than that available experimentally.

This is in itself an important simplification in obtaining data on the frequency dependence of the mechanical and dielectric behaviour of rubbers. However, there is a further step that makes it unnecessary in many cases even to obtain the full composite curves from observations at a range of temperatures as in Fig. 2.14. This comes about in the following way;

If in Fig. 2.15. we select one curve, say number 4, as a reference curve and denote its temperature by T_0

it is clear, that for each of the other curves there is a known difference of temperature from the reference curve and a corresponding frequency change needed to make the curve fit into place on the composite curve. We now write:

$$\text{Temperature difference} = \Delta T = T - T_0 \qquad 2.17$$

$$\text{frequency shift (on log scale)} = \Delta \log n = \log n_0 - \log n \qquad 2.18$$

such that the property measured has the same value at frequency n_0 and temperature T_0 as at n and T (note particularly that in equation 2.17 the reference value T_0 has a negative sign whereas in 2.18, $\log n_0$ is positive).

When ΔT and $\Delta \log n$ for curves 1,2,3,5,6,7 are plotted against each other they give a curve of the shape shown in Fig. 2.16. curve 1. When such curves are obtained for a variety of rubbers (or for that matter many other deformable materials such as amorphous plastics) it is found that all these curves are of the same shape but displaced at various distances along the axes, and so can all be made to coincide with a single

master curve by suitable shifting along the axes.

The master curve has been expressed by the following equation:-

$$\log a_T = -8.86 (T-T_s) / (101.6 + T-T_s) \qquad 2.19$$

where T_s is a characteristic temperature of the material under examination and a_T is the ratio between the frequencies at T_s and T respectively at which the property measured has the same value (a_T was originally defined as the ratio of relaxation time at T and T_s respectively, but since frequency is the inverse of relaxation time, this is identical with the definition just given). This equation is now well known as the WLF equation (The Williams, Landel and Ferry equation) and will be referred to assuch in the rest of this Thesis.

T_s is about 46°C ($\pm$ 5°C) above the so-called 'glass transition temperature' where the rubber assumes a glassy state. It is possible in view of this relationship to use T_g instead of T_s so that equation 2.19 becomes:-

$$\log a_T = -16.2(T-T_g)/(55.6 + T - T_g) \qquad 2.20$$

This latter equation possesses the advantage of avoiding

the use of the rather arbitrary T_s temperature*

To make the experimental curve 1 in Fig. 2.15. coincide with the master curve 2 we have to move the former along the ΔT axis by an amount x and along the $\Delta \log n$ axis by an amount y.

Hence $$\Delta T = (T - T_s) - x \qquad 2.21$$

$$\Delta \log n = \log a_T - y \qquad 2.22$$

x and y, of course, have no absolute significance, since they depend on the particular curve in Fig. 2.14. chosen as the reference curve. If this reference curve happened to be that for the characteristic temperature T_s, x and y would both be zero. Now when T equals T_o, ΔT is zero and hence 2.20 gives

$$T_s = T_o - x \qquad 2.23$$

This enables the characteristic temperature to be determined, since T_o is known and x is found experimentally.

An alternative calculation of T_s is derived from

*A short description of glass transition temperature is given in Appendix 5.2.

equation 2.22 which gives:

$$y = -8.86\,(T_o - T_s)/(101.6 + T_o - T_s) \qquad 2.24$$

The two values of T_s should, of course, agree (since theoretically $y = -8.86x/(101.6 + x)$) and the closeness of agreement will be a check on the accuracy of the experimental data and the curve fitting.

The principle of superposition of property/frequency curves illustrated in Fig. 2.15. has been found to apply over ranges as great as 20 decades of frequency or time and over a temperature range of about $T_s \pm 50^{\circ}C$.

(Further information on this principle will be found in: Andrews,(1952); Davey and Payne (1965), Ferry, Fitzgerald, Grandine, and Williams,(1952); Ferry, Grandine and Fitzgerald,(1953); Fletcher and Gent; (1957); Hutton and Nolle,(1954); Leaderman,(1943); Marvin,(1952); Payne (1957, 1958, 1959a); Payne and Scott (1960), Philippoff, (1953, 1954); Schmieder and Wolf,(1953); Tobolsky and Andrews (1945); Tobolsky (1956), Williams, Landel and Ferry (1955).

An additional note on the time or frequency--temperature superposition principle appears in the

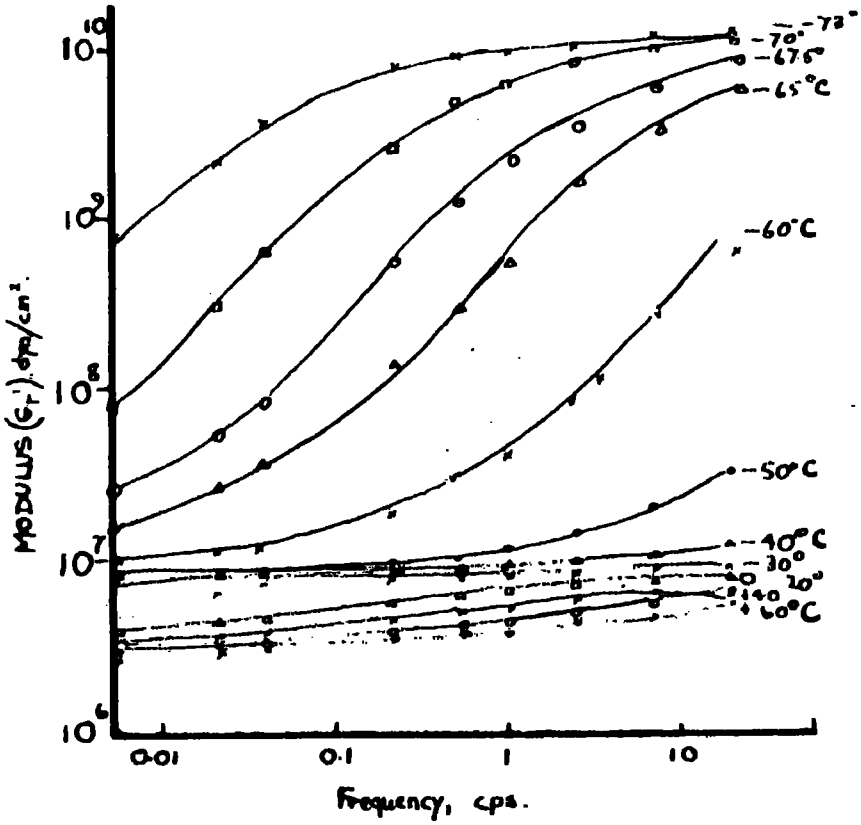

FIG 2·17a Reduced in-phase modulus (G_r') for unvulcanised natural rubber — frequency curve (Payne, '65

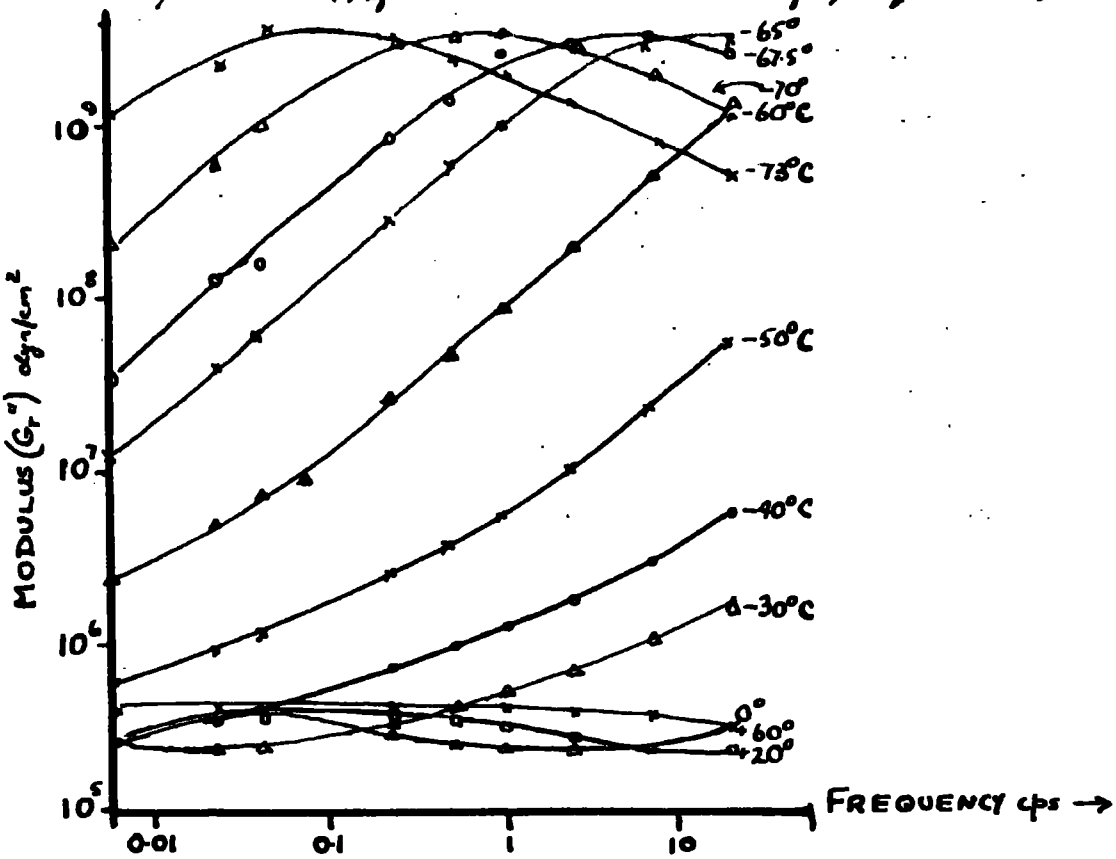

FIG 2·17b. Reduced out-of-phase modulus (G_r'') for unvulcanised natural rubber — frequency

Appendix 5.1 to this Thesis.

The implication of the equation 2.20 relating the temperature frequency equivalence to the glass transition of the polymer is given as a note at the end of this Thesis, Appendix 5.2, where it is shown that the constants in equation 2.20 can be related to the change in the free volume in the polymer below and above the glass transition temperature.

2.5.2 Experimental Results

To illustrate the general principles discussed above, some data obtained with the RAPRA sinusoidal strain machine (Payne and Scott, 1960) will now be given and discussed.

Unvulcanised Natural Rubber

Figs. 2.17a and 2.17b show respectively the values of G_r' and G_r'', that is, the in-phase and out-of-phase components of shear modulus reduced to a reference temperature (T_o) of 25°C by equation 2.14 and 2.15. The value found for the limiting or glassy state compliance, was 8×10^{-11} cm^2/dyne, corresponding to a modulus of 1.25×10^{10} dynes/cm^2 or 1.8×10^5 lb/in^2.

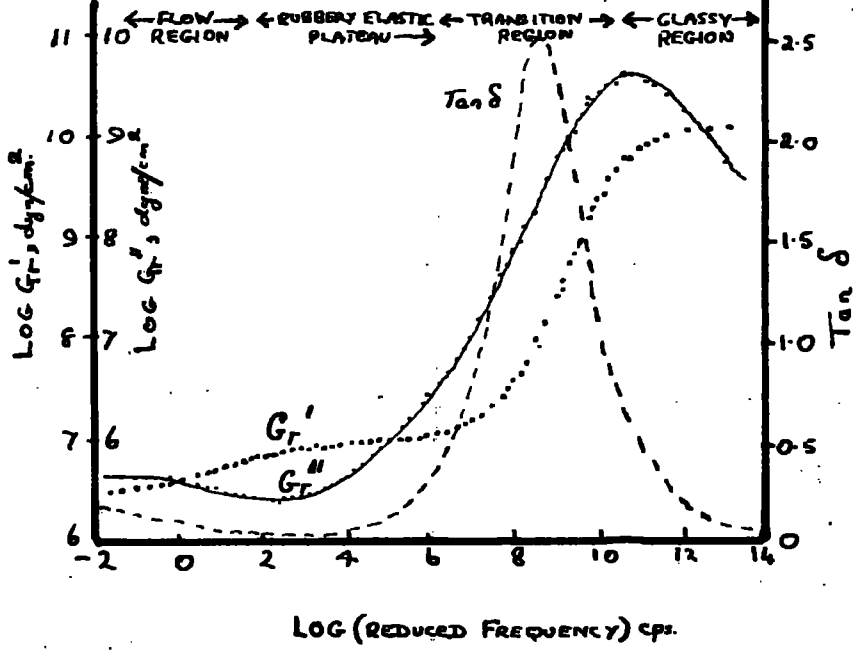

FIG 2·18. Composite curves for variation of reduced moduli (G_r' and G_r'') and tan δ - (G_r''/G_r') for an unvulcanised natural rubber over a wide frequency range; temperature 25°C. Dots represent results from -73° to + 60°C. (c.f. Figs. 2·17a and b)

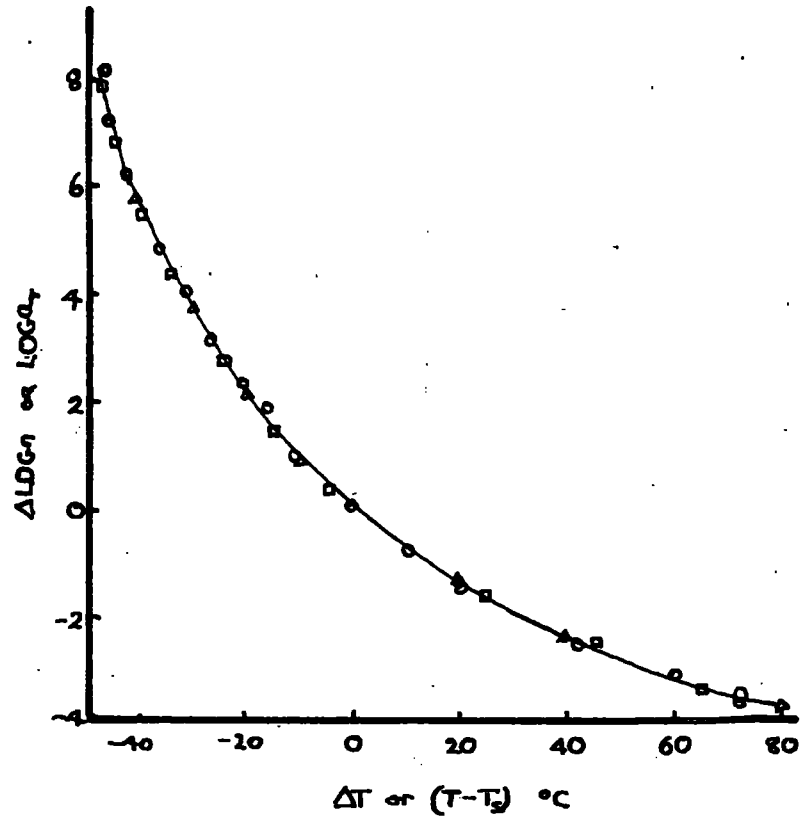

FIG 2·19. Experimental values of temperature difference (ΔT) and log frequency shift ($\Delta \log \eta$) compared with master curve of log a_T versus $(T-T_s)$, for natural rubber. □ - Unvulcanised

Fig. 2.18 gives the composite curves obtained by transposing along the log frequency axis. It is clear from the close fit of the points on the curve that the superposition of the constituent curves can be made with little ambiguity.

When the log frequency shifts required for this superposition were plotted against the corresponding temperature differences, the resulting curve could be closely superimposed on the master curve given by equation 2.3.25 by using an appropriate value of T_s namely, 248°K (-25°C). Fig. 2.19 shows the theoretical master curve with the experimental values from the modulus curves in Figs. 2.17a and 2.17b, and other data.

An important finding from these experiments was that the frequency shifts required were the same for both the in-phase and out-of-phase modulus components, so that the same value of T_s applies to both; this would indeed be expected theoretically since the frequency shifts correspond to the temperature dependence of the molecular relaxation times.

Figs 2.20 and 2.21 show the composite G_r' and G_r'' curves for the following:

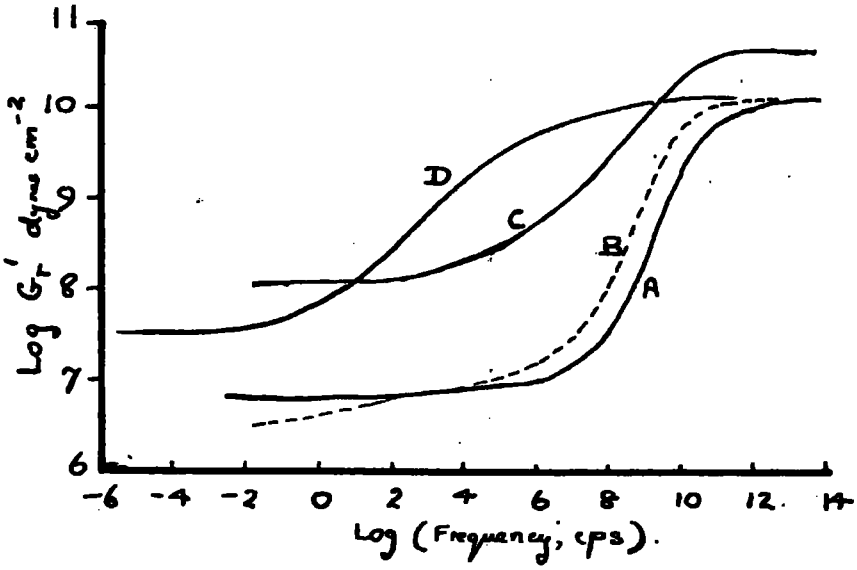

FIG 2·20 *Composite plot of reduced in-phase modulus (G_r') against frequency for natural rubber: A, unvulcanized; B, soft vulcanizate without filler; C, vulcanizate containing carbon black; D, highly vulcanizate (ebonite). Temperature: A, B, C: 25°C; D; 60°C. After Payne (1958).*

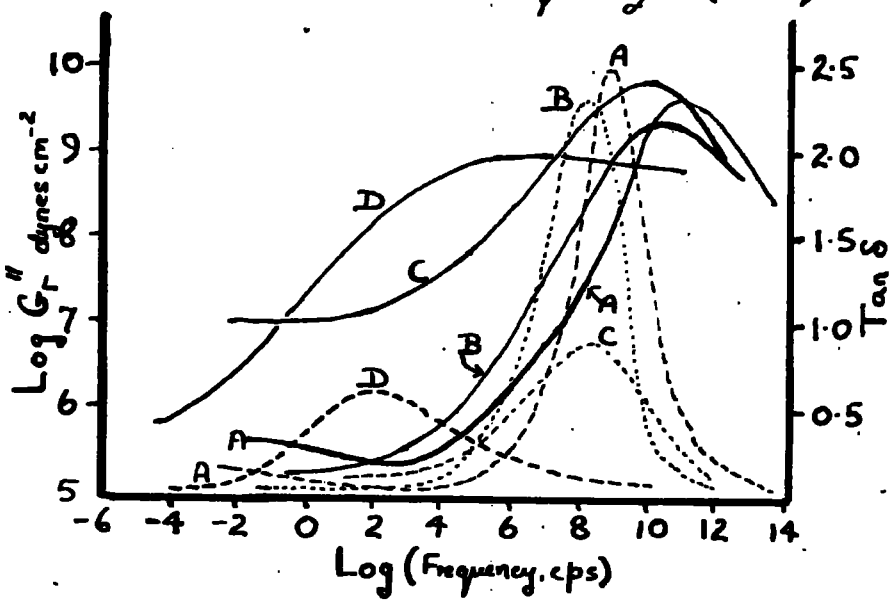

Fig 2·21. *Composite curves of reduced out-of-phase modulus (G_r'') and tan δ against frequency for natural rubber: A, unvulcanized; B, soft vulcanizate without filler; C, vulcanizate containing carbon black; D, highly vulcanized (ebonite). Temperature: A, B, C; 25°C; D: 60°C. After Payne (1958).*

A. Unvulcanised natural rubber.

B. Lightly vulcanised rubber without filler.

C. Rubber containing 50 parts per 100 of carbon black (HAF).

D. Ebonite, that is, very fully vulcanised rubber.

Curves A, B, C are for a temperature of 298°K and curve D for 333°K. It will be noticed that these curves cover 16 decades of frequency, a much wider range than the actual experimental results (3 decades), thus showing the value of the temperature/frequency inter-relation principle in deducing data far outside the range of conditions obtainable by direct experiment.

The relevant data for these four rubbers are shown in Table 2.1

TABLE 2.1

PARAMETERS OF GENERALISED MODULUS/FREQUENCY CURVES FOR NATURAL RUBBER.

Rubber	T_s		J_∞	G' (= G^* approx.), lb/in^2	
	^{0}K	^{0}C	Cm^2/dyne	Elastic region	Glassy region
Unvulcanised	248	-25	8×10^{-11}	c.90	1.8×10^3
Lightly vulcanised	251	-22	8×10^{-11}	90	1.8×10^5
Vulcanised, compounded with carbon black	255	-20	2.5×10^{-11}	1600	5.5×10^5
Ebonite	360	+87	8×10^{-11}	450	1.8×10^5

The G_r' curves in Fig 2.20 all show the three well defined regions strated by Fig. 2.18.

A high plateau at the high frequency end (glassy region).

A steeply rising central portion (transition region)

A lower plateau in the low frequency range (rubbery or elastic region).

The G_r'' curves of Fig. 2.21 likewise show a

central steeply rising region but with a final decrease at the highest frequencies.

At the right-hand or high frequency end of the curves in Figures 2.20 and 2.21 all the materials exhibit behaviour characteristic of the glassy state because the frequency of stress variation is so great that no rubber--like deformation has time to occur. In this region, therefore, deformation is governed by the binding forces between neighbouring atoms, and the modulus for all the four types of rubber is seen to be in the neighbourhood of 1.4×10^{10} dynes/cm^2 and practically independent of frequency or temperature. In this region the loss factor (G_r''/G_r') is relatively small (about 0.1) and decreases with increasing frequency.

In the central region, moving towards the left, the material is passing out of the glassy state as the slower stress variations allow the molecular chain segments of the rubber increasing freedom to move, and finally permit complete mobility. The rubber thus passes through a semi-rigid or leathery condition in which the modulus has intermediate values and the loss factor passes

through a maximum as shown in Fig. 2.21.

Finally, in the low frequency plateau on the left, the material is essentially rubber-like, showing a low modulus and small loss factor, indicating rapid and free response to stress variations. It must be noted that the ebonite curve D relates to a temperture of 60°C, at which the material is no longer rigid but shows more rubber-like behaviour.

The final decrease towards the left shown by the unvulcanised rubber curve A represents a fourth region characteristic of materials in which the absence of cross-links permits flow to occur ('flow region' of Fig. 2.18).

In the above description we have considered the effect of decreasing frequency, that is, moving from right to left in the Figure ; it will be understood that the same sequence of changes would be produced by keeping the frequency the same and raising the temperature.

2.6 DEPENDENCE OF TEMPERATURE/FREQUENCY BEHAVIOUR ON THE NATURE OF THE RUBBER, THE FILLERS, THE PLASTICISERS AND ON THE VULCANISATION SYSTEM.

The above results serve essentially to illustrate how the frequency-temperature superposition relationship has been applied in the case of natural rubber to obtain master curves for the in-phase and out-of-phase modulus components over a very wide frequency range. We must now consider how these master curves can be used to illustrate how the mechanical behaviour depends on the nature of the basic polymer, on the effects of vulcanisation and of added materials such as fillers and plasticisers.

2.6.1 Nature of Polymer

The most important effect of varying the nature of the polymer is to move the modulus/frequency (or modulus/temperature) master curves parallel to the frequency (or temperature) axis. The curves move towards lower frequency or higher temperature, as the polymers become more polar (a polar substance is one whose molecules contain atom groups that are electrically unsymmetrical, having positive and negative poles); thus among the common

types of rubber the polarity increases in the order: Natural rubber and butyl rubber, butadiene-styrene rubber (GR-S or SBR), neoprene, nitrile rubber, while polyvinyl chloride is much more polar than any of these.

2.6.2 Fillers, Plasticisers and Vulcanisation.

The influence of vulcanisation and compounding can be manifested in two ways (i) a bodily movement of the master curve of modulus or tan δ against temperature or frequency along the temperature or frequency axis, (ii) changes in the shape of the curve, representing increases or decreases in the modulus or tan δ in the various regions of the curve.

Considering first the movement of the curve along the temperature or frequency axis, the directions of this movement are as follows:

Vulcanisation:	Towards lower frequency or higher temperature.
Plasticisers:	Towards higher frequency or lower temperature.
Fillers:	Substantially no effect.

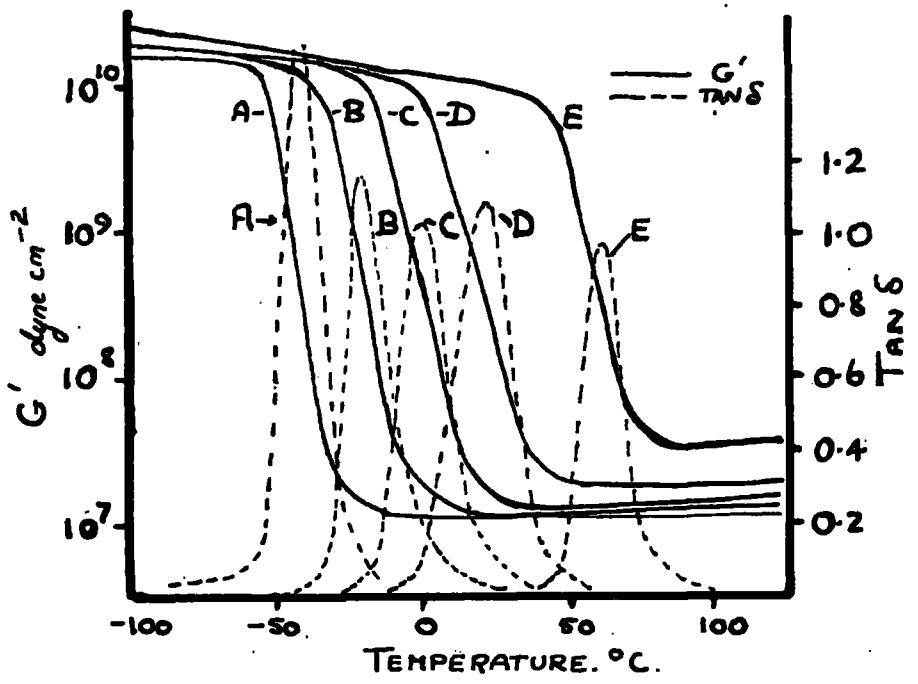

FIG 2·22 Effect of amount of combined sulphur on temperature variation of modulus (G') and tan δ. A, 5%; B, 10%; C, 15%; D, 20%; E, 30% sulphur calculated on raw rubber (Data from Schnieder and Wolf, 1953)

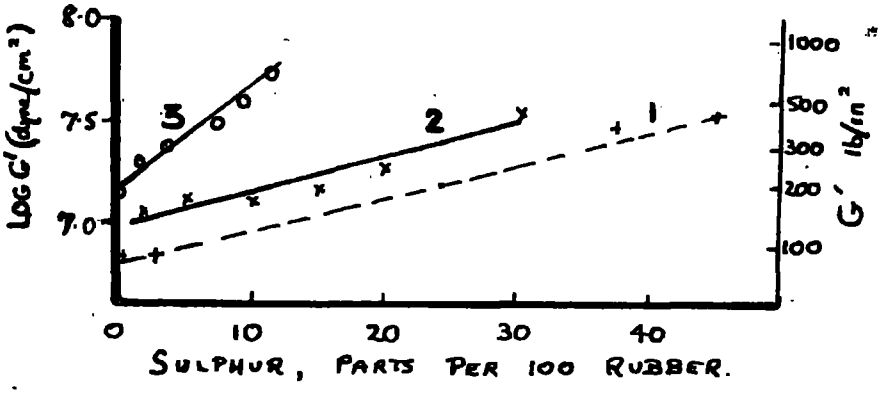

FIG 2·23 Effect of combined sulphur on in-plane modulus (G'). Curve 1: natural rubber (data from Table 2·1); 2: natural rubber (Schnieder and Wolf, 1953) 3: butadiene-styrene rubber (Payne 1959).

The temperature shifts can also be considered as changes in the characteristic temperature T_s; thus vulcanisation increases while plasticiser decreases the value of T_s.

Comparison of the curves in Fig 2.20 for rubber, unvulcanised (A), vulcanised to the soft stage (B), and vulcanised to ebonite (D) illustrates the effect of varying degrees of vulcanisation. Fuller data, in the form of property/temperature curves, are given in Fig. 2.22; from these and other data it may be estimated that for each 1% of combined sulphur (calculated on the rubber content) the curve is moved, that is, T_s is raised about 2.5°C for natural rubber or 3.2°C for a styrene butadiene rubber (Payne 1958b). This effect of vulcanisation is really the same as that of increasing polarity described above, since the sulphur atoms introduced by vulcanisation render the material more polar.

It is not possible to give any fixed quantitative value for the effect of a plasticiser since this will depend on the nature of the plasticiser used. The T_g values for plasticised natural and butadiene styrene

rubbers show T_g to be lowered by some 15^o to 20^o by 20 and 40 parts (per 100 rubber) respectively of plasticiser. (DOP = dioctyl phthalate)

The effects of vulcanisation and compounding on the shape of the property versus frequency (or temperature) curve are summarised in Table 2.2 in terms of the two components of the complex modulus and their ratio tan δ. It has been found convenient to distinguish between the effects in the rubbery and glassy regions of the complete curve in Figure 2.18 since these represent entirely different states of the material. Table 2.2 includes references to Figures illustrating the effects noted.

TABLE 2.2

SUMMARY OF EFFECTS OF VULCANISATION AND COMPOUNDING ON DYNAMIC PROPERTIES.

erty	Region	Vulcanisation	Plasticiser	Filler
hase lus or E')	rubbery	Increase 'plateau' lengthened Fig. 2.20 A, B & D Fig. 2.22	Decrease	Large increase; 'plateau' lengthened Fig. 2.20C
	glassy	Little effect Fig. 2.22	Slight decrease	Increase Fig. 2.20C
of-phase us or E''	rubbery	Increase Fig. 2.20 A & B	Increase	Increase Fig. 2.20C
	glassy	Little effect	Increase	Increase Fig. 2.20C
= 1/Q x. Φ	rubbery	increase	Decrease	Increase
	glassy	Decrease	Decrease	Increase
	transition	Peak lowered and broadened Fig. 2.22	Peak lowered and broadened (at high plasticiser content peak may be raised again)	Peak lowered and broadened

is the peak (maximum) transmissibility, a quantity sometimes used by ngineers in place of tan δ. See Davey and Payne (1965) for lternative definitions.

This table can only present results in broad outline, and must of cessity omit many important details; thus, according to de Meij and n Amerongen (1956) tan δ for a pure gum vulcanisate may be two or ree times as great if an organic sulphide (tetramethylthiuram sulphide) is used as the vulcanising agent instead of sulphur. This pect of the dynamic behaviour of natural rubber vulcanisates is to be scussed in greater detail later in this Thesis.

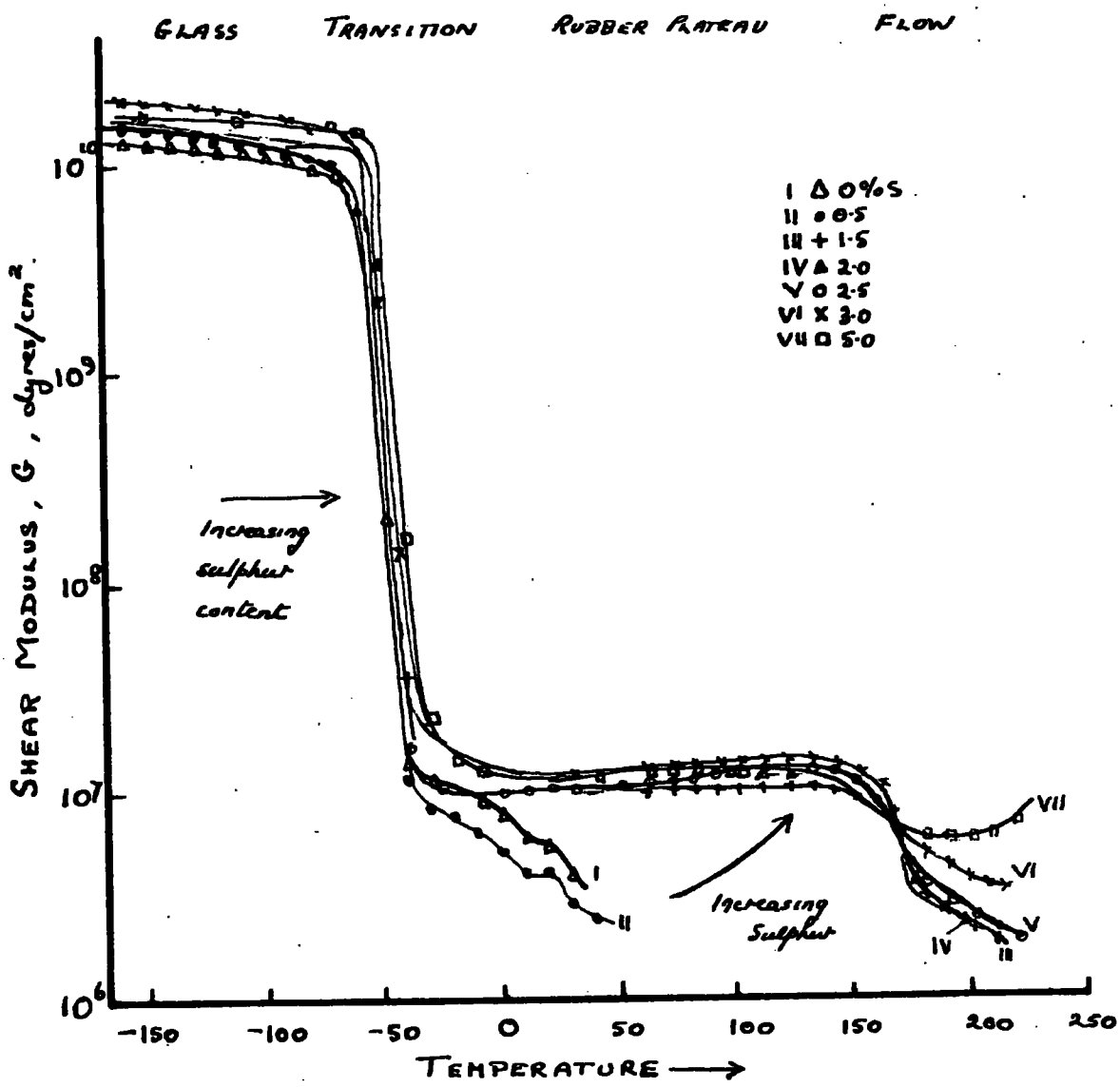

FIG 2·24. Shear modulus - temperature function for natural rubber with increasing sulphur content (Schmieder and Wolf). Frequency of test, 1·5 – 2·0 cycles per second.

The increase in rubbery modulus produced by vulcanisation is due to the introduction of cross-links additional to the pseudo crosslinks provided by the molecular entanglements in the unvulcanised polymer. In normal soft vulcanised rubber, containing say 2 to 3% combined sulphur, the effect of this sulphur level on modulus is relatively small but in a highly cross-linked ebonite containing 20 to 30% sulphur the increase in modulus is considerable (compare curves A and D in Fig. 2.20; see also Fig. 2.23. Note particularly that in these Figures the ebonite is not in the normal hard state with which we are familiar but in the relatively soft rubbery state into which it passes at high temperatures). Even greater increases in the rubber modulus can be produced by compounding with fillers especially carbon black, as is shown by curve C in Fig. 2.20.

2.7 EFFECT OF DIFFERENT TYPES OF CROSS-LINKING

Following on from the observation of de Meij and van Amerongen (1956) that tan δ in the rubbery plateau region for a pure gum vulcanisate may be two or three

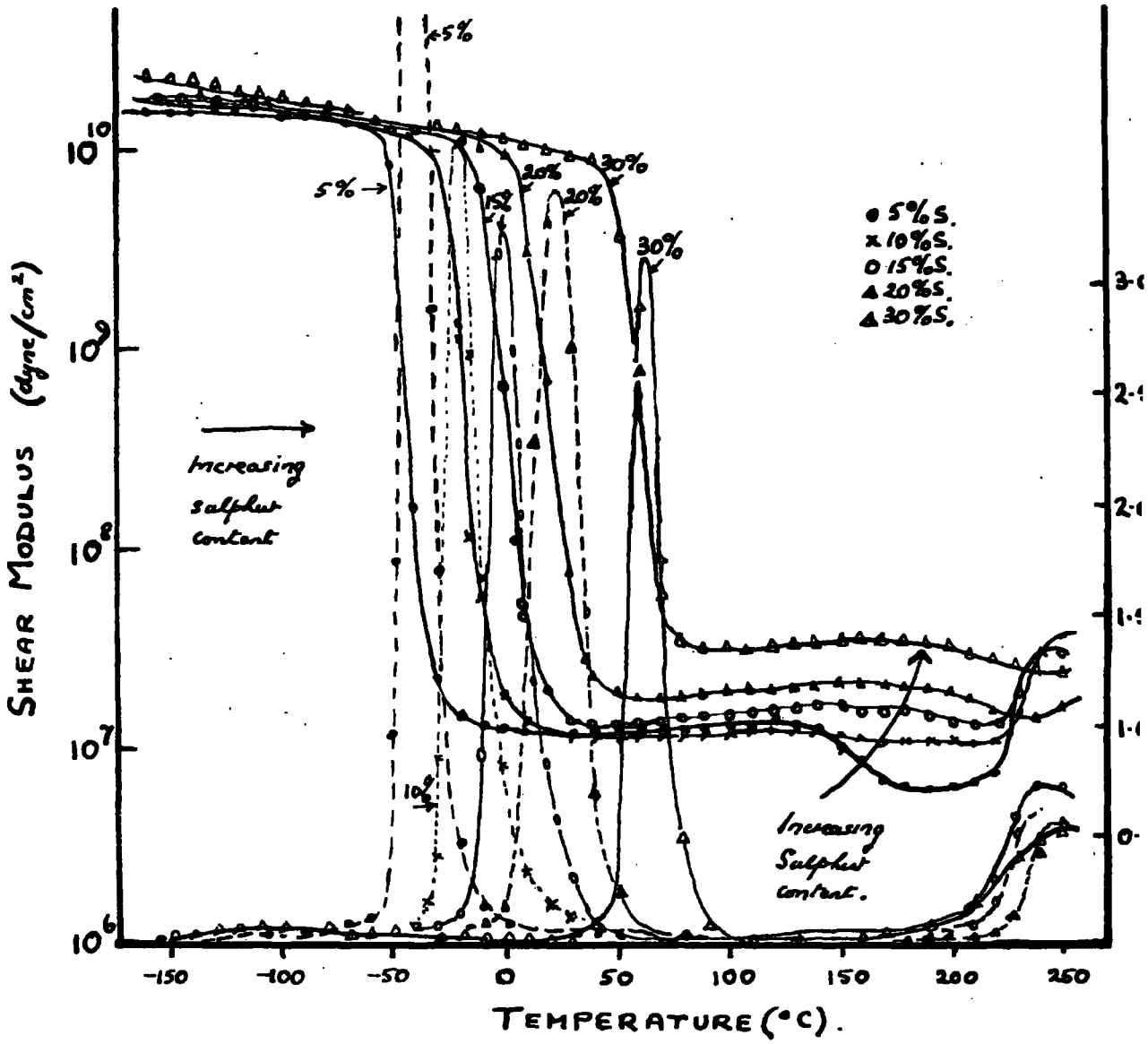

FIG 2·25. Shear modulus and damping decrement - temperature function with increasing amounts of sulphur content (Schmieder and Wolf).

times as great if an organic sulphide (tetramethylthiuram disulphide) is used as the vulcanising agent instead of sulphur. Heinze, Schmeider, Schnell and Wolf (1961) carried out dynamic measurements over a wide temperature range but at a single frequency of test on natural rubber compounds vulcanised by varying amounts of :-

a. Sulphur

b. Dicumyl peroxide

c. Irradiation

Figures 2.24 and 2.25 plot the results for the sulphur vulcanisates, and it can be seen that the transition region changes to higher temperatures, this change being particularly noticeable for sulphur contents about 5%. On the other hand, vulcanisation by dicumyl peroxide hardly alters the transition temperatures, even up to a concentration of curative of 35% or more of dicumyl peroxide. Fig 2.26. Similarly, increased radiation dosage hardly alters the transition, even though the radiation dosage was sufficient to raise the shear modulus value in the rubbery elastic plateau region to levels comparable to that obtained with 30% sulphur. A

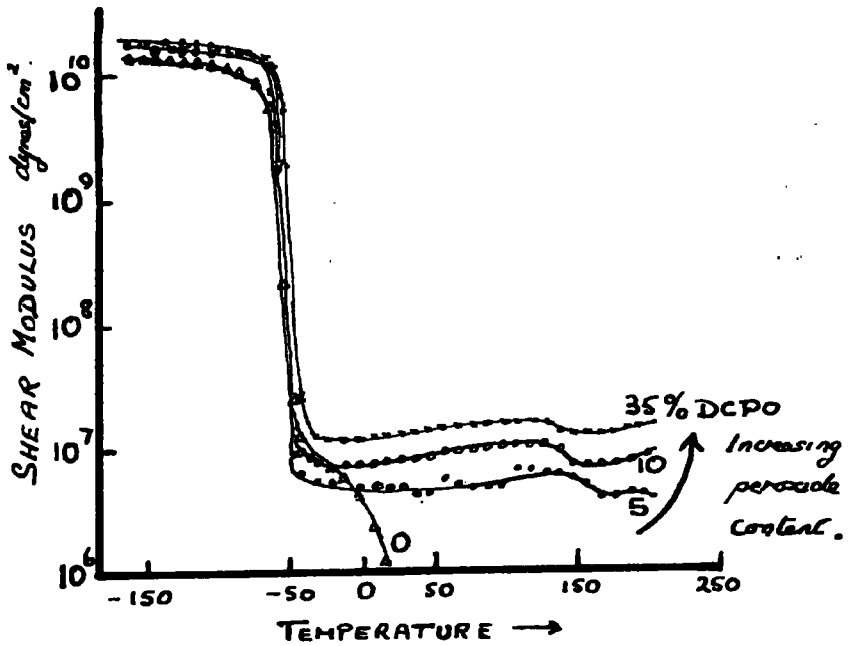

FIG 2·26. Shear modulus, G, of dicumyl peroxide cured natural rubber as a function of temperature. (Heinze, Schmieder, Schell and We 1961).

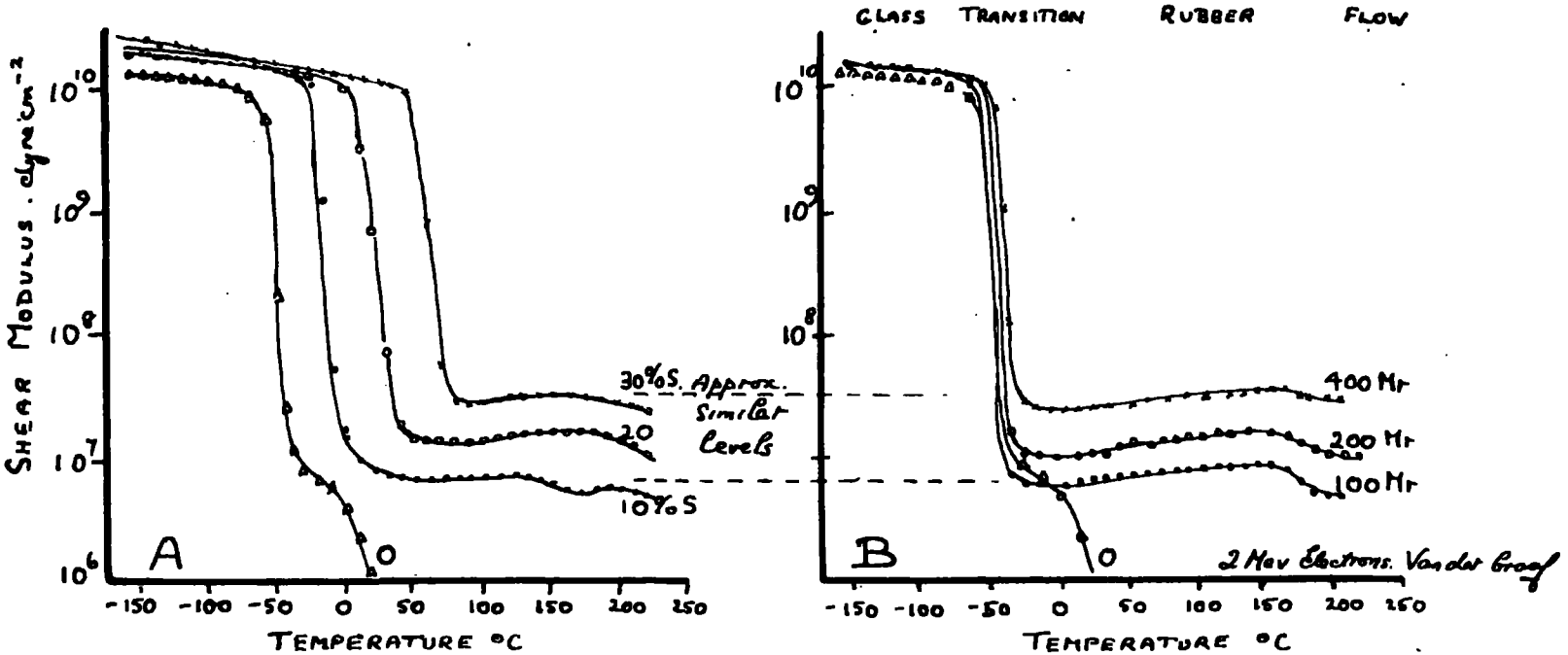

FIG 2·27. A: Natural rubber – varying sulphur content versus temperature.

B: Natural rubber – varying radiation dosage versus temperature.

(Heinze, Salmieder and Wolf, 1961).

comparison of the radiation vulcanisates with the sulphur vulcanisates is given in Fig. 2.27.

Stratton and Ferry (1964) remark on the fact that there is a need for more specific information on two particular points :-

1. The reason for the presence of very slow relaxation mechanisms reflected by an extremely slow approach to elastic equilibrium. Thirion and Chasset (1962), Gent (1962).

2. The presence of elastic loss in periodic deformations at low frequencies, Payne (1958 a and b)

In order to study these observations further, some experiments were carried out using natural rubber crosslinked with sulphur, tetramethylthiuram disulphide, dicumyl peroxide and high energy radiation as the cross linking agents. Table 2.3 is a summary of the composition and properties of the vulcanisates they studied.

TABLE 2.3

COMPOSITION AND PROPERTIES OF VULCANIZATES STUDIED BY FERRY AND STRATTON (1964).

Sulphur vulcanizates (all with 5 parts ZnO, 1 part phenylcyclohexyl-p-phenylenediamine, and 1 part stearic acid)

No.	1	2	3
Hevea rubber[a] (Natural rubber)	100	100	100
% S	3.25	3	4
Mercaptobenzothiazole	...	...	0.5
Diphenyl guanidine	1.25	...	1
Benzthiazylcyclohexyl sulfenamide	...	1	...
Time of vulcanization, min. at 140°	60	40	15
Density, g./cc.	0.969	0.965	0.973
$M_o \times 10^{-3}$, from J_o	4.7	4.3	3.2

Nonsulfur vulcanizates

No.	4[b]	5[c]	6
Hevea rubber[a] (Natural rubber)	100	100	100
Tetramethylthiuram disulfide	...	3	...
Dicumyl peroxide	...	...	3
Time of vulcanization, min. at 140°	...	40	50
Density, g./cc.	0.913	0.963	0.912
$M_o \times 10^{-3}$, from J_o	7.4	6.4	8.9

[a]Smoked sheet except No. 4, which is crepe. [b]Irradiated with γ-radiation. [c]Contains also 5 parts ZnO, 0.5 part phenylcyclohexyl-p-phenylene diamine, and 1 part stearic acid.

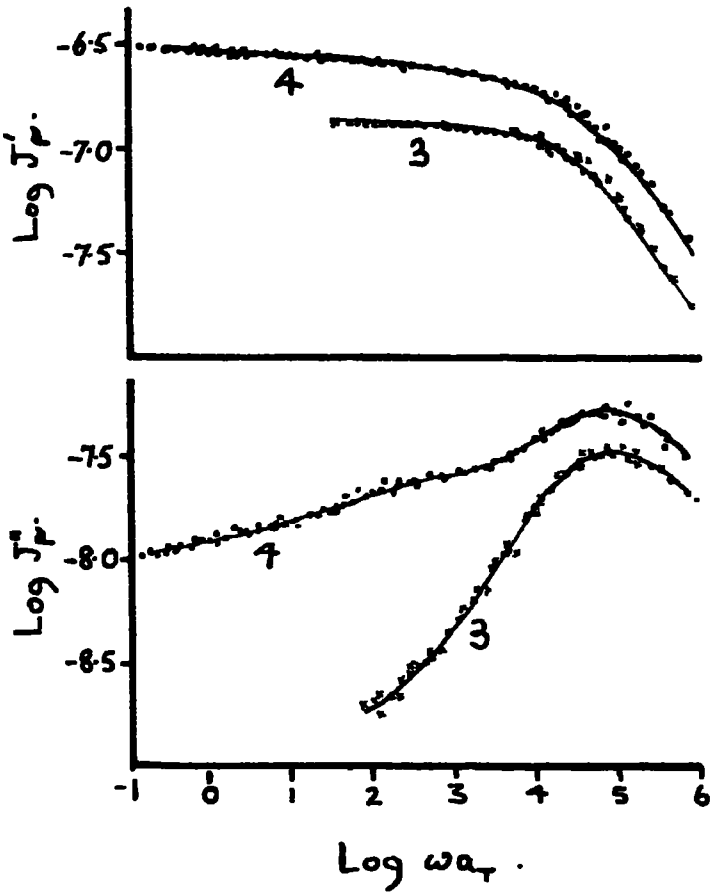

FIG 2·28. Storage and loss compliance reduced to 25° and plotted logarithmically against reduced radian frequency for sample 3 (cross-linked wi sulphur) and sample 4 (cross-linked with γ-radiation). After Ferry and Stratton Master curves derived from data obtained between −10 and +55°C.

In Fig. 2.28 log J_r' and log J_r'' are plotted against log ωa_T for samples 3 and 4. (See Tables 2.3 for details of vulcanisate composition). In each sample J' drops and J'' passes through a maximum with increasing frequency as expected, when the transition zone is entered. At low frequencies, however, there is a striking difference between the two samples. For sample 3, the rubber crosslinked with sulphur, J'' drops rapidly with decreasing frequency and J' becomes almost frequency independent. For sample 4, the rubber crosslinked by radiation, J'' persists with a substantial magnitude at the lowest frequencies measured, and J' continues to rise with decreasing frequency. The results for the other sulphur vulcanisates (samples 1 and 2) resemble those of sample 3, whereas those for the other non sulphur vulcanisates resemble those for sample 4. These observations will be discussed later in this Thesis.

2.8 DISTRIBUTION OF RELAXATION AND RETARDATION TIMES:- METHODS OF DERIVING DISTRIBUTION FUNCTIONS

The distribution of relaxation or retardation times can be obtained from either the G' or G'' or tan δ master curves. If the experimental data are accurate, the same

distributions should be obtained from two or more master curves relating the property to log ω such as G' and G'', or the related J', J'', or J' and tan δ master curves or any combination thereof.

It is not intended to discuss here in any great detail either the exact or the approximation methods of deriving the relaxation or retardation spectra from experimental functions, but only to note the most useful ones. In particular, we will note those used to derive the spectra which are discussed later in this Thesis. The attention of the reader is drawn to the fact that considerable effort has been made by many investigators to develop methods of graphically or numerically deriving the distributions from experimental results.

2.8.1 Relaxation Spectrum from the Storage Modulus, G'

The method of Ferry and Williams (1952) provides two formulae, depending on whether m, the negative slope of H, the relaxation spectrum, on a double logarithmic plot of H versus τ is greater or less than 1. Almost invariably m<1 in which case:-

$$H(\tau) = AG' \alpha(\log G') / \alpha(\log \omega) \Big|_{\frac{1}{\omega} = \tau}$$

where $A = (2 - m)/2\,\Gamma(2 - \frac{m}{2})\,\Gamma(1 - \frac{m}{2})$. If on the other hand $1 < m < 2$, the corresponding formula is

$$H(\tau) = A'G'\left(2 - d \log G'/d \log \omega\right)\Big|_{\frac{1}{\omega} = \tau} \qquad 2.26$$

where $A' = m/2\,\Gamma(1 + \frac{m}{2})\,\Gamma(2 - \frac{m}{2})$

Values of A and m necessary to derive $H(\tau)$ have been computed and tabulated (Ferry), so one can derive $H(\tau)$ by graphical differentiation of the log storage modulus-frequency curve. Okano (1958) and Fujita's (1958) method for deriving the relaxation spectrum is :-

$$H(\tau) = \frac{e^2}{4\pi}\left(\frac{dG'}{d \ln \omega} - \frac{1}{2}\frac{d^2G}{d(\ln \omega)^2}\right)\Big|_{\frac{1}{\omega} = \tau} \qquad 2.27$$

and Ninomiya and Ferry's (1959) numerical method is :-

$$H(\tau) = \frac{G'(a\omega) - G'\omega/a}{2 \ln a} - \frac{a^2}{(a^2-1)^2}\,\frac{G'(a^2\omega) - G'(\omega/a)^2 - 2G'(a\omega) + 2G(\omega/a)}{2 \ln a} \qquad 2.28$$

This last method involves no measuring of slopes, but

utilises in the numerical computation certain values of G', spaced at equal intervals on a logarithmic frequency scale above and below the frequency, $\omega = 1/\tau$ corresponding to the value of τ for which H is derived: viz., at ω/a^2, $a\omega$ and $a^2\omega$ with a=0.2 to 0.4 for accuracy. The numerical calculation can be easily performed with the use of a standard tabulation process and perforated guide cards. Ferry (1961). This method is relatively easy and quick compared to the graphical differentiation methods.

2.8.2 Retardation Spectrum from Storage Compliance.

Schwarzl and Staverman (1956) derived the retardation spectrum from :-

$$L(\tau) = -dJ'/d(\ln\omega) + \tfrac{1}{4} d^3J'/d(\ln\omega)^3 \Big|_{\frac{1}{\omega}=\tau} \qquad 2.29$$

and Fujita (1958) from:-

$$L(\tau) = \frac{-e^2}{4\pi}\left(\frac{dJ'}{d\ln\omega} - \frac{1}{2}\frac{d^2J'}{d(\ln\omega)^2}\right)\Big|_{\frac{1}{\omega}=\tau} \qquad 2.30$$

and Ninomiya and Ferry (1959) from a numerical calculation of:-

$$L(\tau) = \frac{J'(\omega/a) - J'(a\omega)}{2\ln a} - \frac{a^2}{(a^2-1)^2}\,\frac{J'(\omega/a)^2 - J'(a^2\omega) - 2J'(\omega/a) + 2J'(a\omega)}{2\ln a} \qquad 2.31$$

2.8.3 Relaxation Spectrum from Loss Modulus.

Schwarzl and Staverman (1956) from a graphical second approximation method derived relaxation spectrum as follows:-

$$H(\tau) = (2/\pi)\ (G'' - d^2G''/d(\ln \omega)^2 \Big| \qquad \frac{1}{\omega} = \tau \qquad 2.32$$

similarly Fujita from :- 2.33

$$H(\tau) = (e^2/4\pi)(G'' - d^2G''/d(\ln\omega)^2 \Big| \qquad \frac{1}{\omega} = \tau$$

Ninomiya and Ferry (1959) by a first approximation numerical method from:-

$$H(\tau) = \frac{2}{\pi}\left(G''(\omega) - \frac{a}{(a-1)^2}\left\{G''(a\omega) + G''(\omega/a) - 2G''(\omega)\right\}\right)\Big| \qquad \frac{1}{\omega} = \tau \qquad 2.34$$

2.8.4 Retardation Spectrum from Low Compliance.

Schwarzl and Staverman's (1956) second approximation method for deriving the retardation spectrum gave:-

$$L(\tau) = \frac{2}{\pi}\ (J'' - d^2J''/d(\ln\omega)^2) \Big| \qquad 2.35$$
$$\frac{1}{\omega} = \tau$$

Fujita's (1958) first approximation method gave:-

$$L(\tau) = \left(\frac{e^2}{4\pi}\right) J'' \left(1 - (d\ln J''/d\ln\omega)^2 - d^2 \ln J''/d(\ln\omega)^2\right)\Big|_{\frac{1}{\omega}=\tau} \qquad 2.36$$

whereas Nihomiya and Ferry's first approximation numerical method gave:-

$$L(\tau) = \left(\frac{2}{\pi}\right)\left(J''(\omega) - \frac{a}{(a-1)^2}\left\{J''(a\omega) + J''(\omega/a) - 2J''(\omega)\right\}\right)\Big|_{\frac{1}{\omega}=\tau} \qquad 2.37$$

Other methods of deriving H or L have been used, and mention should be made of the following references for a complete description of these and other methods. No comment can be made as to which of the above or other methods are preferable, the only real criterion of their usefulness is whether the same distribution is obtained from simultaneous data, such as analysing two or more of the functions, G', G'', J', J'' or tan δ, which can

usually be obtained from the same physical measurements. If the distributions agree, then the particular method used to derive the spectra is adequate for that particular set of experimental results. The references to the relevant literature on graphical and numerical methods of deriving spectra will be found in Alfrey and Doty (1945), Zener (1948), Schremp, Ferry and Evans (1951), Andrews (1952), Ferry and Williams (1952), Schwarzl and Staverman (1953), Williams and Ferry (1953), Leadermann (1954), Roesler and Twyman (1955), Catsiff and Tobolsky (1955), Roesler (1955), Staverman and Schwarzl (1956), Tobolsky and Catsiff (1956), Benbow (1956), Hopkins and Hanning (1957), Dannhauser, Child and Ferry (1958), Okano (1958), Fujita (1958), Smith (1958), Berge, Saunders and Ferry (1959), Ninomiya and Ferry (1959), Plazek (1960) and in particular Ferry (1961).

2.9 MOLECULAR THEORIES RELATING TO DYNAMIC PROPERTIES

2.9.1 Modified Rouse Theory

Rouse (1953) and later Cerf (1959) derived a molecular theory in which the simultaneous motions of all the segments of a polymer chain can be

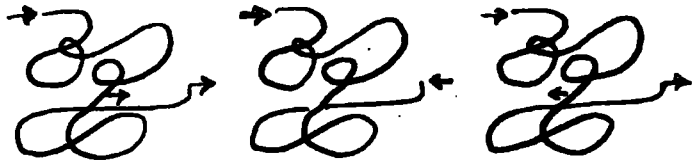

FIG 2.29 Schematic illustration of characteristic modes of coordinated motion of a flexible chain molecule. Arrows indicating direction of motion of a particular segment of a chain

described through a transformation of co-ordinates as the sum of a series of co-operative modes. Each motion represents motion away from a given instantaneous configuration in which the segments are co-ordinated along the molecular contour somewhat similar to the segments of a vibrating string, Fig. 2.29. This is the classical problem of the loaded spring. Bueche (1954). Each mode moreover corresponds to a discrete contribution to the relaxation spectrum. It is convenient to express the results in terms of the spectrum H, and can be expressed as

$$H = nkT \sum_{p=1}^{N} \tau_p \delta(\tau - \tau_p) \quad \text{where} \qquad 2.38$$

$$\tau_p = \sigma^2 f_o \Big/ 24kT \sin^2\left[p\pi/2(N+1)\right] \qquad 2.39$$

where δ is the Dirac delta, and n is the number of polymer molecules per c.c., A line spectrum is predicted, in which each contribution to the shear modulus G_p has the magnitude nkT. f_o is the translational friction coefficient of a sub-molecule. N is the number of sub-molecules in a macromolecule.

The polymer molecule is idealised as a necklace of spherical beads connected by elastic springs. Each bead and associated spring represents a gaussian segment of the polymer. The spring has an elastic constant kT (in shear) arising from the kinetic theory of rubber elasticity as applied to the segment. The moving bead obeys Stoke's law and represents the damping forces retarding the segment motion.

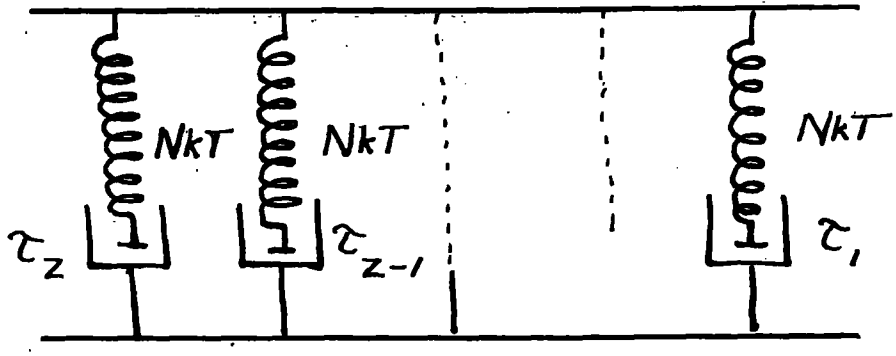

Extending this theory to undiluted polymers, and taking into account the further complication of entanglement coupling we have :-

$$H = ((a\rho N_0)/2\pi M_0)(\xi_0 kT/6)^{1/2}\tau^{-1/2} \quad 2.40$$

and

$$L = ((2/M_0)/\pi a\rho N_0)(6/\xi_0 kT)^{1/2}\tau^{1/2} \quad 2.41$$

where M_o is the monomeric molecular weight. N_o is Avogadro's number, ζ_o is the monomeric friction coefficient (translational friction coefficient per monomer unit).

These last two functions plotted on logarithmic scales (Log H or L versus log τ) should be linear with slopes of $-\frac{1}{2}$ and $+\frac{1}{2}$ respectively. The importance of these relationships is that from the experimentally derived values of H and L which give a slope of $-\frac{1}{2}$ or $+\frac{1}{2}$ when log H or Log L is plotted against log τ, the monomeric friction coefficient, ζ_o, can be determined as the other parameters in equations 2.40 and 2.41 should be known, or could be determined independently, as will be demonstrated later in this review.

Another theoretical treatment of the modified Rouse theory gives :-

$$G' = \frac{\rho RT}{M} \sum_{p=1}^{N} \frac{\omega^2 \tau_p^2}{1 + \omega^2 \tau_p^2} \qquad 2.42$$

and

$$G'' = \frac{\rho RT}{M} \sum_{p=1}^{N} \frac{\omega \tau}{1 + \omega^2 \tau_p^2} \qquad 2.43$$

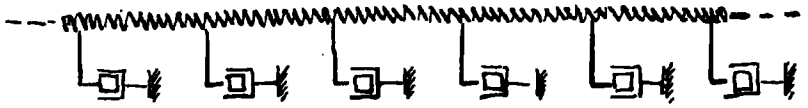

Fig 2·30a Ladder network of Blizard.

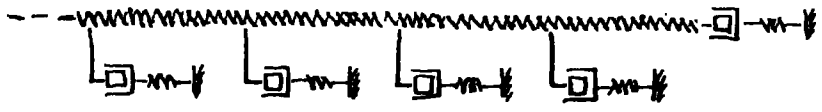

2·30b. Modification of ladder network by Marvin to ac
for limiting value of modulus at high frequencies and short time

where

$$\tau_p = \frac{6\eta_0 M}{\pi^2 \rho R T P^2} \qquad (P = 1, 2, 3 \cdots M/M_e)$$

η_0 is the steady state viscosity at zero rate of shear at a given temperature, T, and molecular weight, M, of the polymer. M_e is the molecular weight between entanglements. P has integral values between 1 and M/M_e. ρ is the density at the absolute temperature T.

For values of P greater than M/M_e, the relaxation times τ_p are given by :-

$$\tau_p = \frac{6\eta_0 M}{\pi \rho R T P^2 (M/M_e)^{2.4}} \qquad 2.44$$

2.9.2 Blizard and Marvin Theories.

Blizard (1951) assumed a model in which polymer molecules are represented as springs moving in a viscous medium. This model is represented in Fig. 2.30a, a model which is analogous to the so-called ladder network in electrical network theory. When the finite (lumped) springs and dashpots are uniformly distributed along the length, the mechanical model becomes exactly analogous

to an electrical model of an inductive transmission line, and can be solved to give :-

$$G' + iG'' = (C_1/M)\left[(iC_2M^2\omega)^{1/2}\coth(iC_2M^2\omega)^{1/2} - 1\right] \quad 2.45$$

where M is molecular weight, and C_1 and C_2 are constants.

Gross and Fuoss (1956) noted that this type of equation corresponds to a discontinuous relaxation spectrum with discrete lines, and therefore :-

$$C_1 = \rho RT/2 \quad 2.46$$

and

$$C_2 = a^2\zeta_0/6M_0^2kT \quad 2.47$$

Using the same model, but using a capacitative transmission line analogy which corresponds to a molecular spring with one end free and one end fixed, Marvin (1960) derived:-

$$G' + iG'' = (C_1'/M)(iC_2'M^2\omega)^{1/2}\tanh(iC_2M^2\omega)^{1/2} \quad 2.48$$

All these treatments are identical at high frequencies. There are slight divergencies at low frequencies. For example the low frequency limiting relation for G' has the form

$$G' = \left(\frac{1}{k}\right) e RT \left(a^2 \zeta_0 / 6 M_0 kT\right)^2 M^3 \omega^2 \qquad 2.49$$

but K has the values 3500, 3240 and 1000 respectively in the Rouse series expression and in the Blizard and Marvin continuous functions respectively.

2.9.3 Summary of Molecular Theories

It is convenient to list the various equations for H and L in Table 2.4 that have been derived from the literature to describe the behaviour of cross-linked systems, without going into details of their derivation.

By converting the relaxation and retardation spectra into loss compliance terms, Ferry (1961) found that the Kirkwood derivation (given in Table 2.4) described closely the experimental data for lightly vulcanised natural rubber at highish frequencies, although he also found that some other cross-linked polymer systems conform more closely to the modified Rouse-Bueche slope of $-\frac{1}{2}$ and $+\frac{1}{2}$ for the

relaxation and retardation spectra at high frequencies. The shapes of the loss compliance - frequency curves predicted by the Bueche, Kirkwood and Hammerle-Kirkwood equations at high frequencies, are nevertheless very similar to each other.

Of great importance, however, is the fact that all the theoretically derived equations quoted in Table 2.4 deviate considerably from the practical results at low frequencies. This deviation will be discussed in detail in a later section of this chapter. At present, the equations quoted in Table 2.4 can only be regarded as of limited value in describing the loss compliance or the distribution functions of cross-linked natural rubber, the limitations arise because of the inability of these equations to describe dynamic behaviour in the rubbery plateau region in cross linked systems, although they are adequate and useful in the transition range where they can be used to derive molecular parameters such as ζ_0, the monomeric friction coefficient.

TABLE 2.4

MOLECULAR THEORIES FOR CROSS-LINKED SYSTEMS:EQUATIONS FOR H OR L.

	H	L
SE	$((a\,e\,N_0)/(2\pi M_0))(\xi_0 kT/6)^{1/2}\tau^{-1/2}$	$(2M_0/\pi a e N_0)(6/\xi_0 kT)^{1/2}\tau^{1/2}$
IFIED SE 30 (ADA)* 4)	$((a\,e\,N_0)/(2\pi M_0))(\xi_0 kT/3)^{1/2}\tau^{-1/2}$	$(2M_0/\pi a e N_0)(3/\xi_0 kT)^{-1/2}\tau^{1/2}$
WOOD		$(M_c/eRT)(\tilde{\tau}/\tilde{\tau}_m)/(1+\frac{\tilde{\tau}}{\tilde{\tau}_m})^2$ where $\tau_m = 2j\,Z_c b^2 \xi_0 kT$ reducing to $(M_0/2eRTN_0 j b^2 \xi_0)\tau$ at short times
ERLE AND WOOD		$(2M_c/eRT)(\frac{\tilde{\tau}}{\tilde{\tau}_0})^2/1+(\frac{\tilde{\tau}}{\tilde{\tau}_0})^3$ where $\tau_0 = e b^3 \eta_0 \sqrt{Z_c}/kT$ reducing to $(2M_0kT/eN_0c^2b^6\eta_0)\tau^2$ at short times
HE		$(8/\pi^2 \eta_c kT)\sum_{\lambda=1}^{N}[(\tau_\lambda/(2\lambda-1)^2)]\,\delta(\tau-\tau_\lambda)$ where $\tau_\lambda = a^2 Z_c^2 \xi_0/3(2\lambda-1)^2\pi kT$

lies to short times:- Differs from the Rouse theories only by a tor of $\sqrt{2}$. Such a difference attributable to the theories rather n aspects of cross-linking.

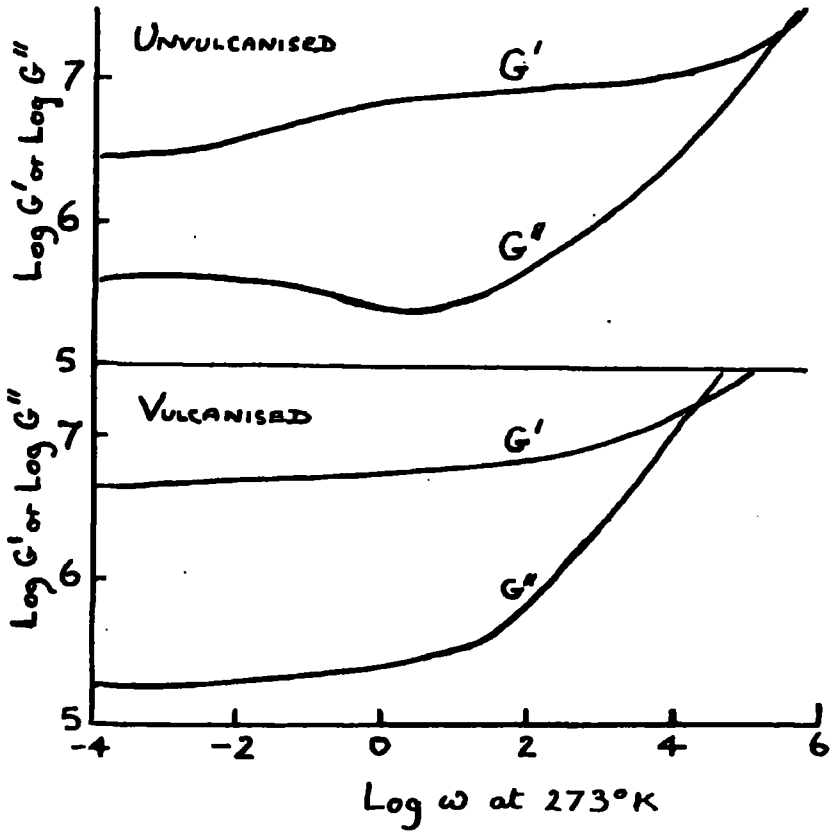

FIG 2·31 Dynamic shear moduli in the rubbery or plateau zone for natural rubber before and after vulcanisation. Upper curves, G'; lower, G''. After Payne (1959).

2.10 DISCUSSION ON EXPERIMENTALLY DERIVED DISTRIBUTION FUNCTIONS

2.10.1 Rubber Plateau Region.

In the transition zone treated in an earlier section of this chapter, viscoelastic properties are dominated by configurational re-arrangements of individual molecules, whereas in the rubbery or plateau zone the properties are dominated by a quite different feature: the presence of a network, due either to actual cross-links or to entanglement coupling, which necessitates co-ordination of the configurational motions of neighbouring molecules or molecular chains. For the slower relaxation processes, the influence of the environment cannot be described solely in terms of an average friction coefficient in the same manner as it is possible to describe the relaxation processes associated with the transition.

In order to discuss these effects further, it is useful now to derive the distribution functions for both unvulcanised and vulcanised natural rubber and compare these spectra in the plateau zone, Fig 2.32.

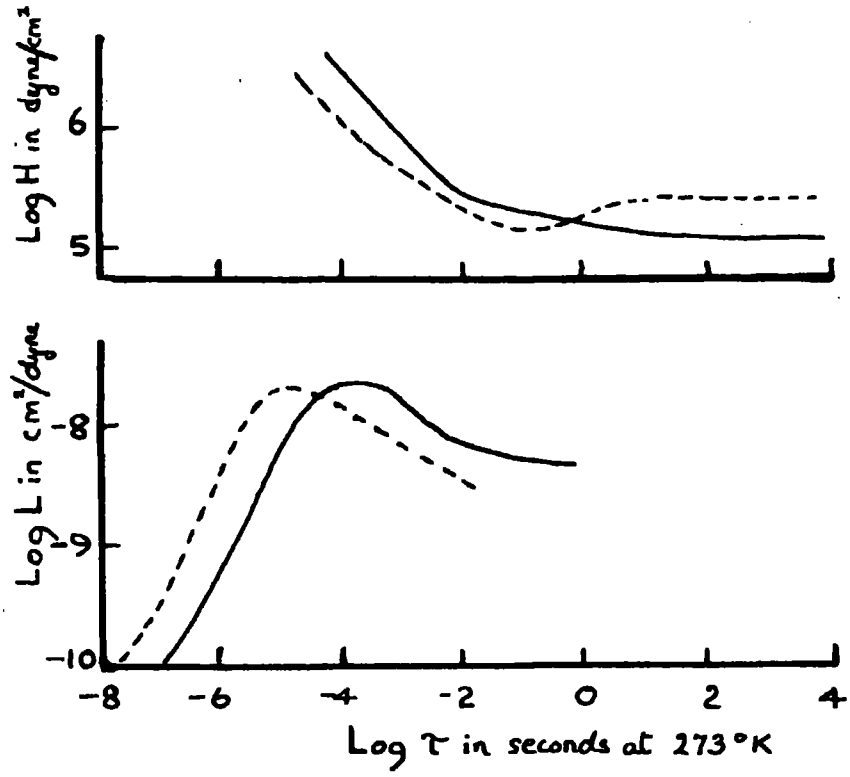

FIG 2·32. *Relaxation and retardation spectra in the plateau zone, calculated from the data of Fig 2·31. Solid curves, vulcanised; dashed curves, unvulcanised. After Payne (1959), Ferry (1961). Using equations 2·26 and 2·31 to derive H and L from experimental data.*

For cross-linked polymers at low frequencies (corresponding to long times), G' changes very little with frequency, and G" is also nearly frequency--independent, with a magnitude considerably below that of G'. This behaviour, exemplified by the curves for lightly vulcanized Hevea rubber in Figs. 2.20 and 2.21, was emphasized by Kuhn, Kunzle and Preissmann (1947) and Philippoff (1953) and its implications in terms of the form of the relaxation spectrum H was demonstrated by Kuhn et.al. (1947). For uncross-linked polymers of high molecular weight, G' and G" also pass through a region where their slopes are relatively small, though more complicated in shape than for the cross-linked case. A representative comparison is shown in Figure 2.31 for natural rubber before and after vulcanization. For the cross-linked polymer, G" is smaller than G' by a factor of about 0.025. For the uncross-linked polymer, the ratio G"/G' is of the order of 0.04, but varies as G" passes through a shallow maximum and shallow minimum.

The corresponding plots of the relaxation spectra are given in Fig. 2.32. At long times, both are flat, the

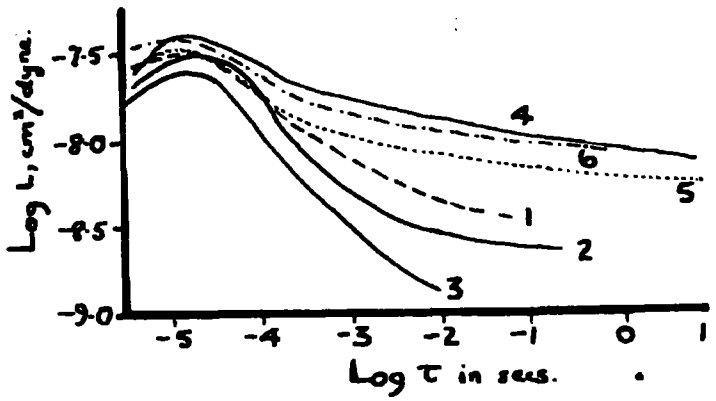

FIG 2·33. *Retardation spectra of six vulcanisates, mean of calculations from J' and J", reduced to 25°C. (Stratton and Ferry). See Table 2·3 for details of the vulcanisates 1, 2 and 3 sulphur vulcanisates. 4, 5 and 6 refer to rubber not cross linked by sulphur.*

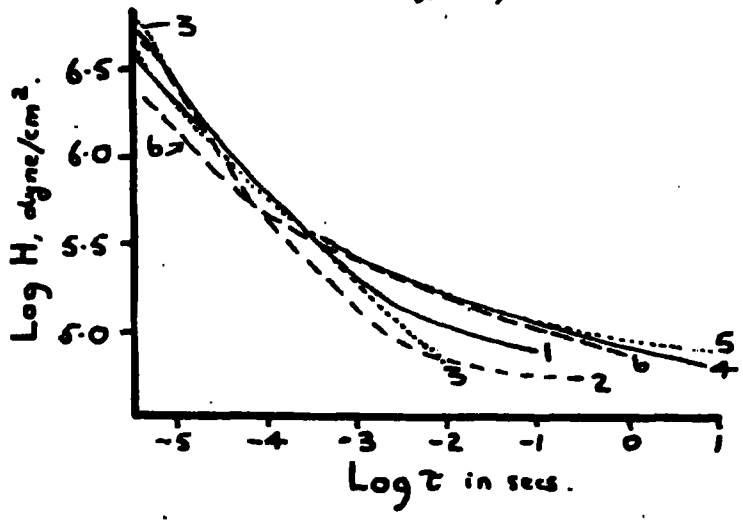

FIG 2·34. *Relaxation spectra of the six vulcanisates, mean of calculation from G' and G", reduced to 25°C. (Stratton and Ferry). See Table 2·3 for details of the vulcanisates*

level for the cross-linked polymer being lower by a factor of 0.46. At shorter times they cross and enter the transition zone parallel but displaced by about 0.8 unit on the logarithmic time scale.

To examine the effect of crosslinking in the rubber or plateau region further it is useful now to consider the retardation spectrum L of the vulcanisates studied by Stratton and Ferry. Fig 2.33 plots L logarithmically against τ , the retardation time. The three non-sulphur vulcanisates (4,5 and 6) clearly represent a class in which the retardation mechanisms extend to much longer times than in the three sulphur vulcanisates. At shorter times on the other hand, the maximum in L characteristic of any network structure is similar for all six vulcanisates.

The same grouping appears in the relaxation spectrum H plotted in Fig 2.34. At short times, the relaxation spectra are all near to each other, though different in shape. At long times, the non-sulphur vulcanisates form a group in which the relaxation mechanisms persist with a considerably greater magnitude.

The differences between the two classes of vulcanisate are again emphasised when $\tan\delta$ is plotted logarithmically

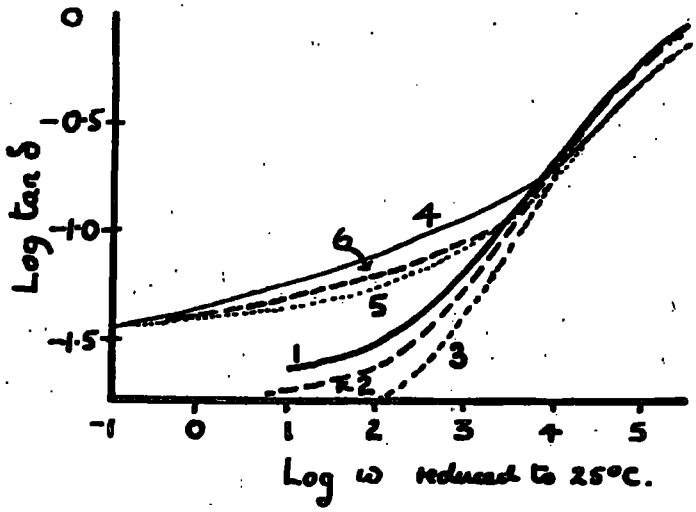

Fig 2·35. Loss tangents of the six vulcanisates, plotted logarithmically against radian frequency reduced to 25°. (Stratton and Ferry).

against radian frequency reduced to 25°C in Fig 2.35. In sample 3, tan δ falls to 0.0% (Payne has recorded values less than 0.01 for highly crosslinked sulphur vulcanisates) whereas in the non-sulphur vulcanisates the lowest value achieved is about 0.033. These differences in L, H and tan δ are, of course, all inter-related and reflect somewhat greater deviations from ideal elastic behaviour in the non sulphur vulcanisates. The source and nature of these deviations will be discussed later in this Thesis.

2.10.2 Transition Region

The maximum in the loss compliance is a useful measure of the network structure as its height and position depend on the number and distribution of the network strands. A knowledge of J''_{max}, the maximum value of the loss compliance, should, therefore, allow one to derive some molecular parameters, as the following two theoretical relationships between J''_{max} and the molecular properties of the network have been proposed. (A further discussion on the derivations and limitations of the following Bueche relationship is presented in Appendix 5.2).

Cross-linked network, (Bueche, 1952).

For cross-linked networks Bueche has shown that:-

$$J''_{max} = 0.42\ Z_c M_o/\rho RT = 0.42\ J_e \qquad 2.50$$

where

Z_c = Average degree of polymerisation of a network strand = M_c/M_o

M_o = Molecular weight per monomer unit

J_e = equilibrium psuedo-equilibrium, or steady state shear compliance and

$$\omega_m = 29.6kT/a^2 Z_c^2\ \zeta_o \qquad 2.51$$

a = root mean square end-to-end distance per square root of the number of monomer units in a rubber molecule

ζ_o = translational friction coefficient per monomer unit.

Uncrossed-linked networks (Morris, 1960)

For rubbers which have not been vulcanised, Morris has derived:-

$$J''_{max} = 0.32 \; Z_e \; M_o/\rho RT \qquad 2.52$$

where

Z_e = average degree of polymerisation between entanglement coupling points = M_e/M_o, and

$$\omega_m = 48kT/a^2 \; Z_e^{\;2} \zeta_o \qquad 2.53$$

It is also useful to note that the value of the retardation spectrum L corresponding to the maximum in J'' is related simply to that of J'' by a factor of $2/\pi$ or $e^2/4\pi$ depending on the type of approximation used to derive $L(\tau)$. The maximum in L should be independent of M, and its position should depend only on Z_c or Z_e in the same manner as given by equations 2.50 to 2.53 above. We shall, therefore, use experimentally derived values of L instead of J'' in the above equations in order to calculate the molecular parameters.

Ferry has noted that in view of the approximate equivalence of the maxima in J'' and L, the location of the maxima of log (L/J_e) is at zero when plotted against log 29.6 $(kT/a^2 \; Z_c^{\;2} \zeta_o$.) Assuming this is correct

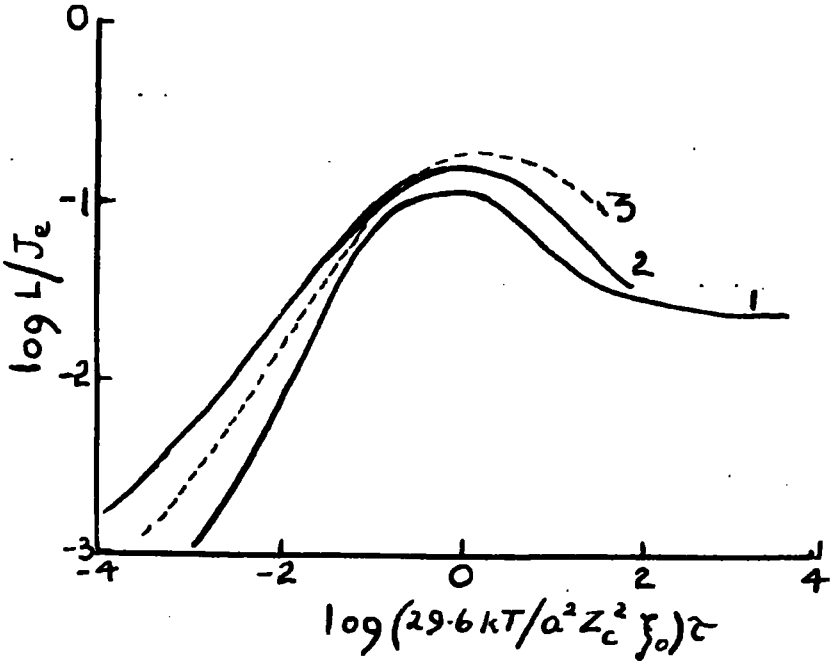

FIG 2·36. Retardation spectra of cross-linked systems, near their maxima, reduced to corresponding states by equations 2·50 and 2·5
Curve 1: natural rubber, 2; polyurethane rubber, 3; 40% polyvinyl chloride in dimethyl thianthrene. (Ferry, 1961).

then Figure 2.36 shows the retardation spectra of cross--linked systems near their maxima reduced to corresponding states in accordance with equations 2.50 and 2.51. The data for this reduction are summarised in Table 2.4. It is to be noted that the shapes of the maxima are roughly the same, their heights varying from 0.115 to 0.19 as compared to the value of 0.26 predicted from equation 2.50 by applying the factor $2/\pi$.

TABLE 2-4

DATA FOR REDUCTION OF L TO CORRESPONDING STATES (CROSS-LINKED SYSTEMS). FERRY (1961).

Polymer system	Ref.	Log J_e	M_c	log $M_o^2/a^2\zeta_o$
Hevea rubber, 0^oC	Payne (1958a)	-6.68	4280	24.75
Polyurethene rubber, 0^oC	Landell (1957)	-7.17	1960	20.48
40% polyvinyl chloride in dimethyl 25%	Ferry & Fitz-gerald (1955)	-6.70	2780	19.40

The viscoelastic properties of polymers are described

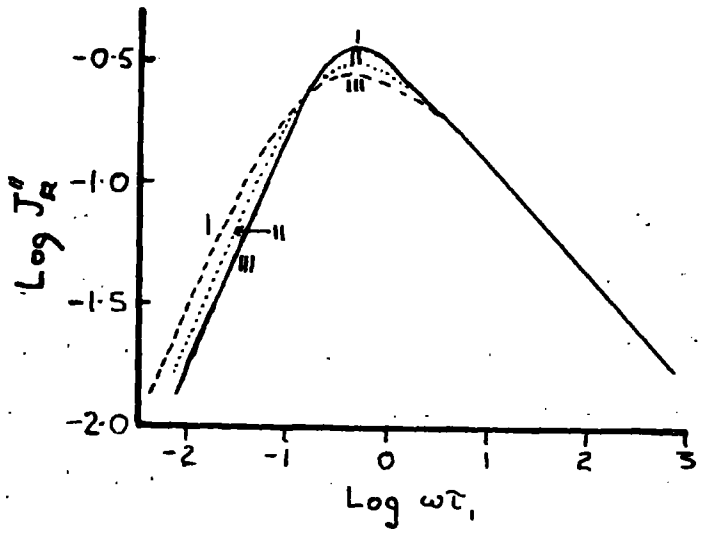

FIG 2·37. Log J'/J_e plotted against log $\omega\tau_1$ for theories based on Blizard model. I, fixed cross-links, uniform strand length; II, movable cross-links with bifurcate branching, uniform strand length; III, fixed cross-links, most probable distribution of strand lengths. (Stratton and Ferry).

adequately in some cases by the theory of Rouse, (which corresponds to the ladder network model of Blizard), so Stratton and Ferry (1964) suggest that the simplest adaptation of the Rouse theories to actual networks can be made by assuming that the cross links are fixed, and the network strands are of a uniform length. (This is provided by Blizard's theory if his Θ is set equal to zero in his expression 14). For instance if J''/J_e is plotted logarithmically against $\omega\tau_1$, where τ_1 is the terminal relaxation time, then curve 1 in Fig. 2.37 is obtained. Here τ_1 is identified with molecular parameters in such a way as to make the high frequency dynamic properties coincide with the predictions of the Rouse theory (Lovell and Ferry, 1961)+. The predicted maxima in J'' is somewhat higher and sharper than any which have been observed experimentally. (Ferry, 1961 p. 279)

Two modifications to the simple basic network model can be made :-

a) The cross links are not fixed:- a given strand ends

+ Specifically, Blizard's expression 14 must be set equal to $2G^*J_e$ where G^* is the complex shear modulus, and his H is $\pi^2\omega\tau_1$.

in a junction with three others, and each of these with three others, and so on. The strand lengths being assumed uniform. (Blizards' eq. 17 where $B = G^{*}J_e$ and $H = \pi\omega\tau_1/4$). Curve 11 in Fig. 2.37.

b) The cross-links are fixed, but the strand lengths are variable with a "most probable" distribution. Curve 111 in Fig. 2.37.

It is interesting to note that these two major modifications to the basic model, which is one in which the cross links are fixed and the network strands are of a uniform length, produce only a moderate broadening of the curves with respect to curve 1 in Fig. 2.37. Lovell and Frederick, (1964). The differences between the curves in Fig 2.37 are really only small, although the heights of the maxima J''/J_e, which are 0.362, 0.310 and 0.286 respectively for the three curves, seem more sensitive to the type of model used. Nevertheless curve 111 is seen to fit the J" data for sample 3 fairly adequately in the region of the maximum, Fig. 2.28. Stratton and Ferry

concluded from this agreement, that the distribution of strand lengths in sulphur vulcanisates is therefore no broader than the "most probable" form. The lower maxima for the non-sulphur vulcanisates suggest a broader distribution of strand lengths than for the sulphur cured rubbers.

The cross-linking produced by γ-radiation is believed to take place by a free radical process, Chapiro (1962), and the same is certainly true for dicumyl peroxide. Braden and Fletcher (1955). Blokl (1959, 1960) from electron spin resonance measurements concluded that the vulcanisation reaction in tetramethylthiuram disulphide vulcanisates also involve free radicals. Stratton suggests that these free-radical chains might tend to concentrate cross links locally, and give a broader distribution of strand lengths than would a random chemical reaction such as that which occurs during sulphur vulcanisation.

The maximum in J" is higher and broader for sample 4 than for 3 and these differences are also reflected in the maxima of L in Fig. 2.33. In Table 2.5, log J''_{max} and

log J_e are listed together with the ratio of J''_{max}/J_e for easy comparison. In terms of the ratio J''_{max}/J_e, the samples again separate into two groups with values of 0.25 for the sulphur vulcanisates, and 0.16 for the others, thus the non-sulphur vulcanisates deviate more strongly from the theoretical predictions discussed above.

TABLE 2-5

PARAMETERS CHARACTERISING TRANSITION AND TERMINAL ZONES AT 25°C (STRATTON AND FERRY).

	Sulphur vulcanisates		
Sample No.	1	2	3
log ζ_0(dyne-sec./cm.)	-6.2	-6.2	-6.2
log J_e (cm^2/dyne)	-6.7	-6.75	-6.89
log J''_{max}(cm^2/dyne)	-7.32	-7.35	-7.46
J''_{max}/J_e	0.24	0.25	0.27
	Non-sulphur vulcanisates		
Sample No.	4	5	6
log ζ_0(dyne - sec/cm.)	-6.4	-6.4	-6.4
log J_e (cm^2/dyne)	-6.49	-6.56	-6.4
log J''_{max}/(cm^2/dyne)	-7.27	-7.36	-7.22
J''_{max}/J_e	0.166	0.158	0.151

2.11 THE MONOMERIC FRICTION COEFFICIENT

The position of the transition zone on the time scale reflects the absolute magnitudes of the relaxation and retardation times, and hence that of the monomeric friction coefficient upon which (according to the flexible chain theories of viscoelasticity) they all depend. By rearranging equation 2.40 as follows

$$\log \zeta_0 = 2 \log H + \log \tau + \log (6/kT) + 2 \log (2\pi M_0/\rho a M_0) \quad 2.54$$

The monomeric friction coefficient can be calculated from the relaxation distribution plots because at the log-time end of the transition region there is a portion of the log H, log τ plot which conforms to the theoretical slope of $-\frac{1}{2}$. This portion occurs between the steeper slope which prevails at short times and the flattening or minimum characteristic distribution associated with the rubbery plateau region. From the position of the tangent to the relaxation distribution curve whose slope is $\frac{1}{2}$, i.e., at the time τ', ζ_0 can be calculated if we know the density ρ, and the monomer molecular weight M_0, as well as a, the root mean square end-to-end length per square root of the

number of monomer units. (The latter is usually taken as the value determined in dilute solution in a Θ solvent, under the assumption that the molecular configuration in the undiluted polymer is unperturbed by long-range effects).

Values of $\log \zeta_0$ for natural rubber, together with the constants M_0 and a used in the calculations of ζ_0 are given in Table 2-6. The friction coefficient, ζ_0, which is the average force per monomer unit required for a chain segment to push its way through its local surroundings at unit velocity, must depend upon the free volume in the polymer, on the intermolecular forces between the chain segment and on the static hindrances to rotating around the bonds. Calculation of an absolute value for ζ_0 is nevertheless uncertain, as the actual relaxation spectrum H for natural rubber rises more steeply at short times than the slope of $-\frac{1}{2}$ on a logarithmic plot required by the Rouse theory (Ferry, 1961 p. 255 and 267). At longer times H flattens out because of the entanglement or vulcanisation network, leaving no intermediate segment with a clear and definite slope of $-\frac{1}{2}$. The limitations and difficulties in applying the Rouse theory to undiluted polymers have been

recently discussed at length by Williams (1962).

TABLE 2-6

VALUES OF ζ_o AT 298°K, AND AT T_g, TOGETHER WITH THE VALUES OF M_o AND a USED TO CALCULATE ζ_o.

Natural Rubber	T_g	M_o	a cm x 10^8	log ζ_o at 298°K	log ζ_o at T_g	Ref.
Unvulcanised	200	68	6.8	-6.74	3.94	1
				-6.87	3.81	1
Cross linked						
sulphur -	203	68	6.8	-5.90	4.66	1
	212	68	6.8	-5.64	4.53	1
	202	68	6.8	-6.20		2
non-sulphur -	203	68	6.8	-6.40		2

1. From data of Payne. Ferry (1961)
2. Stratton and Ferry. (1964)

It can be seen from Table 2-6, that earlier calculations (Ferry, 1961) of the monomeric friction coefficient ζ_o gave log ζ_o = -6.7 to -6.9 for

unvulcanised rubber at 250°K. A small shift in ζ_0 would be expected from the creation of cross links by direct junction of chain carbon atoms in the radiation and dicumyl peroxide vulcanisates instead of the polysulphide links according to an analysis by Mason (1961). For sample rubbers 4 to 6, this would amount to increasing $\log \zeta_0$ by 0.1.

Because of the importance of ζ_0, which, of course, fixes the time scale for visco-elastic behaviour in the transition zone, it would be desirable to obtain an independent measurement of this quantity. At present this is not possible for the polymer chain itself, but the best attempt reported so far was obtained by measuring the translatory friction coefficient of a small foreign molecule similar in size to the monomeric unit and dissolved in the polymer, for instance :-

$$\zeta_1 = KT/D_0 \qquad 2.55$$

where D_0 is the diffusion constant. If D_0 is measured by mass transport, absorption-desorption or by the radioactivity of tagged molecules techniques,

Park (1954), Auerbach, Gehman, Miller, and Kurgla (1958), then ζ_1, the molecular friction coefficient for the foreign molecule in the polymer can be obtained. Aitken and Barrer (1955) have obtained ζ_1 for several foreign molecules in natural rubber, and their results are quoted in Table 2-7.

TABLE 2-7

COMPARISON OF ζ_1 DERIVED FROM DIFFUSION EXPERIMENTS WITH ζ_0 OBTAINED FROM DYNAMIC MEASUREMENTS. (AITKEN AND BARRER (1955), FERRY (1961)

	Mol. Wt.	$\log \zeta_1$	$\log \zeta_0$
n - Butane	58	-6.74	
i - Butane	58	-6.56	
n - Pentane	72	-6.74	
Chain unit	68		-6.90

All measured at $T - T_g = 103^{\circ}C$.

The values of ζ_1 and ζ_0 are clearly similar, and for natural rubber it appears that the monomeric friction coefficient reflects almost wholly the force of pushing

aside neighbouring chains in the environment, and to a negligible extent the difficulty of articulating the chain in which the monomer unit is located.

2.12 LOSS MECHANISMS AT LOW FREQUENCIES

According to all the present theories of visco-elasticity Bueche (1954), Blizard (1951), Kirkwood (1946), Hammerle and Kirkwood (1955), $\tan\delta$ should vanish at long times if the behaviour is ideal. All the dynamic measurements discussed in this Thesis have shown this is not the case, and the reason for the departures from the ideal may be due to one or all of the following causes:-

a) The heterogeneity of strand lengths,

b) the length, and consequently the mobility of the cross-link itself,

c) the presence of loose ends (i.e. network strands attached at one end only).

That the nature of the crosslink does vary is well known. For instance, in vulcanisates obtained by radiation, Chapiro (1960), or dicumyl peroxide, Braden and Fletcher

(1955), the backbone chain carbon atoms of the rubber strands are believed to be bonded directly, forming a rather bulky junction. With tetra methylthiuran disulphide, the chain backbones are joined together with a single interstitial carbon atom. Studebaker and Nabors (1959). In sulphur compounds, on the other hand, the chain backbones are joined by bridges containing one, two, three and often even more sulphur atoms. Studebaker and Nabors (1959), Moore and Trego (1961). Such a flexible junction is, therefore, expected to have considerably less frictional resistance to motion in its environment and to dissipate less energy in co-ordinated motions involving groups of linked strands. Quantitative assessment of these problems have not yet yielded to any theoretical treatments.

Another possible source of the low frequency losses is the effect of loose ends (i.e. network strands attached at one end only) on the motion of the network junctions as treated by Bueche, (1959) (1962), but the theory does not describe quantitatively the persistence of loss mechanism to such very low frequencies such as are evident in the

non-sulphur vulcanisates. Further work on the low frequency loss mechanisms is obviously urgently required particularly with regard to the initial character of the unvulcanised rubber which can be obtained in a very wide range of Mooney viscosities.

2.13 FILLED OR LOADED POLYMERS

For a particulate filler, which does not interact strongly with the polymer, the principal effects arise from the partial occupancy of volume by rigid and immobile masses. Extensive studies by Landel (1956) on polyisobutylene loaded with glass beads of the order of 0.004 cm. in diameter have revealed the changes in the isothermal viscoelastic functions. In this case the particles are large enough so that the average distances between them, even at the highest loading considered, are large compared with the root-mean-square end-to-end separation of the polymer molecules; the latter maintain their Gaussian distributions. Moreover, the particles of filler are too far apart to be bridged by single molecules.

The temperature dependence of relaxation and retardation times in these loaded systems could be described by the Williams, Landel and Ferry, (WLF); equation in the form of equation (2.20), with the value of T_g, the glass transition temperature, elevated slightly over that of unfilled pure polyisobutylene. Here, T_g varied roughly linearly with the volume fraction (ϕ) occupied by filler; For instance, for $\phi = 0.37$, T_g was 7^o higher than for the unloaded polymer. For each individual filled sample, the method of reduced variables could be applied to obtain single composite curves for the viscoelastic functions plotted against reduced frequency or time. The applicability of reduced variables was also apparent in earlier work on filled rubberlike polymers by Becker and Oberst (1956), Blatz (1956), Payne (1958b)

When the samples with different degrees of loading are compared in corresponding temperature states (i.e. 298^oK, for the unloaded polymer, $298^o + T_g$ for each of the loaded samples), the retardation and relaxation spectra fall rather closely together at short times up to a

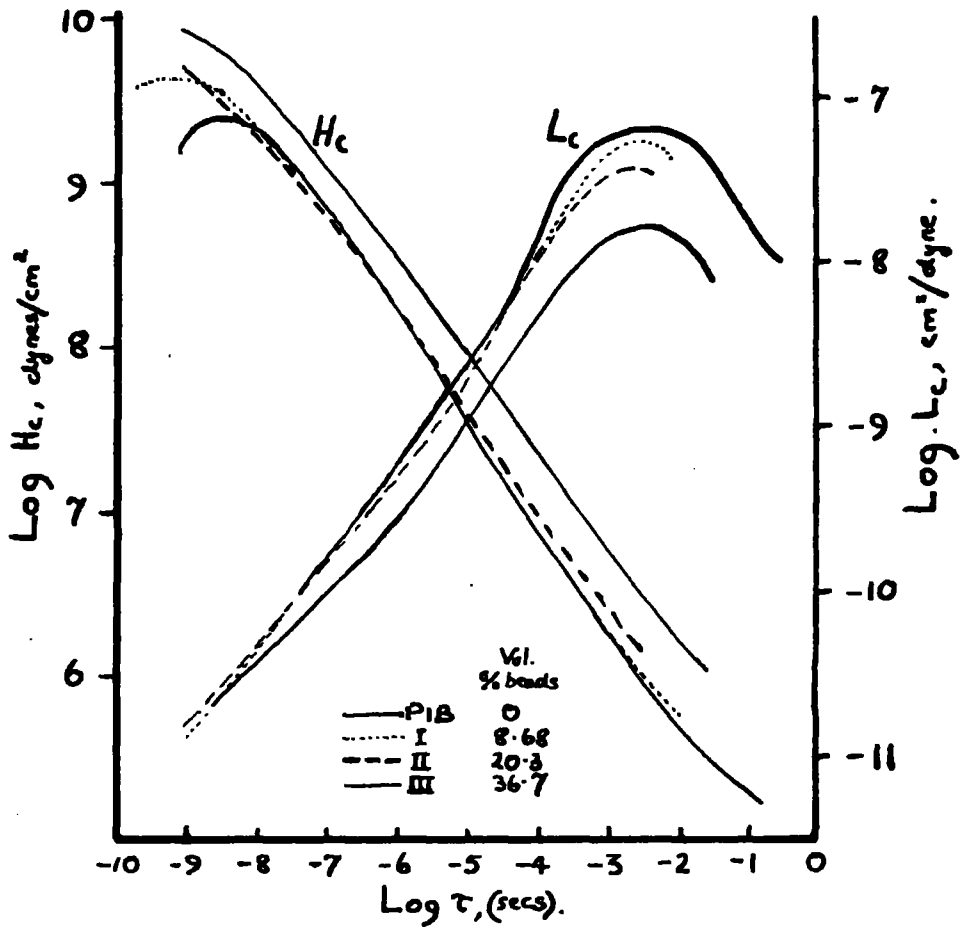

FIG. 2·38. *Relaxation and retardation spectra plotted logarithmically for polyisobutylene and 3 compositions loaded with glass beads, with volume fractions as indicated, reduced to corresponding temperature states (equal values of $T - T_s$). After Landel (1958).*

filler volume fraction of 0.2. At a higher filler loading H is elevated and L is depressed throughout the entire time spectrum; and at longer times the maximum in L is depressed progressively with increasing volume fraction of filler. (Fig 2.38) The last effect does not correspond to a change in entanglement coupling, because the position of the maximum does not shift correspondingly along the time scale.

The pseudo-equilibrium compliance, can be described rather well by a theoretical equation of Eilers: (1941)

$$J_e/J = 1 + k\phi/(1 - S'\phi)^2 \qquad 2.56$$

where J is the compliance of a composition with volume fraction of filler ϕ, and J_0 that of the unfilled polymer; $k = 5/4$ and $1/S' = 0.80$. The latter parameter has the significance of the volume fraction occupied by the filler particles when close packed; it is greater than that for close-packed spheres (0.74) presumably because of some degree of size heterogeneity. Equation 2.56 appears to hold for data on several filled polymer systems, Blatz (1956), including polyurethane rubbers (Ferry 1961). The

drop in compliance (increase in modulus) for large filler particles is analogous to the increase in viscosity caused by suspending rigid spherical particles in a liquid medium, both being due to perturbations in the matrix due to the presence of other particles, Eilers (1941), Robinson (1957), Parkinson (1958), Bueche (1957).

In a rubber loaded with finely divided carbon black, the behaviour is somewhat different. There is good evidence that the polymer molecules are attached to the filler particles by strong absorption forces approaching the nature of chemical bonds. Parkinson (1958), Bueche (1957). Moreover, in a compound containing 50% by weight of particles of the order of 300 A^{o} in diameter, the interparticle separations are of the order of 100 A^{o}, which is similar to the average vector distance between cross-links in a lightly cross-linked rubber vulcanizate. Hence each filler particle may be bridged to others by many polymer chains, and it acts as a multiple cross-link as well as a rigid occupier of space. (Agglomeration of the particles also complicate the picture, Davey and Payne (1965)). The effect on the transition from rubberlike

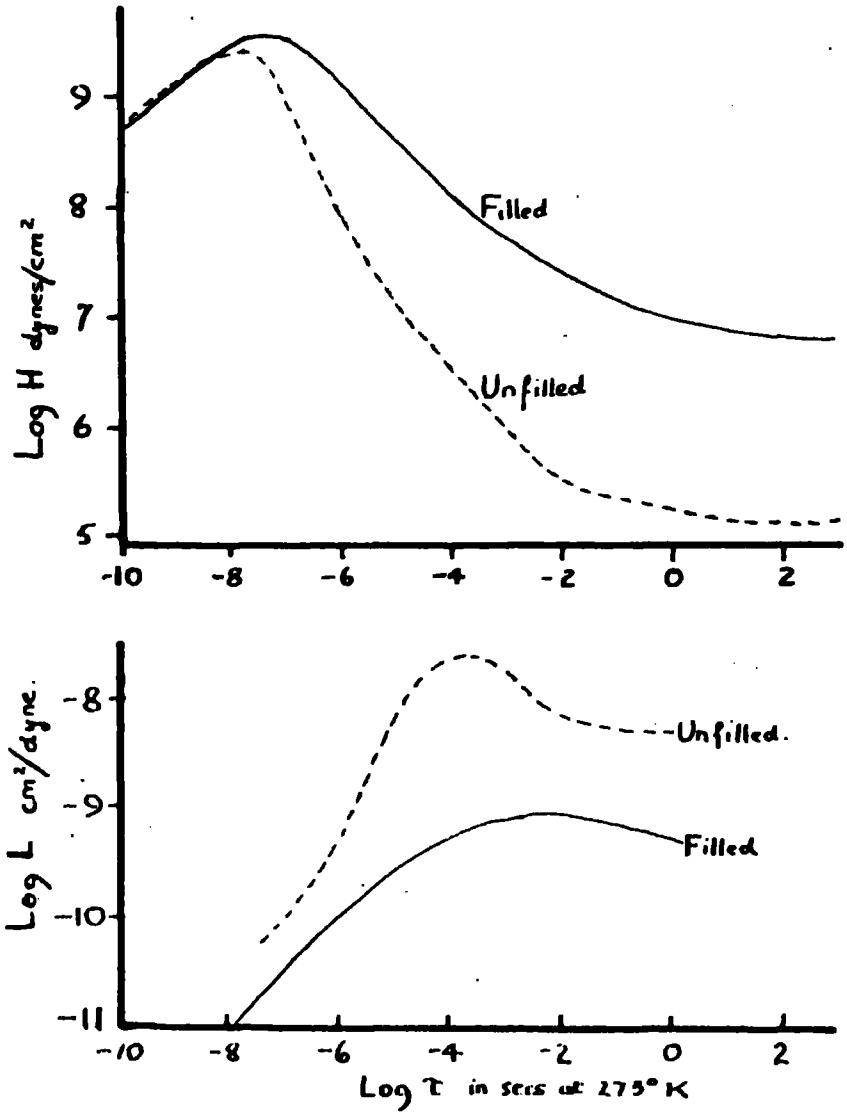

FIG. 2.39. *Relaxation and retardation spectra of vulcanized Natural rubber filled with 50 parts by weight of high-abrasion furnace type carbon black, calculated from data of Payne (1958), and compared with similar spectra for an unfilled vulcanizate (c.f. Figs 2·20 and 2·21), all reduced to 273° K.*

to glasslike consistency is illustrated by data of Payne (1958a) for a carbon-filled rubber vulcanizate in Figs. 2.20 and 2.21, compared with those for an unfilled vulcanizate.

The filler flattens both relaxation and retardation spectra, Fig. 2.39. The former does not attain a slope of ½ on the doubly logarithmic plot in the lower region of the transition zone, where the friction coefficients are usually estimated. Although this slope is reached just to the right of the maximum, the Rouse theory cannot be applied at such short times. At very short times the relaxation spectrum is essentially unaffected by the filler. The maximum in L is depressed, but almost in proportion to the pseudo-equilibrium modulus J_e; the ratio L_{max}/J_e being 0.115 and 0.10 for the unfilled and filled systems respectively.

The level of the pseudo-equilibrium shear modulus was raised by the filler from $10^{6.8}$ to $10^{8.0}$ dynes/cm^2 for rubbers whose spectra data are presented in Fig 2.39. This increase in the rubber plateau region is greater than expected from equation 2.56, an equation which is really only applicable to large spherical particles. The subject

of the dependence of the modulus on the proportion, particle size and chemical nature of the filler has been adequately discussed by Parkinson (1957), Bueche (1957), Houwink and Janssen (1954), (1956), Davey and Payne (1965). From the cited literature, it is evident that the increase in modulus for carbon black filled rubbers cannot be described in terms of the volume filling properties alone, but a further discussion on this point is beyond the scope of this Thesis. The level of the loss modulus in the pseudo-equilibrium zone was raised in Fig 2.39 from $10^{5.2}$ to $10^{7.0}$ dyne/cm^2, representing a proportionally greater increase from that for the shear modulus. The effect of the filler on the temperature dependence of relaxation and retardation times could be described in terms of an increase in T_g of 3^o to 5^oC. Payne (1958a and b). This change is very small in comparison with the other effects of filler and is similar to that produced by the glass beads in polyisobutylene as discussed earlier.

CHAPTER 3

DIELECTRIC PROPERTIES (Temperature and frequency dependence).

3.1 INTRODUCTION

In chapter 1 it was pointed out that energy can be dispersed in a polymer by interaction of electrical as well as mechanical waves with the segmental modes of motion. It is known that the main mechanical and dielectric absorption peaks coincide approximately in the glass-rubber transition region, while the reciprocal of the dielectric constant behaves analogously to the elastic modulus. (See Fig. 2.5) This part of the review shows the close similarity in the behaviour of the dielectric properties in regard to frequency and temperature changes, to the dynamic mechanical behaviour discussed in chapter 2. It also shows how some of the relaxation distribution functions for dielectrics adequately describe the experimental data for natural rubber.

The first part of this chapter is a summary of the earlier published work in the field of dielectric properties of rubber, particularly in regard to variations in dielectric properties due to variations in compounding of the rubber. The main and later parts of this chapter illustrate the use of the WLF transform

techniques to derive master curves of the dielectric properties. These derived master curves are then amenable to analysis for their relaxation distributions. This part of the thesis is based on published data of Payne (1958a), Payne (1958b) and Norman and Payne (1965).

A number of good books and review papers dealing with the relation between the electrical behaviour and the molecular structure of elastomers have appeared, so that it is only necessary here to give a brief summary of the literature. Particular attention is directed to books by Smyth (1955) and von Heppel(1954) and the "General Discussion on Dielectrics" held at the University of Bristol in (1946), Books by Birks (1960), Böttcher (1952), Frölich (1949) and van Vleck (1932), and reviews by Brown (1956) Magat and Reinisch (1962), Schlosser (1960), Wurstlin and Thurn (1956) Wyllie (1960) and Curtis (1960) will also be found useful. A recent review by McPherson (1963) is of great value. A summary article by von Heppel (1958) is included in a recent Handbook of Physics. The fundamental analogies between mechanical and electrical dispersions have been explored by Hoff (1955), Schmieder and Wolf (1951 and 1953).

Staverman (1953), Ferry and Landel (1956), Mikhailov (1951) Payne (1958). Ferry and Strella (1958), Fuoss (1941). Deutsch (1954), Nielsen (1950), Oakes (1954) Thurn (1956) and their respective co-workers.

In many cases attempts to correlate mechanical and electrical properties have been moderately successful, the correlation being best when the dipolar part of the molecule is connected directly to the backbone chain, as it is for instance in polyvinyl chloride. If the dipole is in a side chain, as in polymethyl methacrylate, the main peak does not correlate with the main mechanical damping peak (Deutsch, Hoff and Reddish 1954), because although the mechanical peak is associated with molecular motions of the main backbone of the polymer chain the main electrical peak is associated with the motion of side chains.

LISTS OF SYMBOLS USED IN CHAPTER 3

In this list ϵ_ω is a vector quantity defining real and imaginary parts (ϵ'_ω and ϵ''_ω). Likewise $\epsilon_{\omega,T}$ has real and imaginary parts ($\epsilon'_{\omega,T}$ and $\epsilon''_{\omega,T}$) etc.

SYMBOL	DEFINITION
A	coefficient of cubical expansion
C	capacitance
C_p	capacitance with dielectric between electrodes
C_v	capacitance with vacuum between electrodes
E	voltage gradient in volts per centimetre
E_o	activation energy
F	electric field
F_o	maximum amplitude of oscillation of electric field
$G(\tau)$	distribution function of τ
M	molecular weight
N	Avogadro's number. Number of monomer units/unit volume
N'	number of sulphur atoms/unit volume.
P_o	orientation polarisation.
P_i	induced polarisation.
R	resistance of an equivalent parallel circuit.
T	temperature of measurement (^oK)
T_o	arbitrary reference temperature (^oK)
T_s	value of T at which $\frac{d}{dt}(\log_{10} b'_T) = -0.0872$
V	potential energy
b	curve-width parameter: Wagner- Yager
b_T	τ_T/τ_o when $T_o = T_s$

SYMBOL	DEFINITION
d	density
f	frequency in cycles per second
f'	$\frac{\epsilon'_{\omega,T} - \epsilon_{\infty,T}}{K_T}$ as a function of ωb_T
f''	$\frac{\epsilon''_{\omega,T}}{K_T}$ as a function of ωb_T
K'_T	$\frac{\rho_T}{\rho_o}\frac{T_o}{T} = [1-A(T-T_o)]\frac{T_o}{T}$
K_T	$[1-A(T-T_s)]\frac{T_s}{T}$
m	b_T/b'_T
n	total number of molecular dipoles
n	refractive index
n_1	number of molecules jumping to positive or parallel positions per second.
n_2	number of molecules jumping to negative positions per second.
n_∞	refractive index at very long wavelengths
n_D^T	refractive index for sodium D line at T
N_∞^T	refractive index for infinite wavelength at T
Z	value below which dipole moment of rubber monomer cannot lie.

SYMBOL	DEFINITION
α	Curve-width parameter. Fuoss-Kirkwood or the polarisability of a single molecule.
β	Curve-width parameter : Cole-Cole
γ	Curve-width parameter : Frölich
Δ	general curve-width parameter
$\epsilon_{\omega,T}$	complex dielectric constant $\epsilon'_{\omega,T} - j\,\epsilon''_{\omega,T}$ at ω, T
ϵ_D	dipolar part of dielectric constant
ϵ_τ	contribution to ϵ_D of dipoles of time constant τ
$\epsilon_{s,T}$	static dielectric constant at T
$\epsilon_{\infty,T}$	infinite frequency dielectric constant at T
$\epsilon_{\omega,o}$	$\frac{\epsilon_{\omega,T} - \epsilon_{\infty,T}}{K'_T} + \epsilon_{\infty,o}$
$\epsilon_{\infty,o}$	value of $\epsilon_{\infty,T}$ at $T = T_o$
ϵ_ω	$\frac{\epsilon_{\omega,T} - \epsilon_{\infty,T}}{K_T} + \epsilon_\infty$
ϵ_o	dielectric constant with vacuum between electrodes
ϵ_s	static dielectric constant at T_s
ϵ_∞	infinite frequency dielectric constant at T_s
ϵ''_β	background value of ϵ''_ω
ϵ''_m	maximum value of ϵ''_ω
μ	dipole moment
$\bar{\mu}$	average dipole moment
μ_s	moment of dipole containing 1 sulphur atom
ρ_T	density at T_o
ρ_o	density at T_o
ρ_s	density at T_s
τ	relaxation time
τ_T	value of τ for a given process at T
τ_o	value of τ for a given process at T_o
ψ''	function relating $\frac{\epsilon''_\omega - \epsilon''_\beta}{\epsilon''_m - \epsilon''_\beta}$ to log $\frac{\omega b_T}{\omega_m}$ and Δ
ϕ	average jump or rotation frequency
ϕ_o	average jump or rotation frequency in the absence of an applied field
ω	2π x frequency of measurement
ω_m	value of ωb_T corresponding to ϵ''_m

PLEASE UNFOLD THIS PAGE TO SUPPLY AN EASY REFERENCE

TO A LIST OF SYMBOLS USED IN THIS

CHAPTER 3.

3.2 DEFINITIONS AND ELEMENTARY THEORY OF DIELECTRIC DISPERSION (~~Curtis~~ McPherson 1963)

3.2.1 Dielectric constant. - The fundamental definition of dielectric constant is given in terms of forces between point charges in a homogeneous unbounded medium. The definition involves conditions that can never be realized experimentally, so for practical purposes, dielectric constant is defined in terms of capacitance ratio, and is correctly known as the 'relative dielectric constant'.

The 'relative dielectric constant', ϵ', of an insulating material is the ratio of the capacitance, C_p, of a given configuration of electrodes with the material as the dielectric, to the capacitance, C_v, of the same configuration of electrodes with vacuum as the dielectric.

$$\epsilon' = C_p/C_v \qquad 3.1$$

To indicate its relative nature, dielectric constant is sometimes written as ϵ'/ϵ_o, where ϵ_o the dielectric constant of a vacuum, is taken as unity. For the rest of this review ϵ' will however be referred to as the dielectric constant.

3.2.2 Dissipation factor. - In a capacitor in free space (or for practical purposes, in air) the current, which flows when an electromotive force is applied, is 90 degrees out of phase with the electromotive force, and there is no power loss. When a solid or liquid insulating material is between the plates of the capacitor, however, the current which flows is out of phase with the electromotive force by angle, θ, which differs from 90 degrees by a small angle, δ, thus causing the loss of power. The tangent of this angle is the dissipation factor.

$$\text{Tan}\,\delta = 1/\omega RC, \qquad 3.2$$

where C is the capacitance, R is the resistance of an equivalent parallel circuit, and ω is 2π times the frequency in cycles per second. The dissipation factor is a dimensionless constant and its determination requires no measurement of the dimensions of the specimen. Dissipation factor is often termed power factor.

3.2.3 Loss index (or imaginary part or out-of-phase component of the complex dielectric constant) - Loss index, which is represented by ϵ'', is the product of the dielectric constant and the dissipation factor.

$$\epsilon'' = \epsilon' \tan\delta \qquad 3.3$$

As the name indicates the loss index is a measure of the power lost in an imperfect dielectric when it is subjected to an alternating field. The heat generated in watts/cc for a sinusoidal voltage is:-

$$W/cm^3 = 5/9\ fE^2(\epsilon' \tan\delta) \times 10^{-12}, \qquad 3.4$$

where f is the frequency in cycles per second; E the voltage gradient in volts per centimeter, ϵ' the dielectric constant; and $\tan\delta$ the dissipation factor.

3.2.4 Complex dielectric constant

The complex dielectric constant ϵ^* can be represented by

$$\epsilon^* = \epsilon' - i\epsilon'' \qquad 3.5$$

If the dipoles have a single relaxation time τ, the electrical properties can be defined by the following equations:-

$$\epsilon' = \epsilon_\infty + \frac{\epsilon_s - \epsilon_\infty}{1 + \omega^2\tau^2} \qquad 3.6$$

$$\epsilon'' = \frac{(\epsilon_s - \epsilon_\infty)\omega\tau}{1 + \omega^2\tau^2} \qquad 3.7$$

where ϵ_s is the dielectric constant at zero (or static) frequency and ϵ_∞ is the dielectric constant at infinite frequency. The loss factor goes through a maximum when $\omega\tau = 1$. These last equations are derived in chapter 2 for the real and imaginary part of the dynamic compliance. Actual polymers have many electrical relaxation times instead of a single one, just as polymers have a distribution mechanical relaxation times. The distribution of relaxation times spreads the loss factor curves over a wider frequency range than would have been found with a single relaxation time.

3.2.5 Dielectric Dispersion

If a dipole system is subjected to an alternating electric field, the contribution of the dipoles to the dielectric polarization will depend upon the frequency of the applied voltage. When the dipoles are unable to rotate fast enough to keep up with the field at very high frequencies, the orientational polarisation drops towards zero. This effect may be described in several nearly equivalent ways and a detailed discussion is given in an excellent book by Frölich (1949). It will be useful here to discuss a simplified model to illustrate the mecahnism

of dispersion in dielectrics.

Suppose a dipole of moment μ is rigidly fixed to a small molecule and can only rotate into two positions, one parallel and one antiparallel to the axis, and that for the molecule to rotate from its one equilibrium position to the other, an activation energy E_0 is required. The chance that a given molecule has enough energy to rotate is given by the Boltzmann distribution function and is proportional to exp $(-E_0/kT)$.

If an electric field is applied to the material and if it is directed along the $+x$ axis, the dipoles will preferentially rotate so as to line up with it. In particular, if the potential energy of the dipole (because of the electric field) is taken as zero when the dipole is perpendicular to the field and $\pm V$ when parallel to it, the chance of a molecule rotating so as to be parallel to the field is proportional to:-

$$\exp\ [(-E_0/kT) + (V/kT)] \qquad 3.8a$$

The chance for the antiparallel rotation is proportional to exp. $[-(E_0/kT) - (V/kT)]$. If a 180^0 rotation is designated a jump and if the result is

expressed in terms of the jump frequency ϕ, the average number of molecules jumping to the positive or parallel position per second is

$$n_2 \phi_0 \exp (V/kT) \qquad 3.8b$$

and for the reverse direction

$$n_1 \phi_0 \exp (-V/kT) \qquad 3.8c$$

In these expressions, n_1 and n_2 are the number of molecules parallel and antiparallel to the field respectively. The quantity ϕ_0 is the average jump or rotation frequency in the absence of an applied field. n_1 plus n_2 must equal the total number of molecules.

It is now possible to write an expression for the quantity (dn_1/dt), the rate of change of the number of molecules aligned with the field. This quantity will be the difference between the number of molecules rotating into the positive direction and the number rotating out of the positive direction into the negative direction:-

$$dn_1/dt = n_2\phi_0 \exp (V/kT) - n_1\phi_0 \exp (-V/kT) \qquad 3.8d$$

Also, from the same reasoning,

$$dn_2/dt = - n_2\phi_0 \exp (V/kT) + n_1\phi_0 \exp (-V/kT) \qquad 3.8e$$

As V/kT is very much less than unity, for $V=\mu F$ where F is the electric field, F is seldom larger than 10 ergs/esu/cm and since μ is of the order 10^{-18} esu-cm, $V/kT \simeq 10^{-2}$, it is possible to expand the exponentials of Eqs 4.8d and e to give

$$dn_1/dt = \phi_0[(n_2-n_1) + (n_2+n_1)(\mu F/kT)] \qquad 3.8f$$

and

$$dn_2/dt = \phi [(n_1-n_2) - (n_2+n_1)(\mu F/kT)] \qquad 3.8g$$

The net number of dipoles aligned with the field v is (n_1-n_2) Then from equations 3.8f and g we have

$$dv/dt = 2\phi_0 [-v + n(\mu F/kT)] \qquad 3.8h$$

where n is the total number of molecules. If the field F is oscillating sinusoidally according to the relation $F=F_0 \sin(\omega t)$, the solution of eq. 4.8h is

$$(v/v_0) = (1+\omega^2\tau^2)^{-1} [\sin(\omega t) + \omega\tau \cos(\omega t)] \qquad 3.8i$$

where

$$v_0 = n\mu F_0/kT \qquad \text{and} \qquad \tau = 1/2\phi_0$$

It is clear from this result that the polarisation possesses two components, one in phase and one 90^0 out of phase with the applied field. The component in phase gives rise to the ordinary

dielectric constant, the so-called "real part" of the dielectric constant, which is called ϵ'.
Since the in-phase portion of the polarisation varies as $(1+\omega^2\tau^2)^{-1}$, it is essentially constant at low frequencies and then drops rapidly near $\omega \approx 1/\tau$ and eventually becomes nearly zero at very high frequencies as shown in the figure below

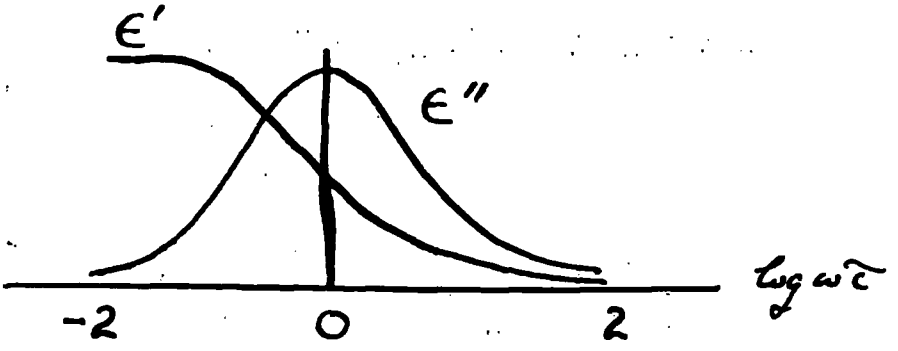

The dielectric constant will not drop to zero in actual materials since induced polarisation will still be present.

The portion of the polarisation out-of-phase with the field gives rise to the so-called "imaginary part" of the dielectric constant. This is seen by considering the energy loss per cycle. Since the force on an average dipole is proportional to $F_0 \sin \omega t$ the energy loss per cycle will be the integral over one cycle of this force times the rate of change

of the net number of aligned dipoles. Hence,

$$\text{Loss} = \oint (dV/dt)\mu F_0 \sin\omega t\,dt \qquad 3.9a$$

On integrating one has:-

$$\text{Loss} = (\text{const})\ \omega\tau/(1+\omega^2\tau^2) \qquad 3.9b$$

Hence the loss is proportional to the out-of-phase portion of the polarisation. It is very low at both high and low frequencies and it goes through a maximum at the frequency where ω is equal to $1/\tau$. The variation of the loss index with frequency is also shown in the sketch above.

The curves shown in the sketch above are referred to as the "Debye dispersion curves", after Debye who was the first to obtain them on dielectrics. There is great similarity between these real and imaginary permittivity curves and the mechanical dynamic compliance and loss curves of Fig. 2.18. In practice, the actual dispersion curves for polymers are wider than for a simple Debye material such as simple polar molecules in dilute solutions.

The exact magnitude of the polarisation, P_o, due to the dipole orientation of molecules with average dipole moment μ is:-

$$P_o = 4\pi\mu^2 N/9kT \qquad 3.10a$$

where N is Avogadros' number.

Another contribution to the total molecular polarisation comes from the dipoles induced in the molecules by the applied electric field. This 'induced' polarisation P_i and the 'orientational' polarisation P_o are related to the observed dielectric constant of the material through the relation:-

$$\frac{(\epsilon-1)}{(\epsilon+2)}\frac{M}{d} = P_i + P_o \qquad 3.10b$$

where M and d are the molecular weight of the molecule and the density of the material respectively.

Since it is known that the electrons can move extremely rapidly within the atoms, P_i would not be expected to change with frequency. The induced polarisation is able to follow fluctuating electric fields even at frequencies as high as the optical range. On the other hand, the orientation polarisation, being the result of the rotation of groups of atoms that form a dipole, will not be able to follow extremely high-frequency oscillations of the electric field. As the dipoles keep alternating in step with the electric field, they experience viscous forces proportional to the velocity of rotation. If the frequency of the applied voltage becomes too high, the dipoles will be

moving too sluggishly under the action of the viscous and electric forces to respond well to the electric field. In fact, at very high frequencies, the dipoles will be unable to keep up with the alternating field, and their contribution to the polarisation drops to zero.

At high frequencies, however, the induced polarisation is essentially unchanged. From electromagnetic theory it may be demonstrated that the dielectric constant at optical frequencies is equal to the square of the index of refraction (more correctly, the index of refraction at very long wavelengths, n_∞) so that

$$P_i = [(n_\infty^2-1)/(n_\infty^2+2)]M/d \qquad 3.10c$$

Therefore, if the refractive index is known, one can substitute from 3.10c into 3.10b, and the orientation polarisation can be computed from a knowledge of the dielectric constant. If the dipoles are able to follow the applied electric field, then equation 3.10a applies, and the average dipole moment for the molecules can be computed.

All the above considerations are based on the premise, that the molecular dipoles are not interacting with each other in such a way as to cause

molecular association or other types of intermolecular restrictions to dipole alignment.

3.3 TYPES OF POLARISATION INVOLVED IN DIELECTRICS (MacPherson, 1963)

When a dielectric material is placed in an electric field, the polarisation that occurs is the result of the formation of electric dipoles in the material. These dipoles may be produced by four different mechanisms and, accordingly, constitute four different components of the total polarization. These components, some of which have already been mentioned, are:

1. Electronic polarization or induced polarization resulting from the displacement of the electronic cloud about each atom with reference to the positively charged nucleus;

2. Atomic polarization, arising from the displacement of atoms as a consequence of the asymmetric distribution of charge within the atom;

3. Dipole or orientation polarization, in consequence of the tendency of electric dipoles, if any are present, to align themselves with the electric field; and

4. Interfacial or space charge polarization, resulting from the motion of ions in the dielectric medium.

Each of these components of the total polarization, will be considered in turn.

3.3.1 ELECTRONIC OR INDUCED POLARIZATION

The electrons occupying shells or orbits around the positively charged nuclei of the atoms are displaced by a small amount with reference to the nuclei when an electric field is applied to a dielectric. The shift or displacement of the positive and negative charges in the atom from their previously symmetrical arrangement gives rise to an induced dipole, which serves to store the energy taken up from the electric field in producing the displacement. On the removal of the field the energy is restored to the system without loss, the action being analogous to that of a perfect spring.

The electronic displacement of induced polarization is responsible for the refraction of light. The time in which it takes place is about 10^{-15} second, an interval which corresponds approximately to the frequency of ultraviolet light. Thus, in the

visible spectrum, the polarization as measured by the index of refraction is affected by the frequency or the wavelength of the light to a significant extent in the violet, and to a progressively lesser extent with decrease in frequency. From the index of refraction measured at different wave lengths it is possible to compute an index for infinite wave length or zero frequency. This index is smaller than the index in the visible spectrum.

Relation of dielectric constant to refractive index

The dielectric constant and the index of refraction have a common basis in the dielectric polarization by the relation found by Maxwell and discussed above, i.e.

$$n^2 = \epsilon', \qquad 3.10d$$

where n is the refractive index and ϵ' is the dielectric constant. This relation holds true to the extent that the dielectric constant is due to electronic polarization, and other types of polarization are non-existent or negligible in amount. Thus, the square of the refractive index, extrapolated to zero frequency, may be taken as the limiting lower value of the dielectric constant

The refractive index of natural rubber, measured for the customary D line of sodium, n_D^{25}, is 1.519. The computed value at zero frequency or infinite wave length n_∞^{25}, corresponds to a dielectric constant of 2.25. The observed value, as noted in a subsequent section, is about 2.36, when measured at a frequency of 10^5 cycles per second. The difference between 2.25 and 2.36 indicates the presence of residual impurities in natural rubber, which give rise to other types of polarization. This is discussed further in Appendix 6.1, which considers experimental results for a range of natural rubber vulcanisates.

The refractive index of a substance is related to the molar refraction, R, by the well-known Lorentz-Lorenz expression,

$$\frac{M(n_\infty^2 - 1)}{d(n_\infty^2 + 2)} = \frac{4\alpha N}{3} = R, \qquad 3.10e$$

where N is Avogadro's number, 6.024×10^{23}, and α is the polarizability of a single molecule; M is the molecular weight or formula weight of the substance, and d is the density.

The usefulness of the Lorentz-Lorenz equation in connection with both the refractive index and the dielectric constant lies in the fact that for most organic substances the molar refraction can be found quite accurately by summing up the refractions of the atoms in the molecule. This additive relation is possible, because the valence electrons and the electrons within the atoms maintain the same configuration in similar compounds. From measurements on a large number of organic compounds, tables have been compiled giving atomic refractions for all common atoms and the increments of molar refraction contributed by particular structural features such as double or triple bonds.

Table 3.1 gives numerical values of atomic refractions and contributions due to structural features that may be of use in calculating the dielectric constant of non-polar elastomers. These values have been taken

TABLE 3.1

INCREMENTS OF REFRACTION BY ATOMS, RADICALS, AND STRUCTURAL FEATURES AT 20°C.

Atom, radical, or bond	Refraction increment
Carbon	2·54
Hydrogen	1·01[a]
Hydroxyl oxygen	1·48
Ether oxygen	1·715
Chlorine	5·75
Fluorine	1·60[b]
Nitrile	5·33
Sulfur (sulfide)	7·60
Thiol (SH)	8·42
Double bond	1·417

[a] The value, 1·03, for hydrogen leads to better agreement between calculated and observed values in some cases.

[b] The value, 1·60, is taken from measurements on fluorine gas. Measurements on some fluorine-containing organic compounds give the value, 0·76.

TABLE 3.2

DIELECTRIC CONSTANT CALCULATED FROM MOLAR REFRACTION

Substance	Density, g/cm^3	Dielectric Constant		Source of observed value
		Calculated	Observed	
Polyethylene	0·9200	2·282	2·276	McCall (1957)
Polyethylene	0·9183	2·273	2·273	Lanza and Herrmann (1958)
Polyethylene	0·9593	2·361	2·357	Lanza and Herrmann (1958)
Gutta-percha	0·961	2·383	2·40	Kemp (1938)
Natural rubber	0·914	2·27	2·36	McPherson (1932) Norman-and Payne (1965), Payne (1958a)
Polytetrafluoroethylene	2·13	1·966	2·009	Ehrlich (1953)
Pentane	0·630	1·841	1·844	Maryott and Smith (1951)
Heptane	0·682	1·913	1·914	Maryott and Smith (1951)

Data from Batsenov (1961) and McPherson (1963) and recently published data Payne (1958) and by Norman and Payne (1965)

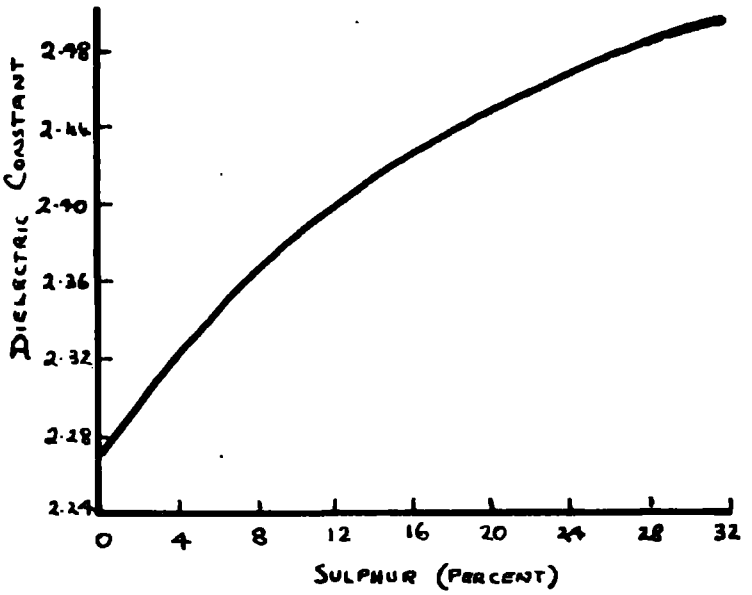

FIG 3·1. Dielectric constant of rubber-sulphur vulcanisates calculated from molar refraction (MacPherson 1963).

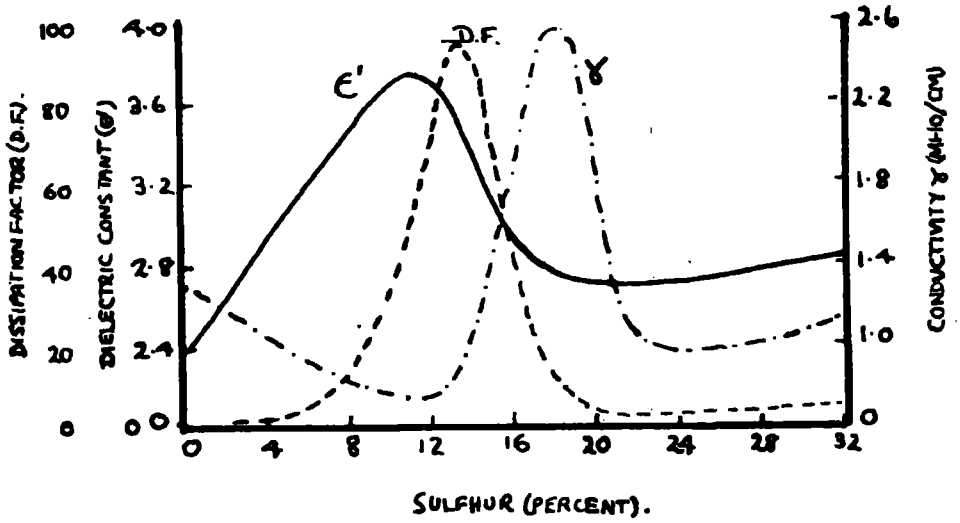

FIG 3·2. Variation of dielectric constant, dissipation factor, and conductivity of rubber-sulphur vulcanisates with sulphur content. Measurements at 1000 cps 25° C. (Scott, MacPherson and Curtis 1923. MacPherson 1963)

from a recent book by Batsenov (1961), but they differ only slightly from values compiled at the beginning of the century.

Calculation of dielectric constant.

Table 3.2 shows values of the dielectric constant of several non-polar elastomers and two liquid hydrocarbons at 20°C, calculated from the observed density and the molar refraction found from data given in Table 3.1. The agreement is good except for natural rubber which, even after purification, probably contained some residual polar substances.

Fig. 3.1 plots the dielectric constant of rubber-sulphur vulcanisates calculated from the molar refraction value in Table 3.1

3.3.2 Atomic Polarization

The second possible effect of an electric field is the displacement of atoms with respect to each other. This action requires about 10^{-12} to 10^{-14} second, a longer time than for the displacement of the electrons. This time corresponds to the frequency of infrared light, however polarization arising from this source is negligibly

small for nonpolar elastomers.

3.3.3 Polarization From Dipole Rotation

The third effect relates to dipoles, which if present, may make a very significant contribution to the total polarization. In polar molecules the valence electrons occupy positions with reference to the positively charged nuclei such that the centre of gravity of the negative charges does not coincide with the centre of gravity of the positive charges. Because of this separation of the charges the molecule behaves as an electric dipole. On the application of an electric field the dipole tends to orient in the direction of the field. This tendency is opposed by thermal agitation and by the rigidity of the molecule. The time involved in orientation may range from 10^{-10} second to minutes, hours, or even days, depending on the molecule and on the size of the structural unit to which it belongs.

3.3.4 Interfacial or Space Charge Polarization

The fourth effect of a field applied to a dielectric, is the transport of ions through the material. With non-polar materials, a very large proportion of the ions come from impurities including water soluble salts and moisture.

Repeated purification and drying of non polar polymers usually raises the resistivity to the limit of measurement and the production of ions from the polymer itself is small in purified natural rubber compounds.

3.4 SUMMARY OF EARLIER WORK ON THE EFFECT OF COMPOUNDING ON DIELECTRIC PROPERTIES WITH PARTICULAR REFERENCE TO TEMPERATURE-FREQUENCY CHANGES.

3.4.1 Effect of vulcanization

The vulcanization of natural and synthetic rubbers is accomplished by the addition of sulphur, oxygen, or other reactive substances to the double bonds in adjacent polymer chains, in such a way as to produce crosslinking. Because of the polar nature of the vulcanizing agents, the dielectric constant and the dissipation factor increases whilst the resistivity decreases.

The effect of sulphur on the electrical properties of rubber may be explained in terms of the increase in polarisation brought about by

1) the electronic polarisation of the sulphur

and 2) the rotation of the electric dipole in the carbon-sulphur bond which tends to align itself with the applied field.

TABLE 3.3

LECTRIC CONSTANT AND DISSIPATION FACTOR OF COMPOUNDS OF PURIFIED NATURAL RUBBER AND SULPHUR AT FREQUENCIES OF 60 TO 300,000 CPS at 25°C

Scott, McPherson and Curtis (1933)

ıur	Property	Frequency, cps				
		60	1000	3000	100,000	300,000
	Dielectric constant	2·36	2·37	2·36	2·36	2·38
	Dissipation factor	0·0023	0·0014	0·0011	0·0008	0·0008
	Dielectric constant	2·67	2·66	2·66	2·69	2·70
	Dissipation factor	0·0019	0·0016	0·0018	0·0116	0·0195
	Dielectric constant	2·93	2·92	2·92	2·98	2·92
	Dissipation factor	0·0016	0·0022	0·0034	0·0312	0·0426
	Dielectric constant	3·51	3·48	3·44	3·05	2·90
	Dissipation factor	0·0033	0·0131	0·0235	0·0748	0·0794
	Dielectric constant	4·04	3·74	3·54	2·83	2·75
	Dissipation factor	0·0284	0·0706	0·0879	0·0642	0·0451
	Dielectric constant	2·84	2·76	2·74	2·68	2·69
	Dissipation factor	0·0256	0·0135	0·0114	0·0094	0·0096
	Dielectric constant	2·74	2·73	2·72	2·70	2·71
	Dissipation factor	0·0017	0·0025	0·0033	0·0063	0·0079
	Dielectric constant	2·84	2·82	2·81	2·78	2·78
	Dissipation factor	0·0035	0·0043	0·0047	0·0072	0·0077

tional note to table 3.3.

The "short time" conductivity exhibits changes with sulphur content, temperature, and frequency that are quite similar to the changes of the dissipation factor under the same conditions, as would be expected.

SULPHUR AT TEMPERATURES OF -75° to 195°C AT 1000 CPS

Sulphur %	Property	-75	-20	0	25	65	125	195
0	Dielectric constant	2·42	2·52	2·40	2·37	2·33		
	Dissipation factor	0·0014	0·0014	0·0012	0·0014	0·0033		
2	Dielectric constant	2·43	1·75	1·73	1·66	2·57	1·51	2·39
	Dissipation factor	0·0011	0·0207	0·0042	0·0016	0·0025	0·0030	0·0037
4	Dielectric constant	2·51	2·93	3·04	2·92	2·80	2·67	2·51
	Dissipation factor	0·0013	0·0493	0·0126	0·0022	0·0019	0·0018	0·0030
8	Dielectric constant	2·55	2·69	3·32	3·48	3·30	3·05	2·82
	Dissipation factor	0·0020	0·0298	0·0699	0·0131	0·0018	0·0008	0·0031
12	Dielectric constant	2·59	2·62	2·83	3·74	3·79	3·44	3·11
	Dissipation factor	0·0022	0·0047	0·0508	0·0706	0·0050	0·0006	0·0056
18	Dielectric constant	2·62	2.66	2·67	2·76	4·10	4·05	3·74
	Dissipation factor	0·0038	0·0030	0·0031	0·0135	0·0749	0·0030	
23	Dielectric constant	2·63	2·68	2·70	2·73	2·87	4·45	
	Dissipation factor	0·0053	0·0043	0·0039	0·0025	0·0203	0·0223	
32	Dielectric constant	2·71	2·77	2·79	2·82	2·83	3·55	
	Dissipation factor	0·0050	0·0051	0·0052	0·0043	0·0043	0·0760	

FROM SCOTT, McPHERSON AND CURTIS (1933)

The relative contributions of these mechanisms will be discussed in the next section and again later in this chapter.

3.4.2 Variation of properties with temperature and frequency.

A summary of the dielectric constant and dissipation factor measurements obtained by ~~Swift~~ Scott, McPherson and Curtis on rubber-sulphur compounds at 25°C as a function of frequency is given in Table 3.3. Additional data obtained at a frequency of 1000 cycles per second but over a wide temperature range is given in Table 3.4 and some typical results shown in Fig. 3.2.

The changes in dielectric constant and dissipation factor with sulphur content are consistent with their being due principally to polarization of the carbon-sulphur dipoles. With increasing sulphur content, the number of dipoles is increased, and at the same time the rigidity of the medium is also increased but the dielectric constant and associated dissipation factor go through maxima, Fig. 3.2. These maxima are shifted to higher percentages of sulfur with increasing temperature, and to lower percentages of sulphur with increasing frequency, and at the hard rubber stage and

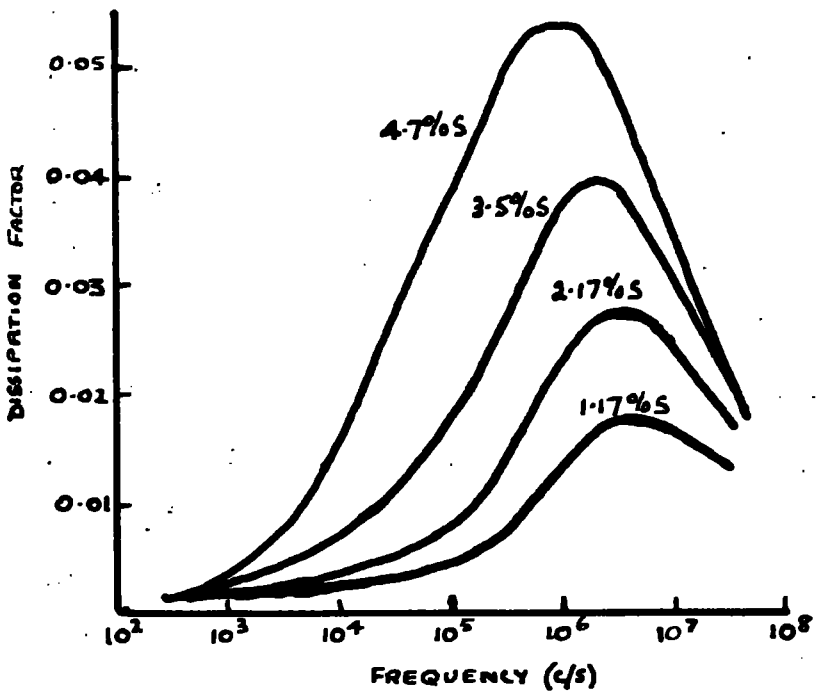

FIG 3·3. *Variation of dissipation factor of soft rubber vulcanisates with frequency. Schallamach (1951).*

at room temperature little more than the contribution of the electronic polarization remains.

Measurements on rubber-sulphur compounds at different temperatures and frequencies have been made by other investigators including Kimura, Aizawa, and Takeuchi (1928), Kitchin (1932), Schallamach (1951) and Waring (1951). The measurements by Kitchin were made at temperatures from 30° to 100°C and at frequencies from 600 cycles to 2 Mc per second. The values found were in good agreement with those reported in Tables 3.3 and 3.4, except at the higher temperatures and frequencies, where the nonhydrocarbon constituents may have increased the values by a small amount. Measurements at the Massachusetts Institute of Technology (1953) on a compound composed of pale crepe, 100 parts, and sulphur, 6 parts, gave a dielectric constant of 2·94 at a frequency of 10^2 cycles per second and 2·36 at 10^8 cycles per second. The former value is in agreement with the value, 2·93, given in Table 3.4 for approximately the same conditions.

Waring and Schallamach conducted extensive investigations of the dissipation factor of natural rubber vulcanizates in the soft rubber range for the purpose of studying the relation between the dissipation factor, on the one hand, and the sulphur content, accelerator types and mechanical

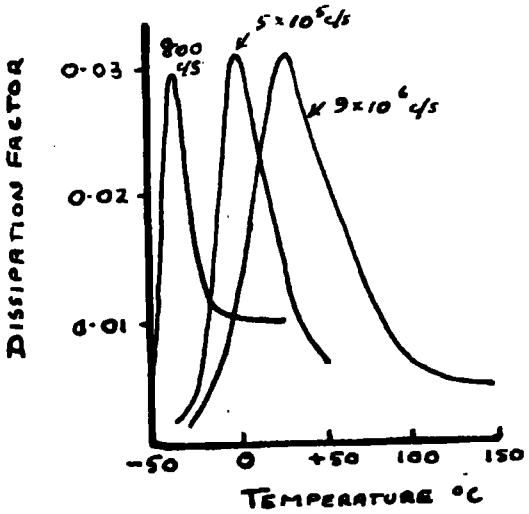

FIG 3·4 Variation of dissipation factor of soft rubber vulcanisates with temperature at different frequencies. (Waring 1951.)

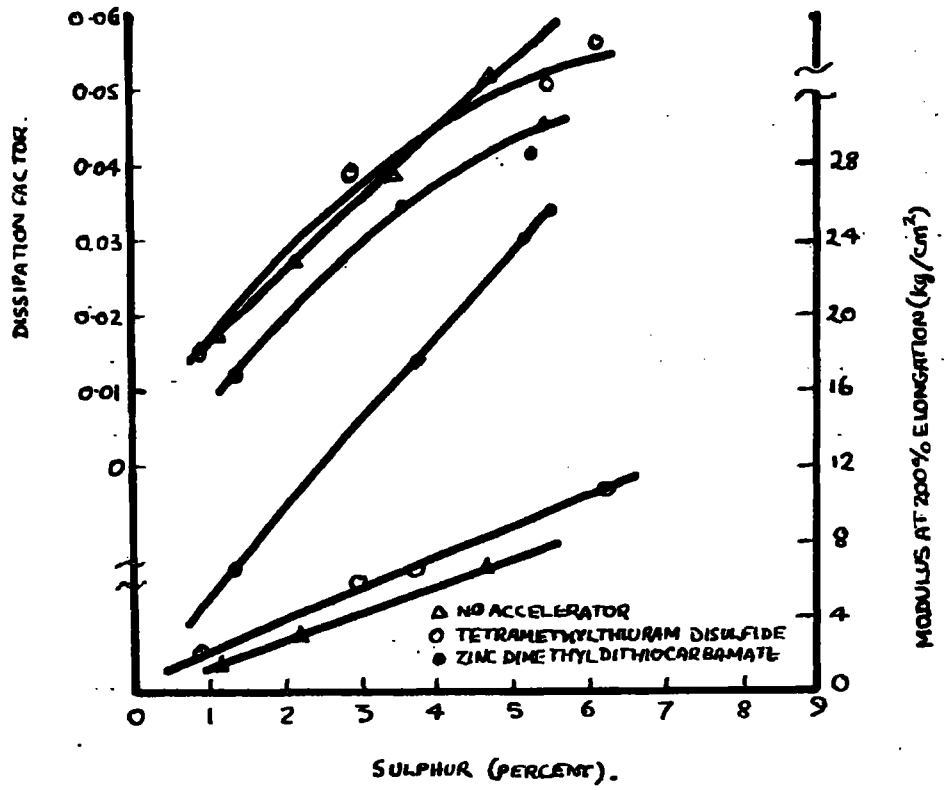

FIG 3·5. Variation of dissipation factor and modulus of soft rubber vulcanisates with per cent of combined sulphur, showing the effect of zinc. (Scheffamack 1957).

properties on the other. Schallamach's measurements were made at room temperature and covered the frequency range from 800 cycles to 40 megacycles per second, while Waring's were made from 0·1 to 40 megacycles per second, with some measurements at temperatures from -50° to 150°C. They found the same effects of frequency and temperature as those noted in the previous paragraphs. Figure 3.3 from Schallamach shows the variation of dissipation factor with frequency for vulcanizates containing different percentages of combined sulphur without accelerator. With increasing combined sulphur content the height of the maximum is increased, its base is broadened, and the frequency of the maximum is shifted in the direction of lower frequencies. This is clearly analogous to the shifting of the transition region to lower frequencies in the mechanical case. Figure 3.4 from Waring relates the dissipation factor at three different frequencies to the temperature. At low frequencies the dissipation factor reaches a maximum at lower temperatures, and the maximum is sharper than at higher temperatures; the height of the maximum is about the same for different frequencies.

Both investigators found significant differences in the dissipation factor of soft rubber vulcanizates cured to the same combined sulphur content with and without accelerators, and with and without zinc oxide. The use of zinc oxide or an accelerator containing zinc, as zinc diethyldithiocarbamate, gives a substantially lower dissipation factor for a given combined sulphur content than vulcanization with sulphur alone or with sulphur and an accelerator containing no zinc. This difference is shown by Figure 3.5 from Schallamach. These observations are interpreted on the basis that sulphur combines with rubber during vulcanization to form at least two types of compounds: crosslinks between the polymer chains, with the disulphide group, —S—S—, and heterocyclic groups arranged at random along the polymer chains, with the monosulphide group, —S—. Sulphur in the latter form contributes more to the polarization than the disulphide crosslinks. Thus, with the use of zinc a higher modulus is obtained along with lower combined sulphur content and lower dissipation factor.

Waring substantiates the explanation of the difference between the two modes of combination of sulphur by citing measurements on dilauryl monosulphide and disulphide. The former has an electric moment of $1{\cdot}66 \times 10^{-18}$ esu and the latter, $2{\cdot}01 \times 10^{-18}$ esu. Thus the

contribution to the polarization of two sulphur atoms in the monosulphide form would be more than one and a half times as great as the contribution of the disulphide group. Therefore the nature of the sulphur crosslink has a marked effect on dielectric properties. Reasonable understanding of the types of crosslink resulting from vulcanisation is only recent, and to date no dielectric experimental work has yet been carried out on very well defined vulcanisation systems. An excellent review of the complexities of sulphur vulcanisation appears in "The Physics and Chemistry of Rubber" by Bateman (1963) and is far too complex a subject to be discussed here.

Schallamach made the observation that prolonged drying of specimens reduced the dissipation factor, and that the effect was greater at the lower frequencies. For example, a specimen cured with zinc diethyldithiocarbamate containing 5·7 per cent of combined sulphur showed a dissipation factor at 800 cycles per second of 0·0045 before, and 0·0015 after drying while at 10^4 cycles per second the values were 0·015 and 0·0135, respectively. Similar observations have been recorded by Norman (1958).

3.5 RECENT EXPERIMENTAL DATA ON VULCANISED NATURAL RUBBER.

Samples of purified rubber were vulcanised for various periods in a frame mould, which was closed rapidly, thus forcing out air before the temperature had time to rise appreciably. The combined sulphur content, as a percentage of total weight of compound, was measured chemically. This data, together with the vulcanisation and reference details and the coefficients of cubical expansion, are given in Table 3.5

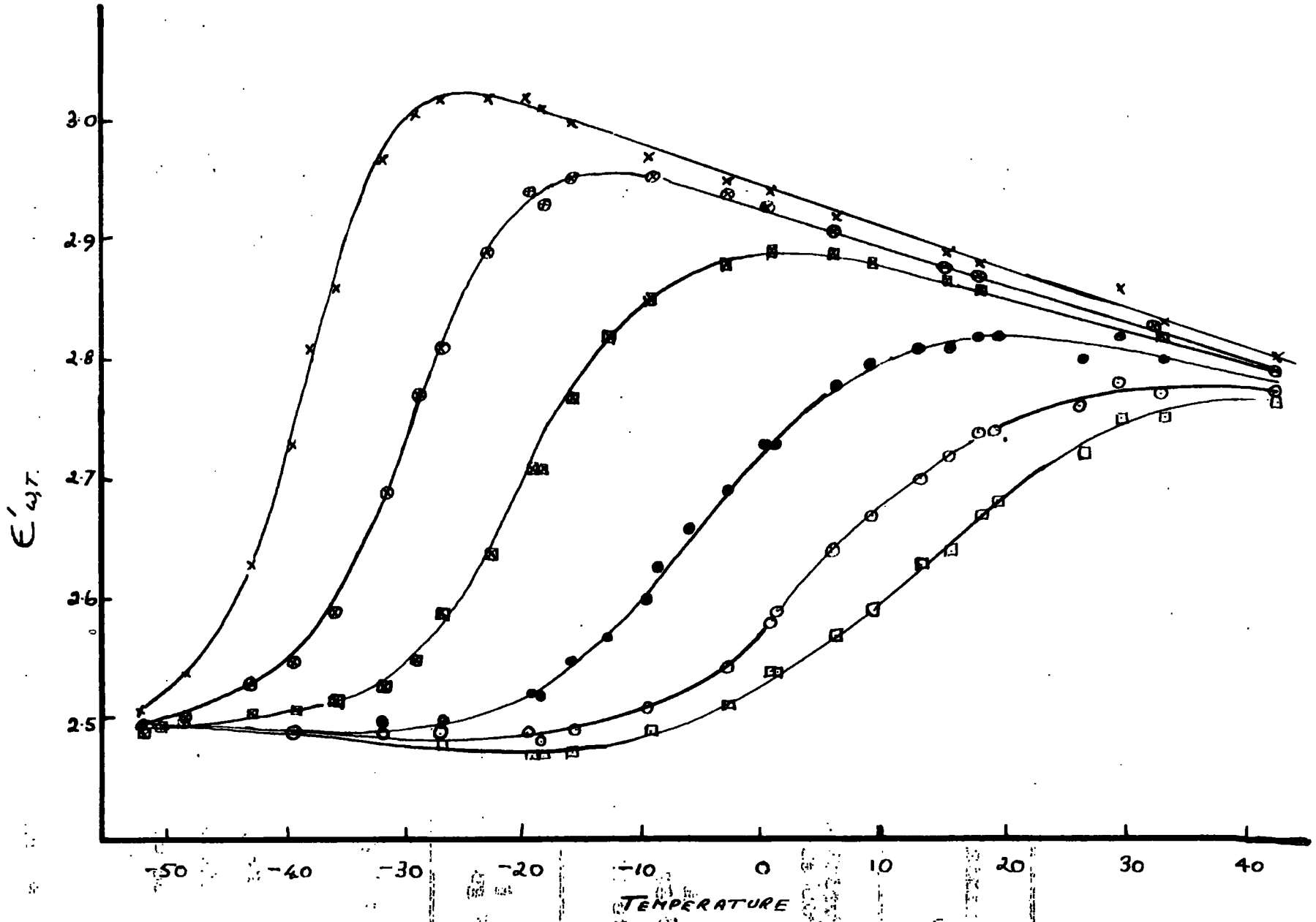
3·0
2·9
2·8
2·7
2·6
2·5
ε'ωT.
-50
-40
-30
-20
-10
0
10
20
30
40
TEMPERATURE

TABLE 3.5

DETAILS OF VULCANISATES

Mixing	Vulcanisation		Reference Code	Combined Sulphur %	Cubical Expansion Coefficient ($^{o}C^{-1}$)
	Time, hours	Temp, ^{o}C			
Purified rubbers					x 10^{-4}
	0·33	120	A 20*	0·1	5·0
	2	148	A 2	1·7	5·1
A 5 gm Sulphur	4	148	A 4	3·0	5·3
to 100 rubber	6	148	A 6	4·3	5·5
B 5 gms Sulphur	3	142	B 3	3·0	5·8

+ 1 gm Mercaptobenzthiazole to 100 parts of rubber.

The measured permittivity and loss factor results for B3* are given in Figs. 3.6 and 3.7. The summarised results for all samples, after the frequency and temperature reductions to be described, will be given and discussed in Sections 3.7 - 3.10.

* The number refers to the time of vulcanisation (in hours).

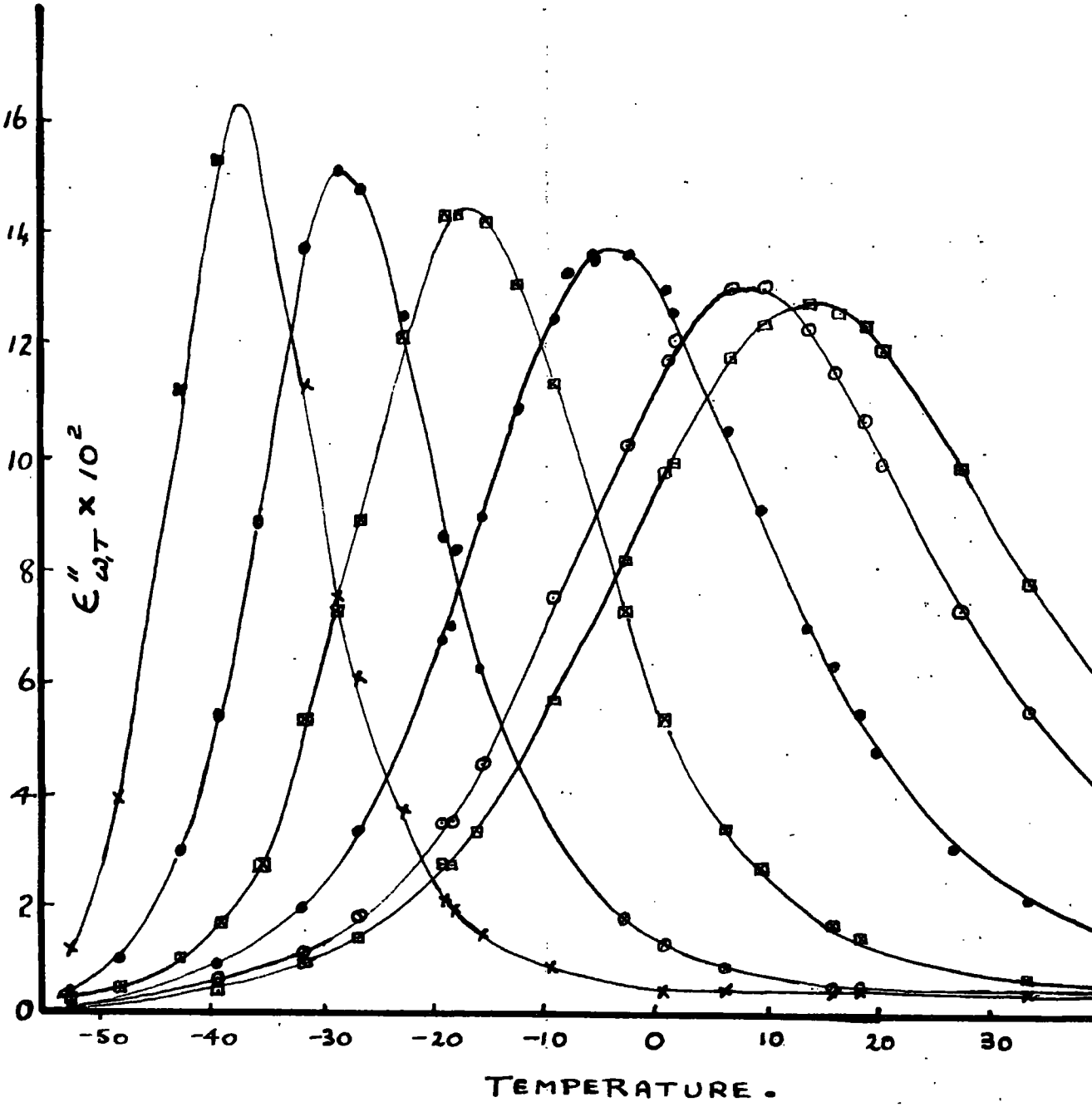

FIG 3.7. Loss factor of B3. Key to frequencies as in Fig. 3.6.

3.6 METHOD OF ANALYSIS OF DATA

The dipolar part of the dielectric constant of a medium is not due to dipoles having a single relaxation time (τ), but to dipoles having a distribution of relaxation times, Bottcher (1952). For a distribution, in which there are $NG(\tau)\,d\tau$ dipoles having relaxation times in an interval τ to $\tau + d\tau$ (N = total number of dipoles per unit volume), the dipolar part ϵ_D of the complex dielectric constant $\epsilon_{\omega,T}$ at an angular frequency ω and temperature T is given by:-

$$\epsilon_D = \epsilon_{\omega,T} - \epsilon_{\infty,T} = (\epsilon_{s,T} - \epsilon_{\infty,T}) \int_0^\infty \frac{G(\tau)}{1+j\omega\tau}\, d\tau \qquad 3.11$$

where $\epsilon_{s,T}$ and $\epsilon_{\infty,T}$, are the static and infinite frequency dielectric constants at T.

Perry and Fitzgerald (1953) made the following assumptions about the behaviour of the value of τ for a given elementary relaxation process and about the contribution of the process to the dielectric constant:-

(1) If τ_T is the value of τ at temperature T, and τ_o is the value of τ for the same elementary

process at temperature T_0,
then $\tau_T / \tau_0 = b'_T$, which is independent of τ .

(2) The contribution (ϵ_τ) of the dipoles having a time constant τ to the value of the dipolar portion ($\epsilon_{s,T} - \epsilon_{\infty,T}$) of the static dielectric constant is proportional to the density (ρ_T) of the material (.i.e. to the number of such dipoles per unit volume) and inversely proportional to the absolute temperature. [This is given by an approximation to the formulae of Debye (1912) and Onzager (1936) combined with the Lorenz-Lorentz (1886) equation if $\epsilon_{\infty,T}$ is constant. The exact expressions should be $\epsilon_\tau \propto \frac{\rho_T}{T} (\epsilon_{s,T} + 2)$ (Debye) and $\epsilon_\tau \propto \frac{\rho_T}{T} \frac{\epsilon_{s,T}}{2\epsilon_{s,T} + \epsilon_{\infty,T}}$ (Onsager), but the added refinement is unnecessary for the materials described here, where $\epsilon_{s,T}$ varies over such a short range. The Debye correction is about twice the Onsager correction, and the model used by either is probably inadequate for a close approximation in the present case. The extrapolation of the results to higher or lower temperatures would be effected by the approximations involved in this step.]

From these assumptions and eq. 3.11 it can be shown that the dipolar part of the complex dielectric

constant at temperature T and frequency ω is given by

$$\epsilon_D = \frac{\rho_T T_o}{\rho_o T} f\left\{\log_{10}(\omega b_T')\right\} \qquad 3.12$$

where ρ_o is the density at T_o.

Thus, if a measure of b_T' is available, and the function f is known for any one temperature, it is possible to compute the results for any other temperature. It is convenient at this stage to write

$$k_T' \equiv \frac{\rho_T T_o}{\rho_o T} \qquad 3.13$$

Determination of b_T' requires measurements at a number of temperatures. If the values of either the real or the imaginary parts of ϵ_D / k_T' are plotted against $\log_{10}\omega$ for a number of temperatures including T_o, a number of curves having identical shapes should result, and each should be displaced along the log ω axis by a distance $\log_{10} b'_T$ relative to the T_o curve. Many authors, Ferry and Fitzgerald, 1953, Ferry 1950, Williams (1955), Williams, Landel and Ferry (1955), Williams and Ferry

(1954) (1955), Zapas, Shufler and de Witt (1955), Payne (1957) (1958 a and b), Fletcher and Gent (1957), have shown this to be true experimentally both for dielectric constant and for its mechanical analogue (compliance) for many materials. The value of $\log_{10} b_T$ so obtained, is not proportional to $(\frac{1}{T} - \frac{1}{T_o})$, as it would be, if the activation energy were constant and the curve $\log_{10} b_T' = \phi' (T - T_o)$ varies with the value of T_o and with the material. Appendix 6.2 discusses further the relationship of activation energy to the WLF equation.

Williams et al (1955) examined the experimental curves of $\phi(T - T_o)$ and found that a particular value of T_o (known at T_s) could be chosen for each material, such that the function $\phi (T-T_s)$ was independent of the material. Since the original definition of T_s was related to a property of a particular material, it is convenient to re-define it as the value of T at which $\frac{\partial}{\partial T}(\log_{10} b_T)$ has the arbitrary value-0·0872. This value arises because T_s was originally defined in terms of the property of a particular material; the value is now too well established to amend the definition. If b_T is defined as the value of b_T' when $T_o = T_s$, the function found by Williams et.al. is

$$\log_{10} b_T = \phi(T-T_s) = - \frac{8.86 (T-T_s)}{101.6 + T - T_s} \qquad 3.14$$

This equation, together with the value of the parameter T_s, defines the activation energy at any temperature in the range over which the equation holds. From the two assumptions of Ferry and Fitzgerald and the experimental equations of Williams et. al. and taking the real and imaginary parts of eq.3,12 with eqs. 3.13 & 3.14 the real and imaginary parts (permittivity and loss factors) of the dielectric constant are given by:-

$$\frac{\epsilon'_{\omega,T} - \epsilon_{\infty,T}}{k_T} + \epsilon_\infty = f'(\log_{10} \omega b'_T) = f''\left(\log_{10} \omega - \frac{8.86(T-T_s)}{101.6+T-T_s}\right) \qquad 3.15$$

and

$$\frac{\epsilon''_{\omega,T}}{k_T} = f''(\log_{10} \omega b_T) = f''\left(\log_{10} \omega - \frac{8.86(T-T_s)}{101.6+T-T_s}\right) \qquad 3.16$$

where

$$k_T = \frac{\rho_T T_s}{\rho_s T} = \frac{T_s}{T}\left[1 - A(T-T_s)\right]$$

ρ_s is the density at $T = T_s$ and A is the coefficient of cubical expansion. ϵ_∞ is the value of $\epsilon_{\infty,T}$ when $T = T_s$.

From equations 3.15 and 3.16, it will be seen that the expression $\frac{\epsilon'_{\omega,T} - \epsilon_{\infty,T}}{k_T} + \epsilon_\infty$ is equal to the real part of the dielectric fonstant at temperature T_s

at a frequency ω and will be denoted by the symbol ϵ'_ω and likewise ϵ''_ω / k_T will be denoted by ϵ'_ω.

Thus the values of $\epsilon'_{\omega,T}$ and $\epsilon''_{\omega,T}$ for any temperature (T) and frequency (ω) within the experimental ranges, and with some uncertainty (principally because of the effects of other dispersion ranges having different values of T_s) outside the experimental ranges, may be calculated from the following parameters and functions, the determination of which will be described in the next section:-

1, A, coefficient of cubical expansion (measured by a conventional method).

2, T_s, a reference temperature.

3, $\epsilon_{\infty,T}$, the infinite frequency dielectric constant (as a function of T).

4, f' and f'' are empirical functions of $[\log_{10}\omega - \frac{8.86(T-T_s)}{101.6+T-T_s}]$. These may be plotted if A and T_s are known and $\epsilon_{\infty,T}$, $\epsilon'_{\omega,T}$, $\epsilon''_{\omega,T}$, are known for a range of T (or ω in the last two cases).

For many materials $f''(\log_{10}\omega b_T)$ passes through a maximum (ϵ''_m) at $\omega b_t = \omega_m$ (say), and for the rubbers described here, the curve of

$$\frac{\int'' \log_{10} \omega b_T - \epsilon''_B}{\epsilon''_\infty - \epsilon''_B}$$

(where ϵ''_B is a constant, termed the back-ground loss factor at $T = T_s$) in the region of the frequency of the maximum loss factor may be expressed as an analytic function $\left[\psi'' \log \frac{\omega b_T}{\omega_m}, \Delta\right]$, where Δ is a parameter, which determines the height/width ratio of the peak for a given form of this function. Then eq. 3.16 becomes

$$\epsilon''_{\omega,T} = \left[1 - A(T-T_s)\right] \frac{T_s}{T} \left[(\epsilon''_m - \epsilon''_B)\psi'' \left\{\Delta, \log_{10}\omega - \log_{10}\omega_m - \frac{8.86(T-T_s)}{101.6 + T - T_s}\right\} + \epsilon_B\right] \quad 3.17$$

Thus, the list of necessary information to calculate the values of $\epsilon''_{\omega,T}$ in the region of the peak value becomes:-

A coefficient of expansion (measured by a conventional method).

T_s a reference temperature.

ω_m the frequency of the peak loss factor at T_s.

ϵ''_m the value of the peak loss factor at T_s.

ϵ''_B a constant (the background loss factor at T_s).

ψ'' an analytic function of $\left(\Delta, \log_{10}\omega - \log_{10}\omega_m - \frac{8.86(T-T_s)}{101.6 + T - T_s}\right)$

Δ an arbitrary constant which occurs in certain forms of ψ''

The derivation of these parameters is described in Sections 3.7 and 3.8.

3.7 ANALYSIS OF THE DATA

In analysing the permittivity data, it is necessary to know $\epsilon_{\infty,T}$ over the experimental range of temperatures in the initial stages of the calculations and additionally at T_s for the later stages. Other authors have assumed that $\epsilon_{\infty,T}$ does not vary with T. In the case of the rubbers used in this investigation it was necessary to allow for the variation. In the absence of any other measure of $\epsilon_{\infty,T}$ it was assumed that an adequate approximation would be given by the square of the refractive index (extrapolated to infinite wavelength using Cauchy's formula) - see the Appendix 6.1. The coefficient of cubical expansion A must also be determined.

The values of $\frac{\epsilon'_{\omega,T} - \epsilon_{\infty,T}}{k'_T} + \epsilon_{\infty,0}$ and $\frac{\epsilon''_{\omega,T}}{k'_T}$ referred to as $\epsilon'_{\omega,0}$ and $\epsilon''_{\omega,0}$ (where $\epsilon_{\omega,0}$ is the value of $\epsilon_{\infty,T}$ at T_0) were calculated for $T_0 = 253^{\circ}K$ ($273^{\circ}K$ for unvulcanised rubber). The inclusion of the term $\epsilon_{\infty,0}$ at this stage does not modify the arguments of the previous section, but brings the method into line with that of previous authors.

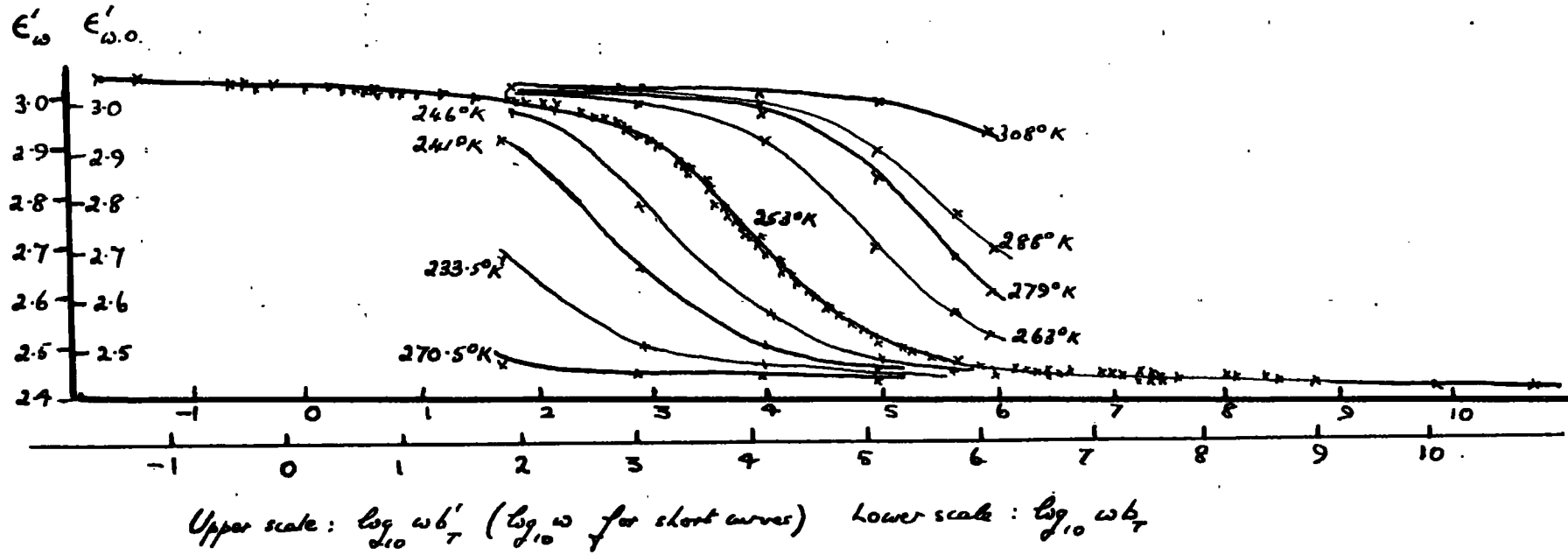

FIG 3·8. Derived curves and master curve for B3.

The derived values, $\epsilon'_{\omega,o}$ and $\epsilon''_{\omega,o}$ were plotted as functions of $\log_{10} \omega$. The points on the short curves and 6 of the points on the centre of the long curve of Fig. 3.8, read in conjunction with the inner scales, show the $\epsilon'_{\omega,o}$ results which were derived from the data of Fig. 3.6. The 6 points on the long curve already mentioned (the results of tests at $T = T_o$) were traced on tracing paper and a curve drawn through them. The tracing paper was then shifted parallel to the log ω axis until the points for a second temperature were made to coincide as closely as possible with the traced curve, which was then extended (and amended if necessary to give a better fit to the double set of points). The new points were added to the curve and the shift ($\log_{10} b'_T$) required was noted. This procedure was repeated for all the temperatures, giving the $\epsilon'_{\omega,o}$ values as a function of $\log_{10} b'_T$. The long curve of Fig. 3.8 gives the resultant "master" curve with all the results.

The values of $\log_{10} b'_T$ were plotted against T on tracing paper. The paper was then laid on the plot of $\log_{10} b_T$ against $(T - T_s)$ calculated from Equation 3.14, and the traced curve shifted (the axes of the two curves being maintained parallel), until the two curves were

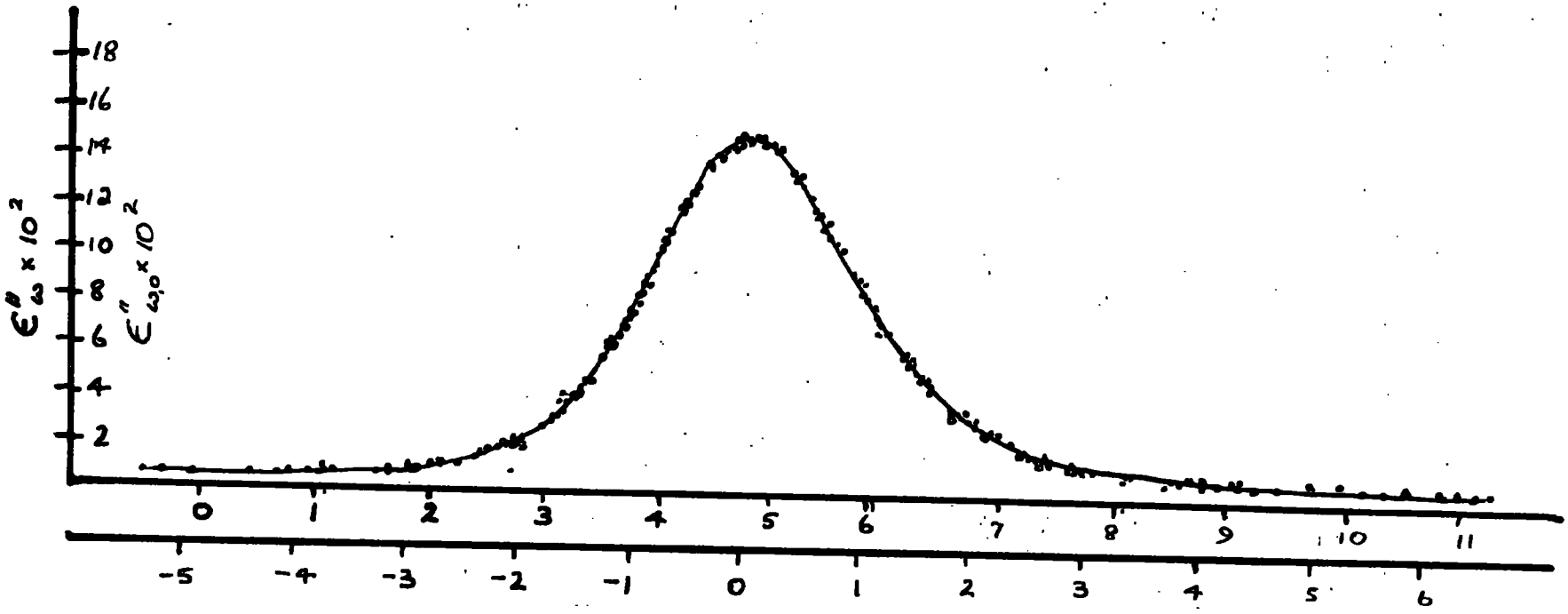

FIG 3·9. Upper scale: $\log_{10} \omega b'_T$. Lower scale: $\log_{10} \omega b_T / \omega_m$. Loss factor of B3 Master curve.

coincident. This is equivalent to finding the reference temperature T_s (the value of T corresponding to $T - T_s = 0$) and a constant m where $b_T = mb'_T$, such that $b_T = 1$ at $T = T_s$; $\log_{10} m$ is minus the value of $\log_{10} b'_T$ corresponding to $\log_{10} b_T = 0$. [The short curves in Fig. 3.8 have been drawn using the calculated values of b_T in conjunction with the value m to provide values of $\log_{10} b'_T$ and then shifting segments of the long curve back along the axis through a distance $(-\log_{10} b'_T)$, in order to show how well the experimental points for individual temperatures can fit the superimposed curve.]

Fig. 3.9 shows the composite master curve obtained from the data given in Fig. 3.7. The value of $\log_{10} \omega_m$ was found by adding $\log_{10} m$ to the value of $\log_{10} b'_T$ at which ϵ''_{ω_0} had its maximum value.

In Fig. 3.10, the values of $\log_{10} b_T$, found by adding $\log_{10} m$ to the experimentally determined values of $\log_{10} b'_T$, for all the rubbers are shown plotted on the curve given by Equation 3.14.

A second set of scales was then set up on drawings of the type shown in Fig. 3.8 as follows:-

(1) The new vertical scale divisions (ϵ'_ω) were made equal in length to the original divisions multiplied

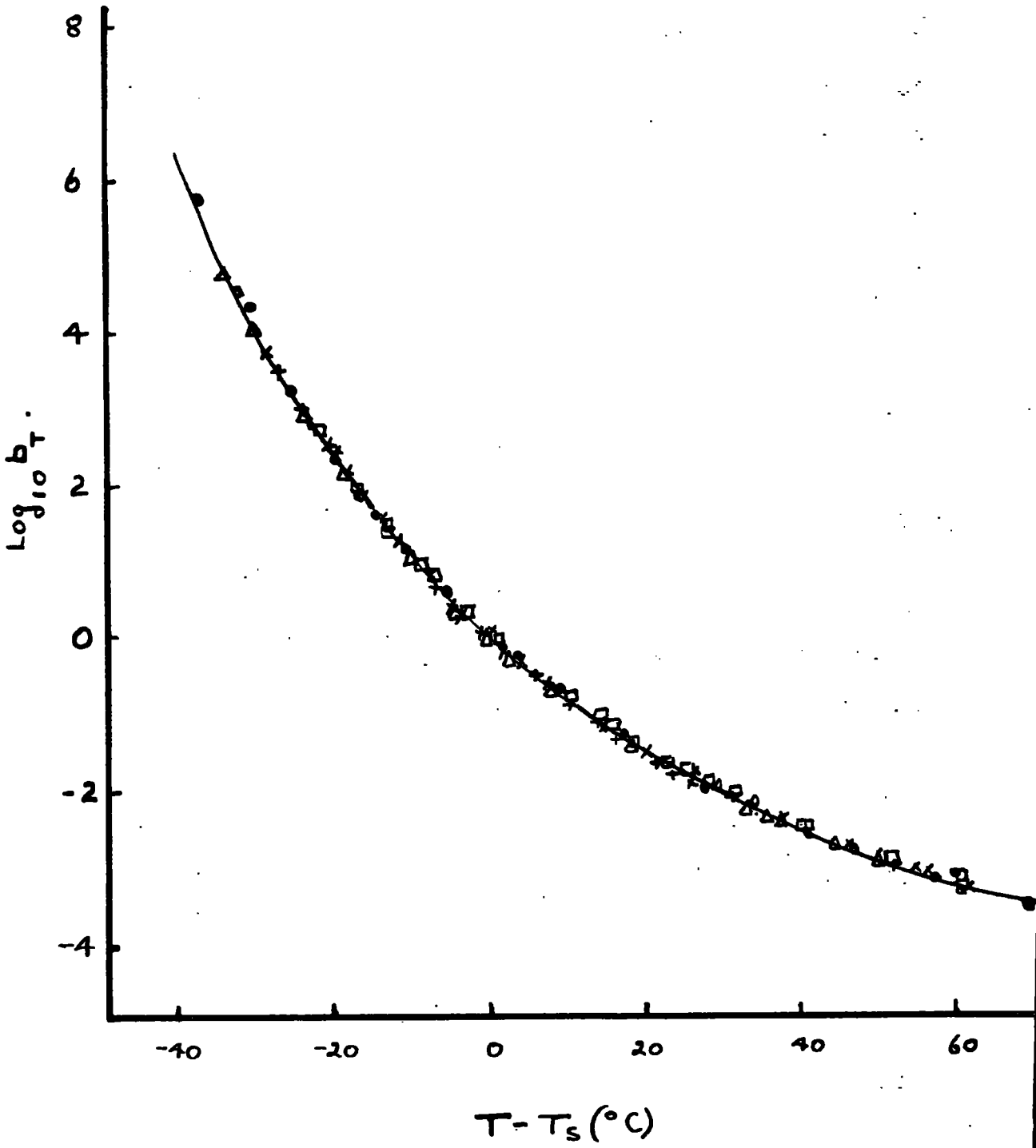

FIG 3·10, Log b_T values. • Unvulcanized. △ A2. □ A4
× A6, + B3, ——— $\log b_T = -8{\cdot}86(T-T_S)/(101{\cdot}6+T$
Payne (1958a).

by $[1-A(T_o-T_s)]\frac{T_s}{T_o}$, and the scale slid along the axis such that $\epsilon'_\omega = \epsilon_\infty$ corresponded to $\epsilon'_{\omega,o} = \epsilon_\infty$ (ϵ_∞ is the value of $\epsilon_{\infty,T}$ at $T = T_s$)

(2) The new horizontal scale ($\log_{10} b_T$) was constructed by shifting the existing scale through a distance ($-\log_{10} m$).

The graph then becomes that of $f'(\log_{10} b_T)$.

A second set of scales was then set up on drawings of the type shown in Fig. 3.9

(1) The new vertical scale division (ϵ''_ω) were made equal in length to the original divisions multiplied by $[1 - A(T_o-T_s)]\frac{T_s}{T_o}$, the scale zero being unaltered.

(2) The new horizontal scale $\log_{10}\frac{b_T}{m}$ was set up with the same length of divisions as the original but with its zero corresponding to the value of $\log_{10}\omega b'_T$ at which ϵ''_ω is a maximum. (If the new horizontal scale had been constructed as was done for Fig. 3.8, the graph would have been that of

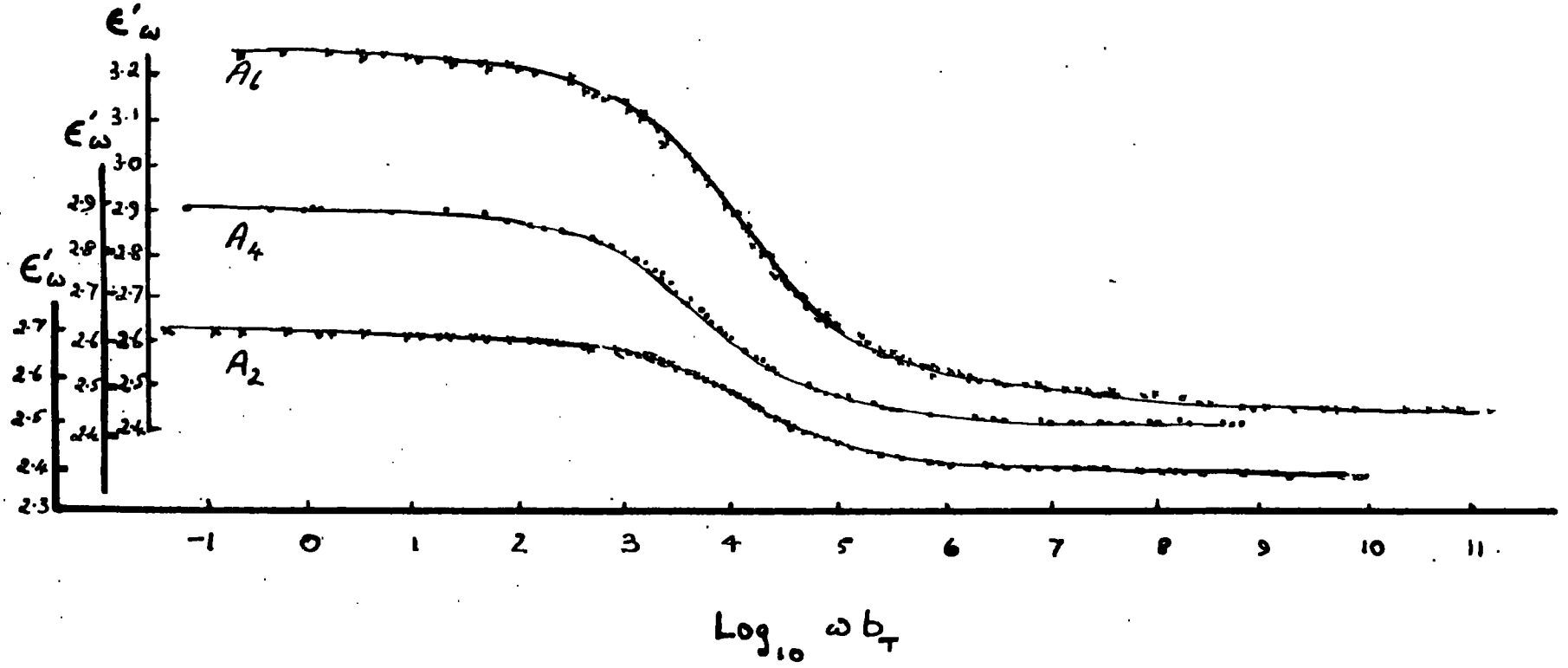

FIG 3·11. *Permittivity of mixing A vulcanisates. Master curves.*

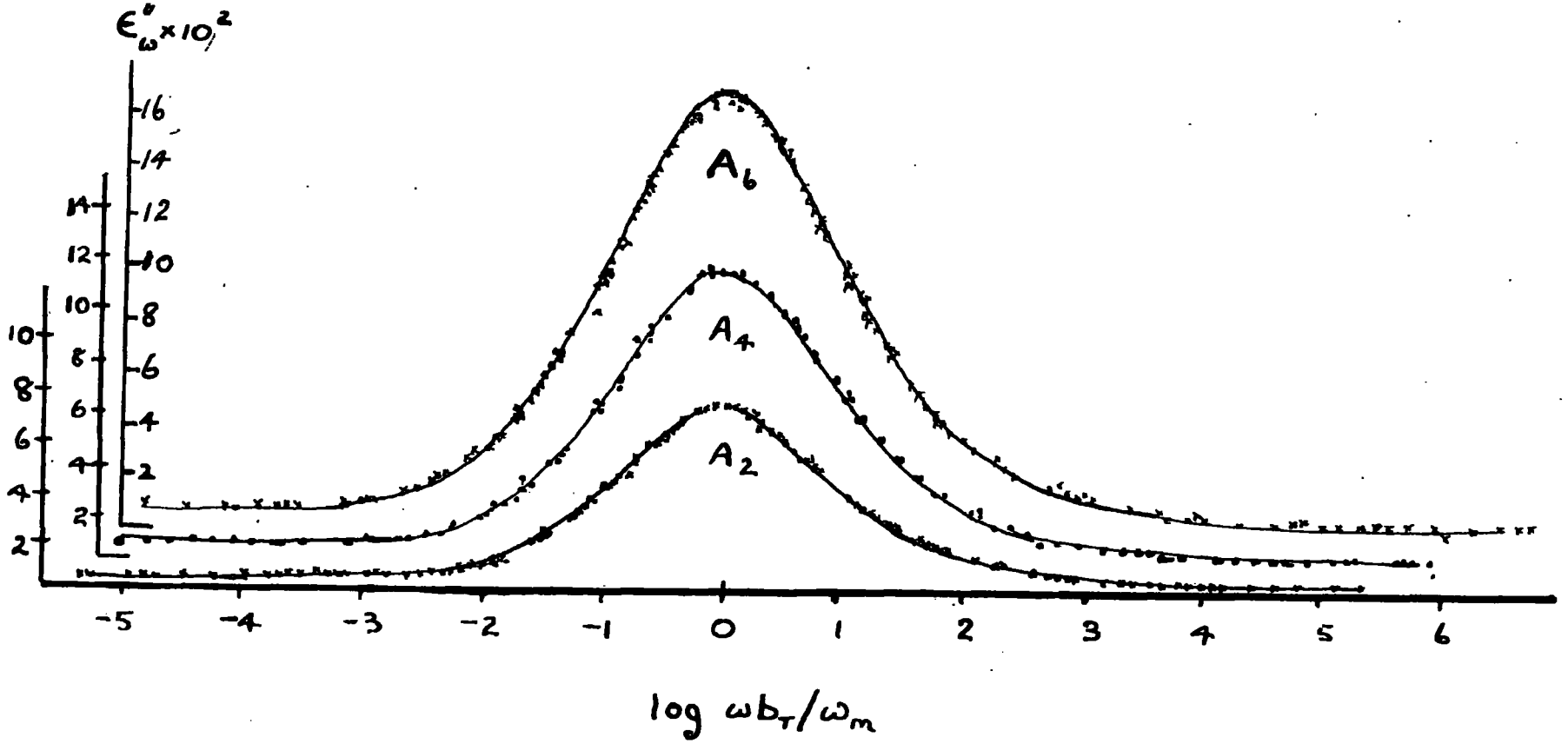

FIG 3·12 Loss factors of mixing A vulcanisates. Master curves.

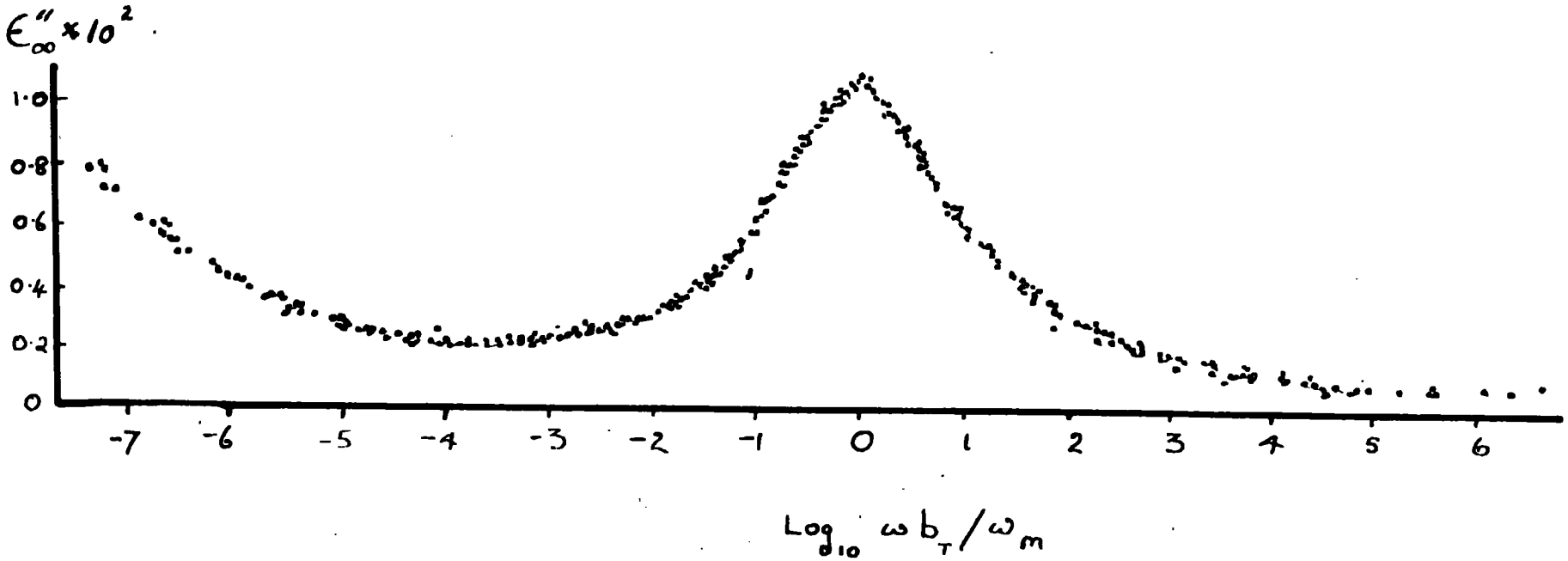

FIG 3·13 Loss factor of unvulcanised purified rubber. Master curve

$f''(\log_{10} \omega b_T)$, its maximum value occurring at $\log_{10} m$.)

Fig. 3.9 thus becomes a "master" curve of

$$(\epsilon''_m - \epsilon''_B)\,\psi''\left[\Delta, \log_{10}\omega - \log_{10}\omega_m - \frac{8.86\,T - T_s}{101.6 + T - T_s}\right] + \epsilon''_B$$

which is designated ϵ''_ω.

The resultant "master" curves for the rubbers from Mixing A are given in Fig. 3.11 - 3.12 and that for the unvulcanised rubber in Fig. 3.13. No graph is given for the permittivity values for the unvulcanised rubber since the range of values observed at different temperatures and frequencies was small compared with the scatter of the results. The peak and lowest values of ϵ''_ω in Figs 3·9, 3·12, and 3·13 provide the values of ϵ''_m and ϵ''_B respectively. The various parameters are given in Table 3.7 in Section 3.8.

3.8 SHAPE OF LOSS FACTOR CURVES AND SUMMARY OF PARAMETERS.

The form of the composite loss factor curves of Figs. 3·9, ·12 and ·13 exhibits the following characteristics:-

(1) A nearly symmetrical Debye-type (but wider) peak, due to a dipolar mechanism. Various authors have compared similar peaks for other materials with various analytic functions for $\epsilon''_\omega / \epsilon''_m$, some of which are purely empirical and some of which are calculated from hypothetical functions for $G(\tau)$. At frequencies remote from the frequency of the peak loss factor, all these loss factor functions tend to zero.

(2) At low values of $\omega\delta_\tau / \omega_m$, the curve rises fairly sharply with decreasing frequency (this is only obvious in the case of unvulcanised rubbers), presumably due to an ionic or Maxwell-Wagner type of loss mechanism. Maxwell (1892), Wagner (1914).

(3) At points of the curve where neither of these mechanisms is predominant, the values of ϵ''_ω do not return to zero, but there is a "background" value ϵ''_B, which is substantially independent of the value of $\omega\delta_\tau$. This is similar to an effect observed by Garton (1946) on relatively non-polar media. Garton showed that it leads to a distribution function of relaxation times of the form $G(\tau) = 1/\tau$

but the theory proposed by Garton is limited to frequencies well above the frequency corresponding to the peak in the loss factor/frequency curve and is not therefore applicable in this case. An attempt to extend the theory to lower frequencies led to results which were at variance with the observations and this line of attack was discontinued.

The experimental values of $\psi''(\Delta, \log_{10}\omega b_\tau - \log_{10}\omega_m) = \frac{\epsilon''_\omega - \epsilon''_\infty}{\epsilon''_m - \epsilon''_\infty}$, in the region of the loss factor peak, have been compared with the various analytic functions (listed in Table 3.6), which have been proposed for ϵ''/ϵ'_m, the best values of Δ being found by trial and error or, when possible, by the use of test plots suggested by previous authors in the references given.

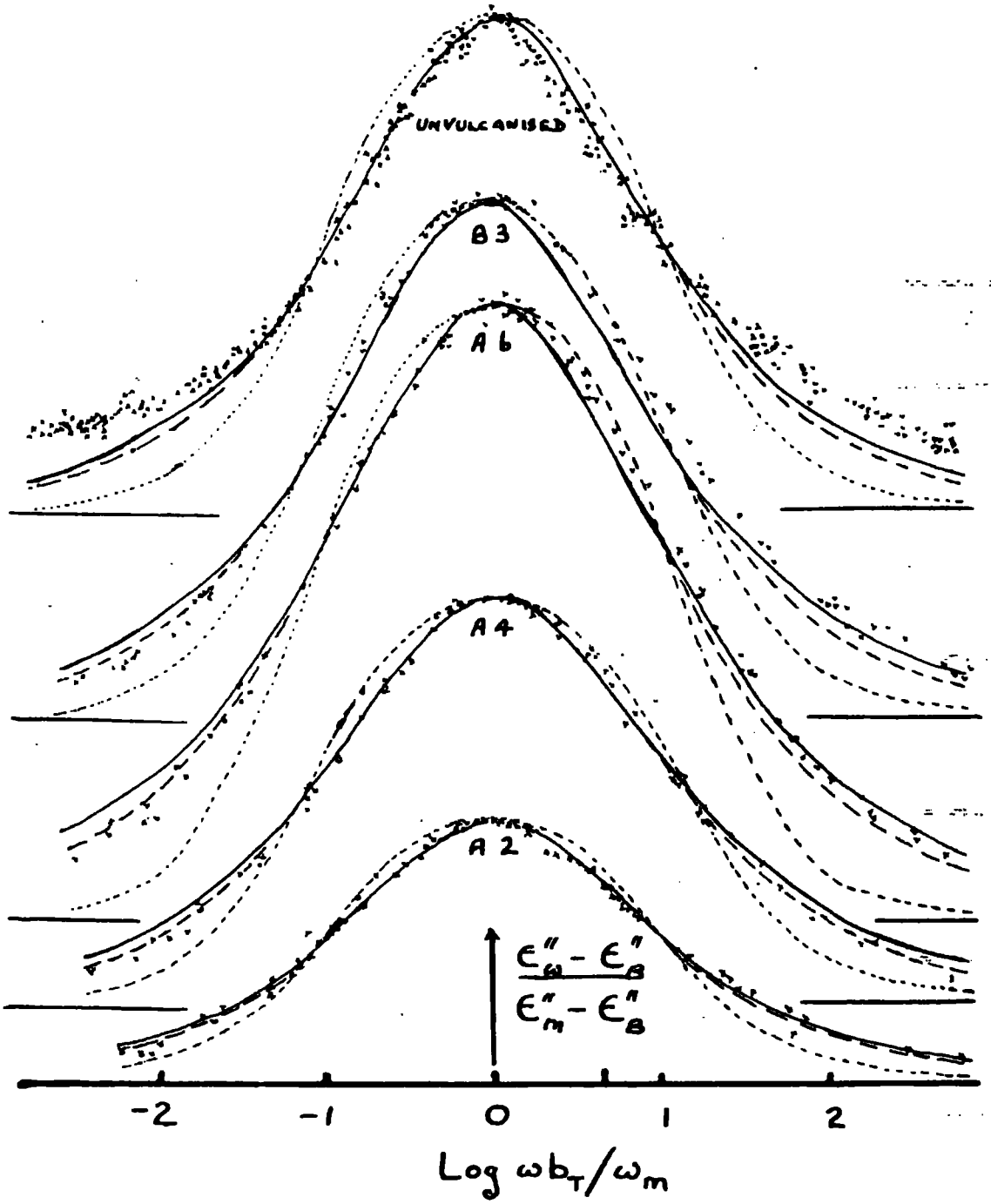

Fig 3·14. Comparison of experimental results with analytic functions
——— Fuoss-Kirkwood, – – – – Cole-Cole, ... Fröhlich.

TABLE 3.6

ANALYTICAL EXPRESSIONS FOR $\epsilon''_\omega/\epsilon''_m$

ssion o.	Author	$\epsilon''_\omega/\epsilon''_m$
	Debye (1929)	$\frac{2X}{1+X^2}$
	Wagner-Yager Wagner (1913, Yager (1936)	$\frac{e^{-b^2X_0^2}\int_0^\infty e^{-b^2u^2}\frac{\cosh 2b^2X_0u}{\cosh u}\,du}{\int_0^\infty \frac{e^{-b^2u^2}}{\cosh u}\,du}$
	Fuoss & Kirkwood (1941a)	$\operatorname{sech}\alpha\,(\log_{10}X)$ *
	Kirkwood & Fuoss I (1941b)	$\frac{4X[(X^2-1)\ln X - X^2+\pi X-1]}{[1+X^2]^2(\pi-2)}$
	Kirkwood & Fuoss II (1941b)	$3.75\int_0^\infty \frac{\rho m}{1+\rho^2 m^2}\left[1+\rho+\rho(\rho+1)e^{\rho}\bar{E}i(-\rho)\right]d\rho$ *
	Cole/Cole (1941)	$\frac{1+\cos\beta\pi/2}{\cosh\beta X_0+\cos\beta\pi/2}$
	Frohlich (1949)	$\frac{\tan^{-1}\gamma X-\tan^{-1}(X/\gamma)}{\tan^{-1}\gamma-\tan^{-1}(1/\gamma)}$

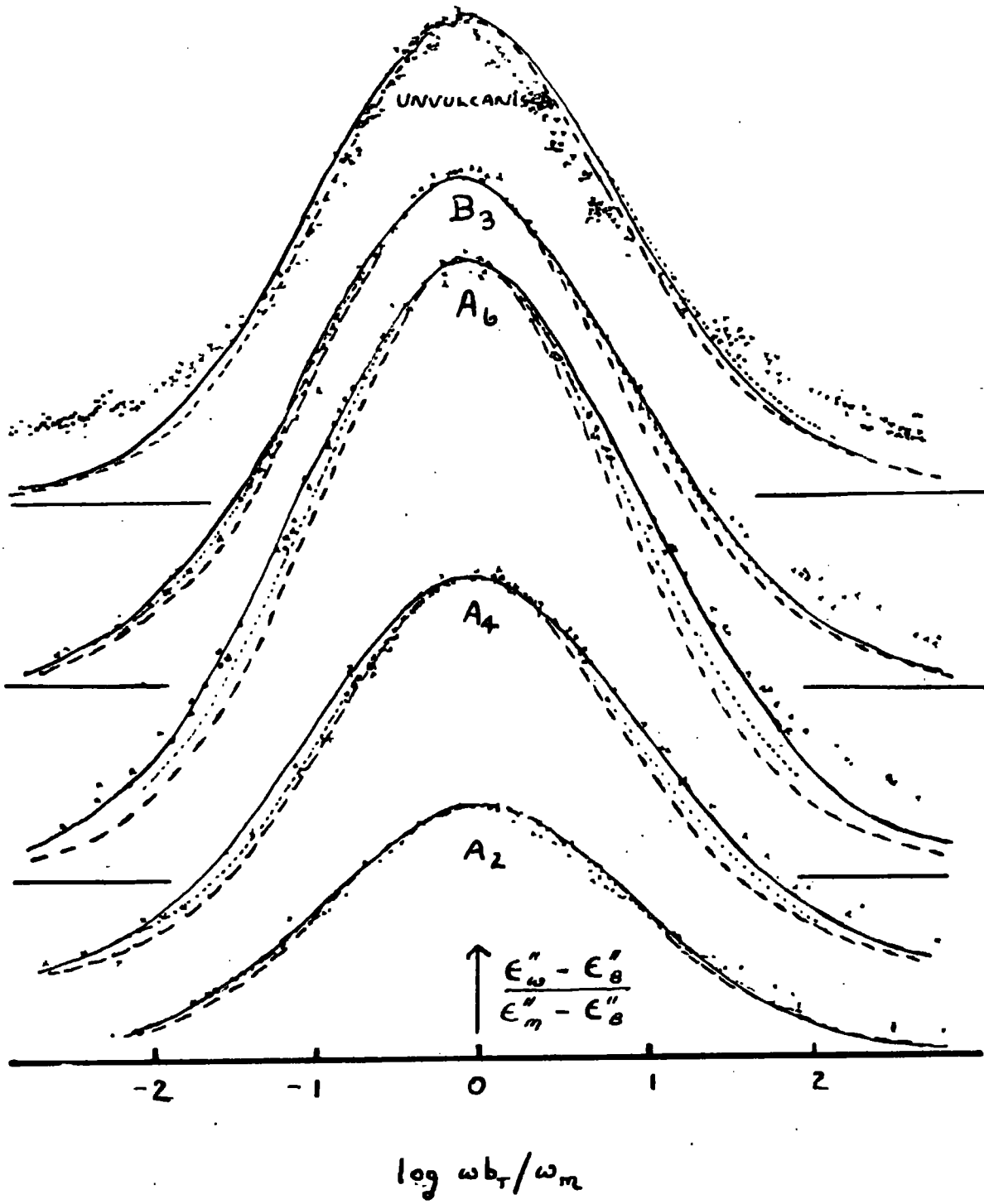

FIG 3·15 Comparison of experimental results with analytic functions (2).

——— Wagner and Yager – – – – Kirkwood and Fuoss (1).

..... Kirkwood and Fuoss (2).

FOOTNOTE TO TABLE 3.6

b, α, β, γ are arbitrary constants

$$X = \frac{\omega b_T}{\omega_m} \qquad m = 0.63 \frac{\omega b_T}{\omega_m}$$

$$X_0 = \ln \frac{\omega b_T}{\omega_m}$$

* These are approximations and $\frac{\epsilon''_\omega (2 + 1/\epsilon'^2_\omega)}{\epsilon''_m (2 + 1/\epsilon'^2_m)}$ should replace $\epsilon''_\omega / \epsilon''_m$ (ϵ'_m is the value ϵ'_ω when $\omega b_T = \omega_m$); the errors of approximation are negligible for the data recorded here. It must be noted, that the theoretical functions 1, 4 and 5 do not contain a disposable parameter A , but the empirical functions 2, 3, 6 and 7 contain such a parameter b, α, β and γ respectively.

Figs. 3.14-15 show values of $\frac{\epsilon''_\omega - \epsilon''_B}{\epsilon''_m - \epsilon''_B}$ in the region of the peak plotted against log $\frac{\omega b_T}{\omega_m}$ superimposed on the lines given by the various graphical relations for $\epsilon''_\omega / \epsilon''_m$. Vertical linear scales, which vary for the different curves, have been omitted for clarity. The functions 3 and 6 appear to give the best fit to the experimental results. The parameters used, together with the various other parameters involved in Equations 3.15, 3.16 and 3.17 and other data on the samples, are given in Table 3.7.

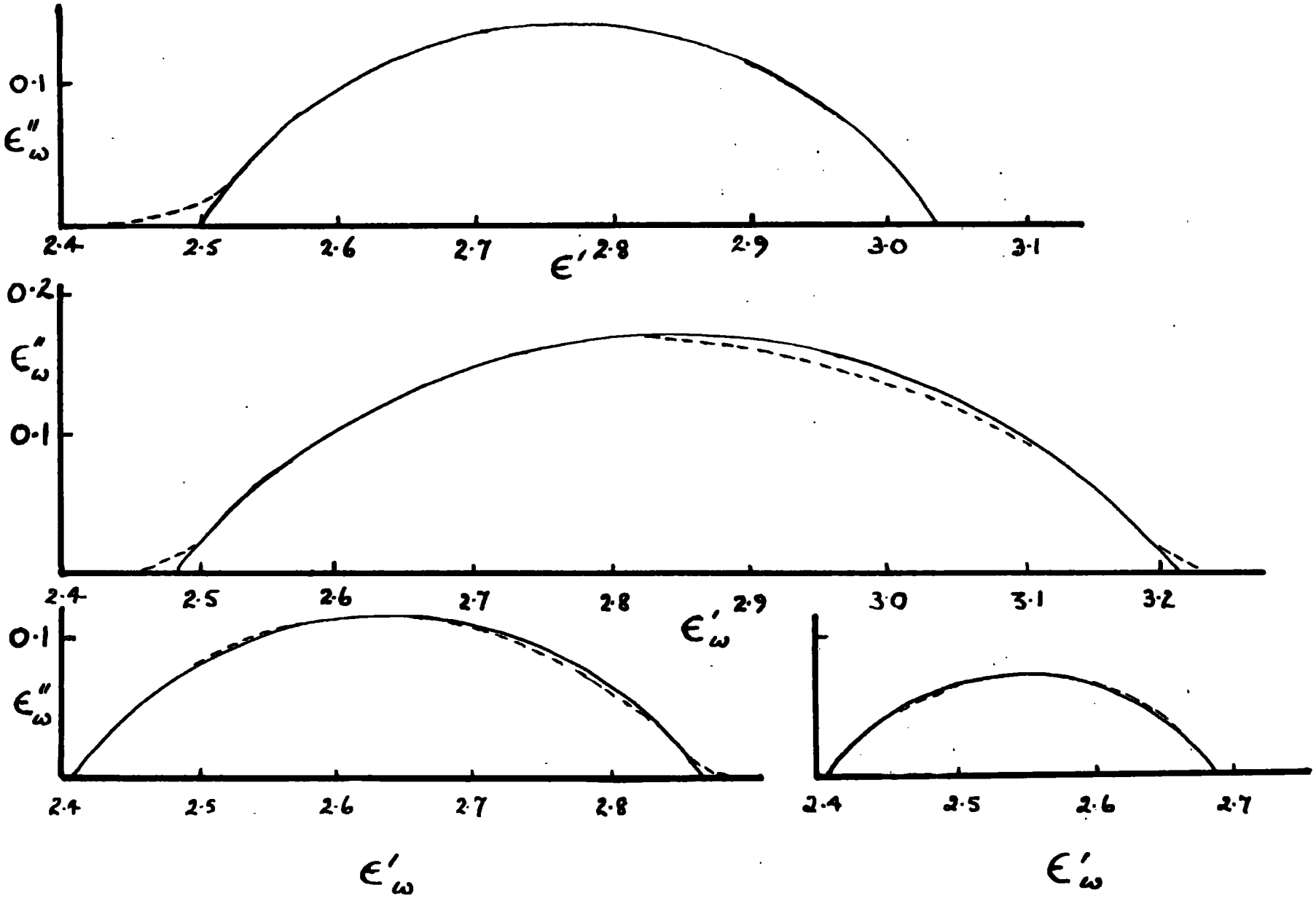

FIG 3·16. *Cole-Cole plots.* ——— circular arcs; - - - - - - - deviations of experimental curves

The Cole-Cole circular arc plots (with no correction for the background loss factor) for the vulcanised rubbers (data reduced to $T = T_s$) are given as full lines in Fig. 3.16. Deviations of the data (derived from the curves of Figs. 3.9, 4.10, 3.11 and 3.12) from the circular arcs are indicated by dotted lines. The accuracy of the $\epsilon''_{\omega,T}$ results for the raw rubber was insufficient to make possible the production of Cole - Cole arc plots for this material. An estimate of ϵ_s (the static dielectric constant at T_s) and a second estimate of ϵ_∞ were made from the Cole-Cole plot.

TABLE 3.7

COLLECTED DIELECTRIC DATA ON ALL RUBBERS

	Unvulcanised	A2	A4	A6	B3
ence temperature T_s; °K	247	251	254·5	259	255
ϵ_∞ (assumed)	-	2·34	2·35	2·37	2·35
T $\frac{d}{dT}\{\epsilon_{\infty,T}\} \times 10^4$ (assumed)	-	4·6	4·6	4·6	4·6
$\epsilon''_m \times 10^2$	1·08	7·4	11·5	76·8	14·5
$\epsilon''_B \times 10^2$	0·07	0·4	0·4	0·4	0·4
ϵ_s (from Figs. 3.8 and 3.11)	-	2·70	2·88	3·22	3·05
o from Cole - Cole plot	+	2·40	2·41	2·48	2·50
s " " " "	+	2·69	2·87	3·21	3·04
α	0·52	0·53	0·48	0·46	0·51
β	0·64	0·65	0·60	0·58	0·63
γ	10	10	13	13	11
Δ	0·40	0·40	0.37	0·35	0·39

+ $(\epsilon_s - \epsilon_\infty)$ too small to permit accurate Cole-Cole plot.

$\log_{10} \omega_m / 2\pi$	5·3	4·0	3·9	2·8	2·9

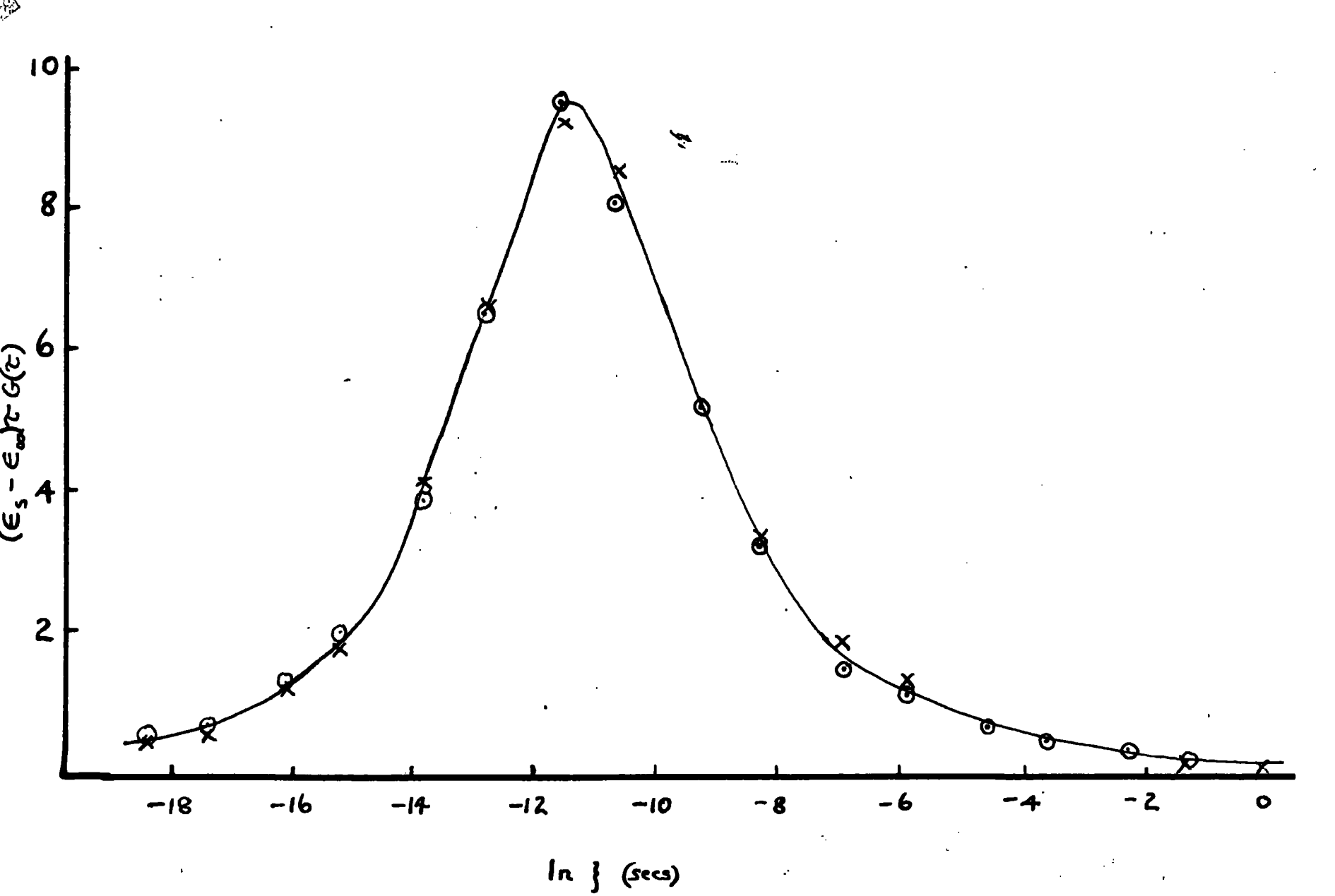

FIG 3·17. Distribution of log relaxation times for B3 at $T = T_s$. × from permittivity data, ⊙ from loss factor data

In the previous discussion it was assumed that $G(\tau)$ could be expressed by various analytic functions, and these hypotheses were tested by comparison of the calculated values of $\epsilon''_\omega / \epsilon''_n$ with the experimental data. It is, however, possible to deduce $G(\tau)$ graphically from the given ϵ'_ω or ϵ''_ω data by a second approximation method given by Ferry & Williams (1952) and by Williams & Ferry (1953). Approximation methods were discussed in the first part of the thesis. The accuracy of the method is not high, since it depends on the graphical differentiation of the experimental curves. The resulting values of $(\epsilon_s - \epsilon_\infty)\tau\, a(\tau)$ at T_s for the sample B3 are given in Fig. 3.17. $\tau\, a(\tau)$ is the distribution function of natural logarithms of the relaxation times and $(\epsilon_s - \epsilon_\infty)\tau\, a(\tau)$ is identical with the function represented by $\psi(\tau)$ in the notation of Ferry and Williams. The agreement between the results from the loss factor and permittivity data is as good as can be expected in view of the approximations and graphical differentiations.

3.9 DIPOLE MOMENTS

From the loss factor/frequency data on raw rubber it is possible to calculate a value z, below which the

dipole moment μ of the rubber monomer cannot lie; the actual dipole moment cannot be calculated since the dispersion is so wide that ϵ''_ω is considerably greater than zero at both ends of the curve and the permittivity data is inadequate to provide a value of $\epsilon_s - \epsilon_\infty$. The value z is derived by assuming that the loss factor at $T = T_g$ is given by

$$\epsilon''_\omega = \left[1{\cdot}01 \times 10^{-2} \operatorname{sech}\left\{0{\cdot}52 \ln(\omega\tau)\right\}\right] + (7 \times 10^{-4})$$

This form of the expression for ϵ''_ω is one which is given by the Fuoss & Kirkwood (1941a) expression superimposed on a constant background loss factor (the constants being as given in Table 3.7). This has been shown to agree with the experimental values if the ionic losses are ignored.

If v and w are the limits of $\ln \omega$ (for $b_T = 1$) in Fig. 3.13, this gives

$$\int_v^w \epsilon''_\omega \, d(\ln \omega) = \left(\frac{\pi}{0{\cdot}52} \times 1{\cdot}01 \times 10^{-2}\right) + (2{\cdot}303 \times 13 \times 7 \times 10^{-4})$$
$$= 8{\cdot}2 \times 10^{-2}$$

but

$$\int_{-\infty}^{\infty} \epsilon''_\omega \, d(\ln \omega) = \frac{\pi}{2} \cdot \frac{4\pi N \mu^2}{27 kT} (\epsilon_s + 2)^2 > \int_v^w \epsilon''_\omega \, d(\ln \omega).$$

(see Oakes & Richards (1946)),

where N = No. of dipoles per unit volume. Putting $N = 8.1 \times 10^{21}$ = No. of monomer units/cm^3, and $\epsilon_s = 2.3$ gives $\mu > z$ where $z = 0.16$ Debye units.

This value of z is much lower than the value $\mu = 0.72D$, obtained by Kambara (1942) for raw crude rubber from measurements on a solution in benzene. It is possible that Kambara's crude rubber was oxidised during the process of solution, thus increasing the dipole moment.

The values of the dipole moment of the vulcanisates per sulphur atom/μ_s have been calculated on the following assumptions:-

(i) that each sulphur atom is involved in a separate dipole;

(ii) that all the dipoles have the same dipole moment;

(iii) that the contribution of the small quantity of accelerator to the dielectric constant is negligible. An attempt to remove the accelerator by extraction resulted in a sample which oxidised rapidly and further tests could not be carried out.

The values of ϵ_s and ϵ_∞ given by the intersection of the circular arcs with the permittivity axis have been used in Onsager's formula (1936)

$\mu_s^2 = \frac{9kT}{4\pi N'} \cdot \frac{(\epsilon_s - \epsilon_\infty)(2\epsilon_s + \epsilon_\infty)}{\epsilon_s(\epsilon_\infty + 2)^2}$ where N' = number of sulphur atoms per unit volume, giving μ = 1·9, 1·8, 1·8, 1·9 D for A2, A4, A6 and B3 respectively. These values are, however, in error due to the contribution of the dipole moment of the rubber molecule. Although no precise values of permittivity of the raw rubber are available, the measured values indicate that, in the absence of the sulphur, $(\epsilon_s - \epsilon_\infty)$ is less than 0·1. If it is assumed that the value of ϵ_s for the vulcanised rubber must be redueed by this figure to allow for the dipole moment of the rubber, then the values of μ_s for the sulphur atom become 1·5, 1·6, 1·7, 1·7 D respectively. These values are similar to that (1·74) calculated by Waring (1951). The use of Cole - Cole plot values of ϵ_∞ and ϵ_s is justified by the fact, that it does not take into account any dipolar dispersion range, which may occur at higher frequencies than those involved here and which has been assumed, therefore, not to be associated with the sulphur atoms. The sulphur combines with the rubber in various chemical groupings and it is

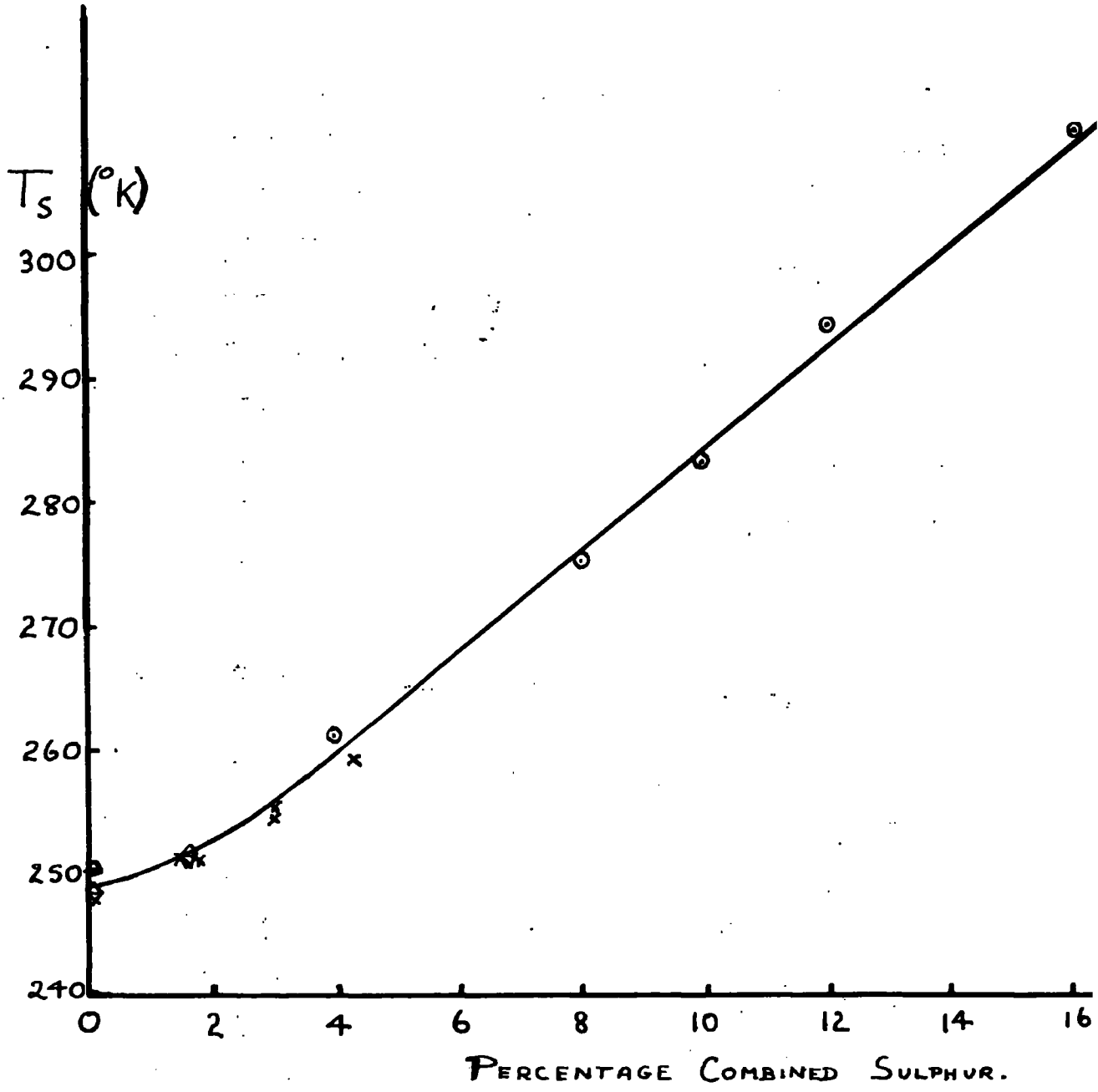

FIG 3·18. Relationship between T_S and combined sulphur content. ×, dielectric results (dielectric - Norman and Payne) ⊙ dielectric results; derived by Payne (1958) from data of Scott, Curtis and McPherson (1933). Δ; dynamic mechanical results from three papers. Zapas, Shufler and de Witt (1955), Fletcher and Gent (1957), Payne (1958), ▽ dynamic mechanical results Payne (1958).

speculative to draw any conclusions from the small range of calculated values of dipole moment.

The value of dipole moment for the isoprene unit is extremely small, so that for most practical purposes, the rubber hydrocarbon is a non-polar substance. Vulcanisation by sulphur adds considerably to the dipolar loss, and the dipole moment per combined sulphur atom (calculated assuming each combined sulphur atom to be a separate dipole) is substantially independent of the percentage combined sulphur or of the acceleration of the reaction.

3.10 DEPENDENCE OF T_s ON COMBINED SULPHUR CONTENT

Table 3.7 indicates that T_s is a function of the combined sulphur content (A2, A4 and A6 had the same total sulphur content). The values of T_s obtained by various authors from dielectric and mechanical data are given in Fig. 3.18. There is a good agreement between the various series of results at the lower end of the curve. Three sets of results give 248°K for unvulcanised rubber, while the other two give 247°K and 250°K, the latter being from experimental data of limited accuracy.

CHAPTER 5

SUMMARY

5.1 SUMMARY OF CHAPTER 2.

1. By the use of the Williams, Landel and Ferry Transform, it was possible to construct master curves of the real and imaginary parts of the dynamic modulus (and related quantities) with respect to logarithm of the angular frequency of oscillation. Analysis of these curves reveal four distinct types of viscoelastic behaviour; flow, highly elastic rubber plateau, transition and glassy.

2. The use of spring and dashpot models was shown to be limited in scope in being able to describe adequately the mechanical response of natural rubber to a sinusoidal oscillation. Use was, therefore, made of several approximation methods to derive either the relaxation or the retardation spectra from actual experimental results.

3. From the maxima in the loss compliance and the retardation spectra, it was possible to derive ζ_0, the monomeric friction coefficient. ζ_0 was shown by Ferry to be similar to the diffusion coefficients of n-Butane, i-Butane and η-Pentane, (materials with a similar

chemical structure to the rubber chain itself) at the same temperature at which ζ_0 was derived. This agreement identifies some aspects of the dynamic behaviour of natural rubber with the properties of the frictional properties of monomer unit in the backbone chain of natural rubber.

4. The nature of the crosslink introduced by vulcanisation clearly influences the modulus and damping in the rubber elastic plateau region. Sulphur compounds, presumably because of the long link of a polysulphide bridge, appear to be more flexible and less hysteretic than compounds possessing smaller junctions.

5. Carbon black fillers considerably modify mechanical properties, especially the relaxation and retardation spectra, but appear to have little influence on the glass transition, or the T_s values of the vulcanisate.

6. The general effects of temperature, frequency, vulcanisation or fillers in modifying the dynamic behaviour of rubber is now known, but much detail still requires ~~still~~ to be established. Considerable attention has to be paid to developing satisfactory molecular theories of network response to mechanical osciallations in the

rubber-plateau region before the finer details of the phenomena can be understood in the region whererubber is normally used in engineering practice.

5.3 SUMMARY OF CHAPTER 3

1. The use of the Ferry and Fitzgerald method (set out in mathematical terms in this thesis) of analysing the loss factor and permittivity data is applicable to the results of both vulcanised and unvulcanised dry purified rubber.

2. The form of the loss factor/frequency function suggests the summation of:-

   (a) a broadened-Debye-type peak; the process is polar.

   (b) a constant "background loss factor"; the process is obscure.

   (c) an ionic loss at very low frequencies; this is only obvious on the unvulcanised rubber.

It is noted that there is no record of (b) having been previously observed in combination with (a) i.e. in a polar material.

3. Of the various theoretical and semi-empirical forms for the distribution of relaxation times giving rise to

the Debye type peak, the Fuoss-Kirkwood and Cole/Cole functions were found to be most in accord with experimental results.

4. Estimates of the dipole moment of raw natural rubber could not be made, although it is deduced that the value cannot be less than 0.16D. The dipole moment per sulphur atom in a vulcanisate (based on the assumption that each combined sulphur atom in the vulcanisate gives rise to a separate dipole and all the dipoles have the same moment) is about 1·6D.

5. The values of T_s obtained from mechanical and dielectric data are almost identical, and furthermore the WLF equation describes the temperature-frequency equivalence of both the dynamic and dielectric properties of natural rubber.

Finally, a general conclusion to be drawn from this work is the great importance of the WLF Transform in relating the temperature and frequency (or time) equivalence of the behaviour of amorphous polymers. Indeed it is now essential for any experimental work on polymers, in which time and temperature are two of the parameters involved, to make use of these Transforms. A recent review by the

author on the use of the WLF transform in nuclear magnetic resonance studies, optical birefringence, friction, abrasion, tear and other studies on polymers (both crystalline and amorphous) accents the practical and theoretical importance of the Transform techniques. Payne (To be published).

CHAPTER 5

5.1 NOTE ON TIME OR FREQUENCY-TEMPERATURE SUPERPOSITION

This thesis has referred the frequency-temperature relationships to the Williams, Landel and Ferry Transform. As in many other scientific fields of endeavour which are progressing rapidly, it is often difficult to state clearly the person or persons actually responsible for some basic principles, especially as the passage of time has modified the original assumptions. There is now however a tendency in the literature to say that the interrelationship between time or frequency and temperature can be treated by the Leadermann-Tobolsky-Ferry time-temperature superposition principle.[1,2,3] The principle was certainly first formalised adequately by Ferry[4] in terms of phenomenological

model and subsequently gives a molecular interpretation by the Rouse,[5] Bueche[6] and Zimm[7] theories. These theories are amply discussed elsewhere.[1,3,8]

1. Ferry, J.D. "Viscoelastic Properties of Polymers", Wiley, New York (1961).
2. Leaderman, H, "Elastic and Creep Properties of Filamentous Materials The Textile Foundation", Washington D.C. (1943).
3. Tobolsky, A.V. "Properties and Structures of Polymers" Wiley, NewYork, (1960).
4. Ferry J.D., J.Am.Chem.Soc., 72, 3746 (1950).
5. Rouse, P.E., Jr., J.Chem.Phys., 21, 1272 (1953)
6. Bueche, F. J.Chem.Phys. 22, 603 (1954)
7. Zimm B.H., J.Chem.Phys. 24, 269 (1956).
8. Bueche, F., J.Appl.Phys., 26, 1133 (1955).

5.2. NOTE ON THE GLASS TRANSITION TEMPERATURE AND THE WLF EQUATION

The glass transition temperature is a well defined singularity in the temperature dependence of any of the intensive properties of the material, e.g. density, compressibility of specific heat, measured in an experiment with a time scale of $1^{o}C$ in several minutes. As an

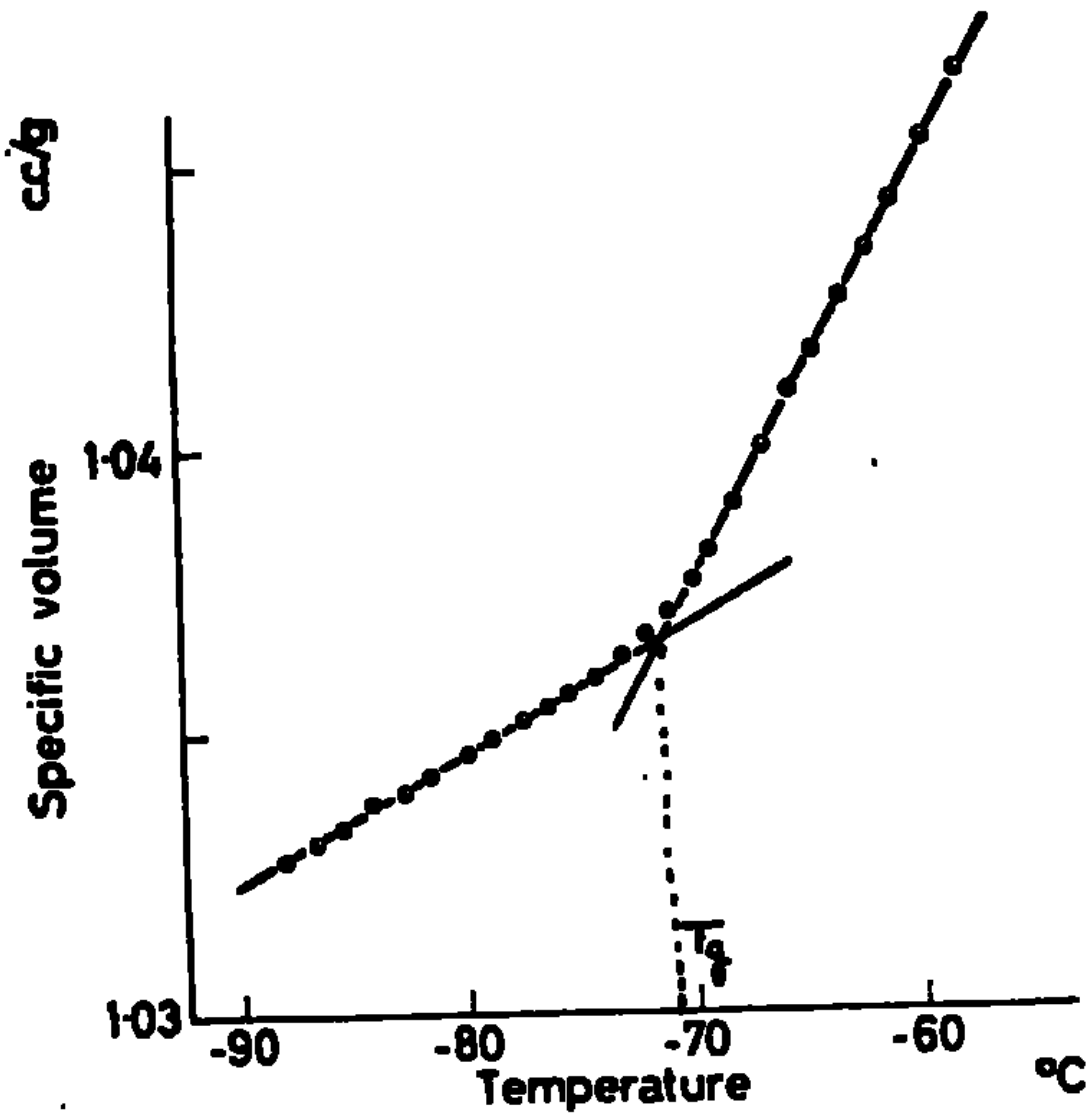

Figure 5.1 Specific volume–temperature relationship for natural rubber

example Fig. 5.1 shows the variation with temperature of specific volume of natural rubber measured with temperature increasing at $1^{\circ}C$ in three minutes.

Below the glass transition point, the material behaves as an amorphous solid; the individual atoms maintain their relative positions during deformation, there being negligible molecular rearrangement in experimentally realizable times.

As the temperature rises above the glass transition point molecular rearrangements take place with increasing ease (in polymers, these usually result from rotations about C-C bonds), giving rise to an additional 'configuration' contribution to specific volume, specific heat, compressibility etc. as appears in Fig. 5.1. This structural effect is zero at the transition point T_g, so that its value at a higher temperature T may be measured by $(T-T_g)$.

The most obvious structural change produced by increasing the temperature is its increase in volume. This thermal expansion may be related to the free volume of the polymer, a quantity which has been variously defined but which here is essentially a measure of the

space available for free molecular motion. If the fractional free volume, f, is defined as the free volume per unit volume of liquid, then the abrupt change $\Delta\alpha$ in thermal expansion coefficient on passing through the glass transition point as shown in Fig. 5.1 may plausibly be taken as the thermal coefficient of f itself, since f_g will be a small fraction. Thus

$$f = f_g + \Delta\alpha \quad (T - T_g) \qquad 5.1$$

where f_g is the fractional free volume at T_g

Following Eyring's introduction of the free volume concept, widely employed in hole-type liquid theories, Doolittle developed a successful equation for viscosity solely in terms of the free volume. Williams, Landel and Ferry, by combining Doolittle's expression for viscosity with the free volume equation above, identified the constants of the general form of the WLF equation

$$\log a_T = C_1 (T - T_s) / (C_2 + T - T_s) \qquad 5.2$$

such that

$$C_1 = 1/2.3 f_g \qquad 5.3$$

$$C_2 = f_g / \Delta a \qquad 5.4$$

Comparison with the established constants in equation 6.2 then indicates that:-

$$f_g = 0{\cdot}025 \quad \text{and} \quad \Delta a = 4{\cdot}8 \times 10^{-4} \text{ deg}^{-1} \qquad 5.5$$

In view of the uncertainty in giving absolute meaning to free volume, the value of f_g, though plausible, cannot be quantitatively tested. The value of the expansion coefficient, however, is a good average of the known value of this quantity, for example the results shown in Fig. 6.1 lead to a value of 4.9×10^{-4} deg^{-1}

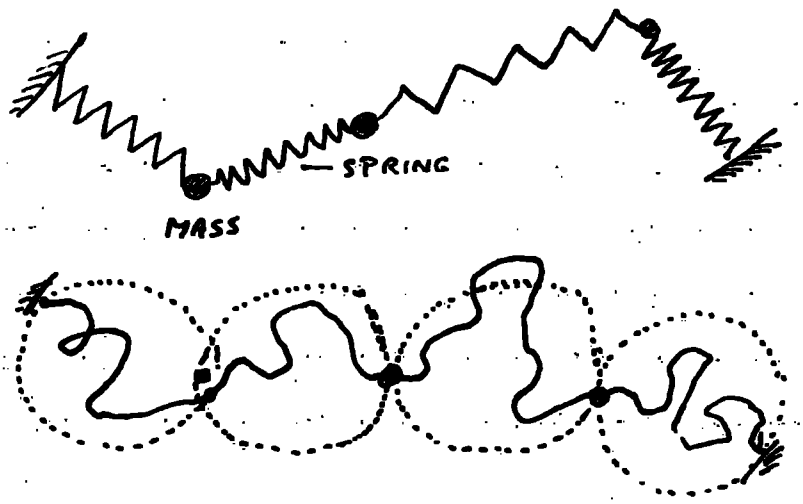

Molecular model corresponding to the theory of Rouse modified for fixed strand ends.

5.3 FURTHER DISCUSSION ON THE MOLECULAR THEORIES USED IN CHAPTER 2 (WITH PARTICULAR REFERENCE TO SECTION 2·10.2)

Bueche takes as his model a three dimensional polymer molecule consisting of masses connected with springs whose stiffness constants equal $3kT/a^2$, where k is Boltzmann's constant, T the absolute temperature, and a^2 the mean square end-to-end distance of the chain per monomer unit. These springs are the so-called "entropy springs", which take into account the effect of Brownion motion on the macromolecules. For mathematical simplicity the valence bond angle is taken as 90^o, and the hindrance potential to internal rotation is assumed to be zero at angle 0^o and 180^o but infinite elsewhere. Energy loss in the system due to the viscous interaction of a segment with its surroundings is introduced into the computation by a segmental fraction coefficient ζ_o .

The equations of motion are set up and solved using a normal mode analysis. For the cross-linked case, the deformation force is applied to the ends of the molecule, which then become cross-link points. The

portions of the overall network between cross links are called 'chains'. Having evaluated the mechanical response for a single 'chain', the total work done on a unit volume of the microscopic sample is assumed to be equally distributed among the v 'chains' comprising the volume and the response of the total network is obtained. The result for a cross-linked polymer is a discrete line spectrum of retardation times. At long times the expression for the shear compliance approaches $\rho RT/M_c$. At short times the discrete spectrum can be replaced by a continuous one, which is independent of M_c and is identical with the Rouse theory except for a numerical factor of $\sqrt{2}$. At these moderately short times the behaviour is not influenced to any extent by the presence of the cross-links. Quantitatively, this is easy to understand since the short times correspond to motions of selectively small segments of the polymer chain and the probability that the segment will include a cross-link is very small if the degree of cross-linking is slight.

At intermediate times the theory predicts a maximum in the retardation spectrum and in the loss compliance due to the presence of the cross-links. The frequency

ω_m of this maximum in the loss compliance is given by the reciprocal of the terminal relaxation time, i.e.

$$\omega_m \doteq 1/\tau_1 = 3\pi^2 kT/a^2 Z_c^2 \zeta_o \qquad 5.6$$

where $Z_c = M_c/M_o$ and M_o is the molecular weight of the monomer unit. Quantitatively, if the maximum is approached by decreasing the frequency, the maximum corresponds to the point, where the experiment first shows that the chain is connected at both ends to the rest of the network (the terminal retardation time corresponds to the fundamental vibration mode of a violin string or to translation of the whole chain). The magnitude of the maximum can be shown to be

$$J''_{max} = 0{\cdot}42 M_c/\varrho RT = 0{\cdot}42\, J_e \qquad 5.7$$

Thus both the height and the position of the maximum depend on the chain length.

Blizard has proposed a ladder network to obtain the viscoelastic response of a network polymer. His model consists of an infinite transmission line. Starting at any point and going in one direction along the line, one comes to a point where the line branches into three lines. Following any of these three lines a given

distance one again comes to a branch point where the line being followed branches into three; this pattern continues ad infinitum. Each portion of the line between branch points has a resistance per unit length and an inductive coupling to ground per unit length. These, when translated into the mechanical analogues, become the elastic contribution (entropy springs) and the viscous contribution (segmental friction coefficient) per monomer unit. This model then would seem to be a fair representation of a polymer network and is somewhat closer to reality than the Bueche model in which no account was taken of how the several chains are connected together (i.e. whether the cross-links have a bi-, tri-, tetra- or higher functionality). Furthermore, the results of the Bueche theory are in terms of a sum, while those of the Blizard theory are obtained in closed, albeit complicated, form. The main disadvantage ot the Blizard treatment is that the equations are given in terms of unspecified constants, which do not provide close identity with molecular parameters.

Other theories for the mechanical behaviour of cross-linked polymers by Kirkwood and by Kirkwood and Hammerle lead to continuous retardation spectrums with the high frequency portions of J'' proportional to ω^{-1}

and ω^{-2} respectively and both independent of M_c.

All of these molecular theories of cross-linked macromolecules have two serious defects which limit their application in real systems. The first defect arises because the theories assume that all the chains in the network are of the same length. Since the vulcanisation of rubber is a random process, M_c will be anything but constant, in fact Watson (1953) has shown that the distribution of M_c should follow the "most probable distribution" expression for large values of $\overline{M}_c$, the number average molecular weight between crosslinks, and furthermore:-

$$\phi(M_c) = (M_o/\overline{M}_c) \exp(-M_c/\overline{M}_c) \qquad 5.8$$

where $\phi(M_c)$ is the fraction of the chains that have a chain molecular weight of M_c, and M_o is the molecular weight of a monomer. From these general considerations J''_{max} should decrease with increasing width of the cross-link density distribution. Since $\omega_m \propto Z_c^{-2}$, this frequency should increase with increasing width of the cross-link density distribution and should be higher the greater the number of short chains present.

The second defect of the molecular theories is their inability to account for the low frequency behaviour. The theories predict, that at low frequencies, J'' will be proportional to ω down to zero frequency. In reality, J'' does not decrease this fast and in fact becomes almost frequency independent at low frequencies and furthermore the loss tangent decreases only very slowly over the low frequency range. This phenomenon is now, due to the recent work of Stratton and Ferry (1964), attributed to the relaxation of groups of chains co-ordinated through their mutual cross-links or entanglements:

CHAPTER 6

APPENDICES

6.1 VALUES OF ϵ_∞, T.

The data of McPherson & Cummings (1935) give the refractive index (n_D^T) for the sodium D line of natural rubber containing S_c % combined sulphur and S_s % free sulphur as

$$n_D^T = 1{\cdot}519 + 0{\cdot}0037S_c - 0{\cdot}00035(T-298) + 0{\cdot}0016S_s, \qquad 6.1$$

if the assumption is made, that the influence of free

sulphur is of the same magnitude in the vulcanisate as it is in the unvulcanised rubber, the data given by Wood (1941) fit Cauchy's formula relating refractive index to wavelength and give an extrapolated value at infinite wavelength (n_{∞}^{25}) which is 0·020 less than n_D^{25}.

Assuming the temperature coefficient remains constant at lower temperatures (-50° to + 20°C) than those over which it was measured (+20° to +60°C), the combined relationships gave values of $(n_{\infty}^{T})^2$ at $T = T_s$ of 2·34, 2·35, 2·37, 2·35 for A2, A4, A6 and B2 respectively, with a temperature coefficient

$$\left(\frac{1}{n_{\infty}^{T}}\right)^2 \frac{\partial}{\partial T}\left(n_{\infty}^{T}\right)^2 \qquad \text{of } -4{\cdot}6 \times 10^{-4} \text{ per } {}^{\circ}\text{C}.$$

Examination of the original data showed that the value of $(n_{\infty}^{T})^2$ was only of the order of 0·12 lower than the lowest values of $\epsilon'_{\omega,T}$ observed, and it was therefore concluded that the effects of atomic polarisability and of any very high frequency (outside the experimental range) dipolar loss mechanism were small. In the absence of any further information it was assumed therefore that $(n_{\infty}^{T})^2 = \epsilon_{\infty,T}$ was an adequate approximation for the present treatment of the results, and the resultant superposition of the curves suggests that the assumption was justified.

6.2 ACTIVATION ENERGIES AND THE WILLIAMS, LANDEL AND FERRY EQUATION.

It does not appear to be generally realised that, for physical processes where the Williams, Landel and Ferry equations applies, the equation requires only a single paramater, the T_s value, in order to specify the activation energies at <u>all</u> the temperature within the range of application. This equation thus specifies a relationship between activation energies and the T_s value is therefore a more useful factor than activation energies at a single or limited number of temperatures.

The Williams, Landel and Ferry equation may be written:-

$$\ln b_T = \frac{2{\cdot}303 \times 8{\cdot}86\ (T-T_s)}{101{\cdot}6 + T-T_s} \qquad 6.2$$

The activation energy is given by

$$E = R\ \frac{d(\ln b_T)}{d(1/T)} = 2{\cdot}07R\left(\frac{T}{101{\cdot}6 + T-T_s}\right)^2 \times 10^3 \qquad 6.3$$

where R is the gas constant ($1{\cdot}987 \times 10^{-3}$ K cal.deg^{-1} mole^{-1})

Thus $$E = 4{\cdot}12 \left(\frac{T}{101{\cdot}6 + T - T_s} \right)^2 \qquad 6.4.$$

and is therefore not a constant as it depends on the temperature and as the <u>difference of temperature</u> away from the reference temperature T_s [or the glass transition temperature, T_g ($T_g = T_s + 50^{\circ}C$)].

CHAPTER 7
REFERENCES.

7.1 References to Chapter 2.

Aitken, A and Barrer R.M., Trans Faraday Soc., 51, 116 (1955).

Alfrey, T., Jnr.,"Mechanical Behaviour of High Polymers", Interscience Publishers, New York (1948).

Andrew, R.D., Ind. Engng. Chem., 44, 707 (1952).

Averbach, I., Gehman, S.D., Mellor, W.R., and Kurgla, W.C., J. Polymer Sci., 28,129 (1958).

Bateman, L., "The Physics and Chemistry of Rubber" Maclarens (1962).

Blatz, P.J., Ind. Engng. Chem., 48, 727 (1956).

Blizard, R.B., J. Appl. Phys., 22, 730 (1951).

Blokl, G.A., Dokl. Akad. Nauk. SSSR. 129, 361 (1959). Rubber Chem., and Technol., 33, 1005 (1960).

Braden, M., and Fletcher, W.P., Trans. Inst. Rubber Ind., 31, 155 (1955).

Bueche, A.M., J. Polym. Sci., 25, 130 (1957).

Bueche, A.M., "Physical Properties of Polymers", Interscience, New York, (1962).

Bueche, F., J. Chem. Phys., 20, 1959 (1952) J. Chem. Phys., 22, 603 (1954).
J. Appl. Phys., 26, 738 (1955).
J. Chem. Phys., 25, 599 (1956).
J. Polym. Phys., 25, 243 (1957).
J. Appl. Polymer Sci. 1, 240 (1959).

Cerf. R., Adv. Polymer Sci. 1, 382 (1959).

Chapiro, A., "Radiation Chemistry of Polymeric Systems". Interscience Publishers Inc., New York (1962).

Davey, A.B., and Payne, A.R., "Rubber In Engineering Practice" Maclaren (1965).

Eilers, H., Kolloid-Z., 97, 313 (1941).

Ferry, J.D., "Viscoelastic Properties of Polymers", John Wiley and Sons Inc., New York (1961).

Ferry, J.D., and Fitzgerald, E.R., J. Colloid Sci., 8, 224 (1953).

Ferry, J.D., Fitzgerald, E.R., Grandine, L., Jnr., and Williams, M.L., Ind. Engng. Chem., 44, 703, (1952).

Ferry, J.D., Grandine, L.D., Jnr., and Fitzgerald, E.R., J. Appl. Phys., 24, 911 (1953).

Ferry, J.D., and Williams, M.L., J. Colloid Sci., 1, 347 (1952).

Fletcher, W.P., and Gent, A.N., Brit. J. Appl. Phys., 8, 194 (1957).

Fujita, H., J. Appl. Phys., 29, 943 (1958).

Gent, A.N., J. Appl. Polymer Sci., 6, 46 and 433 (1962).

Cross, B., and Fuoss, R.M., J. Polym. Sci., 19,39 (1956).

Cross, B., J. Polym. Sci., 20, 123 (1956).

Hammerle, W.G., and Kirkwood, J.G., J. Chem. Phys., 23, 1743 (1955).

Heinze, H.D., Schmieder, K., Schrrell, G., and Wolf, K.A., Kautschuk and Gummi, 14, 208 WT (1961).

Houwink, R., and Janssen, J.J., Kautschuk and Gummi, 7, 82 (1954).

Hutton, A.Q., and Nolle, A.W., J. Appl. Phys., 25, 350 (1954).

Kirkwood, J.G., J. Chem. Phys., 14, 51 and 180 (1946) and Rice, S.A., and Kirkwood, J.G., J. Chem. Phys., 31, 901 (1959).

Kittel, C., "Introduction to Solid-State Physics", Second Edition, Wiley, N.7 (1956).

Kuhn, W., Künzle, O., and Preissmann, A., Helv. Chim. Acta., 30, 307, 446 (1947).

Landel, R.F., J. Colloid Sci., 12, 308 (1957).

Leaderman, H., "Elastic and Creep Properties of Filamentous Materials", Washington, D.C., Textile Foundation (1944).

Lovell, S.E., and Ferry, J.D., J. Phys. Chem., 65, 2274 (1961).

Lovell, S.E., and Frederick, J.E., "Numerical Values Used For G_R', G_R'' and J_R''.
Theoretical Chemistry Institute of the University of Wisconsin (1964).

Marvin, R.S., Ind. Engng. Chem., 44, 696 (1952).

Marvin, R.S., in Bergen T.T., "Viscoelasticity - Phenomenological Aspects", Academic Press, New York, (1960), p. 27.

Mason, P., J. Chem. Phys., 35, 1523 (1961).

Moore, C.G., and Trego, B.R., J. Appl. Polymer Sci., 5, 299 (1961).

Nisomiya, H., and Ferry, J.D., J. Colloid Sci., 14, 36 (1959).

Okano, M., Busseiron Kenkyn, 3, 493 (1958).

Park, G.S., Proc. 2nd Radioisotope Conference. Butterworths, London, 1954, p.11.

Parkinson, D., "Reinforcement of Rubbers", Lakeman and Company, London, (1957).

Payne, A.R., Society of Chemical Industry Publication, S.C.1. Symposium (1958b).

Payne, A.R., and Scott, J.R., "Engineering Design with Rubber", Maclaren and Sons, Ltd. (1961).

Philippoff, W., J. Appl. Phys., 24, 685 (1953).

J. Appl. Phys., 25, 1102 (1954)

Robinson, J.V., Trans. Soc. Rheology, 1, 18, (1957).

Rouse, P.E. Jnr., J. Chem. Phys., 21, 1272 (1953).

Schnieder K., and Wolf, K., Koll Zeits., 134, 149 (1953).

Stratton R.A., and Ferry, J.D., J. Phys. Chem, 67, 2781 (1963)

Staverman, A.J., and Schwarzl, F., in Stuart, H.A., "Die Physik der Hochpolymeres", IV, Chapter 1. Springer - Verlag (1956).

Studebaker M.L., and Nabors, L.G., Rubber Chem. and Technol. 32, 941 (1959).

Thirion, P., and Chasset, R., Proc. 4th Rubber Technol. Conf. London (1962), p. 338.

Tobolsky, A.V., J. Appl. Phys., 27, 673 (1956).

Tobolsky, A.V., and Andrews, R.D., J. Chem. Phys., 13, 3 (1945).

Williams, M.L., J. Polym. Sci., 62, 57 (1962).

Williams, M.L., Landel, R.F. and Ferry, J.D., J. Amer. Chem. Soc., 77, 3701 (1955).

7.2 REFERENCES TO CHAPTER 3

Batsenov, S.S., "Refractometry and Chemical Structure" Consultant Bureau N.Y. (1961) Chapt.2.

Birks, J.B., Editor (1952) "Modern Dielectric Materials", Academic Press Inc., N.Y. (1960).

Bottcher, C.J.F., Theory of Electric Polarisation, Elsevier p. 363.

Brown, W.F., "Dielectrics" Encyclopedia of Physics, 17, Spring-Verlong Berlin (West) Germany (1956).

Curtis, A.J., "Dielectric Properties of Polymeric Systems" in "Progress in Dielectrics" Vol.2 edited by Burks and Schulman, Heywood and Co.Ltd., London, (1900) p.30.

Debye, P., Physik Zietung, 13, 97 (1912).

Debye P., "Polar Molecules" Chemical Catalog Company (1920).

Deutsch K., Hoff, E.A.W., and Reddish, W., J.Polym.Sci., 13, 565 (1954).

Ehrlich P., J. Research Nat. Bur. Std., 51, 185 (1953).

Ferry, J.D., J.Amer.Chem.Soc., 72, 3746 (1950).

Ferry J.D., and Fitzgerald, E.R., J. of Colloid Science, 8, 224 (1953).

Ferry, J.D., and Fitzgerald, E.R. Grandine, L.D. Jnr., and Williams, M.L., Industrial and Engineering Chemistry, 44, 703, (1952).

Ferry, J.D. and Landel, R.F., J. Phys. Chem. 20, 294 (1956).

Ferry J.D. and Strella, S., J. Colloid Sci., 13, 459 (1958).

Fletcher, W.P. and Gent, A.N., Brit. J. Of Applied Physics, 8, 194 (1957).

Fröhlich, H., "Theory of Dielectrics", Clarendon Press Oxford p. 92 (1949).

Fuoss, R.M., J. Amer. Chem. Soc., 63, 369, 378 (1941).

Fuoss, R.M., and Kirkwood, J.G., J. of Amer. Chem. Soc., 63, 385 (1941a).

Gorton, G.C., Trans Faraday Soc., 42A, 56 (1946).

"General Discussion on Dielectrics" held at the University of Bristol England, April 24-26 (1946). Trans Faraday Soc., 42A (1946).

Glasstone, S., Laidler, K.J., and Eyring, H., "The Theory of Rate Processes" p. 544 McGraw-Hill (1941).

Von Hippel, A.R., "Dielectric Materials and Applications", Technology Press of Massachussetts Institute of Technology and J. Wiley and Son Inc., N.Y. 1954.

Hoff, E.A.W., Robinson, D.W. and Willbourn, A.H., J. Polym. Sci., 18, 161 (1955). Deutsch K., Hoff, E.A.W., and Reddish, W., J.Polym.Sci., 13, 565 (1954).

Jenckel, E., and Klein, E., Z. Naturf. 7a, 619 (1952).

Kambara, S., J. of Soc., of the Rubber Industry, Japan 15, 665 (1942).

Kemp. A.R., Proc. Rubber Technol. Conf. London. Hepper p.68 (1938) Rubber Chem. and Technol., 12, 470 (1939).

Kirchin, D.W., Ind. Engineg. Chem., 24, 549 (1932). Rubber Chem. and Technol., 5, 367 (1932).

Kimara, S., Aizawa, T., and Takeuchi, T., J. Inst. Elec. Engnrs. (Japan) Dec. 1274 (1928).

Kirkwood, J.G., and Fuoss, R.M., J. of Chem. Physics, 2, 329 (1941b).

Lanza, V.L., and Hermann, D.B., J.Poly. Sci., 28, 622 (1958).

Lorentz, H.A., Annalen Physik Chemie. 9, 641 (1880).

Lorentz, L.V., Annalen Physik Chemie., 11, 70 (1884).

Magat, M., and Reinisch, L., in "Verhalten in electrischem Washselfeder", edited by Karl A. Wold., Springer Verteg Berlin (1962) pp 519-550. Also Gost Th. Ibid., pp 550-568.

Margott, A.A., and Smith, E.R., "Tables of Dielectrics Constants of Pure Liquids" Natl. Bur. Stds. U.S., Line 514 Washington D.C. (1951).

Massachussetts Indistitute of Technology. "Tables of Dielectric Materials", Vol. IV, Laboratory for Insulation Research, Massachussetts Institute of Technology Technical Report No. 57 Jan. 1953. Also in "Dielectric Materials and Applications", A von Heppel, editor, Technology Press of M.I.T. and John Wiley and Sons Inc., N.Y. (1954).

Maxwell, J.C., "A Treatise on Electricity and Magnetism", 3rd Edition, Volume 1 p. 492, Clarendon Press (1892).

Mc.Call, D.W., in "Polythene" Edited by Renfrew and Morgan, Interscience Publishers Inc. New York (1957), p. 138.

McPherson, A.T., Bur. Std. J. Research, 8, 75, (1932).

McPherson, A.T., Rubber Reviews for 1963. Rubber Chem. and Technol. 36, 1230 (1963).

McPherson, A.T., and Cummings, A.D., J. of Research of The Bureau of Standards, 14, 553 (1935).

Miklaitov, G.P., J.Tech. Phys., Moscow, 21, 1395 (1951).
Norman, R.H., Proc. I.E.E. (1953), 100, II A. 41.
Nielsen, L.E., Buddahl A., and Levrault, R., J.Appl. Phys., 21, 607 (1950).

Oakes, W.G., and Robinson, D.W., J.Polym.Sci., 14, 505 (1954).

Oakes, W.G., and Richards, R.B., Transaction of the Faraday Society, 42A, 197 (1946).

Onsager, L., J. Amer. Chem. Soc., 58, 1486 (1936).

Payne, A.R., J. of App. Phys., 28, 378 (1957).

Payne A.R., Plastics, 23, 182 (1958).

Schallamach, A., Trans. Inst. Rubber Ind., 27, 40 (1951). Rubber Chem. and Technol., 24, 320 (1951).

Schlosser, E., in "Physik der Kunstoffe" edited by Holzmueller and Attenburg, Akademic-Verlog Berlin (1961). pp 487-559.

Schnieder, K. and Wolf, K., Kolloid Zchr. 124, 149 (1953).

Scott, A.H., McPherson, A.T., and Curtis, H.L. Journal of Research of the Bureau of Standards, 11, 173 (1933).

Smyth, C.R., "Dielectric Behaviour and Structure", McGraw Hill Book Co., N.Y. (1955).

Staverman, A.J., Heyboar, J., and Dekking, P., Proc. 2nd Intem. Congress. Rheology. Oxford. 123 (1953)

Thürn, H., and Wolf, K. Kolloid Z., 148, 16 (1956)

Thürn, H. and Wurstlin, F., Kolloid Zeits., 156, 21 (1958)

Van Vleck, J.H., "Electric and Magnetic Susceptibilities", Oxford University Press. London, (1932)

Wagner, K.W., Annalen der Physik. Leipzig, 40, 817 (1913)

Wagner, K.W., "After Effects in Dielectrics", Archives for Electrotechniques, 2, 371 (1914)

Waring, J.R.S., Trans.Inst. Rubber. Ind., 27, 16 (1951)
Rubber Chem. and Technol. 24, 299 (1951)

Williams, M.L., J. of Phys.Chem., 59, 95 (1958)

Williams, M.L., Landel, R.F, and Ferry, J.D., J. of Amer. Chem. Soc., 77, 374 (1955)

Williams, M.L. and Ferry, J.D., J. of Colloid Sci., 9, 479 (1954)
J. of Colloid Sci., 10, 1 (1955)
J. of Polymer Sci., 11, 169 (1953)

Wolf, K., Kunstoffe. 41, 89 (1951)

Wood, L.A., J. of Applied Physics. 12, 119 (1941)

Wurstlin, F., and Thurn, H., in "Theorie and Molekulare Deutung Technologischer Eigenschaften von Hochpolymeren Werkstoffen"., edited by H.A. Stuart. Springer-Varley Berlin. (1956)

Wyllie, A., in "Progress in Dielectrics", Vol. 2.,
Edited by Birks and Schulman. Heywood and Co. Ltd.,
London. (1960)

Yager, W.A., Physics, 7, 434 (1936)

Zapas, L.J., Shufler, S.L. and De Witt.,T.W.,
J. of Polymer Sci., 18 245 (1955).

CHAPTER 8 SUPPLEMENTARY CONTRIBUTIONS.

...n copy from "Rheology of Elastomers" edited by R. Mason and ... Wookey. Pergamon Press. Published on behalf of the ...itish Society of Rheology. This paper was read at the ... British Society of Rheology meeting at Welwyn Garden ... City (1958)

TEMPERATURE–FREQUENCY RELATIONSHIPS OF DIELECTRIC AND MECHANICAL PROPERTIES OF POLYMERS

A. R. PAYNE
Research Association of British Rubber Manufacturers

The method of reduced variables has been applied to the mechanical characteristics of an unvulcanized and a vulcanized natural rubber, a filled natural rubber vulcanizate, and an ebonite, as well as to the dielectric properties of unvulcanized natural rubbers. The overall master curves have been obtained in all cases and the characteristic reference temperature (T_s) determined from the experimental results. The four regions of visco-elastic behaviour in amorphous polymers (glassy amorphous, transition, highly elastic and flow) are discussed.

The second section of the paper discusses the variation with temperature of the frequency at which the tangent of the dielectric loss angle (tan δ) reaches a maximum. This variation was adequately described by Williams, Landel and Ferry's empirical equation. The nature of the polymer had a marked influence on the manner in which the experimental results were described by the empirical equation, and it was found that this behaviour can be separated into distinct groups. The T_s values were derived from the tan δ peak data and compared with the T_s values obtained from other types of physical measurement.

METHOD OF REDUCED VARIABLES

In recent years much consideration has been given to the temperature and frequency dependence of the mechanical and dielectric properties of rubber-like materials.[1–14] It has been recognized that these mechanical and electrical properties are related because they both involve configurational changes of flexible molecules.

The response of polymers to small mechanical or electrical oscillations is found to be affected equally by an increase in the temperature or a decrease in the frequency of the oscillations. Ferry and his co-workers have developed a method for transforming the temperature and frequency scales so that the observed values of a given property, e.g. elastic

modulus or dielectric constant, can be brought on to a single curve covering a very wide range of temperature and frequency. In this method each observation is transformed in two ways: first, in so far as the measured property follows normal kinetic theory, by a linear transformation of the absolute temperature to a suitable reference temperature T_s. Secondly, by a linear shift of log (frequency): this is done in such a way that all of the transformed observations fall on a continuous curve. The striking and convincing feature of this treatment is that the form of the frequency shifting factor log a_T as a function of temperature is determined solely by T_s, and if the appropriate values for T_s are chosen then the relation between a_T and $(T - T_s)$ is identical for all materials so far examined.

The relations used below for reducing the observations may thus be expressed as follows:

Taking the complex shear modulus G^* in terms of its real and imaginary components as

$$G^* = G' + iG'' \qquad \ldots.(1)$$

and the complex compliance J^* as

$$J^* = 1/G^* = J' - iJ'', \qquad \ldots.(2)$$

the kinetic theory transformation from a temperature T, where the density is ρ, to a reference temperature T_0, where the density is ρ_0, is

$$J'_r = (J' - J_\infty)\, T\rho/T_0\rho_0 + J_\infty \qquad \ldots.(3)$$

$$J''_r = J''\,(T\rho/T_0\rho_0) \qquad \ldots.(4)$$

and the linear log (frequency) transformation can be expressed by

$$w_r = wa_T \qquad \ldots.(5)$$

where J_∞ is the limiting compliance for the glassy amorphous state, J'_r and J''_r are the reduced real and imaginary parts of the compliance, and w_r is the reduced value of the circular frequency w. From kinetic theory only the configurational compliance is inversely proportional to absolute temperature, the glassy compliance J_∞ has to be deducted from J' before making the temperature reduction.

An equivalent series of relations holds for the complex dielectric constant ϵ^*, given by

$$\epsilon^* = \epsilon' + i\epsilon'' \quad \ldots.(6)$$

Thus, assuming that all the contributions to the dielectric constant associated with dipole orientation are inversely proportional to the absolute temperature but *directly* proportional to the density,

$$\epsilon_r' = (\epsilon' - \epsilon_\infty)\,(T\rho_0/T_0\rho) + \epsilon_\infty \quad \ldots.(7)$$

$$\epsilon_r'' = \epsilon''\,(T\rho_0/T_0\rho) \quad \ldots.(8)$$

and again,

$$w_r = wb_T \quad \ldots.(9)$$

ϵ_∞ being the limiting high frequency or low temperature value of ϵ'. These relations differ from equations (1) to (5) in respect of the inverted density dependence: the more molecules per unit volume the less the mechanical compliance but the greater the electrical polarization.

The factors a_T and b_T in equations (5) and (9) are interpreted as measures of the temperature dependence of the appropriate relaxation times. From Ferry's work it appears that a_T is given in terms of the reference temperature T_s by the empirical relation[4]

$$\log a_T = -8{\cdot}86\,(T - T_s)/(101{\cdot}6 + T - T_s) \quad \ldots.(10)$$

The parameter b_T is also given by equation (10), and the difference in symbolism is retained in the present paper solely to differentiate the electrical data from the mechanical.

MECHANICAL AND DIELECTRIC PROPERTIES OF NATURAL RUBBER

1. Dynamic Measurements with Natural Rubber

The method of reduced variables has been applied to mechanical measurements made on an unvulcanized, a vulcanized, and a filled, vulcanized, natural rubber and on an ebonite.

The reduction of dynamic data has previously been successfully carried out by the author[9] for a vulcanized acrylonitrile butadiene rubber, notwithstanding published statements[19] that reduction was not possible on vulcanized rubbers because

ross-linking structure affects the mechanical properties at ow frequencies. Recently Fletcher and Gent[46] have reduced he dynamic data of some rubber-like materials, including atural rubber, but their experimental results were limited nainly to the highly elastic plateau region and the lower art of the transition region. However, in these regions heir results are substantially in agreement with those discussed elow where comparison is possible. Zapas *et al.*[8] have also udied the dynamic properties of unvulcanized natural ubber over a wide temperature and frequency range.

Experimental details—In an earlier paper,[15,16] a non-sonant sinusoidal-strain machine for determining the low-equency dynamic properties of visco-elastic polymers was escribed. The principle of the machine was based on a tating eccentric shaft which, moving in a cross-head, could npose a sinusoidal strain on the test sample. The force nerated in the sample was measured by a differential ansformer situated in an extremely stiff type of proof ring.[17] he machine was designed to cover a frequency range of 0001 to 50 c/s and a temperature range of −75°C to 100°C. The rubber test cylinders were bonded to steel plates and static strain of one per cent of the cylinder height was imposed the rubber together with a constant oscillating strain of a alf of one per cent. The temperature increase within the bber being strained under these oscillatory conditions was ver observed to be greater than 0·5°C.

Results for unvulcanized natural rubber—The reduced values G_r' and G_r'' are plotted in Figs. 1 and 2, the experimental lues of G' and G'' having been reduced by equations 3, 4 d 5. All the curves in Figs. 1 and 2 were then translated ng the log frequency axis until superposition occurred, and ratio of the relaxation times was the frequency factor quired to bring about the superposition of the other curves that for temperature T_0. The temperature T_0 was 273°K. the shifting factors, $\log_{10} a_T$, describe the temperature-pendence of the relaxation times, it was expected that the ne values of a_T would be necessary to shift both the G_r' and data, and this was found to be the case.

The overall master curves obtained from superposition of data are shown in Fig. 3. It is apparent from the continuity

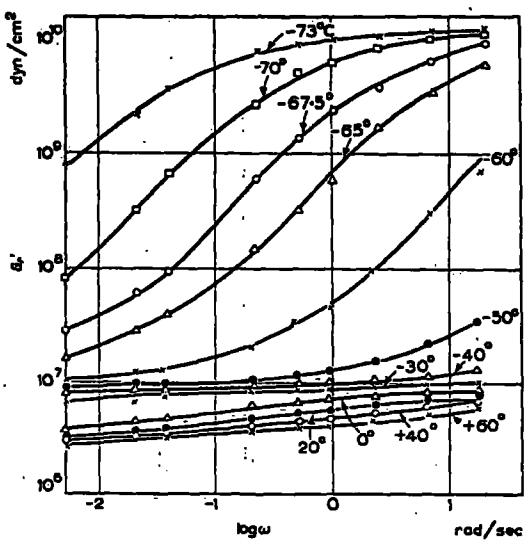

FIG. 1. Reduced modulus G_r' of unvulcanized natural rubber. $T_0 = 273°K.$

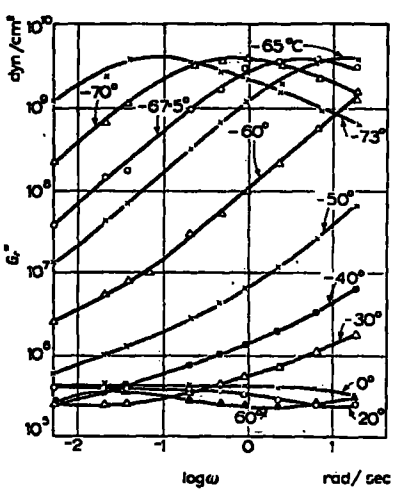

FIG. 2. Reduced modulus G_r'' of unvulcanized natural rubber. $T_0 = 273°K.$

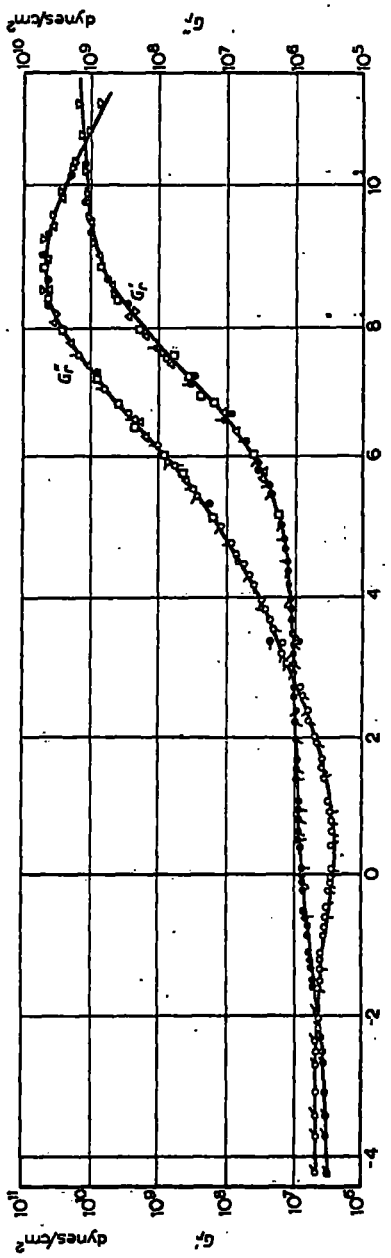

FIG. 3. Overall G_r' and G_r'' curves for unvulcanized natural rubber. Data obtained from Figs. 1 and 2. The different types of point refer to different temperatures.

of the superimposed data that the superposition was carried out with little ambiguity except perhaps at the lower frequencies in the highly elastic plateau region. The value of J_∞, the limiting high-frequency compliance, was taken to be $7{\cdot}7 \times 10^{-11}$ cm²/dyn.

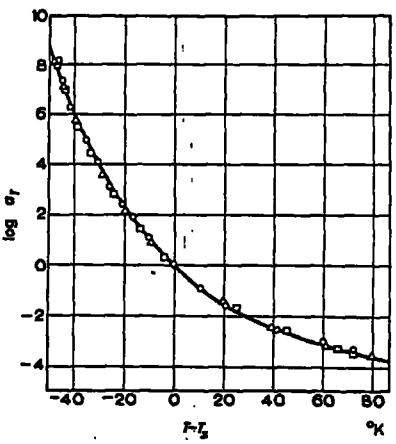

FIG. 4. $\text{Log}_{10}\, a_T$ versus $(T - T_s)$ for several rubbers. The solid line shown is the empirical curve described by equation (12).

○ experimental results of carbon black filled natural rubber vulcanizate. $T_s = -20$°C.

□ experimental results of vulcanized natural rubber. $T_s = -25$°C.

△ experimental results of unvulcanized natural rubber, $T_s = -25$°C.

When the values of a_T were plotted as $\log_{10} a_T$ against temperature T, it was found that the resulting curve could be superimposed on the curve obtained by plotting equation (10) using a suitable value T_0 for temperature T_s; for example, the curve described by equation (10) is shown as a solid line in Fig. 4, and the superimposed $\log_{10} a_T$ values for unvulcanized natural rubber are shown as squares about this line with T_s equal to 248°K. With this value of T_s the experimental results around the curve give an indication of the goodness of fit of equation (10) with the experimental values.

Vulcanized natural rubber—Figs. 5 and 6 show the final composite curves of G_r' and G_r'' for a lightly vulcanized natural rubber (Curve B); the experimental points are not shown

about the curve, but the scatter of the experimental points about the curve was of the same order as that shown in Fig. 3. The $\log_{10} a_T$ values which were necessary for superposition

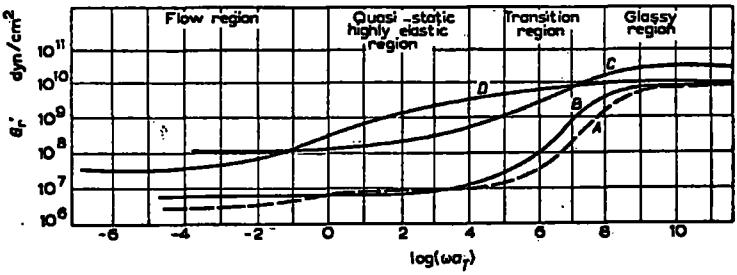

FIG. 5. Overall G_r' curves for several rubbers. $T_0 = 273°K$.
Curve A: unvulcanized natural rubber; from Fig. 3.
Curve B: lightly vulcanized natural rubber.
Curve C: carbon black loaded natural rubber vulcanizate.
Curve D: ebonite.

are included in Fig. 4 and shown as triangles. Again T_0 was 273°K and J_∞ was 8×10^{-11} cm²/dyn. The value of T_s to give the best fit of experimental values of a_T to the empirical equation (10) was 251°K.

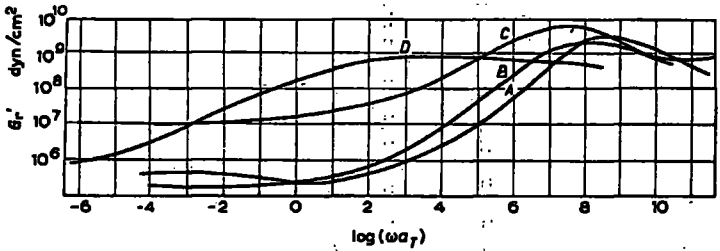

FIG. 6. Overall G_r'' curves for several rubbers.
Key as in Fig. 5.

Filled natural rubber vulcanizate—A natural rubber vulcanizate containing 50 parts by weight of carbon black (High Abrasion Furnace type) was studied, and in view of the known amplitude effect on the measured dynamic modulus values due to a thixotropic phenomenon,[20,21,22] and the normal heat build-up due to frictional energy losses in the rubber, the amplitude was kept as small as possible and constant.

In Figs. 5 and 6 are plotted the final composite curves of G_r' and G_r'' (Curve C). Again, except for the low frequency values, the superposition was obtained with little ambiguity although there was greater experimental scatter about the curve than for the unvulcanized rubber. T_0 was 273°K and J_∞ $2{\cdot}5 \times 10^{-11}$ cm²/dyn. It is evident the that G_r' and G_r'' curves for the filled rubber are flatter than that for the unvulcanized and highly vulcanized natural rubbers.

The corresponding $\log_{10} a_T$ values are included in Fig. 4 plotted as circles and the T_s was 253°K, only 2° higher than for the unfilled natural rubber vulcanizate. This suggests that the presence of an appreciable volume of filler does not affect the temperature dependence of the relaxation rates, which theory suggests are dependent on the free volume into which the relaxing molecules can move;[4] i.e. the free volume for the long-chain molecules in the presence of carbon black particles is little different from the free volume for the long-chain molecules of the unfilled vulcanizate.

Ebonite—Figs. 5 and 6 also show the corresponding overall curves for G_r' and G_r'' for a natural rubber vulcanized to the ebonite stage (Curve D). These curves were obtained by analysing the published results of Becker and Oberst.[23,28] The necessary $\log_{10} a_T$ values were similarly plotted as in Fig. 4 with $T_0 = 333$°K and a suitable value of T_s was found to be 360°K. It is to be noticed that the overall curves for ebonite are much flatter than those for the lightly vulcanized natural rubber. The degree of cross-linking corresponded to approximately one cross-link for every twenty atoms in the main chain, which is practically the maximum density of cross-linking obtainable.

Discussion—Below the so-called second order transition temperature in the 'glassy–amorphous' range, all high polymers appear to be very much alike. In this region the elastic properties are governed by the binding forces between neighbouring atoms, and the elastic modulus G_r' for the four rubbers studied in this paper was practically independent of temperature and frequency and lies in the neighbourhood of 5×10^{10} dyn/cm².

The reduced loss factor, $\tan \delta_r = G_r''/G_r'$ in this region was relatively small ($<0{\cdot}1$), and decreased with increasing $\log wa_T$.

Above the transition temperature, the chain segments of the high polymer become increasingly free, and they eventually attain complete mobility. In the highly elastic plateau range the modulus values were considerably smaller than the values in the glassy–amorphous region and the visco-elastic response to deformations or stresses in this region was reversible. This type of behaviour has been studied theoretically in a number of papers[24].

With higher temperatures (or lower frequencies) there has been found in linear uncross-linked polymers[8,23,28,29,30,36] a range in which they show increasingly plastic flow and pass into a fluid state, and this behaviour is to be seen in the low frequency extreme of the G_r' and G_r'' values for the unvulcanized natural rubber in Fig. 3.

At a given temperature, as the frequency increased the modulus passed through a dispersion range, and the tan δ values attained a maximum in the middle of the dispersion range. With increasing temperature, the dispersion ranges and the tan δ peaks shifted to higher frequencies, and it is now well known that all the high polymers have qualitatively the same behaviour.[12,23,25,26,27]

Fig. 5 summarizes the G_r' curves for the four rubbers studied, all the curves being reduced to a common standard of temperature, $T_0 = 273°K$, except for ebonite which was 333°K. Also indicated on the Fig. 5, but referring specifically to the unvulcanized natural rubber, are the four characteristic regions, i.e. the glassy amorphous region, the transition region, the highly elastic plateau and the region of plastic flow. For the vulcanizates there is no flow region. A study of these curves shows that it is possible to arrange a measure of classification based on the low frequency behaviour of these materials. This classification is based on the elastic moduli values in the highly elastic region. For example, linear polymers like polyvinyl chloride,[23,28] polystyrene[23,26] polymethyl methacrylate,[23,28] polyisobutylene[29,30,36] which have no cross-linking, have values of highly elastic moduli very similar to that of the unvulcanized natural rubber and at low frequencies have a flow region. Cross-linked polymers like vulcanized acrylonitrile butadiene,[9] GR-S,[28] and Vulkollan[28] show a highly elastic plateau similar to that of unfilled natural rubber

vulcanizates. The values of the moduli in this region are constant and dependent on the amount of vulcanization but are higher than for the linear polymers. The dependence on cross-linking is evident from an inspection of the curves, B and D, for lightly and heavily vulcanized rubbers respectively. An increase of cross-linking shifts the dispersion region to lower frequencies. If the ebonite curve had been reduced to 273°K the whole of the curve would have been shifted along the log wa_T axis in the decreasing frequency direction at least eight or nine decades; the exact shift could not be estimated because of the lack of data around 273°K.

Theory[31,32,33,34,35] suggests that the maximum value at low frequencies of G_r' possible by cross-linking is about 1×10^8 dyn/cm^2 and it is only possible to get higher values of this by the use of fillers. The characteristic of filled rubbers in the highly elastic region was to increase the value of G_r' with increasing volumes of filler, but without substantial change in the frequency range of the transition region, although the transition region curve is obviously flatter. Becker and Oberst[23] did attempt a classification on the lines of that discussed above, but it must be remembered that the actual compounding of a material will merge one group in with another; nevertheless the broad classification of the dynamic behaviour of materials into linear, cross-linked and filled can be a useful one in conjunction with the classification of the visco-elastic behaviour of polymers into regions of glassy amorphous, transition, highly elastic and flow.

Fig. 6 shows the corresponding G_r'' curves, and in general the comments on the G_r' apply equally well to these. Figs. 5 and 6 effectively summarize the general effects of compounding on the dynamic properties of natural rubber.

2. Dielectric Measurements on Natural Rubber

The dielectric properties of purified natural rubber have been studied by Norman[36] and discussed by Norman and Payne,[11] and a brief summary of the results is given below. The dielectric measurements were made over a frequency range of 50 to 10^6 c/s and over a wide temperature range. After the results were reduced according to equations (7) and (8) the overall curves for ϵ_r' and ϵ_r'' were obtained

in a similar manner to that described for the dynamic properties.

Fig. 7 shows the overall ϵ_r' values for four different natural rubber vulcanizates containing different percentages of combined sulphur with T_0 as 253°K. Details of the analysis will

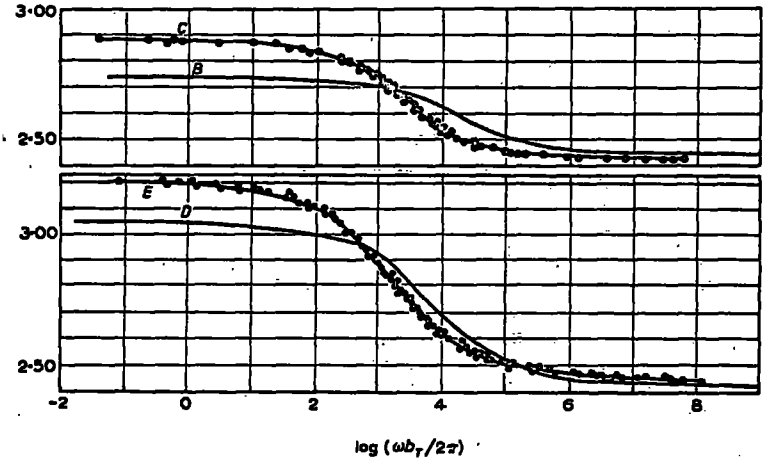

FIG. 7. Overall reduced permittivity ϵ_r' curves for several natural rubber vulcanizates. $T_0 = 253°K$.

Curve B: 1·7 per cent combined sulphur.
Curve C: 3·0 per cent combined sulphur.
Curve D: 3·0 per cent combined sulphur.
Curve E: 4·3 per cent combined sulphur.

be published elsewhere,[11] so the curves shown only summarize the data. The effect of increasing the sulphur content was to reduce slightly the frequency of the transition region and to increase the permittivity values (ϵ_r') at the low frequency end of the overall curve. Fig. 8 shows the corresponding ϵ_r'' values. Increased sulphur also increased the maximum value of the ϵ_r'' peak as well as decreasing the frequency of the position of the maximum value of ϵ_r''. The ϵ_r'' curve for unvulcanized natural rubber is indicated in Fig. 8. However, a characteristic feature of the unvulcanized natural rubber was the anomalous increase of ϵ_r'' due to ionic mechanisms at low frequencies or high temperatures. This behaviour appears to lie in a frequency region comparable to the region of plastic flow in the mechanical curves for unvulcanized natural rubbers.[11]

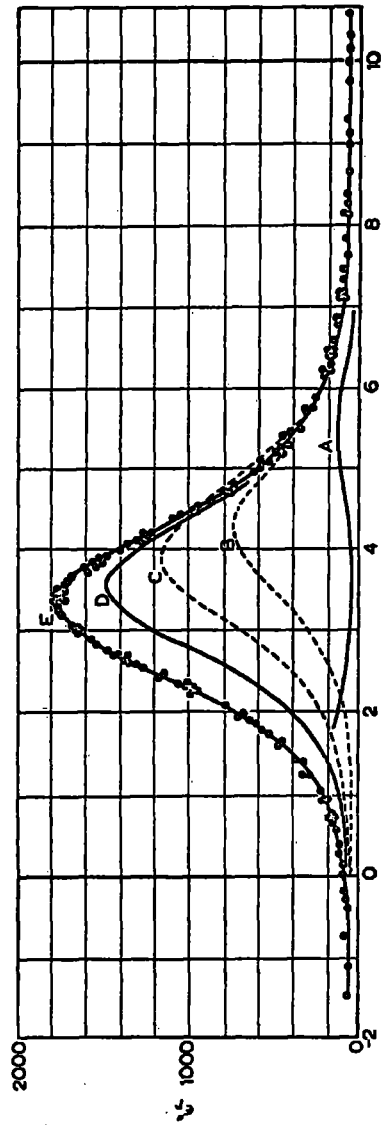

FIG. 8. Overall reduced loss factor ϵ_r'' curves for several natural rubber vulcanizates. $T_0 = 253°K.$

Key as for Fig. 7. Curve A refers to unvulcanized natural rubber.

The necessary experimental b_T values to achieve superposition of the reduced data are shown in Fig. 9, from which it

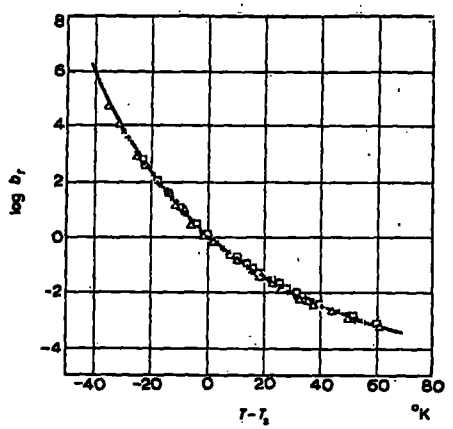

FIG. 9. $\text{Log}_{10}\, b_T$ versus $(T - T_s)$ for several natural rubber vulcanizates.

△ 1·7 per cent combined sulphur: (A.2) unaccelerated mixing.
□ 3·0 per cent combined sulphur: (A.4) unaccelerated mixing.
+ 3·0 per cent combined sulphur: (B.3) accelerated mixing.
× 4·3 per cent combined sulphur: (A.6) unaccelerated mixing.

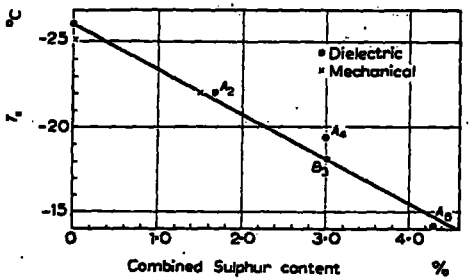

FIG. 10. T_s values as a function of combined sulphur content in natural rubber. The T_s values have been obtained from dielectric and mechanical measurements on unvulcanized and vulcanized natural rubbers.

can be seen that the empirical equation (10) gives an adequate description of the dielectric as well as the mechanical frequency–temperature equivalence of vulcanized and unvulcanized natural rubbers.

3. Comparison of T_g Values

Fig. 10 plots the derived dielectric and mechanical T_g values for the unvulcanized (0 per cent sulphur) and vulcanized unfilled natural rubbers against combined sulphur content. It is clear that to a first approximation there is a linear relationship between T_g and combined sulphur content, at least up to about 4 per cent combined sulphur; that increasing sulphur content increases the T_g value; and that the mechanically derived T_g value agrees with that obtained by dielectric measurements.

The quoted value of T_g, the second-order glass transition temperature, is −73°C for unvulcanized natural rubber.[67] Thus $T_g = T_g + 48$°C, which approximates to the relationship $T_g \simeq T_g + 50$°C, quoted by Williams *et al.*[4] for other materials. Further discussion of these T_g values is given in a later section.

OTHER POLYMERIC MATERIALS

1. Variation with Frequency of the Temperature at which tan δ reaches a Maximum

Thürn and Würstlin[87] give a diagram (their Fig. 1) showing the temperature of the tan δ maxima plotted against frequency for forty-four materials, for which adequate data were obtainable from the literature. They showed that by bearing in mind the chemical nature of these materials, the curves can be separated into two main groups. In the larger of the two groups, (group 1), are the curves with small temperature dependence, and in the smaller group, (group 2), all the maxima which undergo considerably more pronounced temperature shift with frequency.

An examination of the chemical structure of the materials in group 1 suggested further separation into three sub-groups, 1a, 1b and 1c. A complete list of the materials and the groups to which they have been assigned is given in Table 1. Sub-groups 1a contains only those polymers where a strong coupling between the dipoles contributes significantly to the cohesion, e.g. polyvinyl chloride or polyvinyl acetate, or else where strong steric hindrances exist, e.g. polystyrene, polymethyl methacrylate (principal maxima) or in which mobility is

hindered by cross-linking, e.g. vulcanized rubber with more than about 16 per cent of sulphur.

To sub-group 1b belong materials where no, or only very slight, hindrance exists to dipole movement; for instance natural rubber where the dimensions of the meshes of the network in vulcanizates with less than 5 per cent sulphur are so great that there is no perceptible hindrance to dipole movement. Also Thürn and Wolf[47] have shown that the coupling between the dipoles of neighbouring molecular chains in polymethyl acrylate and polyvinyl methyl ether is very much less than with polyvinyl acetate.

In dividing the high polymers into sub-groups a and b we have considered the extreme cases of marked hindrance to movement on the one hand and largely unhindered mobility on the other. There is no doubt that, as the data for plasticized materials and natural rubber with 5–16 per cent sulphur show, there are materials whose properties place themselves between groups 1a and 1b which for convenience will be referred to as group 1c.

The loss-maxima due to chain mobility can only occur when the polymer exhibits high elasticity, i.e. above the glass transition or vitrification temperature, but some materials show secondary and other peaks which cannot be due to the movements of large portions of polymer chains. Group 2 contains for high polymers only their secondary maxima. It is possible to draw certain conclusions by a comparison of the behaviour of these materials with the similar behaviour of the low molecular weight substances containing the same polar groups. In this way Reddish[38] showed that the secondary maxima of Terylene arise from movements of the OH groups of the chain terminations and similar explanations can be made for the other materials placed in group 2.[37,39,40]

2. Empirical Temperature–Frequency Relationships

Consider the variation of the temperature at which the tan δ peak occurs as a function of frequency; and define b_T as the ratio ω/ω_s where ω is the characteristic frequency at temperature T and ω_s is the characteristic frequency at the reference temperature T_s. Then it should be possible to choose T_s to describe the curve in Fig. 1 of Thürn and

Würstlin's paper by the empirical equation (10), if the empirical equation is of universal application to long-chain molecules. The choice of a suitable T_s value is most easily made by a graphical technique now to be described.

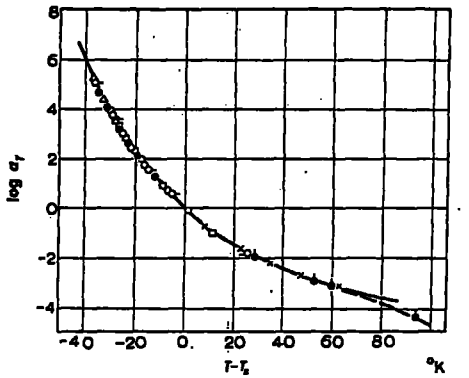

FIG. 11. $(T - T_s)$ versus $(\mathrm{Log}_{10} b_I)$
The solid line shown is the empirical curve described by Eq. (12).

Symbol	Curve number	Material
Open circle	31	Glycerin
Open circle with dash	1	Ebonite. Rubber with 32% sulphur.
Filled circle	2	Polyvinyl formal
Filled circle with dash	44	Monochlorotrifluorethylene
Cross	34	1,2,4,-trimethyl-3,5,6,-trichlorobenzene
Square	5	Terylene (principal maxima)
Triangle	4	Polymethyl methacrylate (principal maxima)

Graphical technique for obtaining suitable T_s values—The solid line in Fig. 11 shows the graphical representation of equation (10), i.e. log b_T versus $(T - T_s)$. By using transparent paper it is possible by vertical and horizontal translations of the data, to superimpose the experimental points about the empirical curve, thus identifying the frequency change of the experimental data with log b_T and the temperature change with

$(T - T_s)$. Space has limited graphical representation to a few materials. With the majority of the data there is little ambiguity about the positioning of the experimental points shown in Fig. 11 about the empirical curve, but of course some ambiguity does exist for materials for which data are limited.

The first conclusion to be drawn, from the fit of the experimental results about the empirical curve, is that except for some group 2 materials positioned at the extreme range of $(T - T_s) > +50°C$, equation (10) gives an adequate description of the temperature–frequency relationship of the tan δ peak position, using T_s as an arbitrary defining parameter. A T_s value for each of these materials can thus be obtained in principle, and a few of these are discussed later.

For three group 2 materials some experimental points occurred at $(T - T_s)$ values greater than $+50°C$ and a divergence from the empirical curve exists. This is not unreasonable since even for ordinary liquids far above their glass transition temperature (or freezing point) the temperature dependence of viscosity varies widely, and is related to specific details of molecular structure.[4,42]

3. Distribution of the Groups on the Empirical Curve

A detailed examination was made of the experimental points (not all reproduced on Fig. 11) about the empirical curve and this again revealed the grouping discussed previously. To examine this distribution of experimental points the position of the experimental tan δ peak at 10^4 c/s of each material on the $\log_{10} b_T$ $(T - T_s)$ curve will now be discussed. Table 1 gives the $\log_{10} b_T$ value for the 10^4 c/s peak ($\log_{10} B_T$), and the materials in the table are in the order of decreasing $\log_{10} B_T$. When so arranged in this order there is seen to be an obvious connection with the grouping. In particular, all the group 1b materials of high molecular weight are clustered within a very narrow range of $\log_{10} B_T$ ($+0{\cdot}20$ to $+1{\cdot}45$), and furthermore, $\log_{10} B_T$ values for group 2 materials are clearly distinct from all group 1 values. A detailed examination of group 1a materials shows log B_T dependent on the temperature at which the tan δ values reach a maximum at 10^4 c/s and this is shown in Fig. 12.

TABLE 1—*Log B_T values*

Thürn and Würstlin's[37] curve number	Material	Original source of data	Group	Log B_T
		Reference		
1	Vulcanized rubber with 32% sulphur	48	1a	+2·80
2	Polyvinyl formal	49	1a	+2·45
3	Polystyrene	50	1a	+2·25
4	Polymethyl methacrylate (principal maxima)	40	1a	+2·14
5	Terylene (principal maxima)	38	1a	+1·89
7	Polyvinyl chloride	51	1a	+1·64
39	Paraffin wax	63	1b	+1·45
28	Polybutyl acrylate	51	1b	+1·32
9	Polyvinyl acetal	49	1a	+1·23
6	Polyacrylonitrile	51	1c	+1·17
10	Polyvinyl isobutyral	48	1c	+1·12
38	Cetyl palmitate	63	1b	+0·90
29	Unvulcanized rubber	48	1b	+0·77
43	Monostearine	66	1b	+0·65
26	Polyvinyl methyl ether	51	1b	+0·56
40	Neoprene GN	64	1b	+0·47
41	Polytrimethylene succinate	65	1b	+0·40
42	Polytrimethylene malonate	65	1b	+0·34
31	Glycerin	58	1b	+0·29
27	Rubber with 4% sulphur	48	1b	+0·24
21	Polymethyl acrylate	56	1b	+0·20
11	Polyhexamethylene sebacamide	53	1c	+0·17
13	Polyvinyl hexenal	54	1a	+0·15
12	Polyvinyl acetate	55	1a	+0·13
14	Polyvinyl-2-ethyl hexanal	54	1a	−0·12
25	Rubber with 8% sulphur	48	1c	−0·16
17	Polyvinyl acetate	52	1a	−0·20
33	Polychlorotrifluoroethylene (low molecular weight fluid)	60	1b	−0·26
19	Rubber with 16% sulphur	48	1a	−0·34
24	Rubber with 10% sulphur	58	1c	−0·44
22	Rubber with 12% sulphur	48	1c	−0·56
20	Polyvinyl propionate	51	1a	−0·70

TABLE 1 (*continued*)

Thürn and Würstlin's[37] curve number	Material	Original source of data	Group	Log B_T
		Reference		
37	Cellophane	62	2	−2·13
36	1,2,3,4-tetramethyl-5,6-dichlorobenzene	61	2	−2·23
34	1,2,4-trimethyl-3,5,6-trichlorobenzene	61	2	−2·42
35	Pentamethyl chlorobenzene	61	2	−2·74
30	Ice	59	2	−3·13
44	Monochlorotrifluoroethylene	66	2*	−3·23
32	Terylene (secondary maxima)	38	2	−3·42
38	Poly-α-chloromethyl methacrylate	63	2*	−3·74
15	Polymethyl methacrylate (secondary maxima)	40	2	−4·14
23	Polyvinyl chloride (secondary maxima)	57	2	−4·27
16	Polymethyl methacrylate (secondary maxima)	51	2*	−4·52

Full line indicates limits of group 2 materials
Dashed line indicates limits of high molecular weight materials of group 1b
Dotted line indicates limits of group 1a materials

* Indicates the group 2 materials whose higher frequency results diverge from the empirical curve about $T - T_s = +50°C$.

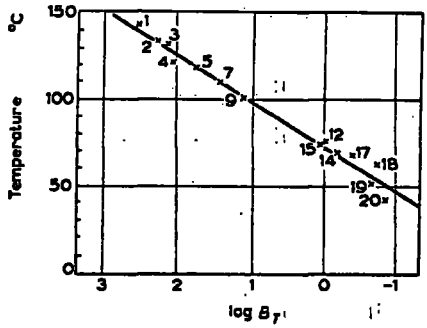

FIG. 12. Temperature of the tan δ peak at 10^4 c/s versus $\log_{10} B_T$ of the group 1a materials. The number beside the plotted points refers to the curve number in Fig. 1 of ref. 37. See Table 1 for identification of the materials.

10^4 c/s was chosen arbitrarily, since it was convenient about the middle frequency of the normal experimental range. Some other frequency could have been chosen, but the form of the distribution would have been the same.

4. Comparison of T_s Values

From the fit of the curves in Fig. 1 of Thürn and Würstlin about the empirical curve in Fig. 11, it was possible to obtain directly the T_s value for the material, and this was done for those materials for which similar values of T_s had been derived from other types of dielectric or mechanical measurement. Table 2 lists the materials so studied together with their T_s values and the form of measurement by which the T_s values were obtained.

An inspection of the T_s values reveals that those for polyvinyl acetate, polyvinyl acetal, and polyvinyl chloride derived from the tan δ peak data, agree well with those values obtained by others who used complete temperature reduction of dielectric and mechanical data for their analyses.

The tan δ derived T_s value for polystyrene, 411°K, is higher than that quoted from dynamic measurements, 408°K but is nearer to the value of 412°K, obtained from the reduction of data of Becker and Oberst[23] by the writer.[28] The tan δ derived T_s value for the principal tan δ peak of polymethyl methacrylate is 431°K; this compares with 435°K obtained from dynamic data, and 433°K obtained from stress relaxation measurements.

The T_s values of unvulcanized natural rubber varies according to the source of data from 247 to 250°K with a mean value of 248°K. The T_s values for vulcanized natural rubber are dependent on the degree of cross-linking.

The agreement of the tan δ derived T_s values with the T_s values derived from other types of measurements implies that the T_s values can be obtained with a reasonable degree of accuracy from a limited amount of experimental data, i.e. the temperature values and the frequency positions of the tan δ peaks.

A more detailed study of the materials discussed in the second part of this paper, especially a comparison of the dielectric grouping with a similar mechanical grouping together with

TABLE 2

Material	Type of measurement	Source of data	T_s Value (°K)
Polystyrene	D	3, 43	408
	D	28 from 23	412
	E	Tan δ peak	411
Polyvinyl acetate	D	5, 3.	349
	E	5, 3.	349
	E	Tan δ peak	351
Polyvinyl acetal	E	3, 44	380
	E	Tan δ peak	380
Polymethyl methacrylate	S	3, 45	433
	D	28 from 23	435
	E	Tan δ peak	431
Polyvinyl chloride	D	28 from 23	396
	E	Tan δ peak	393
	E	28 from 52 (tan δ)	394
Natural rubber, unvulcanized	E	28	247
	E	Tan δ peak	250
	D	First part of paper	248
	D	28 from 8	248
	D	46	248
vulcanized	D	46	251
1·5% combined sulphur	D	First part of paper	251
1·7% combined sulphur	E	First part of paper	251
3·0% combined sulphur	E	First part of paper	254
3·0% combined sulphur	E	First part of paper	255
4·3% combined sulphur	E	First part of paper	259
16% sulphur by weight	E	Tan δ peak	310
12% sulphur by weight	E	Tan δ peak	294
10% sulphur by weight	E	Tan δ peak	283
8% sulphur by weight	E	Tan δ peak	275
4% sulphur by weight	E	Tan δ peak	261
	C	10	256
Polymethyl methacrylate (Secondary peak in the glassy amorphous range)	E	Tan δ peak	295
	E	Tan δ peak	285
	D	28 from 23	285

D = dynamic mechanical, S = stress relaxation, E = dielectric, C = percentage creep or recovery.

the implications of this grouping, is to be given in a subsequent paper.

CONCLUSIONS

A mechanical and dielectric study of natural rubber shows that the method of reduced variables applies whether the material is unvulcanized, lightly vulcanized, heavily vulcanized or loaded with carbon black, and furthermore allows the results obtained over a very wide temperature or frequency range to be presented very concisely by a single overall curve for each material.

A study of the frequency–temperature relationships of the tan δ peaks of a wide variety of polymeric materials in the second part of the paper shows that the empirical equation (10) is an adequate description of the temperature dependence of the relaxation times within $T_s \pm 50°C$, and that the dielectric response of a material follows its chemical grouping. The fit of the group 2 materials also raises the interesting conjecture that the relaxation behaviour of the side groups of the chain backbone of the polymers might be adequately described by the empirical equation (10) over a wider frequency and temperature range than it is possible to obtain experimentally and that there is another glass transition temperature associated with the side groups apart from the glass transition temperature associated with the chain backbone.

The general usefulness of the empirical equation (10) in all sections of the work described in this paper as well as the fact that the temperature reduction principle appears to be quite independent of the relaxation spectrum, justifies the claim by Williams *et al.*[4] that equation (10) is a universal function describing the temperature dependence of viscosity and the mechanical and electrical relaxations in amorphous polymers and other supercooled glass-forming liquids.

The author's thanks are due to the Research Association of British Rubber Manufacturers for permission to publish this paper.

REFERENCES

[1] FERRY, J. D. *J. Amer. Chem. Soc.* **72**, 3746 (1950).
[2] FERRY, J. D., FITZGERALD, E. R., GRANDINE, L. D., Jr. and WILLIAMS, M. L. *Ind. Engng. Chem.* **44**, 703 (1952).

[3] Williams, M. L. *J. Phys. Chem.* **59**, 95 (1955).
[4] Williams, M. L., Landel, R. F. and Ferry, J. D. *J. Amer. Chem. Soc.* **77**, 374 (1955).
[5] Williams, M. L. and Ferry, J. D. *J. Colloid Sci.* **9**, 479 (1954).
[6] Williams, M. L. and Ferry, J. D. *J. Colloid Sci.* **10**, 1 (1955).
[7] Williams, M. L. and Ferry, J. D. *J. Colloid Sci.* **10**, 474 (1955).
[8] Zapas, L. J., Shufler, S. L. and De Witt, T. W. *J. Polymer Sci.* **18**, 245 (1955).
[9] Payne, A. R. *J. Appl. Phys.* **28**, 378 (1957).
[10] Payne, A. R. *Research Association of British Rubber Manufacturers Research Memo.* R. 407 (1957).
[11] Norman, R. H. and Payne, A. R. Submitted to the Institution of Electrical Engineers.
[12] Ferry, J. D. and Fitzgerald, E. R. *J. Colloid Sci.* **8**, 224 (1953).
[13] Alfrey, T. Jr. *Mechanical Behaviour of High Polymers*, Vol. VI. Interscience Publishers, New York (1948).
[14] Alexandrov, A. P. and Lazurkin, J. S. *Acta Physico-Chim. U.R.S.S.* **12**, 647 (1940).
[15] Payne, A. R. *Research Association of British Rubber Manufacturers Research Report* No. 76 (1956).
[16] Payne, A. R. *Rev. Gén. Caout.* **33**, 885 (1956).
[17] Payne, A. R. and Smith, S. F. *J. Sci. Instrum.* **33**, 432 (1956).
[18] Gent, A. N. *Trans. I.R.I.* **30**, 139 (1954).
[19] Hutton, A. Q. and Nolle, A. W. *J. Appl. Phys.* **25**, 350 (1954).
[20] Fletcher, W. P. and Gent, A. N. *Trans. I.R.I.* **29**, 266 (1953).
[21] Payne, A. R. *Proc. 3rd Rubber Tech. Conf.* 413 (1954).
[22] Davies, D. M. and McCallion, H. *Proc. Inst. Mech. Engrs.* **189**, 1125 (1955).
[23] Becker, G. W. and Oberst, H. *Kolloidzschr.* **148**, 6 (1956).
[24] Treloar, L. R. G. *The Physics of Rubber Elasticity.* Clarendon Press, Oxford (1949).
[25] Müller, F. H. *Kolloidzschr.* **120**, 119 (1951).
[26] Wolf, K. *Kunststoffe* **41**, 89 (1951).
[27] Becker, G. W. *Kolloidzschr.* **140**, 1 (1955).
[28] Payne, A. R. To be published.
[29] Marvin, R. S. *Proc. 2nd Int. Congr. Rheol.*, p. 156. Butterworths, London (1954).
[30] Ferry, J. D. and Fitzgerald, E. R. *Proc. 2nd Int. Congr. Rheol.*, p. 140. Butterworths, London (1954).
[31] Auluck, F. C. and Kothari, D. S. *J. Chem. Phys.* **11**, 387 (1943).
[32] Flory, P. J. and Rehner, J., Jr. *J. Chem. Phys.* **11**, 521 (1943).
[33] Wall, F. T. *J. Chem. Phys.* **11**, 527 (1943).
[34] Kuhn, W. and Grün, F. *J. Polymer Sci.* **1**, 183 (1946).
[35] James, H. M. and Guth, E. *J. Polymer Sci.* **4**, 153 (1949).
[36] Norman, R. H. M.Sc. Thesis, London University (1954).
[37] Thürn, J. and Würstlin, F. *Kolloidzschr.* **145**, 133 (1956). These authors had collected together the majority of the dielectric tan δ data on polymers in the literature up to 1956.

[38] REDDISH, W. *Trans. Faraday Soc.* **46**, 459 (1950).
[39] HEYBOER, J., DEKKING, P. and STAVERMAN, A. J. *Proc. 2nd Int. Congr. Rheol.*, p. 123. Butterworths, London (1954).
[40] DEUTSCH, K., HOFF, E. A. W. and REDDISH, W. *J. Polymer Sci.* **13**, 565 (1954).
[41] IWAYANAGI, S. *J. Sci. Res. Inst. Japan* **49**, 23 (1955).
[42] BONDI, A. *Ann. N.Y. Acad. Sci.* 53 (1951).
[43] FITZGERALD, E. R., GRANDINE, L. D., JR. and FERRY, J. D. *J. Appl. Phys.* **24**, 650 (1953).
[44] FERRY, J. D., WILLIAMS, M. L. and FITZGERALD, E. R. *J. Phys. Chem.* **59**, 403 (1955).
[45] BISCHOFF, J., CATSIFF, E. and TOBOLSKY, A. V. *J. Amer. Chem. Soc.* **74**, 3378 (1952).
[46] FLETCHER, W. P. and GENT, A. N. *Brit. J. Appl. Phys.* **8**, 194 (1957).
[47] THÜRN, H. and WOLF, K. *Kolloidzschr.* **148**, 16 (1956).
[48] SCOTT, A. H., MCPHERSON, A. T. and CURTISS, H. L. *Bur. Stand. J. Res. Wash.* **11**, 173 (1933).
[49] FUNT, B. L. and SUTHERLAND, T. H. *Canad. J. Chem.* **30**, 940 (1952).
[50] BAKER, E. B., AUTY, R. P. and RITENOUR, G. J. *J. Chem. Phys.* **21**, 159 (1953).
[51] WÜRSTLIN, F. (unpublished measurements). From THÜRN, H. and WÜRSTLIN, F.[37]
[52] WÜRSTLIN, F. *Kolloidzschr.* **120**, 102 (1950).
[53] BAKER, W. O. and YAGER, W. A. *J. Amer. Chem. Soc.* **64**, 2171 (1942).
[54] SUTHERLAND, T. H. and FUNT, B. L. *J. Polymer Sci.* **11**, 177 (1953).
[55] HOLZMULLER, W. *Phys. Z.* **42**, 281 (1941).
[56] MEAD, D. J. and FUOSS, R. M. *J. Amer. Chem. Soc.* **64**, 2389 (1942).
[57] FUOSS, R. M. *J. Amer. Chem. Soc.* **63**, 369 (1941).
[58] MÜLLER, F. H. *Ergebn. exakt. Naturw. Berlin* **17**, 164 (1938).
[59] SMYTHE, C. P. and HITCHCOCK, C. S. *J. Amer. Chem. Soc.* **54**, 4631 (1932).
[60] REYNOLDS, S. I., THOMAS, V. G., SHARBAUGH, A. H. and FUOSS, R. M. *J. Amer. Chem. Soc.* **73**, 3714 (1951).
[61] WHITE, A. H., BIGGS, B. S. and MORGAN, S. O. *J. Amer. Chem. Soc.* **62**, 16 (1940).
[62] MÜLLER, F. H. In STAGER, H. *Werkstoffkunde.* Berlin (1944).
[63] JACKSON, W. *Proc. Roy. Soc.* A, **150**, 197 (1935).
[64] SCHMEIDER, W. C., CARTER, W. C., MAGAT, M. and SMYTHE, C. P. *J. Amer. Chem. Soc.* **67**, 959 (1945).
[65] PELMORE, D. R. and SIMONS, R. L. *Proc. Roy. Soc.* A, **175**, 468 (1940).
[66] CROWE, R. W. and SMYTHE, C. P. *J. Amer. Chem. Soc.* **72**, 4427 (1950).
[67] BOYER, R. F. and SPENCER, R. S. *Advances in Colloid Science*, Vol. 2, p. 1. Interscience Publishers Inc., New York (1946).

DISCUSSION

A. JOBLING: You stated that some at least of your results were amplitude-dependent. Would you therefore indicate how your comparisons of the properties of different materials were made: for example were all the

measurements taken at some constant amplitude? In theory, the mechanical properties should be amplitude-independent if the amplitude is sufficiently small.

Answer: Only the results on vulcanized natural rubber containing carbon black were amplitude-dependent and comparisons refer to measurements at a constant, small amplitude.

No increased effect of this thixotropic behaviour was observed at the lower temperatures. It appears that if the amplitude is maintained constant then a consistent set of results is obtained.

At very small amplitudes, the mechanical properties of rubber should be amplitude-independent, but this has never been shown, and an investigation into this very point is now being undertaken at R.A.B.R.M.

C. VAN DER POEL: When trying to relate the temperature- and frequency-dependencies of the mechanical properties of bitumens having widely differing rheological characteristics, we found an empirical relationship very similar to that presented by the author. We also found that the behaviour of each material could be characterized by a particular reference temperature. (*vide Proc. 2nd Int. Congr. Rheol.* p. 331, Butterworths, London (1954)). I think, therefore, that you can probably add a class of natural polymers to your impressively long list, viz. bitumens.

A. H. WILLBOURN: 'Transitions' may be associated with specific groups of atoms, at least in certain cases, and these may be present either in side groups or in part of a main polymer chain. Such relevant evidence as exists seems to suggest that all the transitions are associated with processes occurring in the amorphous regions of polymers. Crystallization has only an indirect effect, which may however be very considerable in the temperature region of melting.

Many polymers show more than one transition region: in such cases can you suggest any criterion for deciding which is the glass transition?

Answer: I agree that all of the transitions are associated with processes occurring in the amorphous regions of polymers, and I have made the suggestion, from very meagre data, that there might be separate transitions associated with side groups, and their temperature–frequency relationships might be explained by equation (10). Thus there will be a principal or glass transition associated with the flexible long-chained backbone, and secondary transitions in the amorphous range due to side chains of local grouping. Surely however, the magnitude of the change in modulus is a good criterion for distinguishing between transitions. Thus, for the transition associated with the long-chain backbone this is at least one decade and often (as in most commercial rubbers) three or four decades. Transitions associated with secondary phenomena, on the other hand, are often difficult to identify because the change in modulus is relatively small.

The problems of mixed or co-polymers have not been sufficiently studied to say what is meant by a transition in this case, where, in the highly elastic plateau region, more than one peak often appears. Each peak can be attributed to a statistical distribution of one component within the other, although in the case of Buna S and SS which have two peaks, there is apparently only one glass transition temperature.

A. C. EDWARDS: In the reduction of data by the Ferry method is the limiting value of compliance (J_∞) taken directly from the experimental data or is it derived independently?

Answer: It was taken from the lowest observed experimental value of J'. The exact value of J_∞ was not very critical.

A. CHARLESBY: Could you give data for the various types of polyethylene now available? This may provide some further useful information on the size of the crystallites in linear and branched polyethylene. If T_g for a cross-linked chain is plotted against the distance between successive links, the change should occur at a critical cross-linking density, when interference first occurs between successive links. At lower densities of cross-linking, only rubber-like elasticity should be observed. This may provide some evidence on the length of the segment.

Answer: There are not sufficient data available to check your suggestion, but it is an extremely interesting one.

Future developments on the lines you suggest may well make use of the universal Williams, Landel and Ferry equation (10) which relates the temperature-coefficient of segmental viscosity to a single parameter T_s or T_g. Ferry and his co-workers have shown the wide range of applicability of this equation, and I hope that the present work has strengthened their findings, particularly with regard to rubbers of varying composition and containing fillers. If the interpretation of this equation in terms of free volume can be clarified, then the type of investigation you suggest should prove to be fruitful.

Read at the Silver Jubilee Symposium of the Plastics and Rubber Group 1958. Published in the Society of the Chemical Industry Journal No 5.

THE MECHANICAL AND DIELECTRIC TEMPERATURE/ FREQUENCY EQUIVALANCE OF POLYMERS: GR-S

By A. R. PAYNE

(Research Association of British Rubber Manufacturers, Shawbury, Shrewsbury, Salop.)

The method of reduced variables has been applied to the dielectric and dynamic mechanical measurements of unvulcanized and vulcanized samples of synthetic rubber, GR-S, as well as to the dynamic mechanical properties of carbon-black-loaded GR-S vulcanizates. The overall master curves of property against frequency have been obtained, and the characteristic reference temperatures (T_s) determined from the experimental results by the use of a recently-published empirical equation describing the temperature/frequency equivalence of polymers. A comparison of the dynamic mechanical and dielectric behaviour of the synthetic rubber GR-S with that of natural rubber is given.

Introduction

Much consideration has been given in recent years to the temperature- and frequency-dependence of the mechanical and dielectric properties of long-chain polymers,[1-19] but the vast majority of the work has been confined to non-cross-linked materials and only a few papers[6,16,19] have dealt with the relationships between the dielectric and dynamic mechanical properties of rubber-like materials that are in commercial use in rubber products such as vibration and shock absorbers, tyres and cables. Those used are normally vulcanized and often contain varying proportions of carbon black as a filler, and by far the greatest bulk of rubber used contains either natural rubber or GR-S, a copolymer of butadiene and styrene. An earlier paper[19] in this series relating the dynamic mechanical and dielectric temperature/frequency equivalence of polymers dealt mainly with natural rubber, although many other polymer systems were discussed; the present paper continues the study on the synthetic rubber, GR-S.

Method of reduced variables

The response of polymers to mechanical or electrical oscillations is found to be dependent upon a change of frequency of oscillation or a change of temperature of test. Ferry and his co-workers[1-7,8] have developed a method for transforming the temperature and

limited mainly to the highly elastic plateau region and the lower part of the transition region; their results, however, are substantially in agreement with those discussed below where comparison is possible. Zapas *et al.*[8] have also studied the dynamic properties of a fraction of very high molecular weight of an unvulcanized GR-S over a very wide temperature and frequency range, but there appears to be very little other published data on the dynamic properties of GR-S.

Experimental details

In an earlier paper[23,24] a non-resonant sinusoidal-strain machine for determining the dynamic properties of polymers was described. The rubber was sinusoidally strained in shear and the force generated was measured by means of a differential transformer situated in an extremely stiff type of proof ring.[25] The machine was designed to cover a frequency range of 0·001–50 c/s and a temperature range of −70° to 100°. The rubber cylinders were bonded to steel plates and a static strain of 1% of the cylinder height was imposed on the rubber together with an oscillating strain of 0·5%.

Results for unvulcanized and vulcanized GR-S

The overall master curves of G'_r obtained by reduction and superposition of the data using equations (5) to (9) are shown in Fig. 7. The lowest curve is for the unvulcanized GR-S, and the degree of scatter of the experimental points about the master curve is indicated; this amount of scatter was typical of the particular set of results shown in Fig. 7. The four characteristic regions of viscoelastic behaviour are clearly indicated by the master curve of the unvulcanized GR-S, i.e., at low frequencies (or high temperatures) the G'_r values are dropping rapidly with decreasing frequency, thus indicating the characteristic behaviour of a region of flow. At higher frequencies there is a pseudo-elastic plateau region, which for the GR-S rubbers has a marked slope with frequency compared with that obtained on natural rubber.[8,16,19] At even higher frequencies there is a sharp rise in the shear modulus as the rubber changes from a rubber-like material to a rigid glass. The sharp rise portion is known as the 'transition region', and the final high-frequency plateau as the 'glassy-amorphous'.

The first apparent effect of a small degree of vulcanization is to increase the G'_r values in the pseudo-elastic plateau region: it only alters to a limited extent the onset of a flow region at low frequencies. Higher amounts of vulcanization progressively cause a decrease of the frequency at which the transition region occurs,

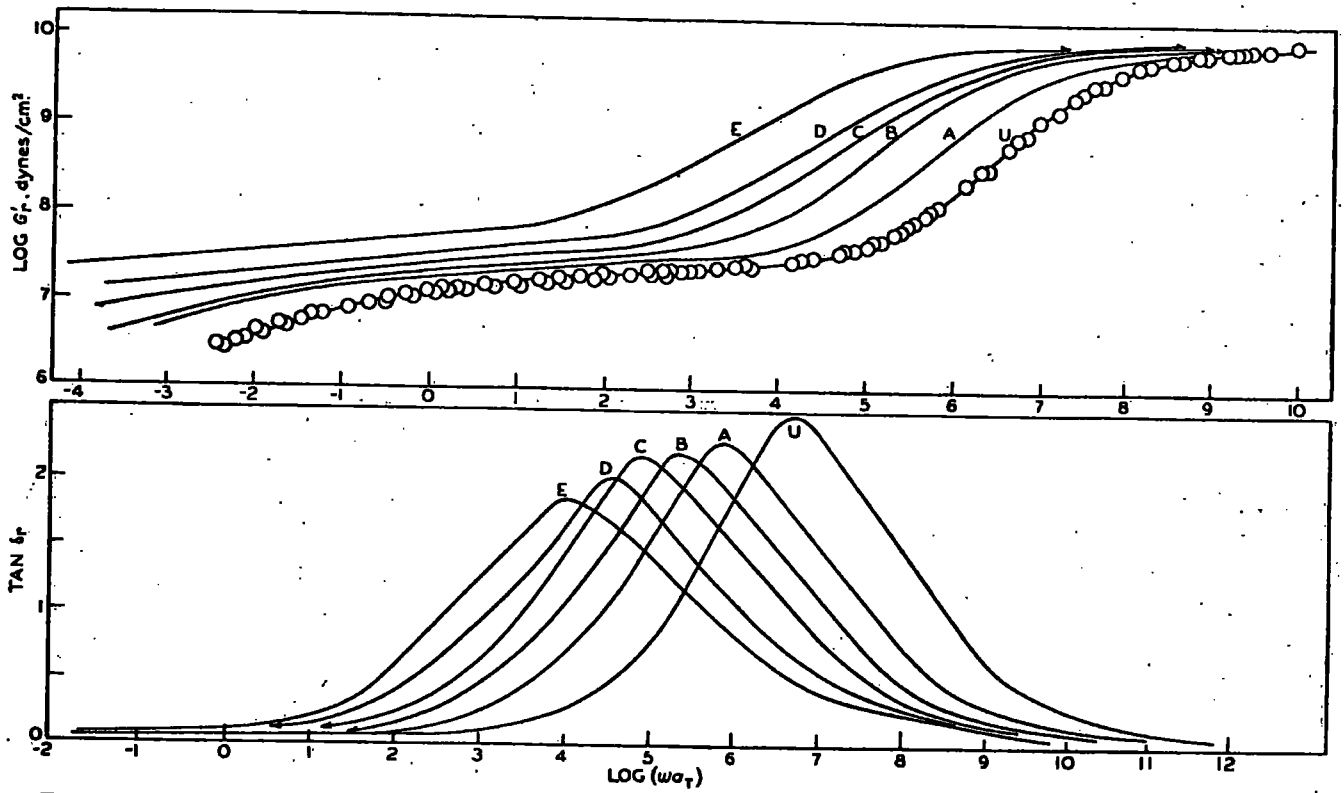

FIG. 7 (top). *Master curves for* G'_r versus $log_{10}\omega a_T$ *for GR-S rubbers*

FIG. 8 (bottom). *Master curves of tan* $\delta_r = G''_r/G'_r$ versus $log_{10}\omega a_T$ *forGR-S rubbers*

analogous to the change of frequency of the dielectric ϵ''_r peaks in Fig. 4. Although increasing vulcanization raises the G'_r values in the pseudo-elastic plateau region, there is very little change of the G'_r value in the glassy-amorphous region.

Fig. 8 gives the master curves for tan $\delta_r = G_r''/G_r'$ for the GR-S rubbers shown in Fig. 7. The decrease of frequency of the tan δ_r peak positions and a broadening of the peaks with increasing vulcanization are apparent, as well as a progressive decrease in the heights of the tan δ_r peaks.

The T_s values obtained from the experimental values of $\log_{10} a_T$ obtained from the superposition procedure are plotted as crosses in Fig. 6, and it can be seen that the T_s values derived dynamically approximate to those from dielectric measurements on the same rubber formulation. The conclusion to be drawn from this agreement is that although the molecular configurations involved in the dynamic oscillations are different from those involved in the dielectric, there is the same temperature/frequency interdependence involved, this being expressed by equation (10). This conclusion is very important from the practical point of view, as the necessary T_s value can be obtained from one type of measurement, e.g., dielectric, and applied in conjunction with equation (10) to the results of other types, e.g., dynamic mechanical, creep, or steady-state viscosity, where time and temperature variations are involved, and furthermore the master curves can be used to predict the dynamic and dielectric values over wide temperature and frequency ranges.

The value of T_s for 1·5% combined sulphur content is 269°K (Mix A), which agrees well with the value of 268°K obtained from creep measurements by Williams *et al.*,[4] and compares with a value of 276°K from dynamic mechanical measurements by Fletcher & Gent.[16]

Carbon-black-filled rubbers

In the reduction of data for the carbon-black-loaded GR-S vulcanizates, it was found necessary to use a value of J_e derived from that of the pure gum vulcanizates, and not the value of J'_r at high frequencies for the carbon-black-filled vulcanizate. In the glassy-amorphous region, the contribution of the carbon black to the shear modulus can be expressed as:[26]

$$G_r = G_1\bar{\Phi}_1 + AG_2\bar{\Phi}_2 \quad \ldots\ldots\ldots \quad (11)$$

where G_r is the total shear modulus, G_1 the shear modulus of the rubber, G_2 the shear modulus of the carbon black, $\bar{\Phi}_1$ and $\bar{\Phi}_2$ are the volume fractions involved ($\bar{\Phi}_1 + \bar{\Phi}_2 = 1$), and A is an adhesion

factor between the carbon black and the rubber. The kinetic theory of rubber-like elasticity applies only to the behaviour of long-chain molecules, and cognizance of this fact requires the subtraction of J_e from the measured J'_r before the kinetic theory correction $T\rho/T_0\rho_0$ is applied. If G_1 is taken as approximately $9{\cdot}5 \times 10^9$ dynes/cm.^{2} (the value obtained from the limiting high-frequency value of G'_r for the unvulcanized GR-S), then the fraction $G_1\bar{\Phi}_1$ can be calculated for the carbon-black-filled vulcanizate. The approximation can then be made that

$$J_e = 1/G_1\bar{\Phi}_1 \quad \ldots\ldots\ldots\ldots \quad (12)$$

and this value has been used to reduce the data. The exact value of J_e is however not very critical.

Fig. 9 shows the derived master curves for G'_r and Fig. 10 the tan δ_r curves. The scatter of the experimental results for Mix I, containing 50 parts by weight of carbon-black-filled GR-S, is markedly greater than that for the unvulcanized rubber. This is probably due not only to uncertainties as to the correct value of J_e to use to reduce the data, but also to errors introduced by the thixotropic behaviour of carbon-black-loaded rubbers.[17,27-35] Fletcher & Gent,[16] discussing the dynamic behaviour of a 50 parts by weight carbon-black-filled natural rubber, found that a better master curve could be obtained if the kinetic theory corrections were ignored. This, however, is not quite the case for GR-S, as the master curve obtained by ignoring the kinetic theory corrections shows more scatter than that shown around curve I in Fig. 9; but it is not markedly different from the latter, so it is probable that the kinetic theory dependence must lie between the two extremes. Further work to establish this dependence is now proceeding.

The most obvious effect of increasing the carbon black content is to raise the G'_r values, both in the pseudo-elastic and the glassy-amorphous regions, but without appreciably changing the frequency range of the transition region. Also, increasing the carbon black content decreases the tan δ_r peaks appreciably, although the tan δ_r value in the pseudo-elastic plateau region is increased. The tan δ_r peaks become more diffuse with increasing carbon black content. This type of behaviour of carbon-black-filled vulcanizates has been remarked upon previously by Fletcher & Gent[16] and Echer,[36] and the increase of tan δ_r in the rubbery elastic plateau region by many authors.[16,33-38]

The T_s values for the carbon-black-filled vulcanizates are within three degrees greater than that obtained for the pure gum vulcanizate ($T_s = 269°$K). This confirms similar results obtained by the

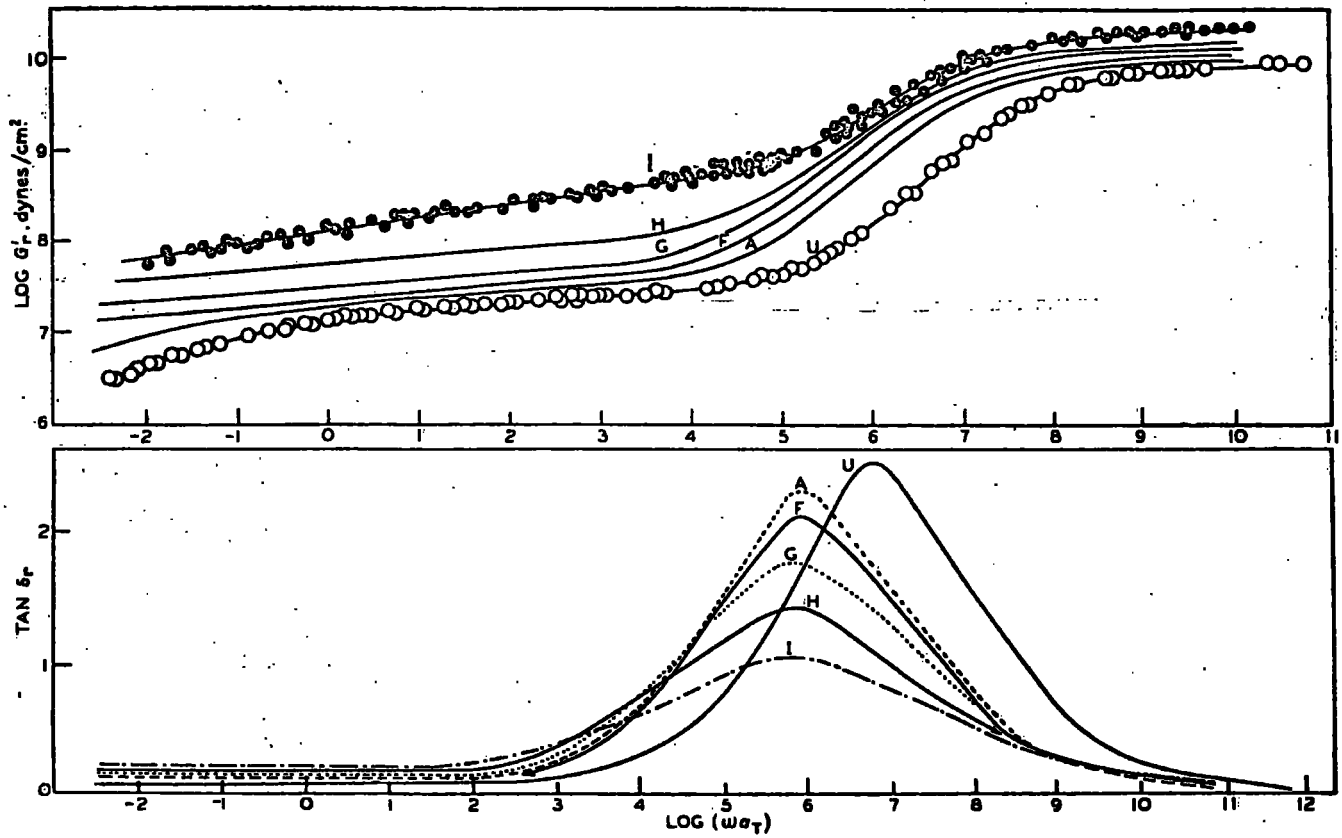

FIG. 9 (top). *Master curves for* G'_r versus $log_{10}\omega a_T$ *for GR-S rubbers*

FIG. 10 (bottom). *Master curves for tan* $\delta_r = G''_r/G'_r$ versus

writer[19] and by Fletcher & Gent[16] on carbon-black-loaded natural rubbers.

Comparison of the GR-S results with those for natural rubber

The comments in this section are mainly based on a comparison of the dynamic results on GR-S with those published in the first paper of this series on the dynamic properties of natural rubber.[19]

The first comparison to be noticed is that the GR-S rubbers have much higher T_s values than the corresponding natural rubbers, the T_s for unvulcanized GR-S, for instance, being about 15° higher than for unvulcanized natural rubber. This difference reflects the differences in the second-order glass transition temperatures of the materials, which have been known for many years.[21]

The second comparison is that the shear modulus in the pseudo-elastic plateau region for unvulcanized natural rubber is about half of that shown in Fig. 7 for unvulcanized GR-S. This difference was noted by Zapas *et al.*,[8] and in a recent paper on the tensile creep of GR-S and natural rubber by Bueche.[37] According to Bueche this difference in modulus levels is an indication of the tightness of the entanglement networks in the polymer, GR-S having the tighter network. The differences in entanglement behaviour are probably the result of differences in chain backbone flexibility, the stiffer chains having the shortest entanglement lengths. GR-S is computed to have an entanglement length of 120 chain backbone atoms between entanglement points, and natural rubber 250.[37]

The third comparison to be made is in the difference in pseudo-elastic plateau lengths, GR-S having a much shorter plateau than natural rubber. Again according to Bueche[37] it would appear that the low number-average molecular weight of GR-S is responsible for the observed short plateau of GR-S as compared with that of natural rubber, which has a much higher number-average molecular weight.

A comparison of the dynamic curves for the vulcanized rubbers also brings out characteristic differences; for example, the vulcanization of natural rubber is successful in so far as the pseudo-elastic plateau is extended to cover a very wide frequency spectrum, thus showing that the primary molecules have been tied into a stable network. Such is not the case for GR-S, for light vulcanization does not seem to have changed the position of the onset of flow to any marked extent, and improvement is effected only by higher degrees of vulcanization; the experiments were not carried out to high enough temperatures with the GR-S rubbers, however, to check the effectiveness of the vulcanization in forming a stable network. It

must be remarked that the use of higher degrees of vulcanization, in order to improve the plateau length by forming a more stable network, is technologically undesirable as GR-S soon becomes too highly cross-linked for optimum tensile strength, and there are processing difficulties in attempting to use a fraction with higher molecular weight to improve the plateau length.[6,37]

Another difference to be noticed is that the slope of the pseudo-elastic plateau region for GR-S is in quite marked contrast with the almost total absence of slope observed with natural rubber. The tan δ_r value in the pseudo-elastic plateau region for all the GR-S rubbers is markedly higher than for the comparable natural rubbers.

Although the experiments were not carried far enough into the flow region, it appears that the presence of carbon black aids the formation of a stable network. This action of carbon black has been known for many years and many interpretations have been propounded.[38-40] The most successful is that due to Guth & Gold[38] who, using modified forms of Einstein's equation for the viscosity of suspensions of spheres in fluids, showed that rigid particles embedded in rubber increase the modulus of the mixture.

An alternative view of the action of carbon black propounded by A. M. Bueche[41] and discussed by F. Beuche[37] postulated that some of the rubber chains are attached to the black at various points, thus introducing some additional cross-links into the system and consequently strengthening the network. Whatever the true physical explanation, it is certain that the inclusion of carbon black does tend to stabilize the network in the pseudo-elastic plateau region for GR-S.

There are no striking differences in the dielectric behaviour of GR-S and natural rubber, the only apparent difference being that the peak ϵ''_r values for unvulcanized GR-S are higher than for unvulcanized natural rubber, but lower in the vulcanizates with the higher concentrations of sulphur. The low-frequency ϵ'_r values are approximately the same for the unvulcanized or lightly vulcanized rubbers, but the ϵ'_r values with higher sulphur content are higher for natural rubber than for GR-S.

Conclusions

The method of reduced variables has been applied to the dynamic mechanical and dielectric properties of unvulcanized GR-S, GR-S vulcanizates of different sulphur contents, and carbon-black-filled GR-S vulcanizates. In each case the master curve showing the variation of the property with frequency has been derived by assuming a suitable T_s value. The T_s values from

the dynamic results agree with those obtained from the dielectric data, so that the temperature/frequency equivalence of GR-S can be expressed adequately by the empirical equation (10). Vulcanization and the inclusion of carbon black do not alter the applicability of equation (10). T_s does, however, increase with increasing vulcanization, although there is little change in the T_s value with increasing carbon black content.

Acknowledgments

The author's thanks are due to the Council of the Research Association of British Rubber Manufacturers for permission to publish this paper.

References

[1] Ferry, J. D., *J. Amer. chem. Soc.*, 1950, **72**, 3746
[2] Ferry, J. D., Fitzgerald, E. R., Grandine, L. D., jun., & Williams, M. L., *Industr. Engng Chem.*, 1952, **44**, 703
[3] Williams, M. L., *J. phys. Chem.*, 1955, **59**, 95
[4] Williams, M. L., Landel, R. F., & Ferry, J. D., *J. Amer. chem. Soc.*, 1955, **77**, 374
[5] Williams, M. L., & Ferry, J. D., *J. Colloid Sci.*, 1954, **9**, 479
[6] Williams, M. L., & Ferry, J. D., *J. Colloid Sci.*, 1955, **10**, 1
[7] Williams, M. L., & Ferry, J. D., *J. Colloid Sci.*, 1955, **10**, 474
[8] Zapas, L. J., Shufler, S. L., & De Witt, T. W., *J. Polym. Sci.*, 1955, **18**, 245
[9] Payne, A. R., *J. appl. Phys.*, 1957, **28**, 378
[10] Payne, A. R., Research Association of British Rubber Manufacturers' Research 1957, Memo. R., p. 407
[11] Ferry, J. D., & Fitzgerald, E. R., *J. Colloid Sci.*, 1953, **8**, 224
[12] Alfrey, T., jun., 'Mechanical Behaviour of High Polymers', Vol. VI, 1948 (New York: Interscience Publishers)
[13] Alexandrov, A. P., & Lazurkin, J. S., *Acta physico-chem. U.R.S.S.*, 1940, **12**, 647
[14] Marvin, R. S., *Proc. 2nd int. Congr. Rheology*, (Oxford, 1953), p. 156 (London: Butterworths Scientific Publications)
[15] Nolle, A. W., *J. Polym. Sci.*, 1950, **5**, 1
[16] Fletcher, W. P., & Gent, A. N., *Brit. J. appl. Phys.*, 1957, **8**, 194
[17] Davies, D. M., & McCallion, H., *Proc. Instn mech. Engrs*, 1955, **189**, 1125
[18] Thürn, H., & Wolf, K., *Kolloidzschr.*, 1956, **148**, 1
[19] Payne, A. R., 'The Rheology of Elastomers', 1958, p. 86 (London: Pergamon Press)
[20] Norman, R. H., M.Sc. Thesis, London University, 1954
[21] Boyer, R. F., & Spencer, R. S., 'Advances in Colloid Science', 1946, Vol. 2, p. 1 (New York: Interscience Publishers)
[22] Hutton, A. Q., & Nolle, A. W., *J. appl. Phys.*, 1954, **25**, 350
[23] Payne, A. R., Research Ass. of British Rubber Manufacturers Res. Rep. 76, 1956
[24] Payne, A. R., *Rev. gen. Caoutch.*, 1956, **33**, 885
[25] Payne, A. R., & Smith, S. F., *J. sci. Instrum.*, 1956, **33**, 432
[26] Nielsen, L. E., Wall, R. A., & Richmond, P. G., *S.P.E.J.*, 1955, **11**, 22
[27] Fletcher, W. P., & Gent, A. N., *Trans. Instn Rubb. Ind.*, 1953, **29**, 266
[28] Gehman, S. D., & Wilkinson, C. S., jun., *Analyt. Chem.*, 1950, **22**, 283
[29] Dillon, J. H., Prettyman, I. B., & Hall, G. L., *J. appl. Phys.*, 1944, **15**, 309
[30] Gehman, S. D., Woodford, D. E., & Stanbaugh, R. B., *Industr. Engng Chem.*, 1941, **33**, 1032

Appendix

Composition of GR-S mixes used (parts by weight)

Ingredient	Mix designation									
	U	A	B	C	D	E	F	G	H	I
GR-S ('Krylene' cold-polymerized) ..	100	100	100	100	100	100	100	100	100	100
Stearic acid	—	2	2	2	2	2	2	2	2	2
Zinc oxide	—	3	3	3	3	3	3	3	3	3
Softener (Dutrex R)	—	—	—	—	—	—	5	5	5	5
C.B.S.*	—	0·95	0·95	0·95	0·95	0·95	0·95	0·95	0·95	0·95
Sulphur	—	1·75	3·5	7·5	10	15	1·75	1·75	1·75	1·75
Carbon black HAF†	—	—	—	—	—	—	10	20	30	50
Vulcanization time, min.	—	60	60	60	60	60	60	60	60	60
Vulcanization temp., °	—	141	141	141	141	141	141	141	141	141
Combined sulphur, %	0	1·5	3·2	6·4	7·6	9·5	1·5	1·5	1·5	1·5

* CBS = *N-cyclo*hexylbenzthiazylsulphonamide

† HAF = high-abrasion furnace

[31] Gui, K. E., Wilkinson, C. S., & Gehman, S. D., *Industr. Engng Chem.*, 1952, 44, 720
[32] Naunton, W. J. S., & Waring, J. R. S., *Proc. 1st Rubber Technology Conf.* (London, 1938), p. 805 (Cambridge: Heffer)
[33] Oberto, S., & Palandri, G., *Rubb. Age*, 1948, 63, 725
[34] Stambaugh, R. B., *Industr. Engng Chem.*, 1942, 34, 1358
[35] Payne, A. R., *Proc. 3rd Rubber Technology Conf.* (London, 1954), p. 426 (Cambridge: Heffer)
[36] Echer, R., *Kautschuk u. Gummi*, 1956, 9, p. W.T.2
[37] Bueche, F., *J. Polym. Sci.*, 1957, 25, 305
[38] Guth, E., & Gold, O., *Phys. Rev.*, 1938, 53, 322
[39] Cohan, L. H., *Proc. 2nd Rubber Technology Conf.* (London, 1948), p. 365 (Cambridge: Heffer)
[40] Guth, E., as reference 39, p. 353
[41] Bueche, A. M., *J. appl. Phys.*, 1952, 23, 154

Discussion

Dr. A. N. Gent: In Figs. 7 and 8, master curves are shown for G'_r and tan δ_r against frequency at a reference temperature of 0° for various vulcanizates of GR-S. Fig. 6 shows, however, that the appropriate reference temperatures (i.e., those directly related to the rubber-to-glass transition temperatures) change by about 30° over the range of crosslinking considered. These changes may largely account for the different positions of the curves in Figs. 7 and 8. Has the author examined the positions of these curves when each is plotted at the appropriate reference temperature, and do they then substantially superpose? In other words, are the observed displacements attributable principally to changes in the respective rubber-to-glass transition temperatures? Measurements we have carried out,* on the effect of incorporating plasticizers and of introducing small amounts of crosslinking into natural rubber, suggests that the master curve is virtually unaltered when this presentation is adopted.

Mr. Payne: Such an effect has been noticed before, and indeed in an earlier paper† there was a definite correlation between the position on the log $a_T/(T-T_s)$ curve for a particular frequency, say 10^4 c/s, of the dielectric tan δ peak, and the type of molecular movement involved, the rubber-like materials with small hindrances to movement falling very closely together. If, however, the frequency position of the tan δ peaks for the dynamic results are considered, then the frequency change in position of the tan δ peak, $\Delta \log \omega a_T$, is obtained from the relationship below when the temperature is reduced from T_0 to T_s:

* Fletcher, W. P., Gent, A. N., & Wood, R. I., *Proc. 3rd Rubber Technology Conf.* (London, 1954), p. 382 (Cambridge: Heffer); Fletcher, W. P., & Gent, A. N., *Brit. J. appl. Phys.*, 1957, 8, p. 194.

† Payne, A. R., 'Rheology of Elastomers', 1958, p. 86 (London: Pergamon Press).

$$\Delta \log \omega a_T = \frac{8{\cdot}86\,(T_0 - T_s)}{(101{\cdot}6 + T_0 - T_s)}$$

These values of log ωa_T are given in Table I together with the log $\dot{\omega} a_T$ value of the tan δ peak at $T = T_s$.

Table I

Rubber	$\Delta \log \dot{\omega} a_T$	Log ωa_T at $T = T_0$ tan δ peak position	Log ωa_T at $T = T_s$ tan δ peak position
U	+0·72	6·80	6·08
A	+0·42	5·95	5·53
B	−0·09	5·43	5·52
C	−0·97	4·92	5·89
D	−1·66	4·50	6·16
E	−2.17	4·00	6·17
			Mean 5·89

The last column shows approximate constancy in the mean $\dot{\omega} a_T$ value, and a variation in the T_s value of about two degrees is sufficient to account for the variations about the mean. This is approximately the error in obtaining the T_s value from the log $a_T/(T - T_s)$ coincidence, besides any error in obtaining the correct tan δ peak for an asymmetrical peak. Also the effect of continuous superposition is that the errors in shifting, especially in the plateau regions, is cumulative, and may well account for a 0·2 or 0·3 variation in the tan δ peak position of $\dot{\omega} a_T$. Taking all these points into consideration it is shown that within the experimental accuracy, when all the curves are reduced to their respective T_s values, the tan δ peak positions coincide, so that, in fact, the observed displacements are attributable mainly to changes in the respective rubber-to-glass transition temperatures. It is expected that at higher combined sulphur contents a variation from this rule will appear because of the large hindrance to movement offered by the cross-linking, probably in a manner similar to that shown to occur for natural rubber vulcanizates.

Similar behaviour with the effect of plasticizer in polyvinyl chloride and polyvinylidene chloride on the dielectric properties is quite marked.

Mr. B. F. Read: What justification is there for using results of the equilibrium kinetic theory to reduce data obtained under non-equilibrium conditions (i.e., dynamic data)?

Mr. Payne: If the contribution to a process (dielectric) has a given value of τ the dipolar part of the dielectric constant is given by

$$(\epsilon_\omega - \epsilon_\infty)_T = \left(\frac{\epsilon_s - \epsilon_\infty}{1 + i\tau\omega}\right)_T \quad . \quad . \quad (1)$$

$\epsilon\omega$ is the dielectric constant, ϵ_s the static dielectric c onstant, ω is the angular frequency, τ the relaxation time, ϵ_∞ is the dielectric constant at infinite frequency, T is the temperature.

Similarly at T_o

$$(\epsilon\omega - \epsilon_\infty)_{T_o} = \left(\frac{\epsilon_s - \epsilon_\infty}{1 + i\omega\tau}\right)_{T_o} \quad . \quad . \quad (2)$$

Now from the kinetic theory, the equilibrium condition is given by

$$(\epsilon_s - \epsilon_\infty)_T = (\epsilon_s - \epsilon_\infty)_{T_o} \cdot \frac{T_o}{T} \quad . \quad . \quad (3)$$

which is independent of τ. Then if there are a number of mechanisms with different values of τ, the total dipolar contribution at T is then given by

$$\Sigma(\epsilon_\omega - \epsilon_\infty)_T = \frac{T_o}{T} \Sigma(\epsilon_\omega - \epsilon_\infty)_{T_o} \quad . \quad . \quad (4)$$

This follows from equations (1), (2) and (3) as $\omega\tau$ is a constant and equation (4) is the relationship for the non-equilibrium condition.

Similar arguments can be advanced for the mechanical properties.

The best justification is perhaps to put the question the other way round, as reduction can be carried out separately on both ϵ'' and ϵ' components of the dielectric constant to produce single continuous curves: then the assumption of the kinetic theory dependence must be the correct one.

frequency scales so that the observed physical values, i.e., the dynamic modulus or the dielectric permittivity, can be brought on to a single master curve covering a very wide range of frequency and temperature. In order to obtain this master curve, each observation is transformed in two ways: firstly, in order to account for normal kinetic theory changes with temperature, by a linear transformation of the temperature to a suitable reference temperature T_s, and secondly by shifting the property *versus* log frequency curves along the frequency axis in such a way that all the observations fall on a single continuous curve. The most interesting and striking feature of this treatment is that the form of the frequency-shifting factor $\log_{10}a_T$ (or $\log_{10}b_T$ from dielectric measurements) as a function of temperature is determined solely by T_s, and if the appropriate values of T_s are chosen, then the relationship between $\log_{10}a_T$ and $(T-T_s)$ is identical for all materials so far examined.

The relationships used for transforming the observations are as follows: the complex dielectric constant ϵ^* is given as

$$\epsilon^* = \epsilon'+i\epsilon'' \quad . \quad . \quad . \quad . \quad . \quad . \quad . \quad . \quad . \quad . \quad (1)$$

where ϵ' and ϵ'' are the real and imaginary parts of the complex permittivity. Then the reduced values of ϵ' and ϵ'', i.e., ϵ'_r and ϵ''_r

$$\epsilon'_r = (\epsilon'-\epsilon_\infty)(T\rho_0/T_0\rho)+\epsilon_\infty \quad . \quad . \quad . \quad . \quad . \quad . \quad (2)$$

$$\epsilon''_r = \epsilon''(T\rho_0/T_0\rho) \quad . \quad . \quad . \quad . \quad . \quad . \quad . \quad . \quad . \quad (3)$$

$$\omega_r = \omega b_T \quad . \quad . \quad . \quad . \quad . \quad . \quad . \quad . \quad . \quad . \quad . \quad . \quad (4)$$

ϵ_∞ is the limiting high-frequency or low-temperature value of ϵ', ρ and ρ_0 are the densities at any temperature T and at an arbitrarily chosen reference temperature T_0 respectively. ω_r is the reduced value of the circular frequency ω. A full description of the derivation of these equations is given in earlier papers by Ferry and co-workers and by others.[5-7,14,19]

Similarly the complex modulus G in terms of its real and imaginary parts is:

$$G^* = G'+iG'' \quad . \quad . \quad . \quad . \quad . \quad . \quad . \quad . \quad . \quad . \quad . \quad (5)$$

and the complex compliance J^* is

$$J^* = 1/G^* = J'-iJ'' \quad . \quad . \quad . \quad . \quad . \quad . \quad . \quad . \quad . \quad (6)$$

and

$$J'_r = (J'-J_\infty)(T\rho/T_0\rho_0)+J_\infty \quad . \quad . \quad . \quad . \quad . \quad (7)$$

$$J''_r = J''(T\rho/T_0\rho_0) \quad . \quad . \quad . \quad . \quad . \quad . \quad . \quad . \quad . \quad (8)$$

$$\omega_r = \omega a_T \quad . \quad . \quad . \quad . \quad . \quad . \quad . \quad . \quad . \quad . \quad . \quad . \quad (9)$$

J_∞ is the limiting high-frequency or low-temperature compliance

obtained from the experimental results. J_r' and J_r'' are the real and imaginary parts of the reduced compliance.

The factors a_T and b_T are interpreted as measures of the temperature dependence of the appropriate relaxation times. It has recently been shown that a_T is given in terms of the reference temperature T_s by the empirical relationship,[3,4,8]

$$\log_{10} a_T = -8{\cdot}86(T-T_s)/(101{\cdot}6+T-T_s) \quad . \quad . \quad . \quad (10)$$

The parameter b_T is also given by equation (10) and the difference in symbolism between a_T (mechanical) and b_T (dielectric) is retained in the present paper solely to differentiate the mechanical data from the dielectric.

Dielectric measurements on GR-S

Dielectric measurements were made on a series of GR-S vulcanizates containing increasing amounts of sulphur. (The details of the compounds are given in the Appendix.) The experiments were carried out on modified Schering and megacycle bridges[20] over a frequency range of 50 to 10^6 c/s, and over a temperature range of -50 to $+50°$. All the results were reduced by the use of equations (2) and (3) to give ϵ'_r and ϵ''_r at a standard reference temperature $T_0 = 273°$K. ϵ_∞ (refractive index squared) was chosen as 2·25 for all the rubbers studied.

As an example of the technique required to produce the master curves, the reduced loss factor ϵ''_r results for the GR-S with 6·4% of combined sulphur are plotted in Fig. 1 where the ϵ''_r results are plotted against the frequency of test at different temperatures. It is clear that the segments of each curve can be translated along the $\log_{10}$(frequency) axis until superposition occurs on the curve for temperature $T_0 = 273°$K (in this case the curve for $T_0 = 273°$K is interpolated from the data). The distance of translation along the $\log_{10}$(frequency) axis is the shifting factor or $\log_{10} b_T$ value. The overall master curve obtained by this superposition is shown in Fig. 2. It is apparent from the continuity of the superimposed data that the superposition was carried out with little ambiguity over the ϵ''_r peak region, although some ambiguity exists at the high-frequency end. When the necessary shifting factors, $\log_{10} b_T$, were plotted against the temperature T of the corresponding curves, it was found that the resulting curve could be superimposed on that obtained by plotting equation (10) using a suitable value for temperature T_s. For example, the curve described by equation (10) is shown as a solid line in Fig. 3, and the superimposed $\log_{10} b_T$ values for GR-S taking $T_s = 277°$K are shown as points about this line.

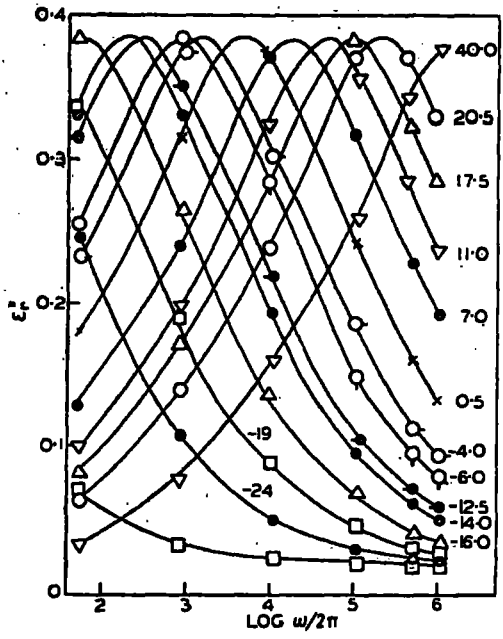

FIG. 1. *Reduced loss factor* ϵ_r'' versus *frequency of test at various temperatures*
Mix C. GR-S vulcanizate

With this value of T_s, the experimental results shown give an indication of the goodness of fit of equation (10) with the experimental values. It was found that for all the rubbers studied, both dynamically and dielectrically, equation (10) gave an equally satisfactory description of the experimental $\log_{10} b_T$ values, provided a suitable T_s value was chosen. No further examples will be given in this paper, but only the appropriate T_s values quoted.

Fig. 4 shows the master curves of the ϵ''_r results for unvulcanized and vulcanized GR-S with $T_0 = 273°K$. It is seen that increasing sulphur content decreases the frequency of the maximum of ϵ''_r but increases both the breadth and the height of the peaks up to 6·4% of combined sulphur, after which the height decreases slightly; there is no apparent explanation to be given at the moment for this decrease. The experimental results about some of the master curves give an indication of the scatter obtained by the superposition process.

The corresponding ϵ'_r results are shown in Fig. 5. The master curves, except those for high sulphur contents (curve E), are less

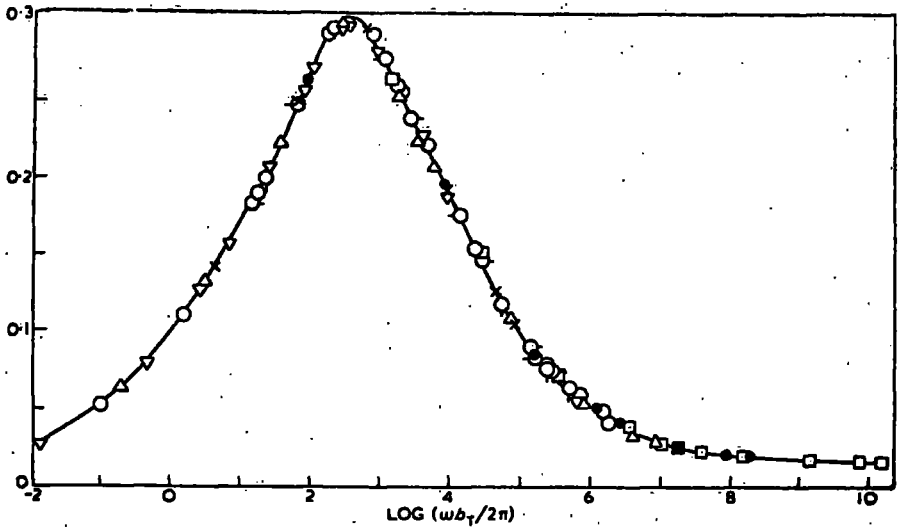

FIG. 2. *Master curve for* ϵ_r'' versus $log_{10}\omega b_T/2\pi$
$T_0 = 273°K$. Mix C

clearly defined, as can be seen from the curve for unvulcanized GR-S, where the scatter of the experimental results is of about the same order as the overall change in ϵ'_r between high and low frequencies. This inaccuracy limits the usefulness of the technique

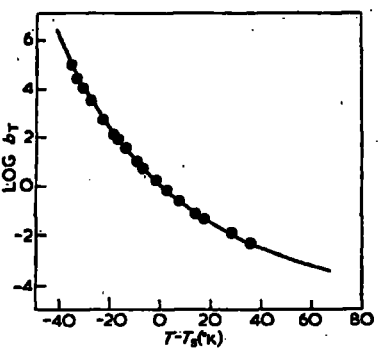

FIG. 3. Log_{10} b_T versus $T-T_0$ (°K)
Mix C

of superposition and reduction of data to obtain a master curve for ϵ'_r; nevertheless for the higher sulphur contents, the $\log_{10}b_T$ values necessary to bring about superposition are the same as those required to superimpose the ϵ''_r data and this provides a check on the internal consistency of the experimental results.

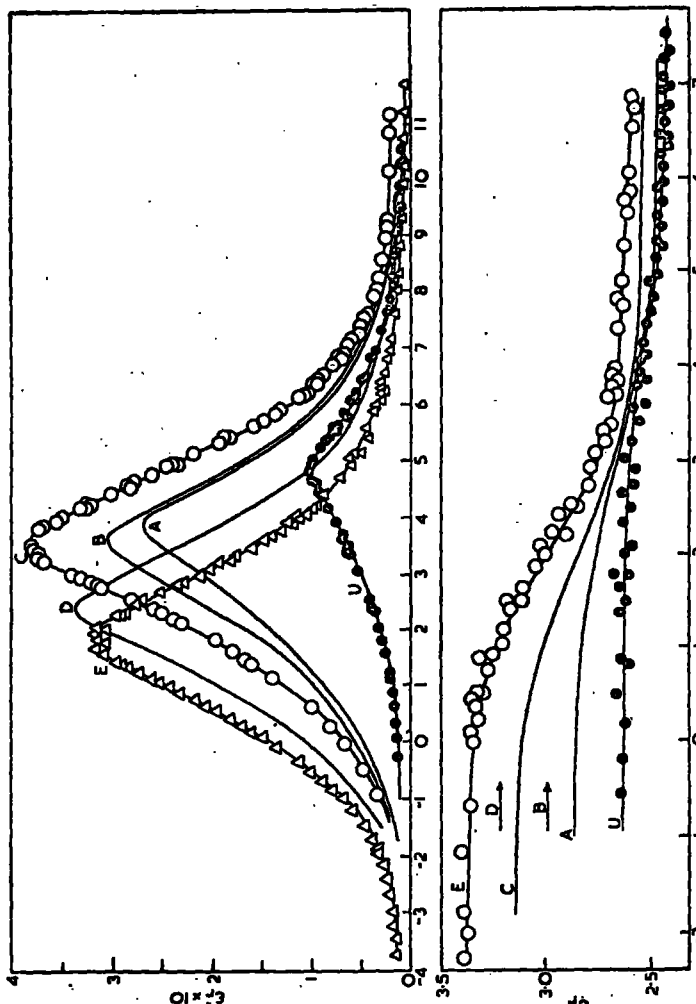

FIG. 4 (top). *Master curves of* ϵ'' *versus* $\log \omega b_T/2\pi$ *for GR-S*
FIG. 5 (bottom). *Master curves of* ϵ'_T *versus* $\log_{10} \omega b_T/2\pi$
(Letters on curves refer to vulcanisate mixes)

From the curve relating the derived T_s values for the GR-S rubbers to combined sulphur content (Fig. 6), it can be seen that an

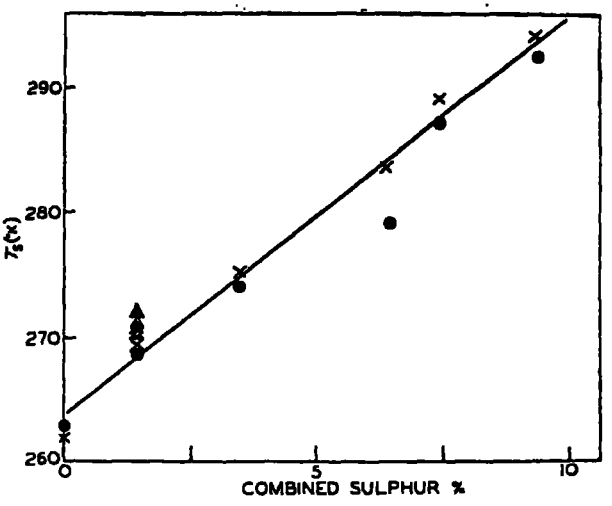

FIG. 6. T_s (°K) versus *percentage combined sulphur*
● dielectric measurements
× dynamic measurements on pure gum GR-S rubbers
▲ dynamic mechanical measurements on carbon-black-filled GR-S rubbers

approximately linear relationship exists between T_s and the percentage combined sulphur, the T_s value increasing with sulphur content.

The quoted value of T_g,[21] the second-order glass transition temperature, is $-61°$ for unvulcanized GR-S; thus $T_s = T_g + 51°$, which approximates to $T_s = T_g + 50°$, quoted by Williams *et al.*[4] for other materials.

Dynamic measurements on GR-S

The method of reduced variables has been applied to dynamic mechanical measurements made on an unvulcanized, several vulcanized and several carbon-black-loaded vulcanizates of GR-S. (The compounding details are given in the Appendix.)

The reduction of dynamic data has been successfully carried out by the author for a vulcanized acrylonitrile–butadiene rubber,[9] notwithstanding published statements that reduction was not possible on vulcanized rubbers because the cross-linking affects the mechanical properties at low frequencies.[22] Recently Fletcher & Gent[16] have reduced the dynamic data of some rubber-like materials, including a vulcanized GR-S, but their results were

TRANSACTIONS
of the
INSTITUTION OF THE RUBBER INDUSTRY

VOL. 41, No. 5 OCTOBER, 1965

Dielectric Properties of Purified Natural Rubbers

BY R. H. NORMAN, M.Sc., A.INST.P., F.I.R.I.* and
A. R. PAYNE, B.Sc., F.INST.P., F.I.R.I.†

RAPRA Code No.: 41C1–982

SUMMARY

Loss factor and permittivity data on both raw and vulcanised dry purified natural rubber are presented and analysed using the Ferry and Fitzgerald method of relating the effects of frequency and temperature. This leads to the possibility of summarising all the experimental data at various temperatures and frequencies in terms of a small number of parameters and a curve representing the data at a specific temperature. Alternatively, the loss factor curve in the region of its peak may be expressed in terms of only six physically significant parameters and an analytic function. The form of the distribution function of relaxation times is given for one vulcanised sample. The dipole moment of the combined sulphur, and a value below which the dipole moment of the raw rubber must lie, are estimated.

INTRODUCTION

IN a previous paper[1] the permittivity and power factor results for purified and crude unvulcanised natural rubber under dry and moist conditions were presented. It may be noted that, on these unvulcanised rubbers, the dielectric results were almost identical provided that the rubbers were very dry.

In this paper, the corresponding measurements on dry purified vulcanised rubber are presented and analysed. The method of preparation of the purified rubber and the test methods were described in Ref. 1. The electrodes were of tin foil, attached by vaseline and backed by brass.

* Rubber and Plastics Research Association of Great Britain, Shawbury, Shrewsbury, Shropshire, England.
† Natural Rubber Producers' Research Association, Welwyn Garden City.

Details of Samples and Presentation of Data

Two mixings were prepared from purified rubber, in a Bridge Banbury internal mixer, under nitrogen. Each contained 200 g. rubber and 10 g. sulphur, and mixing B also contained 2 g. mercaptobenzthiazole. Chemical analysis[2] showed that, owing to a certain quantity of sulphur sticking in the apparatus and to losses from the glands of the mixer (especially during mixing B), the actual quantity of sulphur in the mixings was 4·45 and 3·50 per cent. of the total weight of the mixings for A and B respectively. Since the sulphur and accelerator in mixing B were premixed, and both powders were in a similar state of aggregation, it may be assumed that the loss of accelerator was in proportion to the loss of sulphur, giving a final accelerator concentration of 0·74 per cent. by weight.

Samples were vulcanised for various periods in a frame mould which was closed rapidly, thus forcing out air before the temperature had time to rise appreciably. The combined sulphur content, as a percentage of total weight of compound, was estimated.[3] The combined sulphur data, together with the vulcanisation and reference details and the coefficients of cubical expansion, are given in Table 1.

TABLE 1

Details of Vulcanisates

Mixing	Vulcanisation		Reference code	Combined sulphur, per cent.	Cubical expansion coefficient ($°C.^{-1}$)
	Time	Temp., °C.			$\times 10^{-4}$
A	20 min.	120	A20	0·1	5·0
	2 hr.	148	A2	1·7	5·1
	4 hr.	148	A4	3·0	5·3
	6 hr.	148	A6	4·3	5·5
B	3 hr.	142	B3	3·0	5·8

The measured permittivity and loss factor results for B3 are given in Figures 1 and 2. The summarised results for all samples, after the frequency and temperature reductions to be described, will be given and discussed in later Sections of this paper.

The results on A20 were of poor accuracy owing to the wrinkling of the sheet after moulding (due to residual stresses). These results will not therefore be quoted, but they showed that mixing the rubber with 4·45 per cent. of sulphur and vulcanisation to 0·1 per cent. combined sulphur caused an increase of the peak loss factor (above that of the rubber alone) of about 0·003 compared with an increase of 0·07 for A2, which contained 1·7 per cent. combined sulphur. Since an approximately linear relationship has been found between the peak loss factor and combined sulphur content, the results on A20 suggest that the mixing process and the presence of more than 4 per cent. free sulphur alone had little effect on the peak loss factor. The background loss factor (i.e. the loss factor at a considerable frequency difference on either side of the peak)

was slightly increased by mixing and/or by the presence of free sulphur, and high loss factors at 50 c./s. above 10° C. (even above those of A2, A4, A6 and B3) suggest that the ionic component of the dielectric loss was increased. The effect of mixing on permittivity is uncertain owing to the difficulties of measurement, but the results obtained suggest that the increase over that for the raw purified rubber is less than 1 per cent.

Temperature/Frequency Analysis

Using the analysis which follows, it is possible to express all the experimental results in terms of mathematical expressions containing a few arbitrary constants together with a single curve for each material. Over certain temperature and frequency ranges, the loss factor curves

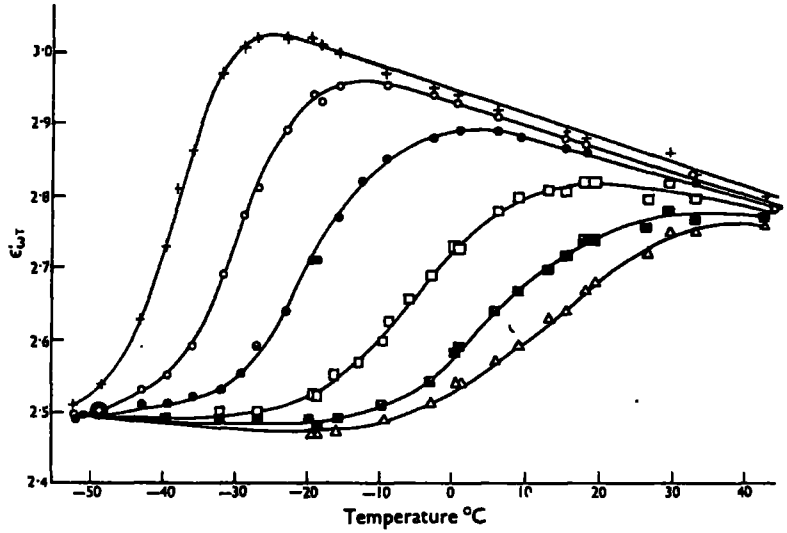

Fig. 1. Permittivity of B3.

+	50 c/s.	□	10^5 c/s.
○	800 c/s.	■	5×10^5 c/s.
●	10^4 c/s.	△	10^6 c/s.

may alternatively be expressed by a mathematical function involving two additional arbitrary parameters. A complete list of symbols is given in Appendix E.

For the distribution of dipolar relaxation times in which there are $N.G(\tau)\delta\tau$ dipoles having relaxation times (τ) in an interval τ to $\tau + \delta\tau$ (N = total number of dipoles per unit volume), the dipolar part ϵ_D of the complex dielectric constant ($\epsilon_{\omega,T} = \epsilon'_{\omega,T} + i\epsilon''_{\omega,T}$) at an angular frequency ω and temperature T is given by

$$\epsilon_D = \epsilon_{\omega,T} - \epsilon_{\infty,T} = (\epsilon_{s,T} - \epsilon_{\infty,T}) \int_0^\infty \frac{G(\tau)}{1 + i\omega\tau}\, \partial\tau \qquad .. \qquad (1)$$

where $\epsilon_{s,T}$ and $\epsilon_{\infty,T}$ are the static and infinite frequency dielectric constants at T.

Ferry and Fitzgerald[4] made the following assumptions about the behaviour of the value of τ for a given elementary relaxation process and about the contribution of the process to the dielectric constant:

(1) The ratio of the relaxation times at two temperatures, T and T_o, for any given elementary relaxation process, is independent of the particular element chosen; i.e. τ_T/τ_o (where the subscripts refer to the temperature of measurement and an arbitrary reference temperature T_o

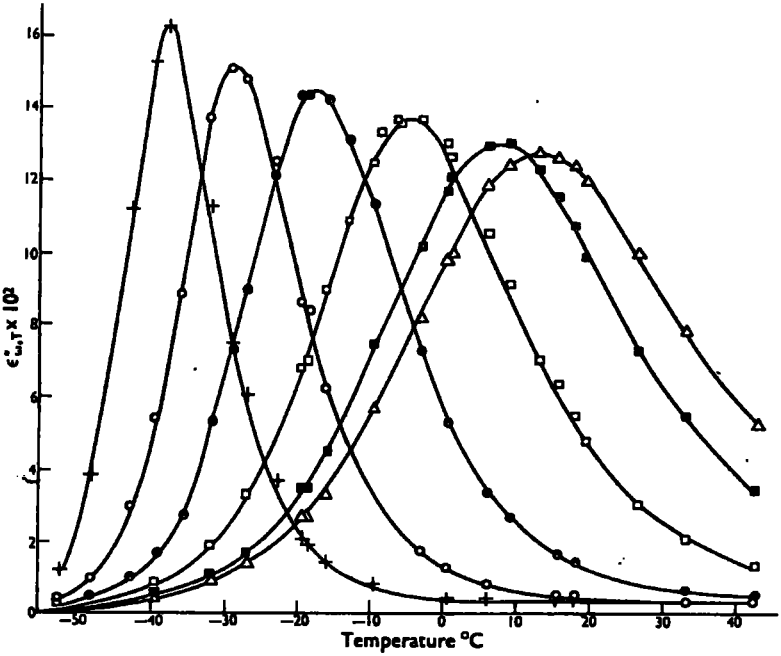

FIG. 2. Loss factor of B3.

+ 50 c/s.	□ 10^5 c/s.
○ 800 c/s.	■ 5×10^5 c/s.
● 10^6 c/s.	△ 10^6 c/s.

respectively) is characteristic of the material as a whole and can be replaced by, for convenience, a parameter b'_T.

(2) The contribution (ϵ_τ) of the dipoles having a time constant τ to the value of the dipolar portion ($\epsilon_{s,T} - \epsilon_{\infty,T}$) of the static dielectric constant is proportional to the density (ρ_T) of the material (i.e. to the number of such dipoles per unit volume) and inversely proportional to the absolute temperature (see also Appendix C).

From these assumptions and Equation 1, it can be shown that the

dipolar part of the complex dielectric constant at temperature T and frequency ω is given by

$$\epsilon_D = \frac{\rho_T T_o}{\rho_o T} f\{\log_{10}(\omega b'_T)\}, \qquad \ldots \quad \ldots \quad (2)$$

where ρ_o is the density at T_o, f being a function which can be derived experimentally in the manner described in Appendix A.

Thus, if a measure of b'_T is available, and the function f is known for any one temperature, it is possible to compute the results for any other temperature. It is convenient at this stage to write

$$k'_T \equiv \frac{\rho_T T_o}{\rho_o T}. \qquad \ldots \quad \ldots \quad \ldots \quad \ldots \quad (3)$$

Determination of b'_T requires measurements at a number of temperatures. If the values of either the real or the imaginary parts of ϵ_D/k'_T are plotted against $\log_{10}\omega$ for a number of temperatures, including T_o, a number of curves having identical shapes should result, each displaced along the $\log_{10}\omega$ axis by a distance $\log_{10}b'_T$ relative to the T_o curve. Many authors [5–16] have shown such relations to be true experimentally, both for dielectric constant and for its mechanical analogue (compliance) for many materials. (In the case of compliance, $k'_T = \frac{\rho_o T_o}{\rho_T T}$). The value of $\log_{10}b'_T$, so obtained, is not proportional to $\frac{1}{T} - \frac{1}{T_o}$ as it would be if the activation energy were constant and the curve $\log_{10}b'_T = \phi(T - T_o)$ varies with the material.

Williams *et al.*[8] examined the experimental curves of $\phi(T - T_o)$ and found that a particular value of T_o (known as T_s) could be chosen for each material, such that the function $\phi(T - T_s)$ was independent of the material. T_s is the value of T at which $\frac{\partial}{\partial T}(\log_{10}b'_T)$ has the arbitrary value $-0{\cdot}0872$. This rather odd value arises because T_s was originally defined in terms of the property of a particular material; the value is now too well established to amend the definition. b_T is defined as the value of b'_T when $T_o = T_s$. The function found by Williams *et al.* is

$$\log_{10}b_T = \phi(T - T_s) = -\frac{8{\cdot}86\,(T - T_s)}{101{\cdot}6 + T - T_s} \qquad \ldots \quad (4)$$

This equation, together with the value of the parameter T_s, defines the activation energy at any temperature in the range over which the equation holds (see Appendix D).

From the two assumptions of Ferry and Fitzgerald[4] and the experimental equation of Williams *et al.*,[8] the real and imaginary parts (permittivity and loss factor) of the dielectric constant are given by

$$\frac{\epsilon'_{\omega,T} - \epsilon_{\infty,T}}{k_T} + \epsilon_\infty = f_1(\log_{10}\omega b_T) = f_1\left\{\log_{10}\omega - \frac{8{\cdot}86\,(T - T_s)}{101{\cdot}6 + T - T_s}\right\} \quad (5)$$

$$\frac{\epsilon''_{\omega,T}}{k_T} = f_2(\log_{10}\omega b_T) = f_2\left\{\log_{10}\omega - \frac{8{\cdot}86\,(T - T_s)}{101{\cdot}6 + T - T_s}\right\} \quad .. \quad (6)$$

where $k_T = \frac{\rho_T T_s}{\rho_s T} = \frac{T_s}{T}\left[1 - A(T - T_s)\right]$, ϵ_∞ is the value of $\epsilon_{\infty,T}$ when $T = T_s$, ρ_s is the density at $T = T_s$ and A is the coefficient of cubical expansion.

From Equations 5 and 6, it will be seen that the expression $\frac{\epsilon'_{\omega,T} - \epsilon_{\infty,T}}{k_T} + \epsilon_\infty$ is equal to the real part of the dielectric constant at temperature T_s at a frequency ω and will be denoted by the symbol ϵ'_ω, and likewise $\epsilon''_{\omega,T}/k_T$ will be denoted ϵ''_ω.

Thus the values of $\epsilon'_{\omega,T}$ and $\epsilon''_{\omega,T}$ for any temperature (T) and frequency (ω) within the experimental ranges (and with some uncertainty, principally because of the effects of other dispersion ranges having different values of T_s, a little outside the experimental ranges) may each be calculated from the following parameters and functions:

A coefficient of cubical expansion (measured by a conventional method).

T_s a reference temperature.

$\epsilon_{\infty,T}$ the infinite frequency dielectric constant (as a function of T).

f_1 and f_2 empirical functions of $\left[\log_{10}\omega - \frac{8{\cdot}86\,(T - T_s)}{101{\cdot}6 + T - T_s}\right]$.

The method of determination of the values of the above parameters and functions from the experimental data is given in Appendix A.

The resulting "master" curves of $\epsilon'_\omega = f_1(\log_{10}\omega b_T)$ and $\epsilon''_\omega = f_2(\log_{10}\omega b_T)$ for B3 are given in Figures 3 and 4. (The inside scales and the short lines should be ignored, except in conjunction with Appendix A.) The resultant "master" curves for the rubbers from mixing A are given in Figures 5 and 6 and that for the unvulcanised rubber in Figure 7.

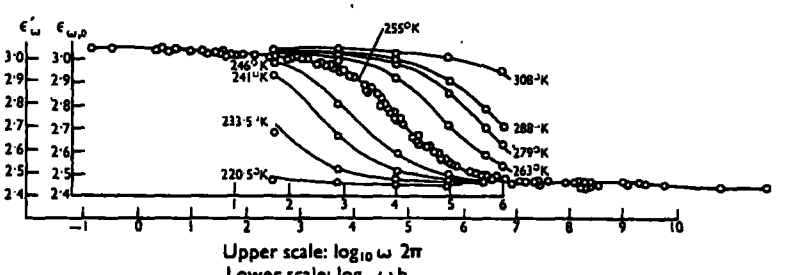

FIG. 3. Permittivity of B3. Derived curves and master curve.

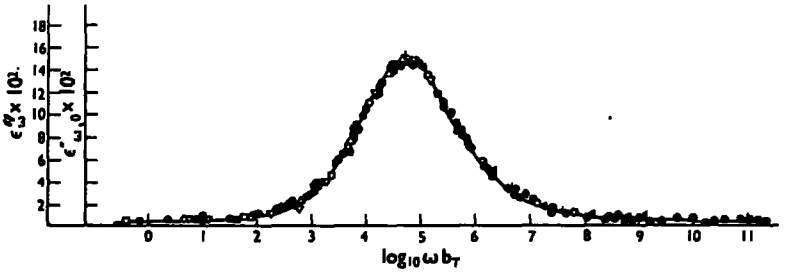

FIG. 4. Loss factor of B3. Master curve.

Temperatures (° K.)

□	315·5	◆	253·5
△	288·5	+	246
▽	279	○	241
■	270	◁	233·5

● All other points

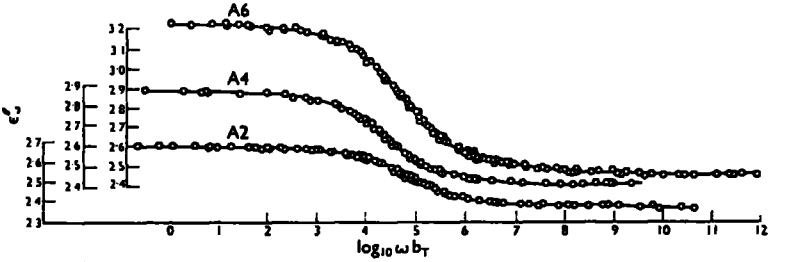

FIG. 5. Permittivity of mixing A vulcanisates. Master curves.

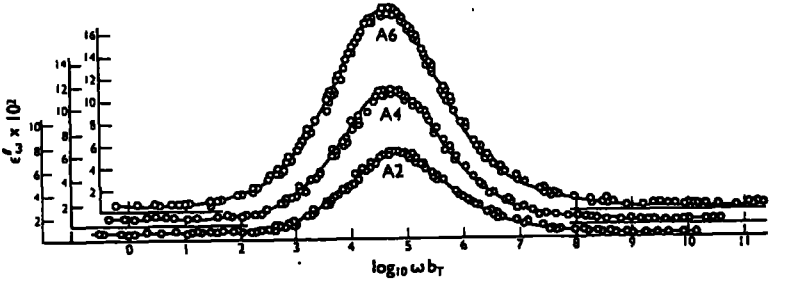

FIG. 6. Loss factor of mixing A vulcanisates. Master curves.

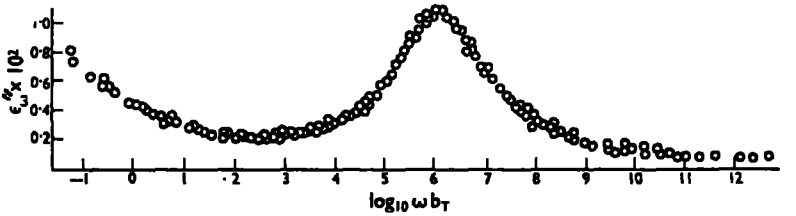

FIG. 7. Loss factor of unvulcanised purified rubber. Master curve.

No graph is given for the permittivity values for the unvulcanised rubber since the range of values observed at different temperatures and frequencies is small compared with the scatter of the results.

Shape of Loss Factor Curves and Summary of Parameters

The form of the composite loss factor curves of Figures 4, 6 and 7 suggests that they may be divided into the following features:

(1) A nearly symmetrical Debye-type (but wider) peak having a maximum which will be designated ϵ''_m occurring at a value of ωb_T which will be designated ω_m. This is due to a dipolar mechanism. Various authors have compared similar peaks for other materials with various analytic functions for $\epsilon''_\omega/\epsilon''_m$, some of which are purely empirical and some of which are calculated from hypothetical functions for $G(\tau)$. At frequencies remote from the frequency of the peak loss factor, all these loss factor functions tend to zero.

(2) At very low values of $\omega b_T/\omega_m$, the curve rises fairly sharply with decreasing frequency (this is only obvious in the case of unvulcanised rubbers), presumably due to an ionic or Maxwell-Wagner[17,18] type of loss mechanism.

(3) At points of the curve where neither of these mechanisms is predominant, the values of ϵ''_ω do not return to zero, but there is a "background" value ϵ''_B which is substantially independent of the value of ωb_T. This is similar to an effect observed by Garton[19] with relatively non-polar media. Garton showed that it leads to a distribution function of relaxation times of the form $G(\tau) = 1/\tau$, but the theory proposed by Garton is limited to frequencies well above the frequency corresponding to the peak in the loss factor/frequency curve and is not therefore applicable in this case. An attempt to extend the theory to lower frequencies led to results which were at variance with the observations and this line of attack was discontinued.

In the region of the peak, the curve may be considered to be the superposition of features (1) and (3), and $\dfrac{f_2(\log_{10}\omega b_T) - \epsilon''_B}{\epsilon''_m - \epsilon''_B}$ may be approximately expressed as an analytic function $\psi_2(\Delta, \log_{10}\omega b_T/\omega_m)$, where Δ is a parameter which determines the height/width ratio of the peak for a given form of this function. Then Equation 6 becomes

$$\epsilon''_{\omega,T} = [1 - A(T - T_s)] \times \frac{T_s}{T}\left[(\epsilon''_m - \epsilon''_B)\,\psi_2\left\{\Delta, \log_{10}\omega - \log_{10}\omega_m - \frac{8{\cdot}86\,(T - T_s)}{101{\cdot}6 + T - T_s}\right\} + \epsilon''_B\right] \quad .. \quad .. \quad (7)$$

Thus, the list of necessary information to calculate the values of $\epsilon''_{\omega,T}$ in the region of the peak value becomes:

A coefficient of expansion (measured by a conventional method).

T_s a reference temperature (found as described in Appendix A).

ω_m the frequency of the peak loss factor at T_s (read from "master" curves).

ϵ''_m the value of the peak loss factor at T_s (read from "master" curves).

ϵ''_B a constant—the background loss factor at T_s (the lowest value on the "master" curves).

ψ_2 an analytic function of $\left[\Delta, \log_{10}\omega - \log_{10}\omega_m - \frac{8{\cdot}86\,(T - T_s)}{101{\cdot}6 + T - T_s}\right]$.

Δ an arbitrary constant which occurs in certain forms of ψ_2.

The experimental values of $\psi_2\,[\Delta, \log_{10}\omega b_T - \log_{10}\omega_m] = (\epsilon''_\omega - \epsilon''_B)/(\epsilon''_m - \epsilon''_B)$, in the region of the loss factor peak, have been compared with the various analytic functions (listed in Table 2) which have been proposed for ϵ''/ϵ''_m, the best values of Δ being found by trial and error or, where possible, by the use of test plots suggested by previous authors in the references given.

TABLE 2

ANALYTICAL EXPRESSIONS FOR $\epsilon\omega''/\epsilon''_m$

No.	Author	$\epsilon''\omega/\epsilon''_m$
1.	Debye[20]	$\frac{2X}{1 + X^2}$
2.	Wagner–Yager[21,22] ..	$\frac{e^{-b^2X_o^2}\int_0^\infty e^{-b^2u^2}\frac{\cosh 2b^2X_o u}{\cosh u}\,du}{\int_0^\infty \frac{e^{-b^2u^2}}{\cosh u}\,du}$
3.	Fuoss and Kirkwood[23] ..	$\operatorname{sech}\alpha(\log_{10}X)$*
4.	Kirkwood and Fuoss I[24] ..	$\frac{4X\,[(X^2 - 1)\,ln\,X - X^2 + \pi X - 1]}{[1 + X^2]^2\,(\pi - 2)}$*
5.	Kirkwood and Fuoss II[24]	$3{\cdot}75\int_0^\infty \frac{pm}{1 + p^2m^2}\left[1 + p + p(p + 2)e^p\,Ei(-p)\right]\partial p$*
6.	Cole and Cole[25]	$\frac{1 + \cos\beta\pi/2}{\cosh\beta X_o + \cos\beta\pi/2}$
7.	Frölich[26]	$\frac{\tan^{-1}\gamma X - \tan^{-1}X/\gamma}{\tan^{-1}\gamma - \tan^{-1}1/\gamma}$

b, α, β, γ are arbitrary constants.

$X = \omega b_T/\omega_m$. $\quad m = 0{\cdot}63\ \omega b_T/\omega_m$. $\quad X_o = ln(\omega b_T)/\omega_m$.

* These are approximations and $\frac{\epsilon''\omega(2 + 1/\epsilon'\omega^2)}{\epsilon''_m(2 + 1/\epsilon'^2_m)}$ should replace $\epsilon''\omega/\epsilon''_m$ (ϵ'_m is the value ϵ'_ω when $\omega b_T = \omega_m$; the errors of approximation are negligible for the data recorded here). It must be noted that the theoretical functions 1, 4 and 5 do not contain a disposable parameter Δ, but each of the empirical functions 2, 3, 6 and 7 contains such a parameter b, α, β and γ respectively.

Figure 8 shows values of $(\epsilon''_\omega - \epsilon''_B)/(\epsilon''_m - \epsilon''_B)$ in the region of the peak plotted against $\log(\omega b_T/\omega_m)$ superimposed on the lines given by functions 3, 6 and 7 for $\epsilon''_\omega/\epsilon''_m$. Vertical linear scales, which vary for

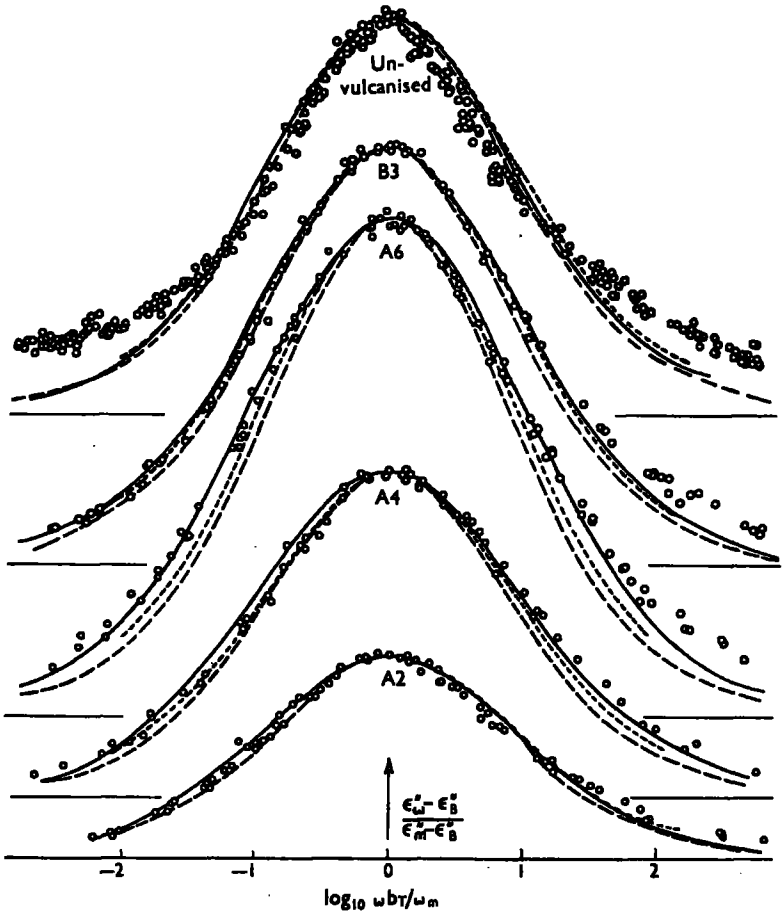

FIG. 8. Comparison of experimental results with analytic functions.

———— Fuoss–Kirkwood
— — · — — Cole–Cole
---------- Fröhlich

the different curves, have been omitted for clarity. Figure 9 shows the same values with the lines for functions 2, 4 and 5. The functions 3 and 6 give the best fit to the experimental results. The parameters used,

together with the various other parameters involved in Equations 5, 6 and 7 and other data on the samples, are given in Table 3.

The Cole-Cole circular arc plots[25] (with no correction for the background loss factor) for the vulcanised rubbers (data reduced to $T = T_s$) are given

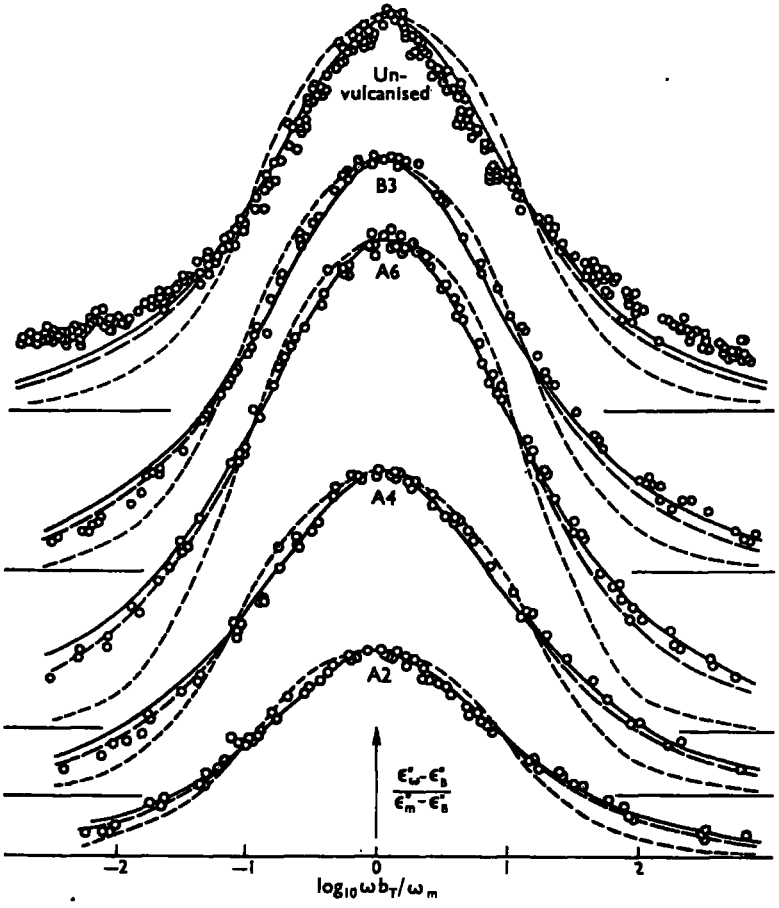

FIG. 9. Comparison of experimental results with analytic functions.

———— Wagner–Yager

— — — — Kirkwood and Fuoss I

---------- Kirkwood and Fuoss II

s full lines in Figure 10. Deviations of the data (derived from the urves of Figures 3–6) from the circular arcs are indicated by dotted lines. ın estimate of ϵ_s (the static dielectric constant at T_s) and a second stimate of ϵ_∞ were made from the Cole-Cole plot.

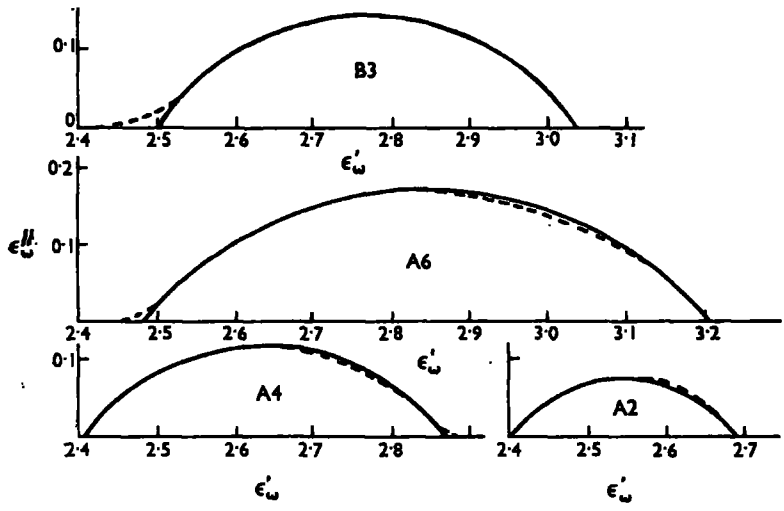

FIG. 10. Cole–Cole plots.

——— circular arcs

---------- deviations of experimental curves (from Figs. 3, 4, 5 and 6)

TABLE 3

COLLECTED DIELECTRIC DATA

	Unvulcanised	A2	A4	A6	B3
Reference temperature T_s; ° K. ..	247	251	254·5	259	255
ϵ_∞ (assumed)	—	2·34	2·35	2·37	2·35
$-\frac{1}{\epsilon_{\infty,T}} \cdot \frac{\partial}{\partial T}(\epsilon_{\infty,T}) \times 10^4$ (assumed)	—	4·6	4·6	4·6	4·6
$\log_{10}(\omega_m/2\pi)$	5·3	4·0	3·9	3·8	3·9
$\epsilon''_m \times 10^2$	1·08	7·4	11·5	16·8	14·5
$\epsilon''_B \times 10^2$	0·07	0·4	0·4	0·4	0·4
ϵ_s (from Figs. 3 and 5)	—	2·70	2·88	3·22	3·05
ϵ_∞ from Cole–Cole plot	†	2·40	2·41	2·48	2·50
ϵ_s from Cole–Cole plot	†	2·69	2·87	3·21	3·04
α	0·52	0·53	0·48	0·46	0·51
β	0·64	0·65	0·60	0·58	0·63
γ	10	10	13	13	11
b	0·40	0·40	0·37	0·35	0·39

† $\epsilon_s - \epsilon_\infty$ too small to permit accurate Cole–Cole plot.

In the previous discussion it was assumed that $G(\tau)$ could be expressed by various analytic functions, and these hypotheses were tested by comparison of the calculated values of $\epsilon''_\omega/\epsilon''_m$ with the experimental data. It is, however, possible to deduce $G(\tau)$ graphically from the given ϵ'_ω or ϵ''_ω data by a second approximation method given by Ferry and Williams[27] and by Williams and Ferry.[28] The accuracy of the method is not high, since it depends on graphical differentiation of the experimental curves. The resulting values of $(\epsilon_s - \epsilon_\infty)\,\tau G(\tau)$ at T_s for the sample B3 are given in Figure 11. $\tau G(\tau)$ is the distribution function of natural

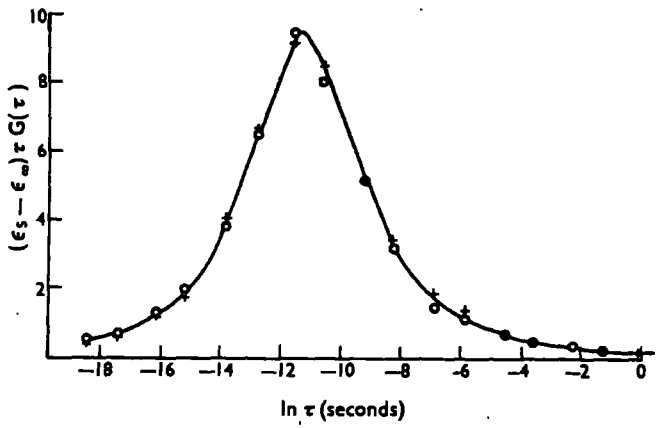

FIG. 11. Distribution of log relaxation times for B3 at $T = T_s$.
+ from permittivity data
⊙ from loss factor data

logarithms of the relaxation times and $(\epsilon_s - \epsilon_\infty)\,\tau G(\tau)$ is identical with the function represented by $\psi(\tau)$ in the notation of Ferry and Williams. The agreement between the results from the loss factor and permittivity data is as good as can be expected in view of the approximations and graphical differentiations.

DIPOLE MOMENTS

From the loss factor/frequency data on raw rubber it is possible to calculate a value z below which the dipole moment μ of the rubber monomer cannot lie; the actual dipole moment cannot be calculated since the dispersion is so wide that ϵ''_ω is considerably greater than zero at both ends of the curve, and the permittivity data is inadequate to provide a value of $\epsilon_s - \epsilon_\infty$. The value z is derived by assuming that the loss factor at $T = T_s$ is given by

$$\epsilon''_\omega = [1{\cdot}01 \times 10^{-3}\,\mathrm{sech}\{0{\cdot}52(ln\ \omega/\omega_m)\}] + (7 \times 10^{-4}).$$

This form of the expression for ϵ''_ω is one which is given by the Fuoss and Kirkwood[23] expression superimposed on a constant background loss

factor (the constants being as given in Table 3). This has been shown to agree with the experimental values if the ionic losses are ignored.

If v and w are the limits of $ln\ \omega b_T$ in Figure 7, this gives

$$\int_v^w \epsilon''_\omega\, \partial(ln\omega) = [(\pi/0{\cdot}52) \times 1{\cdot}01 \times 10^{-2}] + [2{\cdot}3 \times 13 \times 7 \times 10^{-4}]$$

$$= 8{\cdot}2 \times 10^{-2}$$

$$\text{but} \int_{-\infty}^{\infty} \epsilon''_\omega\, \partial(ln\omega) = \frac{\pi}{2} \cdot \frac{4\pi N\mu^2}{27kT}\,(\epsilon_s + 2)^2 > \int_v^w \epsilon''_\omega\, \partial(ln\omega)$$

(see Oakes and Richards[29]),

where N = No. of dipoles per unit volume.

Putting $N = 8{\cdot}1 \times 10^{21}$ = No. of monomer units/cm.^{3},

and $\epsilon_s = 2{\cdot}3$, gives $\mu > z = 0{\cdot}16$ Debye units.

This value of z is much lower than the value $\mu = 0{\cdot}72$D, obtained by Kambara[30] for raw crude rubber from measurements on a solution in benzene. It is possible that Kambara's crude rubber was oxidised during the process of solution, thus increasing the dipole moment.

The values of the moment μ_s of a dipole containing one sulphur atom have been calculated on the following assumptions:

(i) that each sulphur atom is involved in a separate dipole;

(ii) that all the dipoles have the same dipole moment;

(iii) that the contribution of the small quantity of accelerator to the dielectric constant is negligible. An attempt to remove the accelerator by extraction resulted in a sample which oxidised rapidly and further tests could not be carried out.

The values of ϵ_s and ϵ_∞ given by the intersection of the circular arcs with the permittivity axis have been used in Onsager's formula,[31] $\mu_s^2 = \frac{GkT}{4\pi N'} \cdot \frac{(\epsilon_s - \epsilon_\infty)(2\epsilon_s + \epsilon_\infty)}{\epsilon_s(\epsilon_\infty + 2)^2}$, where N' = number of sulphur atoms per unit volume, giving $\mu_s = 1{\cdot}9$, $1{\cdot}8$, $1{\cdot}8$, $1{\cdot}9$D for A2, A4, A6 and B3 respectively. These values are, however, in error due to the contribution of the dipole moment of the rubber molecule. Although no precise values of permittivity of the raw rubber are available, the measured values indicate that, in the absence of the sulphur, $\epsilon_s - \epsilon_\infty$ is less than $0{\cdot}1$. If it is assumed that the value of ϵ_s for the vulcanised rubber must be reduced by this figure to allow for the dipole moment of the rubber, then the values of μ_s become $1{\cdot}5$, $1{\cdot}6$, $1{\cdot}7$, $1{\cdot}7$D respectively. These values are similar to that ($1{\cdot}74$) calculated by Waring.[32] The use of Cole–Cole plot values of ϵ_∞ and ϵ_s is justified by the fact that it does not take into account any dipolar dispersion range which may occur at higher frequencies than those involved here and which has been assumed therefore not to be associated with the sulphur atoms. The sulphur combines

with the rubber in various chemical groupings and it is speculative to draw any conclusions from the small range of calculated values of dipole moment.

The value of dipole moment for the isoprene unit is extremely small, so that for most practical purposes, the rubber hydrocarbon is a non-polar substance. Vulcanisation by sulphur adds considerably to the dipolar loss, and the dipole moment per combined sulphur atom (calculated assuming each combined sulphur atom to be a separate dipole) is substantially independent of the percentage combined sulphur or of the acceleration of the reaction.

Dependence of T_s on Combined Sulphur Content

Table 3 indicates that T_s is a function of the combined sulphur content (A2, A4 and A6 had the same total sulphur content). The values of T_s obtained by various authors from dielectric and mechanical data are given in Figure 12. There is a good agreement between the various series

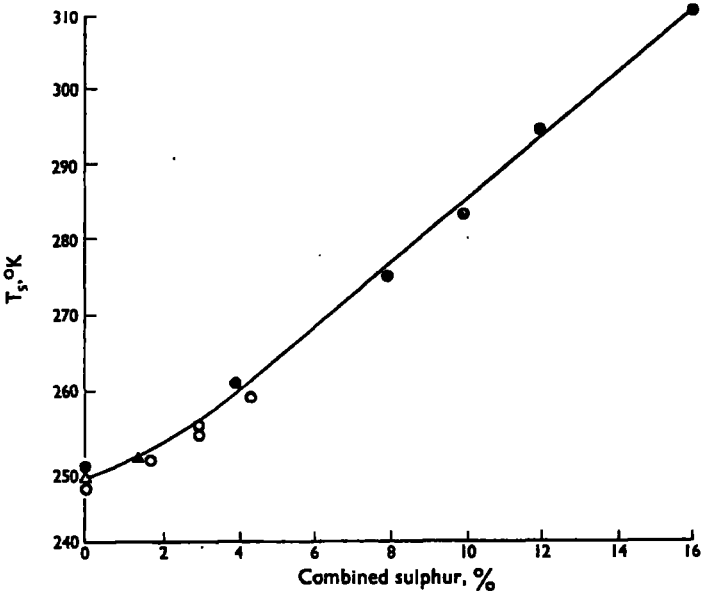

Fig. 12. Relationship between T_s and combined sulphur content.

○ dielectric results: present paper

● dielectric results: derived by Payne[23] from data of Scott, McPherson and Curtis[24]

△ dynamic mechanical results from three sources[15,16,23]

▲ dynamic mechanical result[23]

of results at the lower end of the curve. Three sets of results give 248° K. for unvulcanised rubber while the other two give 247° K. and 250° K., the latter being from experimental data of limited accuracy.

Conclusions

1. The Ferry and Fitzgerald method (set out in mathematical terms in this paper) of analysing the loss factor and permittivity data is applicable to measurements on both vulcanised and unvulcanised dry purified rubber.

2. The form of the loss factor/frequency function suggests the summation of

(*a*) a broadened-Debye-type peak; the process is polar;

(*b*) a constant "background loss factor"; the process is obscure;

(*c*) an ionic loss at very low frequencies; this is only obvious on the unvulcanised rubber.

3. Of the various theoretical and semi-empirical forms for the distribution of relexation times giving rise to the Debye-type peak, the Fuoss–Kirkwood[23] and Cole–Cole[25] functions were found to be most in accord with experimental results.

4. Estimates of the dipole moment of raw natural rubber could not be made, although it is deduced that the value cannot be less than 0·16D. In a vulcanisate, the moment of the dipole containing one sulphur atom (based on the assumptions that each combined sulphur atom in the vulcanisate gives rise to a separate dipole and all the dipoles have the same moment) is about 1·6D.

Acknowledgements

The authors are indebted to the Rubber and Plastics Research Association of Great Britain for permission to publish this paper.

(*Received 6th September, 1965*)

Appendix A

Method of Carrying out Temperature/Frequency Analysis.

In analysing the permittivity data, it was necessary to know $\epsilon_{\infty,T}$ over a range of temperatures which must include all the experimental temperatures and T_g. Other authors have assumed that $\epsilon_{\infty,T}$ does not vary with T. However, in the case of the rubbers used in this investigation it was necessary to allow for the variation. In the absence of any other measure of $\epsilon_{\infty,T}$ it was assumed that an adequate approximation would be given by the square of the refractive index (extrapolated to infinite wavelength using Cauchy's formula)—see Appendix B. The coefficient of cubical expansion A must also be determined.

The values of $\frac{\epsilon'_{\omega,T} - \epsilon_{\infty,T}}{k'_T} + \epsilon_{\infty,o}$ and $\epsilon''_{\omega,T}/k'_T$, referred to as $\epsilon'_{\omega,o}$ and $\epsilon''_{\omega,o}$ (where $\epsilon_{\infty,o}$ is the value of $\epsilon_{\infty,T}$ at T_o), were calculated for $T_o = 253°$ K. (273° K. for unvulcanised rubber). The inclusion of the term $\epsilon_{\infty,o}$ at this stage does not modify the arguments of the previous section, but brings the method into line with that of previous authors.

The derived values of $\epsilon'_{\omega,\rho}$ and $\epsilon''_{\omega,\rho}$ were plotted as functions of $\log_{10}(\omega/2\pi)$; see the short curves and inner scales in Figure 3. The displacement ($\log_{10} b'_T$) along the $\log_{10}\omega$ axis of the curve for the reference temperature from each of the other curves was then plotted against T. The value of T_s was then read off as the temperature at which the slope was $-0{\cdot}0872$ deg^{-1} C. The logarithm of the parameter m in the relationship $b_T = mb'_T$ was then found as the value of $-\log_{10} b'_T$ at $T = T_s$. In Figure 13, the values of $\log_{10} b_T$ found by adding $\log_{10} m$ to the experi-

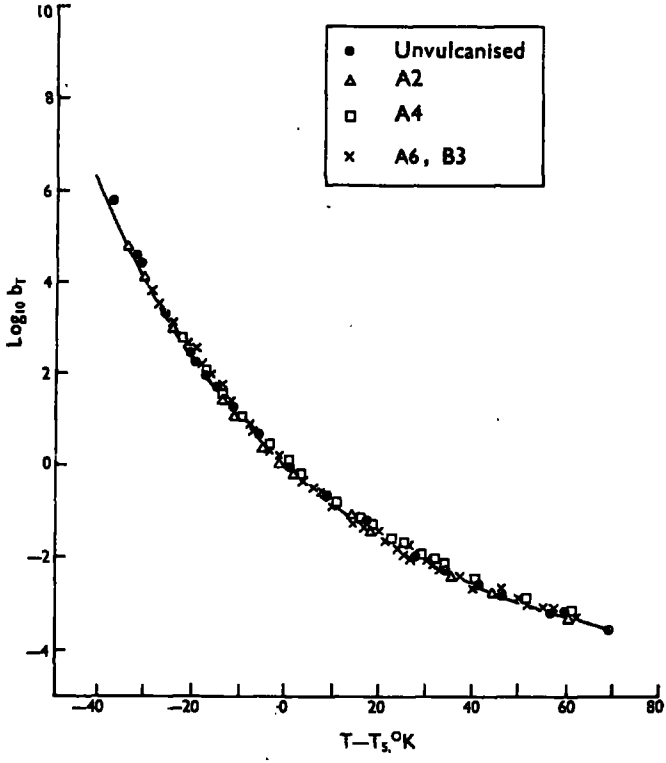

FIG. 13. Log b_T values.

● Unvulcanised × A6, B3
△ A2
□ A4

$$\log b_T = -\frac{8{\cdot}86\,(T - T_s)}{101{\cdot}6 + T - T_s}$$

mentally determined values of $\log_{10} b'_T$, for all the rubbers, are shown plotted against $T - T_s$, superimposed on the curve given by Equation 4.

The curves of $\epsilon'_{\omega,\rho}$ and $\epsilon''_{\omega,\rho}$ were then shifted along the $\log_{10}\omega$ axis for distances $\log_{10} b_T$ given by Equation 4, thus giving plots of the real

and imaginary parts of $\epsilon_{\omega,o}$ as functions of $\log_{10}\omega b_T$ as shown in Figures 3 and 4. The vertical scales were then amended to turn the graphs of $\epsilon_{\omega,o}$ into graphs of ϵ_ω as follows. In both cases, the lengths of the scale divisions were multiplied by a factor of $\frac{T_s}{T_o}[1 - A(T_o - T_s)]$. For the ϵ' graph the position of the scale was adjusted so that ϵ'_∞ on the new scale corresponded with $\epsilon'_{\infty,o}$ on the original scale.

Appendix B

Values of $\epsilon_{\infty,T}$.

The data of McPherson and Cummings[35] give the refractive index (n_D^T) for the sodium D line of natural rubber containing S_c per cent. combined sulphur and S_s per cent. free sulphur as

$$n_D^T = 1{\cdot}519 + 0{\cdot}0037S_c - 0{\cdot}00035(T-298) + 0{\cdot}0016S_s,$$

if the assumption is made that the influence of free sulphur is of the same magnitude in the vulcanisate as it is in the unvulcanised rubber. The data given by Wood[36] fit Cauchy's formula relating refractive index to wavelength and give an extrapolated value at infinite wavelength $(n)_\infty^{25}$ which is 0·020 less than n_D^{25}.

Combining these relationships and assuming the temperature coefficient remains constant at lower temperatures (−50° to +20° C.) than those over which it was measured (+20° to +60° C.), gives values of $(n_\infty^T)^2$ at $T = T_s$ of 2·34, 2·35, 2·37, 2·35 for A2, A4, A6 and B3 respectively, with a temperature coefficient $\left(\frac{1}{n_\infty^T}\right)^2 \frac{\partial}{\partial T}(n_\infty^T)^2$ of $-4{\cdot}6 \times 10^{-4}$ per ° C.

Examination of the original data showed that the value of $(n_\infty^T)^2$ was only of the order of 0·12 lower than the lowest values of $\epsilon'_{\omega,T}$ observed, and it was therefore concluded that the effects of atomic polarisability and of any very high frequency (outside the experimental range) dipolar loss mechanism were small. It was therefore assumed, in the absence of any further information, that $(n_\infty^T)^2 = \epsilon_{\infty,T}$ was an adequate approximation for the present treatment of the results, and the resultant superposition of the curves suggests that the assumption was justified.

Appendix C

Comparison of Ferry and Fitzgerald Assumptions with Debye and Onsager Theories.

Ferry and Fitzgerald's second assumption is equivalent to an approximation to the formulae of Debye[37] and Onsager[31] combined with the Lorenz–Lorentz[38,39] equation if $\epsilon_{\infty,T}$ is constant. The exact expressions should be $\epsilon_\tau \propto \frac{\rho_T}{T}(\epsilon_{s,T} + 2)$ (Debye) and $\epsilon_\tau \propto \frac{\rho_T}{T} \cdot \frac{\epsilon_{s,T}}{2\epsilon_{s,T} + \epsilon_{\infty,T}}$ (Onsager), but the added refinement is unnecessary for the materials

described here, where $\epsilon_{s,T}$ varies over such a short range. The Debye correction is about twice the Onsager correction and the model used in either is probably inadequate for a close approximation in the present case. The extrapolation of the results to higher or lower temperatures would, however, be affected by the approximation involved in this step.

Appendix D

Activation Energies and the Williams, Landel and Ferry Equation.

It does not appear to be generally realised that, for physical processes where the Williams, Landel and Ferry equation applies, the equation requires only a single parameter, the T_s value, in order to specify the activation energies at *all* the temperatures within the range of application. The equation thus specifies a relationship between activation energies, and the T_s value is therefore a more useful factor than activation energies at a single or limited number of temperatures.

The Williams, Landel and Ferry equation may be rewritten

$$ln\, b_T = -\frac{2{\cdot}303 \times 8{\cdot}86\,(T - Ts)}{101{\cdot}6 + T - T_s}.$$

The activation energy is given by

$$E = R\frac{\partial(ln\, b_T)}{\partial(1/T)} = 2{\cdot}07\,R\left(\frac{T}{101{\cdot}6 + T - T_s}\right)^2,$$

where R is the gas constant ($1{\cdot}987 \times 10^{-3}$ kcal. deg.$^{-1}$ mole^{-1}).

$$\text{Thus } E = 4{\cdot}12\left(\frac{T}{101{\cdot}6 + T - T_s}\right)^2.$$

Appendix E

List of Symbols.

In this list ϵ_ω is a vector quantity defining real and imaginary parts (ϵ'_ω and ϵ''_ω). Likewise $\epsilon_{\omega,T}$ has real and imaginary parts ($\epsilon'_{\omega,T}$ and $\epsilon''_{\omega,T}$) etc.

Symbol	Definition
A	coefficient of cubical expansion
b	curve-width parameter: Wagner–Yager
b_T	τ_T/τ_o when $T_o = Ts$
b'_T	τ_T/τ_o
f_1	$\frac{\epsilon'_{\omega,T} - \epsilon_{\infty,T}}{k_T}$ as a function of ωb_T
f_2	$\epsilon''_{\omega,T}/k_T$ as a function of ωb_T
$G(\tau)$	distribution function of τ
k'_T	$\frac{\rho_T T_o}{\rho_o T} = [1 - A(T - T_o)]\frac{T_o}{T}$

Symbol	Definition
k_T	$[1 - A(T - T_s)]\frac{T_s}{T}$
m	b_T/b'_T
N	number of dipoles/unit volume
N'	number of sulphur atoms/unit volume
n_D^T	refractive index for sodium D line at T
n_∞^T	refractive index for infinite wavelength at T
T	temperature of measurement
T_o	arbitrary reference temperature
T_s	value of T at which $\frac{\partial}{\partial T}\log_{10}b'_T = -0{\cdot}0872$
z	value below which dipole moment of rubber monomer cannot lie
α	curve-width parameter: Fuoss–Kirkwood
β	curve-width parameter: Cole–Cole
γ	curve-width parameter: Frölich
Δ	general curve-width parameter
$\epsilon_{\omega,T}$	complex dielectric constant $\epsilon'_{\omega,T} + i\epsilon''_{\omega,T}$ at ω,T
ϵ_D	dipolar part of dielectric constant
ϵ_τ	contribution to ϵ_D of dipoles of time constant τ
$\epsilon_{s,T}$	static dielectric constant at T
$\epsilon_{\infty,T}$	infinite frequency dielectric constant at T
$\epsilon_{\omega,o}$	$\frac{\epsilon_{\omega,T} - \epsilon_{\infty,T}}{k'_T} + \epsilon_{\infty,o}$
$\epsilon_{\infty,o}$	value of $\epsilon_{\infty,T}$ at $T = T_o$
ϵ_ω	$\frac{\epsilon_{\omega,T} - \epsilon_{\infty,T}}{k_T} + \epsilon_\infty$
ϵ_s	static dielectric constant at T_s
ϵ_∞	infinite frequency dielectric constant at T_s
ϵ''_B	background value of ϵ''_ω
ϵ''_m	maximum value of ϵ''_ω
μ	dipole moment
μ_s	moment of dipole containing 1 sulphur atom
ρ_T	density of material at T
ρ_o	density at T_o
ρ_s	density at T_s
τ	relaxation time

Symbol	Definition
τ_T	value of τ for a given process at T
τ_o	value of τ for a given process at T_o
ψ_2	function relating $\frac{\epsilon''\omega - \epsilon''_B}{\epsilon''_m - \epsilon''_B}$ to $\log(\omega b_T/\omega_m)$ and Δ
ω	$2\pi \times$ frequency of measurement
ω_m	value of ωb_T corresponding to ϵ''_m

References

1. Norman, R. H., *Proc. I.E.E.*, 1953, **100**, IIA, 41.
2. B.S. 903: 1958: Part B6, Section 1.
3. B.S. 903: 1958: Parts B6, Section 1 and B8.
4. Ferry, J. D. and Fitzgerald, E. R., *J. Colloid Sci.*, 1953, **8**, 224.
5. Ferry, J. D., *Viscoelastic Properties of Polymers*, New York, John Wiley and Sons, Inc.
6. Ferry, J. D., Fitzgerald, E. R., Grandine, L. D., Jr. and Williams, M. L., *Ind. Eng. Chem.*, 1952, **44**, 703.
7. Williams, M. L., *J. Phys. Chem.*, 1955, **59**, 95.
8. Williams, M. L., Landel, R. F. and Ferry, J. D., *J. Am. Chem. Soc.*, 1955, **77**, 3701.
9. Williams, M. L. and Ferry, J. D., *J. Colloid Sci.*, 1954, **9**, 479.
10. Williams, M. L. and Ferry, J. D., *J. Colloid Sci.*, 1955, **10**, 1.
11. Williams, M. L. and Ferry, J. D., *J. Colloid Sci.*, 1955, **10**, 474.
12. Zapas, L. J., Shufler, S. L. and Dewitt, T. W., *J. Polym. Sci.*, 1955, **18**, 245.
13. Payne, A. R., *J. Appl. Phys.*, 1957, **28**, 378.
14. Payne, A. R., *Plastics*, 1958, **23**, May, 182.
15. Payne, A. R., Society of the Chemical Industry Monograph No. 5, p. 273, London, Society of the Chemical Industry.
16. Fletcher, W. P. and Gent, A. N., *Brit. J. Appl. Phys.*, 1957, **8**, 194.
17. Maxwell, J. C., *A Treatise on Electricity and Magnetism*, 3rd Edition, Vol. 1, p. 492, Oxford, Clarendon Press Ltd.
18. Wagner, K. W., *Archives Elektrotechniques*, 1914, **2**, 371.
19. Garton, C. G., *Trans. Faraday Soc.*, 1946, **42A**, 56.
20. Debye, P., *Polar Molecules*, New York, Chemical Catalog Co.
21. Wagner, K. W., *Ann. Physik*, 1913, **40**, 817.
22. Yager, W. A., *Physics*, 1936, **7**, 434.
23. Fuoss, R. M. and Kirkwood, J. G., *J. Am. Chem. Soc.*, 1941, **63**, 385.
24. Kirkwood, J. G. and Fuoss, R. M., *J. Chem. Phys.*, 1941, **9**, 329.
25. Cole, K. S. and Cole, R. H., *J. Chem. Phys.*, 1941, **9**, 341.
26. Fröhlich, H., *Theory of Dielectrics*, p. 92, Oxford, Clarendon Press Ltd.
27. Ferry, J. D. and Williams, M. L., *J. Colloid Sci.*, 1952, **7**, 347.
28. Williams, M. L. and Ferry, J. D., *J. Polym. Sci.*, 1953, **11**, 169.
29. Oakes, W. G. and Richards, R. B., *Trans. Faraday Soc.*, 1946, **42A**, 197.
30. Kambara, S., *J. Soc. Rubber Ind.*, Japan, 1942, **15**, 665.
31. Onsager, L., *J. Am. Chem. Soc.*, 1936, **58**, 1486.
32. Waring, J. R. S., *Trans. Inst. Rubber Ind.*, 1951, **27**, 16.
33. Payne, A. R., *Rheology of Elastomers*, p. 86, London, Pergamon Press.
34. Scott, A. H., McPherson, A. T. and Curtis, H. L., *J. Res. Nat. Bur. Stand.*, 1933, **11**, 173.
35. McPherson, A. T. and Cummings, A. D., *J. Res. Nat. Bur. Stand.*, 1935, **14**, 553.
36. Wood, L. A., *J. Appl. Phys.*, 1941, **12**, 119.
37. Debye, P., *Physik Z.*, 1912, **13**, 97.
38. Lorentz, H. A., *Ann. Physik Chemie*, 1880, **9**, 641.
39. Lorenz, L. V., *Annalen Physik Chemie*, 1880, **11**, 70.

(*Received 6th September, 1965*).